The University of Nottingham
UNITED KINGDOM · CHINA · MALAYSIA

USC UNIVERSIDADE DE SANTIAGO DE COMPOSTELA

Novel gel-associated drug loaded nanocarriers for intratumoural delivery

Ivana Štaka

M.Sc. pharmaceutical engineer (Hons.)

Submitted to The University of Nottingham for the degree of Doctor of Philosophy

September 2017

Table of Contents

Declaration i

Abstract ii

Acknowledgements iv

Abbreviations vi

List of Figures x

List of Tables xxii

1 Introduction 1

1.1 Cancer – the disease 1

1.1.1 Cancer statistics 2

1.1.2 Treatment of cancer 3

1.2 Considerations impacting decisions regarding injection or resection 4

1.2.1 Inoperable and late stage cancers 4

1.2.1.1 Metastasised cancers 5

1.2.1.2 Cancer location 5

1.3 Nanomedicines for cancer 6

1.3.1 Liposomes 7

1.3.2 Polymer conjugates 8

1.3.3 Dendrimers 9

1.3.4 Surfactant and polymeric micelles 10

1.3.5 Nanoparticles (NPs) 11
1.3.6 Nanocapsules (NCs) 12
1.3.7 Nanocarriers on the market 13
1.3.7.1 Nanoplatforms in clinical trials 16
1.4 Systemic vs. local chemotherapy 18
1.5 Platforms for local delivery in cancer 21
1.5.1 Gels as a drug delivery platform 23
1.5.1.1 Polymeric gels 26
1.5.1.2 Low molecular weight gels (LMWGs) 27
1.5.1.3 Gel-nanoparticle composite 30
1.6 Gemcitabine 33
1.6.1 Uptake and mechanism of action 34
1.6.2 Gemcitabine resistance 37
1.6.3 Gemcitabine prodrugs 38
1.7 The proposed platform 40
1.7.1 Aim of the project 40
2 Development of polymeric nanocapsules 42
2.1 Materials and methods 46
2.1.1 Self-emulsification method 46
2.1.2 Materials used for production of nanoemulsions and nanocapsules 49
2.1.3 Preparation and optimisation of NCs 50

2.1.3.1 Optimisation of nanoemulsions 51

2.1.3.2 Influence of oil nature on physico-chemical characteristics of nanoemulsions 52

2.1.3.3 Preparation of cationic nanoemulsions and polymer introduction 53

2.1.3.4 Drug encapsulation 54

2.1.3.5 In vitro drug release 55

2.1.4 Methods of characterisation 56

2.1.4.1 Physicochemical characterisation of NCs 56

2.1.4.2 Isolation of nanocapsules and quantification of the drug loading 56

2.1.4.3 Morphological analysis by transmission electron microscopy - TEM 57

2.1.4.4 Freeze drying of NCs 57

2.1.4.5 Stability of the nanocapusules 58

2.1.4.6 Statistical analysis 58

2.2 Results and discussion 59

2.2.1 Development and characterisation of nanoemulsions 59

2.2.1.1 Ratios between non-ionic surfactants (Tween® 80 and Kolliphor® HS 15) 60

2.2.1.2 Total amount of surfactants 63

2.2.1.3 Oil content 64

2.2.1.4 Influence of the type of oil on size of nanocapsules..... 67
2.2.2 Production of polymeric NCs from cationic nanoemulsions.. 70
2.2.2.1 TEM characterisation of polymeric NCs..... 75
2.2.3 Encapsulation of anticancer drugs and purification of NCs .. 77
2.2.4 Stability of the NCs upon storage, in PBS and in cell culture medium 80
2.2.5 Stability of the NCs in PBS and in cell culture medium 84
2.2.6 In vitro release of GEM C14 from NCs..... 86
2.2.6.1 Release of GEM C14 from HA NCs..... 90
2.3 Summary 94
3 In vitro activity of drug loaded nanocapsules in cancer cells 95
3.1 Material and methods 98
3.1.1 Cell lines used: 98
3.1.2 Assays: 99
3.1.2.1 Growth inhibition assay:..... 99
3.1.2.2 Colony formation assay.....101
Results and disussion 102
3.2 Effect of NCs on cancer cell lines 102
3.2.1 Growth inhibition of HCT 116 and MiaPaCa-2.....102
3.3 Colony formation after the treatment with NCs.....109
3.3.1 The clonogenic cell survival of HCT 116 and MIA PaCa-2 cancer cells 110

3.3.2 IC_{50} values 117
3.4 Can NCs overcome drug resistance? 121
3.4.1 Are vincristine (VC) resistant cells resistant to gemcitabine? 123
3.4.2 GEM resistant cell line 124
3.5 Summary 130
4 Gel-nanocapsule composites for localised cancer therapy 132
4.1 Systems designed for localised cancer therapy 132
4.1.1 Chitosan gels.....133
4.1.2 LMWGs for localised cancer delivery 134
4.2 Materials and Methods 137
4.2.1 Materials used for manufacture of gels and gel-NCs associated formulations 137
4.2.2 Preparation of gels and gel-NCs composites 138
4.2.2.1 Preparation of polymeric gels 138
4.2.2.2 Preparation of hydrogels from LMW gelators 139
4.2.3 Encapsulation and quantification of fluorescent dye 140
4.2.4 Characterisation of NCs loaded with fluorescent dye 141
4.2.5 In vitro release experiment procedure 141
4.2.5.1 Release of fluorescent dyes from NCs 141
4.2.5.2 Release from the gel-NCs formulation 142
4.2.6 Injectability of the Gel-NC system 143

4.2.7 Methods for gel characterisation 144

4.2.7.1 Vial inversion 144

4.2.7.2 Measurment of storage and loss modulus 144

4.2.7.3 Transmission Electron Microscopy (TEM) 145

4.3 Results and discussion 146

4.3.1 Hyaluronic acid - chitosan gels 146

4.3.2 Hyaluronic acid – chitosan gels with nanocapsules 148

4.4 Low molecular weight organic gels - LMWGs 151

4.4.1 LMW hydrogels - N4-octanoyl-2'-deoxycytidine gelator 152

4.4.2 LMWGs -NCs composites.....157

4.4.2.1 Gels with 80 nm nanocapsules coated with hyaluronic acid 157

4.4.2.1.1 Rheological studies 158

4.4.2.1.2 Influence of amount of NCs on characteristics of gel-NCs 160

4.4.2.2 Comparison of gel strength between different nanocapsules.....167

4.4.3 Fate of the nanocapsules at 60 °C 169

4.5 Analysing the microscopic behaviour.....170

4.5.1 Nano structure determination by electron microscopy studies 170

4.6 In vitro release of fluorescent dyes from NCs and gel-NCs system 172

4.6.1 Release of Nile Red 173
4.6.1.1 Release of NCs from the LMW hydrogel 175
4.6.2 Release of porphyrin 179
4.6.2.1 IVIS imaging 182
4.6.3 Injectability of the NC-gels 182
4.7 Summary 186
5 Conclusions and future perspectives 188
5.1.1 Development of polymeric nanocapsules < 100 nm 188
5.1.2 In vitro activity of nanocapsules in cancer cells 189
5.1.3 Gel-nanocapsules associated system for localised cancer therapy 190
5.2 Future work 192
5.2.1 Further optimization of NCs formulation 192
5.2.2 NCs on cellular level 192
5.2.3 Localisation of gel-NCs formulation upon intratumoural injection 193
5.2.3.1 Polymeric gel-NCs composite 193
5.2.3.2 LMW gel-NCs composite 194
References 196
Appendices 238

Declaration

Unless otherwise acknowledged, the work presented in this thesis is my own. No part has been submitted for any other degree at The University of Nottingham or any other institution.

As the project was part of NanoFar doctorate programme, part of experimental work was done at University of Santiago de Compostela.

This doctoral dissertation was conducted under supervision of:

Dr. Maria Jose Alonso Fernandez, Full Professor at the Department of Pharmaceutical Technology at the University of Santiago de Compostela, Spain;

Dr. Maria Marlow, Associate Professor at School of Pharmacy at the University of Nottingham, UK;

Dr. Tracey D. Bradshaw, Assistant Professor at School of Pharmacy at the University of Nottingham, UK.

Ivana Štaka

August 2017

Abstract

Cancer is one of the leading causes of death worldwide with approximately 14 million new cases reported in 2012. Systemic chemotherapy is widely used to treat cancer and can often result in toxicity and adverse side effects. To reduce these adverse side effects and potentially increase efficacy, the focus of this thesis is to create a new intratumoural drug delivery platform for patients who are too ill to receive systemic chemotherapy or with inoperable tumours.

Herein, an injectable formulation composed of a hydrogel and drug-loaded polymeric nanocapsules (NCs) was developed, to deliver the chemotherapeutic locally within the tumour and hence reduce the adverse side effects. The hydrogel is used to control the release of the NCs within the tumour, while small NCs (<100 nm) aim to promote NC penetration throughout the tumour mass.

Self-emulsification, a low energy and solvent-free method, was used to produce the polymeric NCs. The lipid core of the NCs was suitable for encapsulation of anticancer drugs: docetaxel (DCX) and 4*N*-myristoyl-gemcitabine (GEM C14).

NCs with diameters of 40 and 80 nm and with zeta potential values of ~ -4 ± 1 to –19 ±1 mV were produced. Both anticancer drugs, DCX and GEM C14 were encapsulated with efficiencies of greater than 90%. GEM C14 was released from the NCs by diffusion with 63 ± 8 and 66 ± 10 % released in 30 days from 40 and 80 nm NCs respectively. Additionally, GEM C14-loaded NCs showed activity against various cancer cell lines *in vitro* where the following GI_{50} values were obtained: 15 ± 6, 10 ± 9, 13 ± 3 nM in HCT 116, MIA PaCa-2 and Panc-1 cell lines respectively. Although not as potent in a GEM-resistant pancreatic cancer cell line (Panc-1 GEM resistant),

GEM C14 NCs (GI_{50}= 410 ± 463 nM) were significantly more active than GEM C14 alone (GI_{50}=8300 ± 5523 nM).

Hydrogels were prepared using a low molecular weight (LMW) gelator - *N*4-octanoyl-2'-deoxycytidine. This amphiphilic molecule self-assembles in water forming a 3D nanofibre network with the ability to reform after the application of stress, making it suitable for injection through a syringe/needle. *N*4-octanoyl-2'-deoxycytidine was used to gel the NC suspension *via* a heat-cooling cycle. The strength of gel-NC composite was determined by oscillatory rheology and its 3D nanofibre structure containing spherical NCs was confirmed by TEM. The gel-NCs formulation reformed instantly into a gel after injection through the needle and formed a depot when injected in an *in vitro* simulation of intratumoural delivery i.e. chicken tissue.

In summary, a novel NCs-gel composite has been designed demonstrating appropriate characteristics for intratumoural drug delivery.

Acknowledgements

There are numerous people that I would like to express gratitude for their contribution to this project.

I would like to start with my supervisors; Dr. Maria Marlow and Dr. Tracey D. Bradshaw from University of Nottingham and Dr. Maria Jose Alonso from University of Santiago de Compostela for their support and guidance throughout the PhD. It was indeed a remarkable opportunity to work with such experts which would not be possible without the European Commission, Education, Audiovisual and Culture Executive Agency (EACEA), Erasmus Mundus programme, NanoFar doctorate funding.

Next, the accomplished work would not have been possible without the technical support provided by staff both from NanoBioFar group of CIMUS and the one from Boots Science building. Additionally, assistance provided by Mike Fay and Christopher Parmenter in Nottingham Nanotechnology and Nanoscience Centre for TEM imaging is greatly appreciated. Special thanks go to Kathryn Skilling for synthesis of compounds I had used in this project.

Along this road, I had pleasure working with magnificent young scientists whose friendship on top of everything will always be remembered, hence I extend my gratitude to Carmen, Sonia, Adri, Jose, Jacqueline, Anne, Floor and Masar. The ones with whom I went through thick and thin during these few years are NanoFar colleagues with special thanks to Emma, Ana, Lara and Rahmet for all lovely moments we have shared. Nothing would have been possible without a close circle of friends: Jovana, Gorice, Mima, Anja, Ema and Pilići thank you for your unwavering support from the overseas.

I would like to extend the biggest thanks to my boyfriend Miloš. This work definitely wouldn’t have been possible without you.

In the end, I will never have enough words to express gratitude to my parents, little brother and aunt, whose unconditional support follows me every step of the way.

Abbreviations

ACT	Adoptive Cell Therapy
SMANCS	Styrene-maleic acid (SMA) and neocarzinostatin (NCS)
PAMAM	Polyamidoamine
PPO	Poly (propylene oxide)
PLA	Poly (L-lactide acid)
PCL	Poly-ε-caprolactone
PNIPAM	Poly(N-isopropylacrylamide)
PDMA	Poly(dimethylacrylamide)
PPF	Poly (propylene fumarate)
PU	Poly(urethane)
NPs	Nanoparticles
PLGA	Poly- (lactic-co-glycolic acid)
EGF	Epidermal Growth Factor
NCs	Nanocapsules
DOX	Doxorubicine
PEG	Polyethylene glycol
FDA	Food and Drug Administration
PCX	Paclitaxel
OS	Overall survival
NSCLC	Non-Small Cell Lung Cancer
mAb	Monoclonal Antibody
VEGF	Vascular Endothelial Growth Factor
LMW	Low Molecular Weight

LMWGs	Low Molecular Weight Gels
s.c.	Subcutaneous
i.t.	Intratumoural
i.v.	Intravenous
i.p.	Intraperitoneal
i.m.	Intramuscular
SAFIN	self-assembled fibrillar networks
HAMC	Hyaluronan/Methyl Cellulose
HPMC	Hydroxypropyl methylcellulose
NR	Nile Red
GEM; dFdC	Gemcitabine; 2',2'-difluoro-2'-deoxycytidine
GEM-HCl	Gemcitabine hydrochloride
hNTs	Human Nucleoside Transporters
dFdCMP	Gemcitabine Monophosphate
dFdCDP	Gemcitabine Diphosphate
dFdCTP	Gemcitabine Triphosphate
dCK	Deoxycytidine Kinase
CDA	Cytidine Deaminase
DCTD	Deoxycytidylate Deaminase
RNR	Ribonucleotide Reductase
TS	Thymidylate Synthase
GEM C14	4*N*-myristoyl gemcitabine
MTD	Maximum Tolerated Dose
HPH	High Pressure Homogeniser
PIT	Phase Transition Temperature
SEDDS	Self-Emulsified Drug Delivery Systems
SMEDDS	Self-Microemulsified Drug Delivery Systems

SNEDDS	Self-Nanoemulsified Drug Delivery Systems
MCT	Medium Chain Triglyceride
CTAB	Hexadecyltrimethylammonium bromide
HA	Sodium Hyaluronate
PGA	Poly-L-glutamic Acid
DCX	Docetaxel
PDI	Polydispersity Index
ZP	Zeta Potential
mV	Milliivolt
SEC	Size Exclusion Chromatography
RT	Room Temperature
ANOVA	One-way Analysis of Variance
P-gp	P-glycoprotein
nm	Nanometre
OR	Ostwald Ripening
SS	Sample and Separate
DM	Dialysis Membrane
CF	Continuous Flow
PBS	Phosphate Buffer Serum
FBS	Foetal Bovine Serum
ATCC	American Type Culture Collection
CFU	Colony Forming Units
MRP	Multidrug Resistance associated Proteins
ABC	ATP-binding Cassette
VCR	Vincristine
CPT	Camptothecin
HA MMW	Hyaluronic Acid of Medium Molecular Weight

CS	Chitosan
Porphyrin	4,4’,4’’,4’’’-(Porphine-5,10,15,20-tetrayl) tetrakis(benzoic acid)
G'	Storage/elastic modulus
G''	Loss modulus
TEM/SEM	Transmission/Scanning Electron Microscopy
LVE	Linear-Viscoelastic

List of Figures

Figure 1-1 Cancer progress and prognosis adapted from Macmillan research on cancer prevalence in UK. Number of people getting cancer for the first time is presented in blue, while number of people dying is shown in black rectangles. Purple circles represent number of people living with cancer, while green rectangles indicate how long people live on average. Macmillan estimations are based on data from Office for National Statistics. http://www.macmillan.org.uk/documents/aboutus/research/thechangingstoryofcancer.pdf 3

Figure 1-2 Schematic representation of liposomal structure. Black circle symbols with two tails present a lipid bilayer while blue curvy lines attached to it are representation of PEG molecules. Encapsulated drugs (red triangles and blue star) and targeting moieties in green are marked on the scheme. 8

Figure 1-3 Schematic representation of polymer conjugates. Black curvy line symbolises polymer to which drug (small molecule) and targeting moieties in green are marked on the scheme. 8

Figure 1-4 Schematic representation of dendrimer structure. Branched macro molecules are drawn using black colour while drug (blue triangles) and targeting moieties (green structures) are marked on the scheme. 9

Figure 1-5 Schematic representation of micelle structure. Hydrophobic part is presented with straight line while zig-zag line presents hydrophilic part of surfactant or polymer. A blue triangles present drug and green structures targeting moieties. 10

Figure 1-6 Schematic representation of NP structure. Curvy black lines present polymer matrix while drug (blue stars and red

triangles) and targeting moieties (green structures) are marked on the scheme. 11

Figure 1-7 Schematic representation of NC structure. Bright grey circle present outer polymer shell and dark grey a lipid core with various surfactants presented in black rectangles with circle or diamond endings. A drug (blue stars) and targeting moieties (green structures) are marked on the scheme. 12

Figure 1-8 Gel classification in terms of the source of the gelator, the medium it gels, constitution and the type of crosslinking. 25

Figure 1-9 Schematic representation of LMWG self-assembly. Non-covalent bonding of single molecules into hierarchical assemblies as their primary structure followed by fibre formation and their entanglement into macroscopic form of a gel. Blue-purple area presents often diverse gelator structure (polar and non-polar regions) and yellow lines present non-covalent bonding between the molecules. 28

Figure 1-10 The chemical structure of gemcitabine..... 34

Figure 1-11 Schematic representation of gemcitabine uptake, cellular and mechanism of action. 1) Internalisation of gemcitabine (dFdC) by human nucleoside transporters (hNTs). 2) Gemcitabine phosphorylation to gemcitabine monophosphate (dFdCMP) by deoxycytidine kinase (dCK); phosphorylation of dFdCMP by monophosphate pyrimidine kinase (UMP-CMP) to gemcitabine diphosphate (dFdCDP) and its subsequent phosphorylation to gemcitabine triphosphate (dFdCTP) by di phosphate pyrimidine kinase (DPK). 2) Deamination of dFdC and dFdCMP by cytidine deaminase (CDA) and deoxycytidylate deaminase (DCTD) respectively. 4) Dephosphorylation with 5’-nucleotidase (5’-NT). Mechanisms of action are indicated by blue dashed lines: 5) incorporation into DNA; 6) incorporation into RNA; 7) inactivation of

ribonucletide reductase (RNR); 8) inhibition of deoxycytidine monophosphate deaminase (DCTD); 9) inhibition of thymidylate synthase (TS). 36

Figure 2-1 Schematic representation of nanocapsule's formulation development. From left to right i) non-ionic emulsion preparation; ii) cationic nanoemulsion preparation; iii) polymeric nanocapsules formulation; iv) drug loaded polymeric nanocapsules formulation preparation. 51

Figure 2-2 Structural representation of a) hyaluronic acid and b) poly-L-glutamic acid. 54

Figure 2-3 The chemical structure of GEM C14. 54

Figure 2-4 Influence of ratio of non-ionic surfactants in oil phase on size of nanoemulsions. Total amount of surfactants is 105 mg where ratio of Tween 80 and Kolliphor HS 15 varies 1:5, 1:2, 1:1, 1:1.5, 1.5:1, 2:1, 3:1, 5:1, 24:1 w/w. Amount of Miglyol 812N oil used was 55 mg and oil:water ratio was kept constant at 1:8. Mean values (n=3) are shown, error bars represent standard deviation of the mean, where n is number of independent trials. 61

Figure 2-5 Effect of total surfactant amount on size of nanoemulsions. The total amount of surfactants was varied from 105, 90, 85, 75, 60 and 55 mg. The amount of Miglyol 812N was 55 mg with constant ratio of Tween® 80:Kolliphor® HS 15 as 1:1. The oil:water ratio was kept constant at 1:8. Mean values (n=3) are shown, error bars represent standard deviation of the mean, where n is number of independent trials. 63

Figure 2-6 Effect of the amount of oil (55 mg to 70 and 90 mg) on the size of nanoemulsions. Amount of surfactants (Tween 80 and Kolliphor HS 15) has kept constant (45 mg of each), as well as the lipid-aqueous phase ratio at 1:8. Mean values (n=3) are shown,

error bars represent standard deviation of the mean, where n is number of independent trials. 64

Figure 2-7 Effect of oils with different chemical structure on physico-chemical characteristics of nanoemulsions. Amount of Miglyol 812N and Maizine 35-1 was 70 mg while the total amount of surfactants was 90 mg and the oil:water ratio was 1:8. Mean values (n=3) are shown, error bars represent standard deviation of the mean, where n is number of independent trials. 67

Figure 2-8 Change in charge of nanoemulsions (system A and B) with the addition of cationic surfactant (CTAB) and subsequent polymer coating (HA or PGA). The amount of CTAB used was 0.25 mg. The amounts of polymers were 2 mg/mL, while the oil aqueous phase ratio was 1:8 and the final volume of 1.5 mL was used. Mean values (n=3) are shown, error bars represent standard deviation of the mean, where n is number of independent trials. 74

Figure 2-9 TEM images of A) HA 40 nm and B) HA 80 nm NCs imaged under cryo conditions. Scale bars are 200 nm. 76

Figure 2-10 Physico-chemical characteristics of elutions after HA 80 nm NCs loaded with a lipophilic dye is run through the SEC column. Mean values (n=3) are shown, error bars represent standard deviation of the mean, where n is number of independent trials.. 78

Figure 2-11 Stability of NCs upon the storage at room temperature and its influence on size of NCs. HA 80, HA 40, PGA 80 and PGA 40 nm NCs were stored in a cupboard at RT and size was evaluated weekly. Mean values (n=3) are shown, error bars represent standard deviation of the mean, where n is number of independent trials.. 81

Figure 2-12 Stability of NCs upon storage in fridge at temperature of 8 °C and its influence on size of NCs. HA 80, HA 40, PGA 80 and PGA 40 nm NCs were stored in the fridge and size was evaluated weekly.

Mean values (n=3) are shown, error bars represent standard deviation of the mean, where n is number of independent trials.. 82

Figure 2-13 Influence of the storage conditions (room or fridge temperature) on the size of NCs after 4 weeks. Size of HA 80, HA 40, PGA 80 and PGA 40 nm NCs was assessed after storage in a cupboard at RT or in the fridge at 8 °C. Mean values (n=3) are shown, error bars represent standard deviation of the mean, where n is number of independent trials. 1 way ANOVA Dunnett's multiple comparison test, size of NCs after 4w storage compared with initial size at day 0. *($p<0.05$). 84

Figure 2-14 Physico-chemical characteristics (size and PDI) of HA 80 and HA 40 nm NCs after incubation with PBS and RPMI medium. Measurements were performed on the day of the incubation at RT. Mean values (n=3) are shown, error bars represent standard deviation of the mean, where n is number of independent trials.. 85

Figure 2-15 Release of GEM C14 from HA 80 and HA 40 NCs with drug loading of 0.1%. Volume of NCs formulation used was 0.5 mL with 37.5 mL of PBS (pH=7.4). Experiments were performed at 37 °C. Mean values (n=3) are shown, error bars represent standard deviation of the mean, where n is number of independent trials.. 91

Figure 2-16 Fitting the release data indicating that GEM C14 is released from NCs by Fickian diffusion. Mean values (n=3) are shown, error bars represent standard deviation of the mean, where n is number of independent trials. 92

Figure 3-1 Example dose-response curves generated from 72 h MTT assay data for (top) HCT 116 and (bottom) MiaPaCa-2 cells treated with HA 80 nm NCs (blank or loaded with GEM C14), GEM C14 and GEM-HCl. Blank NCs do not contain drug and are diluted in the same way as loaded NCs in order to match amount of NCs. 104

Figure 3-2 Growth inhibition studies on all blank and loaded NCs compared to drugs alone on HCT 116 cell line. One-way ANOVA Tukey's multiple comparisons test ****(p<0.0001); ***(p<0.001); **(p<0.01); *(p<0.05). Mean values (n=3) are shown, error bars represent standard deviation of the mean, where n is number of independent trials. 106

Figure 3-3 Growth inhibition studies on all blank and loaded NCs compared to drugs alone on MiaPaCA-2 cell line. One-way ANOVA Tukey's multiple comparisons test ****(p<0.0001); ***(p<0.001); **(p<0.01); *(p<0.05). Mean values (n=3) are shown, error bars represent standard deviation of the mean, where n is number of independent trials. 107

Figure 3-4 Influence of NC concentration on number of colonies formed after the treatment of HCT 116 cells with the blank NCs. Blank NCs do not contain drug but they are diluted in the same way as loaded ones. 1 way ANOVA Dunnett’s multiple comparison test, NCs compared with number of colonies in control *(p<0.05); **(p<0.01). 111

Figure 3-5 Influence of GEM C14 concentration on number of colonies formed after the treatment of HCT 116 cells with the loaded NCs. Control presents number of colonies for non-treated cells. 1 way ANOVA Dunnett’s multiple comparison test, NCs compared with number of colonies in control. ***(p<0.001); **(p<0.01). 113

Figure 3-6 Influence of GEM C14 versus GEM-HCl concentration on number of colonies formed after the 24h treatment of HCT 116 cells with drug alone. 1 way ANOVA Dunnett’s multiple comparison test, NCs compared with number of colonies in control. ****(p<0.0001); ***(p<0.001). 114

Figure 3-7 Influence of NCs’ concentration on number of colonies formed after the treatment of MIA PaCa-2 cell line with the blank

NCs. 1 way ANOVA Dunnett's multiple comparison test, NCs compared with number of colonies in control. *(p<0.05); **(p<0.01). 115

Figure 3-8 Influence of GEM C14 concentration on number of colonies formed after the treatment of MIA-PaCa-2 cell line with the loaded NCs. Control presents number of colonies for non-treated cells. 1 way ANOVA Dunnett's multiple comparison test, NCs compared with number of colonies in control. *(p<0.05) ***(p<0.001); **(p<0.01). 116

Figure 3-9 Influence of GEM C14 versus GEM-HCl concentration on number of colonies formed after the 24h treatment of MIA PaCA-2 cells with drug alone. 1 way ANOVA Dunnett's multiple comparison test, NCs compared with number of colonies in control. ***(p<0.001); **(p<0.01). 117

Figure 3-10 IC_{50} values for all systems of blank, loaded NCs and non-encapsulated drug on HCT 116 cell line calculated from clonogenic assay data. ***(p<0.001); **(p<0.01). 119

Figure 3-11 IC_{50} values for all systems of blank, loaded NCs and non-encapsulated drug on MIA-PaCa-2 cell line calculated from clonogenic assay data. **(p<0.01); *(p<0.05). 120

Figure 3-12 Growth inhibitory profiles of HA 80 nm NCs blank or loaded with GEM C14 and for GEM-HCl or modified GEM on Panc-1 cell line. 124

Figure 3-13 Growth inhibitory profiles of HA 80 nm NCs blank or loaded with GEM C14 and for GEM-HCl or modified GEM on GEM resistant Panc-1 cell line. 125

Figure 3-14 Mean GI_{50} values (nM) ± s.d. of Panc-1 cell line following 72 h treatment, with HA 80 nm NCs blank or loaded with GEM C14 and for GEM-HCl or GEM C14. 127

Figure 3-15 Mean GI_{50} values (μM) ± s.d. of GEM resistant Panc-1 cell line following 72 h treatment, with HA 80 nm NCs blank or loaded with GEM C14 and for GEM-HCl or modified GEM. 1-way ANOVA: *($p<0.05$); **($p< 0.005$). 128

Figure 4-1 Photographed image of double barrel syringe..... 139

Figure 4-2 CS – HA gel produced by a double barrel syringe, CS and HA were used in concentration of 5 mg/mL. Gel is shown with an arrow. 147

Figure 4-3 Polymeric gels produced by a double barrel syringe. a) CS - NCs HA 80 nm/ HA 40 nm b) CS - NCs HA 80 nm - HA MMW; c) CS - NCs HA 40 nm - HA MMW. In case a) barrel A contains only HA NCs 80 or 40 nm NCs and barrel B contains a solution of CS; while in b and c) barrel A contains HA polymer of medium molecular weight dissolved in nanocapsules (HA NCs 80 and 40 nm), barrel B contains a solution of CS. Concentrations of both polymers are 5 mg/mL and HA 40 or HA 80 nm NCs were used at a concentration of 8% w/v. Gels were imaged in the same hour of the preparation. 149

Figure 4-4 Polymeric gels formed by magnetic stirring of chitosan in various concentrations and hyaluronic acid at concentrations of 5 mg/mL with and without NCs HA 80 nm. Concentrations of Chitosan used are: a) 5 mg/mL; b) 10 mg/mL; c) 30 mg/mL. White object marked with an arrow is a magnetic bar, while gel is wrapped around it. 150

Figure 4-5 The structural formula of N4-octanoyl-2'-deoxycytidine gelator 152

Figure 4-6 Vial inversion of N4-octanoyl-2'-deoxycytidine gelator in water. Final component concentration in % w/v is a) 0.5; b) 1; c) 1.5; d) 2; e) 2.5. 153

Figure 4-7 Rheological data for N4-octanoyl-2'-deoxycytidine gelator in water. Gelation time was ≤ 30 minutes. Testing was performed a

day after gel preparation. Amplitude sweeps (G’ and G’’) of 0.5, 1, 1.5, 2 and 2.5% w/v, at 37 °C, γ= 0.05 – 100% and ω=10 rad/s. Mean values (n=3) are shown, error bars represent standard deviation of the mean, where n is number of independent trials.154

Figure 4-8 Influence of concentration of N4-octanoyl-2’-deoxycytidine gelator on gel strength (G') in gel-water systems. Measurements were performed at 37 °C, γ= 0.05 – 100% and ω=10 rad/s and G values derived from LVE region at 0.1% strain. Mean values (n=3) are shown, error bars represent standard deviation of the mean, where n is number of independent trials. 156

Figure 4-9 Rheological data for N4-octanoyl-2’-deoxycytidine gelator in 8% w/v HA 80 nm NCs. Gelation time was ≤ 30 minutes. Test was performed a day after gel preparation. Amplitude sweeps (G’ and G’’) of 2, 2.5, 3, 3.5 and 4% w/v, at 37 °C, γ= 0.05 – 100% and ω=10 rad/s. Mean values (n=3) are shown, error bars represent standard deviation of the mean, where n is number of independent trials. 159

Figure 4-10 Influence of concentration of gelator on gel strength (G') in gel-8% w/v HA 80 nm NCs systems. Test was performed a day after gel preparation at 37 °C, γ= 0.05 – 100% and ω=10 rad/s and G values derived from LVE region at 0.1% strain. Mean values (n=3) are shown, error bars represent standard deviation of the mean, where n is the number of independent trials. 160

Figure 4-11 Rheological data for N4-octanoyl-2’-deoxycytidine gelator in 4% w/v HA 80 nm NCs. Gelation time was ≤ 30 minutes. Test was performed a day after gel preparation. Amplitude sweeps (G’ and G’’) of 1, 1.5, 2, 2.5, 3, w/v, at 37 °C, γ= 0.05 – 100% and ω=10 rad/s. Mean values (n=3) are shown, error bars represent standard deviation of the mean, where n is number of independent trials. 161

Figure 4-12 Rheological data for N4-octanoyl-2'-deoxycytidine gelator in 2% w/v HA 80 nm NCs. Gelation time was ≤ 30 minutes. Test was performed a day after gel preparation. Amplitude sweeps (G' and G'') of 1, 1.5, 2, 2.5, 3% w/v, at 37 °C, γ= 0.05 – 100% and ω=10 rad/s. Mean values (n=3) are shown, error bars represent standard deviation of the mean, where n is number of independent trials. 163

Figure 4-13 Influence of concentration of gelator on gel strength in a) gel-4% w/v HA 80 nm NCs and b) gel-2% w/v HA 80 nm NCs systems. Gelation time was ≤ 30 minutes. Test was performed a day after gel preparation at 37 °C, γ= 0.05 – 100% and ω=10 rad/s and G values derived from LVE region at 0.1% strain. Mean values (n=3) are shown, error bars represent standard deviation of the mean, where n is number of independent trials. 164

Figure 4-14 Influence of concentration of nanocapsules on gel strength (G') in gel-HA 80 nm NCs systems, where gelator concentration is constant at 2% w/v, while concentration of nanocapsules varies from 2, 4 and 8% w/v. Gelation time was ≤ 30 minutes. Test was performed a day after gel preparation at 37 °C, γ= 0.05 – 100% and ω=10 rad/s. Mean values (n=3) are shown, error bars represent standard deviation of the mean, where n is number of independent trials..... 166

Figure 4-15 Vial inversion of N4-octanoyl-2'-deoxycytidine gelator in presence of NCs: a) PGA 80 nm; b) PGA 40 nm; c) HA 40 nm. Final gelator component concentration in all systems is 2 % w/v; and amount of NCs used is 4 % w/v. Gelation time was ≤ 30 minutes. 167

Figure 4-16 Effect of different NCs on gel strength. NCs of 40 or 80 nm in size coated with either hyaluronic acid or polyglutamic acid were used in these experiments. Concentration of gelator and NCs are constant, where N4-octanoyl-2'-deoxycytidine gelator a

concentration was 2% w/v with 4% w/v NCs. Amplitude sweeps (G' and G'') at 37 °C, γ= 0.05 – 100% and ω=10 rad/s. Mean values (n=2) are shown where n is a number of independent trials. Gelation time was ≤ 30 minutes. 168

Figure 4-17 Size (nm) of HA 40 or HA 80 nm NCs at 60°C with and without gelator. Black bars present size of nanocapsules before heating or mixing with gelator at room temperature. Black bars with grey lines present size of nanocapsules exposed to heat at 60-70°C without presence of gelator. Grey bars present size of the nanocapsules-gel system together, when heated/dissolved at 60-70°C. Mean values (n=3) are shown, error bars represent standard deviation of the mean, where n is number of independent trials. 169

Figure 4-18 TEM images of N4-octanoyl-2'-deoxycytidinegelator in a) water 2% w/v; scale bar is 500 nm; b) HA 80 nm NCs (2% w/v gelator – 8% w/v NCs); scale bar is 1000 nm. Samples were vacuum dried before imaging. c) and d) cryo-TEM imaging of 2% w/v gelator – 8% w/v HA 80 nm NCs. 171

Figure 4-19 Encapsulated NR separation from free dye by SEC columns using PBS buffer as eluent. b) Release of NR from HA 80 nm NCs over 72h, where 1 mL of NCs was incubated with 4 mL of PBS. Mean values (n=2) are shown where n is number of independent trials. 175

Figure 4-20 2% (w/v) gel - 8% HA 80 NCs system gelled release medium after 24h incubation in water bath (37 °C). PBS, pH=7.4, was used as a release medium. Gels were prepared in 0.5 mL of NCs and toped up with a) 1.25; b) 2.5; c) 5 mL of PBS. 176

Figure 4-21 Cumulative release of Nile Red/NCs from gel-NCs system at 37°C in PBS medium, pH=7.4. Concentration of gelator in all systems is 2% w/v and NCs used in this experiment are: HA 80 nm NCs of 4 and 8% w/v and HA 40 nm NCs in concentration of 4% w/v.

Gels were prepared with 0.5 mL volume of NCs and gel was incubated with 12.5 mL of PBS. Mean values (n=3) are shown, error bars represent standard deviation of the mean, where n is number of independent trials. 177

Figure 4-22 Schematical representation of gelator participation in gel-NCs composite. Apart from gelator self-assembly into fibers, it can hypothetically participate at oil-water interface due to its amphiphilic structure. Additionally, connection between gelator and polymer coating (HA) of NCs is presented in red rectangle through hydrogen bonds. Chemical groups with potential for hydrogen bonding are presented in red. 178

Figure 4-23 Size (nm) and PDI of the sample taken from the release medium over 72h of the experiment. a) 2% gel- 4% HA 80 nm system and b) 2% gel- 4% HA 40 nm system. Mean values (n=3) are shown, error bars represent standard deviation of the mean, where n is number of independent trials. 179

Figure 4-24 a) Encapsulated porphyrin separation from free dye by SEC columns using PBS buffer as eluent. b) Release of porphyrin from HA 80 nm NCs and gel system over 24 h, where formulation to PBS ratio is 1:25. Mean values (n=3) are shown, error bars represent standard deviation of the mean, where n is number of independent trials. 181

Figure 4-25 Gel formulations dispensed through the syringe (top picture) using needle (25G) into the vial (bottom picture). Formulation used are: a) 0.5% (w/v) gelator-water; b) 3.5% (w/v) gelator – 8% NCs; c) 3% (w/v) gelator – 4% NCS; d) 3% (w/v) gelator – 2% NCs..... 183

Figure 4-26 Images of 2% w/v gelator in a) 4% w/v HA 80 nm NCs or b) 8% w/v HA 80 nm NCs. Gels formed after dissolution at 60°C were stored in the syringe for 1 hour and dispensed into a vial or in

a chicken muscle tissue. Images were taken 5-10 minutes after dispensing gels in into a vial/chicken tissue. 184

List of Tables

Table 1-1 Examples of marketed nanomedicines for cancer 14

Table 1-2 Examples of cancer nanomedicines undergoing clinical trials 17

Table 1-3 Examples of local cancer drug delivery platforms 21

Table 1-4 Examples of gel-NPs for localised drug delivery 31

Table 2-1 Influence of surfactants amount and their ratio as well as oil amount on size of nanoemulsions. The oil:water ratio was kept constant at 1:8. Mean values (n=3) are shown, error bars represent standard deviation of the mean, where n is number of independent trials. 59

Table 2-2 Composition and physico-chemical characteristics of 2 nanoemulsion systems that are chosen from wide range of sizes for progression. Amount of surfactants and oil is provided below, while the oil:water ratio used was 1:8. Mean values (n=3) are shown, error bars represent standard deviation of the mean, where n is number of independent trials. 66

Table 2-3 Influence of Tween® 80: Kolliphor® HS 15 ratio on size of nanoemulsions when Maizine® 35-1 was used as the oil. The total amount of surfactants was 90 mg and oil amount 70 mg while the oil:water ratio was kept constant at 1:8. The number of independent trials was n=2. 69

Table 2-4 Physicochemical characteristics of polymeric NCs and their primary cationic nanoemulsions. First two rows present non-ionic

nanoemulsions prepared as shown in Table 2-2 where the primary nanoemulsion (A) is 60-70 nm in size, while primary nanoemulsions (B) are smaller in size approximately between 30-40 nm. Cationic surfactant, CTAB, is added in order to get cationic nanoemulsions, followed by addition of polymer coating (hyaluronic acid or poly-L-glutamic acid) to form polymeric NCs. All amounts are expressed in mg per formulation, where final formulation volume is 1.5 mL.... 72

Table 2-5 Characterisation of final systems that are going to be used in future experiments. The compositions of NCs are the ones highlighted in orange from Table 2-4. 75

Table 2-6 Physico-chemical characteristics of NCs loaded with either DCX or GEM C14. HA 80, HA 40, PGA 80 and PGA 40 nm NCs loaded with DCX or GEM C14 (0.1% w/w). Mean values (n=3) are shown, error bars represent standard deviation of the mean, where n is number of independent trials. 79

Table 2-7 Conditions of in vitro drug release evaluation from nanocarriers that are described in the literature. Abbreviations: PTX - paclitaxel; ACSF - artificial cerebrospinal fluid; BSA – Bovine Serum Albumin; OR – oil red; DW – deionised water; SC – subcutaneous; *several formulations variations were tested; i.c. – intracavitary; DOX – doxorubicin; DCX – docetaxel; n.a.- in some papers the ratio of formulation to release medium is not provided. 88

Table 2-8 Release exponent (n) and correlation coefficient (R) by fitting the GEM C14 release profiles for HA 40 and HA 80 nm NCs. 92

Table 3-1 Mean GI_{50} values (nM) ± s.d. of tumour cell lines following 72 h treatment, with all types of blank or GEM C14 loaded NCs and with GEM-HCl or modified GEM alone, generated by MTT cell viability assay. 105

Table 3-2 IC_{50} values (nM) of all blank and loaded NCs on colorectal and pancreatic cancer cell line. 118

Table 3-3 Mean GI_{50} values (nM) ± s.d. in tumour cell lines following 72 h treatment, with HA 80 nm NCs blank or loaded with GEM C14 and for GEM-HCl or modified GEM, generated by MTT cell viability assay. Resistance factor (Rf) is ratio of GI_{50} values of the same system compared between sensitive and resistant cell lines. 126

Table 4-1 Size (nm) and polydispersity (PDI) index of the HA 80 nm NCs after encapsulation of Nile Red. Mean values (n=3±SD), where n is a number of independent trials, are shown. 174

1 Introduction

The goal of this thesis is the development of a hydrogel and drug-loaded polymeric nanocapsules (NCs) for localised delivery in cancer therapy. Hence, in this introductory chapter the general characteristics of cancer and its treatment are briefly described with further focus on nanomedicines in cancer therapy. Also, platforms for local delivery that are commercially available or under research are reported including gel-particle formulations. Furthermore, a cancer that could potentially benefit from the proposed platform is pancreatic cancer and therefore gemcitabine as a first line treatment for this cancer was incorporated as a lipophilic prodrug in the NCs. Hence gemcitabine is reviewed in terms of mechanism of action and resistance as well as novel prodrugs.

1.1 Cancer – the disease

Cancer is comprised of 200 different diseases with diverse causes and symptoms. Despite the variety of different cancers, a general feature is that their formation is due to gene mutations which result in the 6 hallmarks of cancer – (1) sustaining proliferative signalling, (2) evading growth suppressors, (3) resisting cell death, (4) enabling replicative immortality, (5) inducing angiogenesis, and (6) activating invasion and metastasis as discussed in detail by Hanahan and Weinberg[1]. The most important feature is sustaining proliferative signalling which means the cells proliferate in an uncontrolled manner, which for some cancers can lead to the formation of a solid tumour mass.

1.1.1 **Cancer statistics**

According to cancer research UK approximately 357,000 people were diagnosed with cancer in 2014 in the UK, which is around 980 people every day and one person in every two minutes[2]. 163,444 of this 350 thousand died from cancer in the UK in that same year. Whilst globally there were 14.1 million new cases and 8.2 million deaths in 2012.

Lung, liver, stomach and bowel cancers have been the four most common causes of cancer death since 1975 and accounting for nearly half of all cancer deaths today. Generally considered as a disease of old age, 50% of all cancer cases in the UK each year are diagnosed in people aged 70 and over (2012-2014). 50% of people diagnosed with cancer in England and Wales survive their disease for ten years or more (2010-11). Cancer survival is improving and has doubled in the last 40 years in the UK. In the early 1970's the median survival time after diagnosis was one year, by 2007 it was six years and by 2011 it was ten years.

Also, the Macmillan cancer support organisation have reported similar survival rates[3]. The number of people who have survived five or more years since diagnosis has increased by over 260,000 (or 21%) in the five years to 2015. The number of people living with cancer in the UK is increasing by 3.2% every year. Due to advances in cancer treatment as well as a greater focus on earlier diagnosis, cancer prevalence is set to continue to rise which could bring four million people living with cancer by 2030 (Figure 1-1).

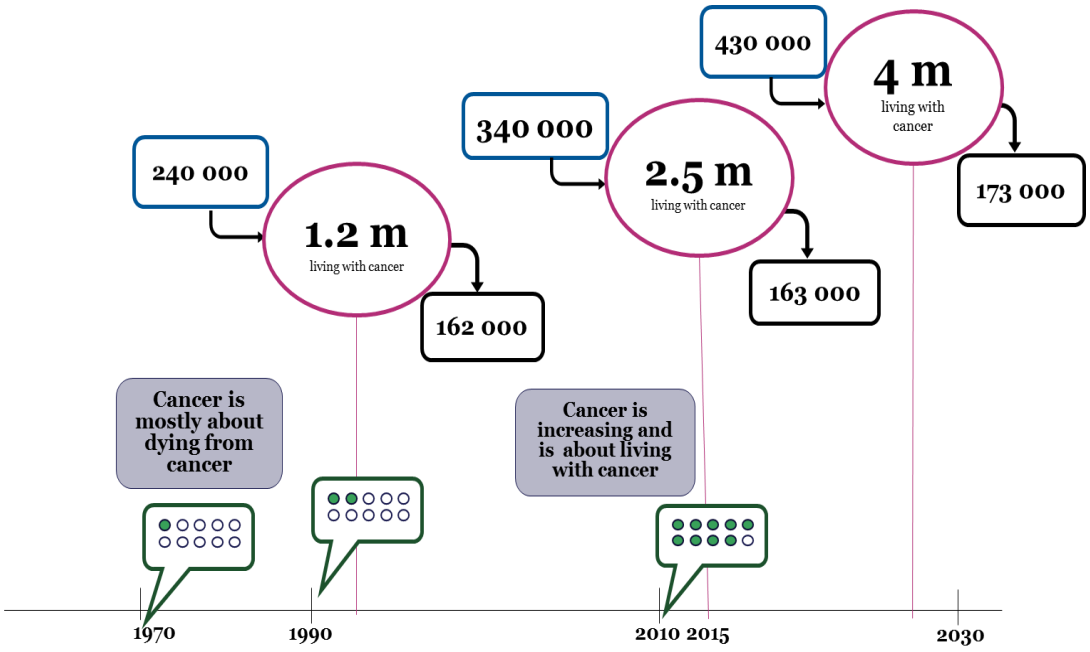


Figure 1-1 Cancer progress and prognosis adapted from Macmillan research on cancer prevalence in UK. Number of people getting cancer for the first time is presented in blue, while number of people dying is shown in black rectangles. Purple circles represent number of people living with cancer, while green rectangles indicate how long people live on average. Macmillan estimations are based on data from Office for National Statistics. http://www.macmillan.org.uk/documents/aboutus/research/thechangingstoryofcancer.pdf

1.1.2 **Treatment of cancer**

Cancer patients, due to a complexity of the disease, suffer from numerous symptoms depending on the type of tumour, its location and the stage it has reached. Therefore, there are various treatment options which include surgery, radiation, chemotherapy, hormonal therapy, immunotherapy, gene therapy and often their combinations.

Surgery is one of the oldest techniques and is used to remove whole tumours or parts of the tumour when there is a chance of damaging surrounding tissue. In some cases, surgery is just performed to ease symptoms in cancers that otherwise cause pressure on vital organs which can be painful for patients and result in poor functioning of

other organs. Surgery can be done as an open incision or laparoscopy. There are ways of performing surgery that do not involve incisions and they include: cryosurgery, lasers, hyperthermia, and photodynamic therapy[4].

The surgical procedure is often accompanied with radiotherapy or chemotherapy. Radiotherapy uses high-energy radiation such as X-rays, gamma rays, and charged particles that kill cancer cells[5,6]. Radiotherapy is used for eliminating tumours, preventing recurrence or shrinking tumours before surgery.

Chemotherapy uses drugs that stop the growth of cancer cells or kills them. It is widely used for many cancer types in order to treat or prevent recurrence. As the work in the thesis is relevant to the improvement of chemotherapeutics, a detailed review on chemotherapeutic marketed drug delivery platforms and ones that are under research is provided in this chapter.

1.2 Considerations impacting decisions regarding injection or resection

1.2.1 Inoperable and late stage cancers

Not all cancers can be removed by surgery which is commonly related to late and advanced stages of the disease. Several reasons for not choosing surgery include:

1. Late stage metastasised cancers that have spread to distant sites and/or are micro-metastases and difficult to detect;
2. Sensitive cancer location such as in spinal cord, deep in the brain tissues or in/near important vessels (e.g. arteries);
3. Patients are not fit enough to withstand surgery.

1.2.1.1 *Metastasised cancers*

Small cell lung cancer (SCLC) presents as small lung tumours in multiple locations which are often spread to the brain. Therefore, its elimination would require many mini surgeries increasing the risk for the patient with negligible improvement. Additionally, resection in brain would mean severing the connection between brain and the rest of the body. In these cases, radiotherapy and targeted chemotherapy are treatment options[7,8]. Similarly, with bowel/colorectal cancer when diagnosed will have already metastasised to the liver and spread to multiple sites in between such as the peritoneal cavity or then to bone. Sometimes chemotherapy serves to shrink a tumour and to allow resection, but even when this is possible recurrence rates are high[9]. Metastasis and poor prognosis are as well reported for advanced oesophageal cancer due to a prior lack of symptoms. Around 7 in 10 oesophageal cancer cases are diagnosed at a late stage in England (2014) and since the early 1970s, its mortality rates have increased by almost a half (46%) in the UK. Oesophageal cancer also spreads to other organs even in the early stages of the disease, which often makes it inoperable[10].

In these instances, local therapy cannot guaranty the appropriate efficacy. It was reported for polymeric implants in brain tumours to be mainly 1-2 mm from the site of implementation with the longest distance of 17 mm achieved after 72 hours[11]. Hence, in case of metastised tumours, formulation that will also reach lymphatics is needed.

1.2.1.2 *Cancer location*

A sensitive cancer location is another reason for inoperability. In these cases, cancer cells infiltrate an important blood vessel or are very close to it in which makes resection impossible due to

unstoppable mass bleeding that would occur during the resection. One example of this is pancreatic cancer, which can easily invade the abdominal aorta[12]. Pancreatic cancer is the 11th most common cancer in the UK with 9600 new cases and 8817 deaths in 2014[2]. In the 1970s, 1% of people diagnosed with pancreatic cancer survived their disease beyond ten years and that percentage is the same today. Around 8 in 10 pancreatic cancer cases are diagnosed at a late stage and inoperable therefore systemic chemotherapy and palliative care are currently the only treatment options. Since gemcitabine is first line treatment for pancreatic cancer, we have chosen it as a model drug for the gel-nanocapsule formulation developed in this project, therefore its characteristics and role in cancer treatment are described below.

1.3 Nanomedicines for cancer

Chemotherapy is the main treatment for tumour recurrence and for the late stage tumours. However, it is difficult for the chemotherapeutic drugs to reach the tumour tissues selectively which causes undesirable side effects in normal healthy tissues during therapy. Development of nanomedicines and their enormous progress in last 50 years has focused on reducing the toxic side effects of chemotherapy.

A nanomedicine is a complex nanometre-scale size system consisting of at least two components, of which one is the active drug. The nanomedicine has a special function related to the diagnosis, treatment, prevention of the disease or quality of life improvement, using molecular tools and molecular knowledge of the human body[13]. For this project, nanomedicines developed for drug delivery in cancer are of interest.

It all started with the concept of the "magic bullet" where Paul Erlich proposed that a drug that could be directed into the cells of interest circumventing healthy tissue[14]. Indeed, the first nanocarrier was a liposomal lamellar structure[15] developed in 1964 and 15 years later was used for drug delivery[16] paving the way for various nanocarriers for targeted cancer drug delivery. Specifically, this was followed by further development of nanocarriers for drug delivery such as polymer conjugates, micelles, nanoemulsions, nanocapsules, nanoparticles and dendrimers. Anticancer drugs are often highly metabolised to more polar conjugates and hence are then rapidly excreted by the kidney giving short-lifes. However, nanocarriers have afforded longer drug half-lifes due to prolonged drug-nanocarrier circulation times; followed by targeted intracellular delivery and/or tumour targeting. Also in some instances nanocarriers have increased drug stability during storage[17,18].

1.3.1 **Liposomes**

Liposomes are spherical carriers composed of at least one lipid bilayer ranging in size from approximately 50 nm to a few μm. Since they are formed from amphiphilic phospholipids, they have the ability to incorporate both hydrophilic and hydrophobic molecules[19,20]. Over the time, liposomal formulations have increased in complexity. For example PEGylated phospholipids have been used to create liposomes with prolonged circulation times[21] and/or surface modified with different ligands (peptides, proteins (including antibodies), or small molecules) that actively target overexpressed tumour receptors[22,23]. Since it was the first nanocarrier to be developed, it is the most extensively explored system which has resulted in many commercial formulations or progression to clinical trials (see section Nanocarriers on the market).

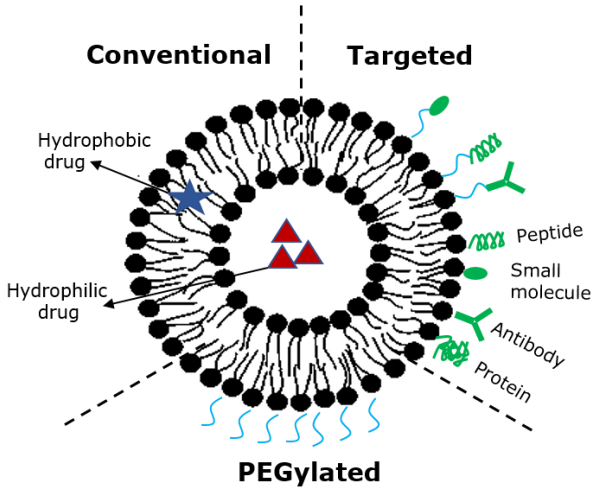


Figure 1-2 Schematic representation of liposomal structure. Black circle symbols with two tails present a lipid bilayer while blue curvy lines attached to it are representation of PEG molecules. Encapsulated drugs (red triangles and blue star) and targeting moieties in green are marked on the scheme.

1.3.2 **Polymer conjugates**

Polymer conjugates are covalently bonded drugs to a polymer backbone. The conjugation is designed to target and release drug at the tumour site. The most explored polymers are polyglutamate[24], HPMA[25] and PEG[26,27] which sometimes are additionally decorated with targeting ligands such as antibodies, sugars or peptides[28].

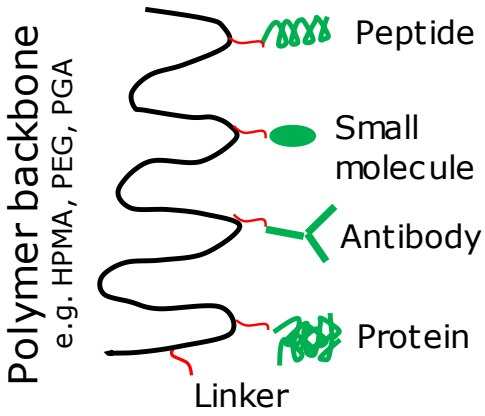


Figure 1-3 Schematic representation of polymer conjugates. Black curvy line symbolises polymer to which drug (small molecule) and targeting moieties in green are marked on the scheme.

1.3.3 **Dendrimers**

Dendrimers are macromolecular well defined "tree-like" structures where branches are symmetrically growing from the core with a precise number of groups at each step. An anticancer drug can be covalently attached to the dendrimer repeating units or encapsulated by non-covalent interactions.

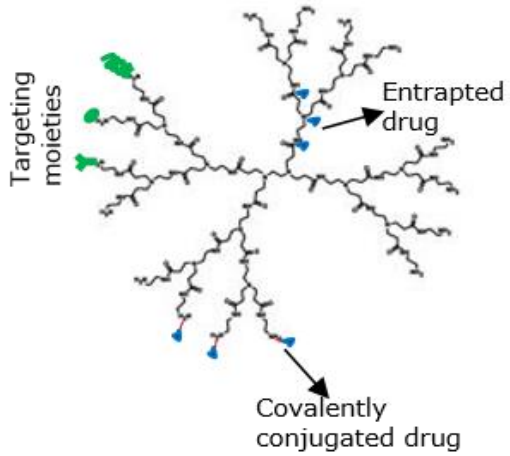


Figure 1-4 Schematic representation of dendrimer structure. Branched macro molecules are drawn using black colour while drug (blue triangles) and targeting moieties (green structures) are marked on the scheme.

Similar to previously described systems, ligands can be attached to achieve active targeting. Despite high density, monodispersity and a well-defined number of ligands on the surface, dendrimers, due to expensive synthesis and sometimes toxicity, they have not been progressed to a commercial formulation for delivering anticancer drugs[29].

1.3.4 **Surfactant and polymeric micelles**

The micelles are supramolecular assemblies of surfactant molecules in an aqueous phase where hydrophilic "heads" are located towards the solvent and hydrophobic "tails" are oriented towards the centre due to the solvophobic forces[30]. Polymeric micelles have similar structures where amphiphilic co-polymers that contain both hydrophobic and hydrophilic blocks are involved in micelle formation.

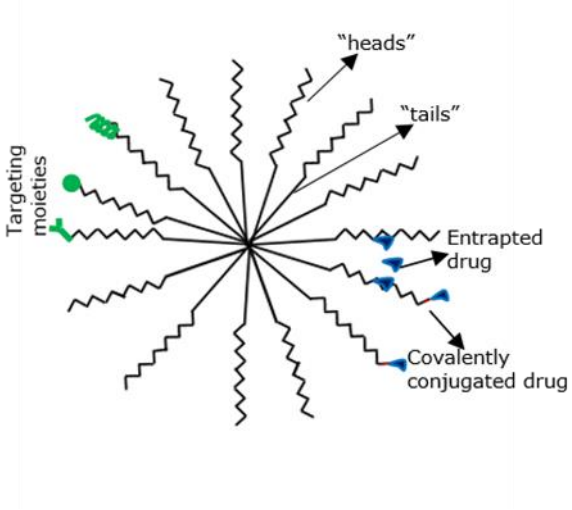


Figure 1-5 Schematic representation of micelle structure. Hydrophobic part is presented with straight line while zig-zag line presents hydrophilic part of surfactant or polymer. A blue triangles present drug and green structures targeting moieties.

The most investigated polymers are PEG, poly(propylene oxide) (PPO), their triblock copolymer (Pluronics), PEG with poly(L-lactide) (PLA), poly-ε-caprolactone (PCL) and PEG conjugated to lipids instead to another polymer[31]. A drug can be chemically conjugated, physically encapsulated or both methods can be used in the same micellar formulation[32]. Although demicellisation in biological media is often reported, these nanocarriers have progressed to the clinical trials.

1.3.5 **Nanoparticles (NPs)**

Nanoparticles are solid matrix systems made of polymer. A drug can be initially conjugated to the polymer or encapsulated into the matrix later.

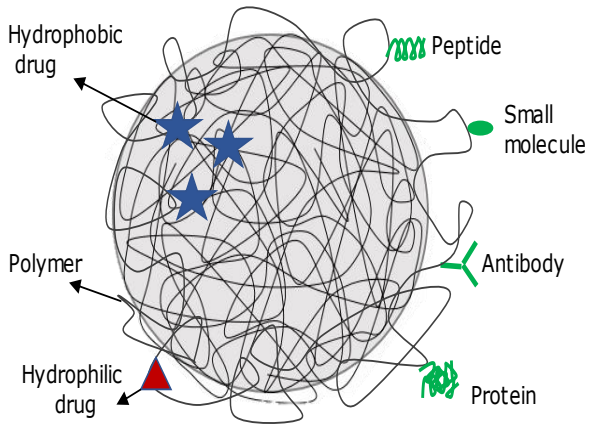


Figure 1-6 Schematic representation of NP structure. Curvy black lines present polymer matrix while drug (blue stars and red triangles) and targeting moieties (green structures) are marked on the scheme.

Various natural, semisynthetic and synthetic polymers such as: dextran, hyaluronic acid, chitosan, polyhydroxyalkanoates (linear polyesters), poly-(lactic-co-glycolic acid) (PLGA) and a group of cyclical saccharides (cyclodextrins) have been intensively investigated for more than 30 years[33–35]. Cyclodextrins have a hydrophobic core suitable for drug encapsulation, and hydrophilic outer surface for the association of hydrophilic compounds, ions, proteins[36]. To introduce targeting properties various ligands (peptides, proteins/antibodies, small molecules) are associated on the surface of the nanoparticles to target human epidermal growth factor (EGF), folate, integrins and amongst others, kinase receptors[37].

1.3.6 **Nanocapsules (NCs)**

NCs have a lipid core stabilised by a mixture of surfactants to form a nanoemulsion. Upon addition of polymers to the nanoemulsion, they form an outer polymeric shell to create nanocapsules. When the polymer shell is simply composed of surfactants and PEG, the NCs are named as lipid NCs, in the rest of the cases they are called NCs or polymeric NCs[38,39].

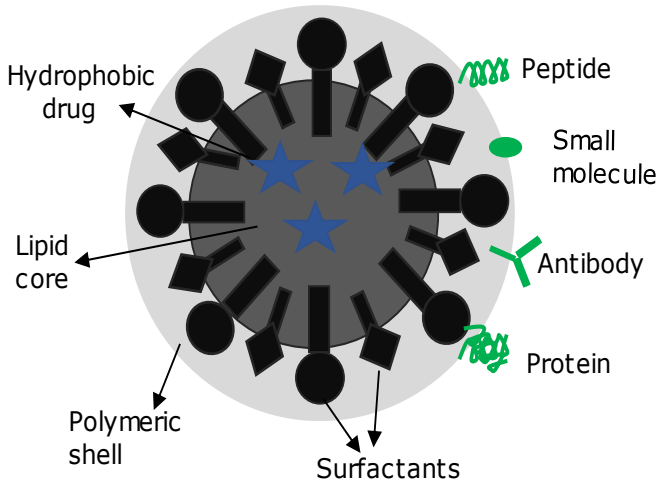


Figure 1-7 Schematic representation of NC structure. Bright grey circle present outer polymer shell and dark grey a lipid core with various surfactants presented in black rectangles with circle or diamond endings. A drug (blue stars) and targeting moieties (green structures) are marked on the scheme.

Since NCs are basically nanoemulsions with a polymer coating , their methods of preparation are similar[40]. The presence of polymer brings stability in media and influences drug release[17]. NCs with different polymer coatings, sizes and targeting properties are further described in Chapter 2. Since NCs have only recently been developed in comparison to other formulations, there are as yet no formulations that have translated to a commercial formulation. However, a few have progressed to clinical studies.

1.3.7 **Nanocarriers on the market**

In the last two decades, over 10 cancer nanomedicine formulations have been commercialised (Table 1-1). The first approved nanoformulation for cancer treatment was Doxil®, a liposomal formulation of Doxorubicin (DOX). Firstly, DOX was associated to a lipid bilayer and later enhancements involved drug loading in the intraliposomal aqueous phase and coating with polyethylene glycol (PEG) which improved safety and efficacy resulting in Food and Drug Administration (FDA) approval of Doxil® in 1995. Doxil® has shown to be well tolerated in humans and exhibited reduced side effects especially drastically lower cardiotoxcity[41]. Another liposomal formulation of DOX - Myocet® is approved in Europe for metastatic breast cancer after showing an improved therapeutic index, fewer side effects and the same efficacy as DOX alone[42]. Additionally, daunorubicin citrate liposome formulation - DaunoXome® was approved as a first-line cytotoxic therapy for the treatment of advanced, HIV-associated Kaposi's sarcoma as it was shown to be as effective as the three-drug regimen (adriamycin, bleomycin and vincristine), but with a reduced incidence of side effects[43]. Other nanomedicines include Marquibo® - vincristine sulphate liposomal injection for treatment of leukaemia[44] and Onyvide® - PEGylated liposome of irinotecan approved for post-gemcitabine metastatic pancreatic cancer treatment[45]. Mifamurtide (Mepact®), an adjuvant liposomal formulation containing muramyl tripeptide phosphatidyl ethanolamine, activates macrophages, monocytes and other immune cells of the reticuloendothelial system increasing production of cytokines and chemokines. These activated cells then attack the cancer cells[46]. This formulation is approved in Europe, Mexico, South Korea, Switzerland, and Israel for non-metastatic osteosarcoma[47].

Table 1-1 Examples of marketed nanomedicines for cancer

Generic name	***Nano-technology platform***	***Active ingredient***	***Cancer type***	***Status***	***Ref.***
Doxil	PEGylated Liposome	DOX	HIV-related Kaposi sarcoma, ovarian cancer, multiple myeloma	Approved by FDA	[41]
Myocet	Liposome	DOX	Metastatic breast cancer	Approved in Europe	[42]
DaunoXome	Liposome	daunorubicin	HIV-associated Kaposi's sarcoma	Approved by FDA	[43]
Marquibo	Liposome	vincristine	Leukaemia	Approved by FDA	[44]
Onyvide	PEGylated liposome	irinotecan	Post-gemcitabine metastatic pancreatic cancer	Approved by FDA	[45]
Mifamurtide (Mepact)	Liposome	Muramyl tripeptide phosphatidyl ethanolamine	Nonmetastatic osteosarcoma	Approved in Europe	[47]
Nab-paclitaxel (Abraxane)	NPs	PCX	Breast, lung and pancreatic cancer	Approved by FDA	[48]
Genexol-PM	Polymeric micelles	PCX	Breast and NCSLS cancer	Approved in Korea, India, Philippine, Vietnam	[49]
NanoTherm	Iron Oxide NPs	NA	Glioblastoma	Approved in Europe	[50]
Oncaspar	PEG-conjugate	L-asparagine amidohydrolase	Lymphoblastic leukaemia	Approved in Europe	[51]

SMANCS (Zinostatin)	Polymer-conjugate	neocarzinostatin	Hepatocellular carcinoma	Approved in Japan	[52]

The first non-liposomal formulation approved for cancer treatment was Abraxane® that is composed of paclitaxel (PCX) loaded albumin nanoparticles (NPs). Abraxane® significantly improved overall survival (OS) when used with gemcitabine in metastatic pancreatic cancer compared to patients treated with gemcitabine only. It still resulted in at least 20% incidence of common adverse effects. Similarly, significant OS was shown when Abraxane® was used in combination with carboplatin for the initial treatment of patients with locally advanced or metastatic non-small cell lung cancer (NSCLC). However, some serious adverse effects (anaemia and thrombocytopenia) were noted in both groups. Better tolerability of Abraxane® compared to patients who received only paclitaxel was achieved in the treatment of breast cancer[48]. An example of micellar formulation that have also progressed to the market is Genexol-PM. It is a polymeric micelle formulation of paclitaxel and in combination with gemcitabine reached market in Europe and Korea for patients with NSCL cancer[49,53].

There are also a few commercialised polymer-conjugate formulations. For instance, Oncaspar® is PEG-L-asparaginase formulation marketed for acute lymphoblastic leukaemia[51] or Zinostatin, a conjugate of styrene-maleic acid (SMA) and an antitumour protein neocarzinostatin (NCS) SMANCS, approved for hepatocellular carcinoma in Japan[52].

In 2010, iron-oxide NPs (NanoTherm®) received European regulatory approval for treatment of glioblastoma by hyperthermia[50]. These small (15 nm) particles agglomerate following direct injection into the tumour and activation by a magnetic field produces heat. Depending on the temperature reached and length

of treatment, the tumour cells are either directly destroyed or sensitised before chemotherapy or radiation.

1.3.7.1 *Nanoplatforms in clinical trials*

Chemotherapeutical nanoplatforms continue to develop and there are many undergoing clinical trials (Table 1-2). Again, liposomal formulations are more numerous than others. These formulations are improved as they contain additional moieties with potential targeting characteristics. For instance, MM-302 are HER-2 targeting DOX-loaded liposomes designed for treatment of HER-2 positive breast cancer. HER-2 is human epidermal growth factor receptor which normally controls the growth of healthy breast cells. However, its overexpression is an indication of faster tumour growth that is more likely to spread and reoccur compared to HER2-negative breast cancers. DOX-loaded liposomes with an anti-HER2 monoclonal antibody (MAb) (MM 302) for targeting overexpressed HER-2 receptors in breast cancer treatment were progressed to Phase II/III of clinical trials[54]. Although there was no new or unexpected side effects, MM-302 had a shorter than expected median progression free survival which resulted in trial termination[55]. Also, MBP-426, an oxaliplatin encapsulated transferrin conjugated N-glutaryl phosphatidylethanolamine (NGPE) liposome, demonstrated direct drug binding to Tf receptor (TfR) and reached phase II clinical trials for gastric, oesophageal and gastro-oesophageal adenocarcinoma[56].

An example of polymeric micellar formulation of PCX is NK-105 that reached phase III clinical trials for metastatic or recurrent breast cancer (trial ID: NCT01644890)[57].

From dendrimer formulations, currently there is DCX-dendrimer conjugate[58] (DEP™ docetaxel) that is progressing through a phase I clinical trial in Australia for patients with advanced solid tumours (trial ID ACTRN12614000171617).

Table 1-2 Examples of cancer nanomedicines undergoing clinical trials

Name	***Nanotechnology platform***	***Active ingredient***	***Cancer type***	***Status***	***Ref.***
MM-302	HER-2 targeting liposome	DOX	HER-2 positive breast cancer	Phase II/III	[54]
MBP-426	TfR- targeting liposome	Oxaliplatin	Gastric, oesophageal and gastro-oesophageal adenocarcinoma	Phase II	[56]
NK-105	Polymeric micelle	PCX	Metastatic or recurrent breast cancer	Phase III	[59]
DEP-docetaxel	Dendrimer	DCX	Advanced solid tumours	Phase I	[58]
SGT53	TfR-targeting liposome	Plasmid encoding normal human wild-type p53 DNA	Metastatic pancreatic cancer	Phase II	[60]
Atu027	Liposome	siRNA against protein kinase N3	Metastatic pancreatic cancer	Phase I/II	[61]
TKM-080301	Lipid NPs	siRNA against PLK1	Neuroendocrine tumours, adrenocortical carcinoma and advanced hepatocellular carcinoma	Phase I/II	[62]
ALN-VSP02	Lipid NPs	siRNAs against KSP and VEGFA	Solid tumours	Phase I	[63]

Furthermore, gene therapy in association with nanocarriers is making remarkable progress in cancer treatment with more than 10 formulations in clinical trials. For instance, SGT53, a liposomal formulation decorated with antibody fragment and loaded with a

plasmid containing the normal human p53 gene was designed for metastatic pancreatic cancer. P53 is cellular tumour antigen that functions as a tumour suppressor and it is often found mutated in cancer, hence delivery of wild type P53 should restore tumour suppressor function and control tumour growth. Furthermore, Phase I clinical trials showed the accumulation of SGT53 in metastatic lesions but not in normal tissue[60]. Another class of molecules widely used in cancer therapy are small interfering RNA molecules. Some formulations that have reached clinical trials are Atu027, a liposomal formulation of siRNA against protein kinase N3[61], TKM-080301 and ALN-VSP02 that are lipid NPs against polo-like kinase 1 (PLK1)[62] or vascular endothelial growth factor (VEGF)-A and kinesin spindle protein (KSP)[63].

Recently, cancer care has improved; this is not just that treatment improved but also diagnosis, prevention and palliative care. However, development of nanomedicines has probably contributed to the increased number of years that patients live after the diagnosis (Figure 1-1). In last few decades many formulations were marketed and used clinically. However, from almost 3 million publications in the cancer category (search term was cancer excluding reviews) between 1985 and 2005, only 3% of these are related to clinical trials[64]. From the formulations that are already on the market, we saw that usually, they are as effective as current treatments but with fewer side effects. However, these side effects do not completely disappear. Therefore, there is a need for constant improvement both in identifying potential targets in cancer and developing platforms for their targeting.

1.4 Systemic vs. local chemotherapy

The potential of local cancer delivery instead of systemic therapy has been recognised by many groups and there is a growing number of

reports on the superiority of intratumoural (i.t.) treatments compared to intravenous (i.v.) administration. For instance, Lammers *et al.* designed poly(HPMA)–Gly-Phe-Leu-Gly-DOX conjugate and evaluated its localisation after i.v. or i.t. application, as well as the efficacy, compared to free DOX in rat prostate carcinoma model (R3327-AT1). After i.t. administration DOX-polymer conjugate was detected only at the site of administration for 24 h, whilst 4 h after i.v. administration it was detected in high doses in heart/lungs, spleen and liver. Furthermore, the i.t. administered DOX-conjugate was significantly more effective than DOX-conjugate (i.v.) or free DOX administered by i.v. or i.t routes[65]. Another formulation containing DOX in supramolecular gel showed a 20% reduction in the tumour volume and approximately a 60% decrease in the tumour weight as compared to i.v. administration of drug in solution, in an early stage colon cancer mouse model. The same formulation was tested in a breast tumour model and showed a 40% reduction in tumour volume relatively to i.v. injection of DOX[66]. Similarly, a Taxol® derivative (Taxol-succinic acid-glutathione) formed a supramolecular gel and reduced tumour growth by half in breast tumour bearing mice upon i.t. injection compared to i.v. administration of equivalent concentration of Taxol® with final relative tumour volumes of 432 and 865% respectively. Additionally, a fatal dose of Taxol® in the hydrogels was at least 7.5 times higher than that of Taxol®[67].

The work of Yang *et al.* evaluated the influence of i.t., intraperitoneal (i.p.) and s.c. administration of DCX loaded mixed micelles gel (MMG) in the ovarian SKOV-3 cancer tumour model in mice. Although not significantly different, MMG administered i.t. resulted in the lowest tumour growth rate when compared with i.p. and s.c. administration of the same formulation. Also, all three groups (i.t., i.p. and s.c.) showed a significant reduction in tumour volume as compared to the untreated control. Additionally, after s.c injection,

MMG was compared with the gel alone i.e does not contain micelles and showed a significantly lower tumour growth rate[68].

An example of local delivery of gel loaded monoclonal antibody formulation for colorectal cancer was designed by Lee *at al.* The monoclonal antibody, Avastin®, was loaded in a vitamin D –PEG triblock gel and its efficacy was compared with Avastin® solution in two tumour models. In the first, subcutaneous colorectal (HCT 116) murine model, a subcutaneously administered gel formulation significantly reduced the tumour growth rate relative to i.p. and i.v. administration of the Avastin® solution. Evaluation in another colorectal cancer peritoneal metastatic tumour model showed that s.c. injection of the hydrogel formulation had higher survival rates than i.v. injection of Avastin® solution, respectively 87 and 55 % survival over 62 days[69].

The following report compares the effect of a microcapsules injected i.t. with other routes of administration and presents some interesting features of particles in local delivery. Microspheres, loaded with DOX, cisplatin or 5-fluoruracil, were tested in two mammary adenocarcinoma mice models. One tumour in mice was developed subcutaneously and another intramuscularly (i.m.) and results were not dependent on the model used. Data showed that efficacy in tumour reduction was achieved only if microspheres were applied at 6 injection sites around the tumour perimeter, while the same systems administered in the centre of the tumour were ineffective. Also, it was shown that 5 separate treatments, every 14 days, were significantly more effective than a single treatment. Systemic and intratumourally bolus injections of chemotherapy at maximum tolerated dose (MTD) did not show an effect on tumour growth[70].

Overall i.t. administered formulations proved to be superior for cancer treatment whether they were in a form of polymer conjugates, gels or particles with better efficacy and less toxic side

effects and also with less frequent administration. If these preclinical outcomes could be translated to the clinical setting, they could bring significant advantages for patients undergoing chemotherapy.

1.5 Platforms for local delivery in cancer

Local delivery is administration of the active drug/formulation directly into the tumour or injecting into the resection site. Benefits of local delivery are described in 1.4. however, there are only a few types of formulations that show promising clinical data. They are mainly polymer depots and include particles, gels, films, wafers and rods (Table 1-3).

Table 1-3 Examples of local cancer drug delivery platforms

Name	***Drug delivery platform***	***Active ingredient***	***Cancer type***	***Status***	***Ref.***
Gliadel®	Wafer	Carmustin	Brain cancer	Approved by FDA	[71]
Paclimer	Microspheres	PCX	NSCLC and ovarian cancer	Phase I/II	[72,73]
NA	Millirods	DCX	Liver cancer	Preclinical	[74]
NA	Films	PCX	Lung cancer	Preclinical	[75]
OncoGel®	Hydrogel	PCX	Oesophageal cancer	Phase II	[76]

One of the first commercialised implants for cancer therapy was Gliadel®, a wafer developed by the Langer research group and approved by the FDA in 1996. Gliadel wafers (14 mm diameter) are composed of spray dried and compressed polymeric microparticles (1-20 µm). Microparticles were loaded with carmustin and a copolymer of 1,3-bis-p-carboxyphenoxy propane and sebaic acid was used for their preparation. The formulation has shown to be

present in the resection site up to 6-8 weeks after implantation[77]. Gliadel® wafers are used in the treatment of aggressive brain cancer-glioblastoma usually after complete or partial surgical resection of the tumour. This treatment has improved median survival with comparable side effects to patients that only underwent surgical removal of tumour[71].

Another formulation progressed to phase I clinical studies is Paclimer® a microsphere formulation with median diameter of 53 μm made of polyphosphoester polymer with a high loading of paclitaxel (PCX) (10% w/w). These microspheres provided slow release of PCX for a period of 90 days. In subcutaneously developed lung tumours in mice, the Paclimer® formulation administered i.t., reduced significantly the tumour growth rate compared to i.t. administration of a commercial PCX formulation with the same dose[72]. Intraperitoneal administration of Paclimer® formulation was investigated in patients with recurrent ovarian cancer and progressed to a phase I clinical study. Tolerated dose was found to be up to 1200 mg/m^2. Paclitaxel was slowly released for 8 weeks and polymer residues were found even months after administration. However, this formulation was not progressed further and the reasons for this decision were not disclosed[73].

An additional successful local delivery system are rods, with a dowel shaped structure, whose diameter is usually smaller as compared to its length and vary from nano to millimetres. The composition of rods can be polymers (usually amphiphilic) which self-assemble first to micelles and by varying the system conditions (polymer concentration, a presence of surfactants, temperature) can be transformed into a rod or even result in hydrogel formation[78]. Weinberg *et al.* designed PLGA millirods loaded with DCX and tested them in a liver cancer model in rabbits. The millirods were implanted inside the tumours and reduced tumour growth significantly where

the tumour size was 10 times smaller compared to untreated controls[74].

As an alternative to polymer depots for localised delivery, polymer films have also been prepared. Liu *et al.* designed flexible poly(glycerol monostearate co-e-caprolactone) films with 10% w/w PCX for treatment of local recurrence[75]. After complete tumour removal in a lung cancer model in mice, films were implanted and prevented recurrence in >80% of animals, while 0% was prevented when commercial PCX was locally administered.

The most explored platforms for local cancer delivery are gels and they will be reviewed in more details below.

1.5.1 **Gels as a drug delivery platform**

Gels are not easy systems to define due to their diversity and chemical complexity. The first definition dates back to 1861 and was given by Thomas Graham. While working on a distinction between a crystalline and colloidal condition of matter, he noted that the softness of the gelatinous colloid partakes of fluidity and enables the colloid to become a medium for liquid diffusion[79].

A more explicit definition was proposed in 1926 by Jordon Lloyd and was stated as: "only one rule seems to hold for all gels and that is that they must be built up from two components, one which is a liquid at the temperature under consideration and the other which, the gelling substance proper, often spoken of as the gelator, is a solid. The gel itself has the mechanical properties of a solid, i.e. it can maintain its form under stress of its own weight and under any mechanical stress it shows the phenomenon of strain."

In the following years, numerous definitions arose. For instance, John D. Ferry in his research on viscoelastic behaviour proposed that gel is a substantially diluted system which exhibits no steady flow,

where he basically excluded viscoelastic liquids from term gel[80]. The generally accepted definition is that proposed by Flory in 1974: ‘‘a gel has a continuous structure that is permanent on the analytical time scale and is solid-like in its rheological behaviour’’.

Several other definitions appeared in the literature and the simplest definition suggests that gels are systems composed mainly of a liquid and minor amount of gelating compound (gelator) that together form continuous phase resulting in a solid or solid like behavior[81,82].

Considering their complexity, gels are usually classified in terms of the source of the gelator, the solvent it gels and the type of crosslinking (Figure 1-8). Firstly, considering the source of the gelator, gels can be formed from naturally occurring gelators or ones that are derived from synthetic compounds (artificial gels). Naturally derived gelators are mainly macromolecules and examples include gelatin, collagen, agar, starch and gellan gum. Artificial gels can further be divided to polymeric (macromolecular) or supramolecular (molecular) gels. The best known synthetic polymer gelators are polyester, polyamide, poly(vinyl alcohol), polyethylene, polyacrylate, polymethacrylate[83]. Supramolecular gels are formed from low molecular weight (LMW) compounds. While macromolecular gels result from either physical or chemical crosslinking or both[84], supramolecular gels are formed through a combination of physical non-covalent interactions. The type of crosslinking impacts the mechanical characteristics of the gel. Polymer chains in chemically cross-linked hydrogels are interconnected by permanent non-reversible bonds. These hydrogels are utilised when tough and stable properties are required. In contrast, physical hydrogels result in weaker gels which are more vulnerable to shearing by mechanical forces. Nonetheless, their dynamic nature brings two characteristics: viscous flow under shear stress (shear-thinning) and time dependent recovery upon

relaxation (self-healing) properties, making them desirable for injectable formulations.

Also, depending on the solvent used for the gelation, gels are divided into two major groups of hydrogels and organogels. If an organic solvent is used gels are characterised as organogels[85]. Conversely, hydrogels are formed in an aqueous medium, where a small amount of solvent maybe used to solubilise the gelator.

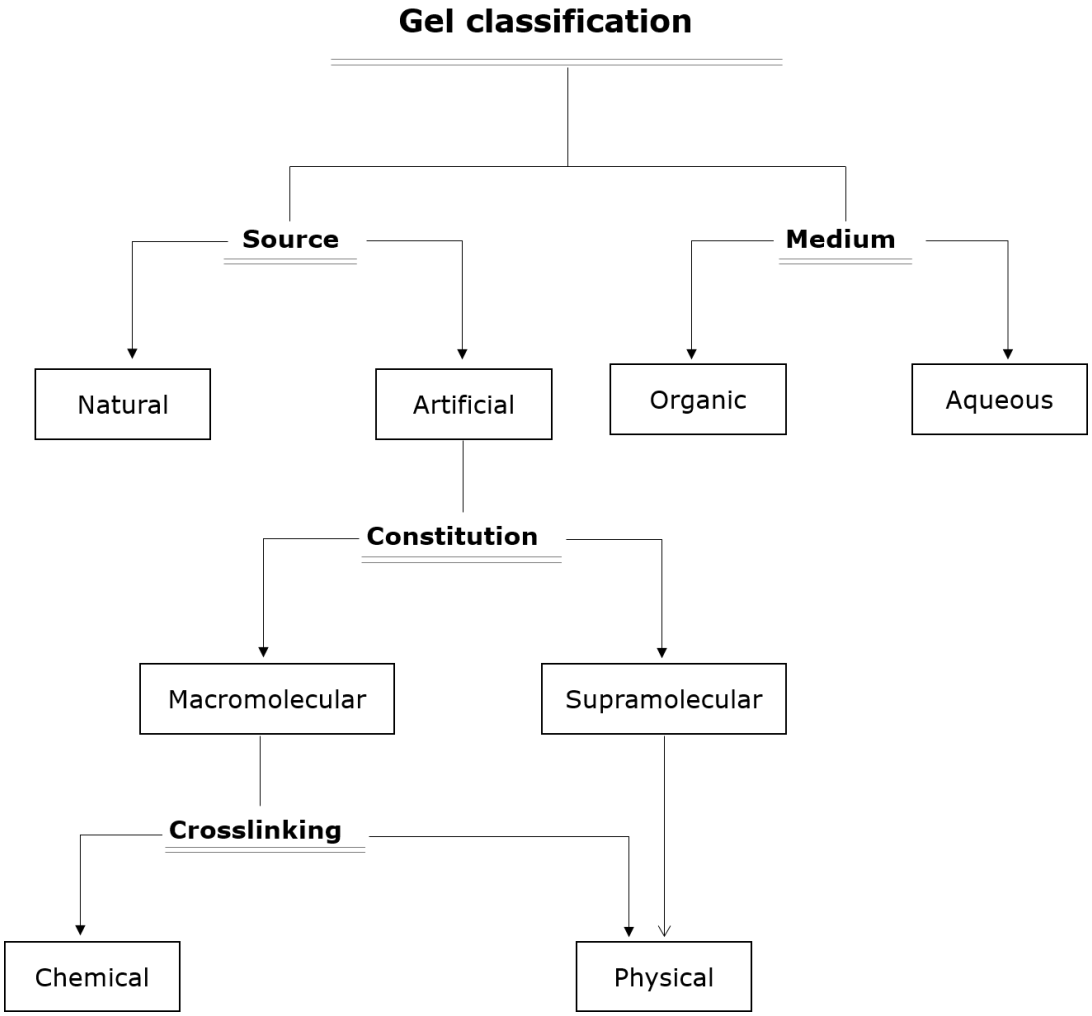


Figure 1-8 Gel classification in terms of the source of the gelator, the medium it gels, constitution and the type of crosslinking.

The presence of an organic solvent brings a certain toxicity into the formulation and it is often the limiting factor for organogels being used in drug delivery. Therefore, hydrogels are more common. Additionally, an advantage of physically crosslinked hydrogels is

their ability to be injected through a syringe and delivered in a low invasive manner *in vivo*. When applying a shear stress upon injection, these soft and responsive materials flow, with subsequent gel reformation in situ once the stress is removed, which is of importance in drug delivery to maintain controlled release *in vivo*[86].

1.5.1.1 *Polymeric gels*

A conventional group of hydrogels consists of a macromolecular network formed using a crosslinker, a small reactive molecule that forms a bridge between polymer chains. Indeed, these gels were characterised as covalently irreversible structures, through which drug can diffuse[87]. Due to crosslinker related toxicity and non-flexible structure, another group of hydrogels that are formed using environmental triggers (temperature, pH or ionic strength) have gained considerable interest. Sol-gel chemistry or reverse thermal gelation uses polymers with moderate hydrophobicity for hydrogel preparation. These polymers are rarely used alone but rather as copolymers (combination of multiblocks)[88]. Polymers with such characteristics include: poly (propylene oxide) – PPO; poly (lactide-co-glycolic acid) - PLGA; poly(N-isopropylacrylamide) - PNIPAM; poly (propylene fumarate) - PPF; poly(caprolactone) - PCL; poly(urethane) - PU and many others. They are soluble in the aqueous medium at low temperatures. However, as temperature increases they interconnect and form a gel. To minimise the hydrophobic parts of the polymer chain in contact with water, their hydrophobic parts tend to aggregate and crosslink.

One of commercialised tri block copolymer gels is OncoGel®. This formulation is PCX loaded PLGA–PEG–PLGA thermosensitive gel which demonstrated controlled release of PCX for 6 weeks. When injected intratumourally in a breast tumour model in mice at 1/10 of the systemic dose resulted in a similar number of long-term

survivors as i.v. Taxol® alone. Furthermore, OncoGel® combined with radiation therapy for inoperable oesophageal cancer was well-tolerated with no dose-limiting toxicities and negligible systemic exposure[76]. However, in phase IIb clinical trials, where OncoGel® was evaluated as adjunctive therapy to systemic chemotherapy and radiation for localised oesophageal cancer, neither a statistically significant difference in overall tumour response nor difference in the 12-month survival between these two groups was observed[89].

In addition, gels can be formed as a result of electrostatic interactions between two polymers of two opposite charge or a polymer and a small molecule of opposite charge. The, extensively used polymer, chitosan, was crosslinked using β- glycerophosphate salts as a base for a thermogel platform developed by BioSyntech for regenerative medicine and therapeutic delivery[90]. Berrada *et al.* used this platform for encapsulation of camptothecin and showed its slow release of over 30 days. In a radiation-induced fibrosarcoma 1 (RIF-1) tumour model, the gel delayed tumour growth more effectively than systemically administered camptothecin, where animals were sacrificed when the tumour reached 4 times of its initial volume at 25 and 6 days respectively[91].

1.5.1.2 *Low molecular weight gels (LMWGs)*

In the recent years, there has been immense interest in gels obtained from low molecular mass gelators, also known under the name of supramolecular gels. Materials used for their formation are molecules smaller than 3 kDa and compared to polymeric gelators, they have the ability to gel medium at concentrations as low as 1% wt. Small molecules self-assemble into long fibres, whose entanglement leads to hydrogel formation or self-assembled fibrillar networks (SAFINs)[92]. The mechanism of self-assembly from single molecules into higher-order hierarchical assemblies and

characteristics of gel on macroscopic scale are not well defined. Initial assembly of LMW gelator molecules is driven by non-covalent bonds between molecules, where these weak forces are responsible for one dimensional anisotropic aggregation of single molecules into fibrils (Figure 1-9). On the next level growth of these assemblies is continued as they form fibers or take other shapes such as rods, sheets, tapes. Finally, fibers interact into crosslinked networks that can support the solvent phase which results in a "solid-like" gel on the macroscopic level[93].

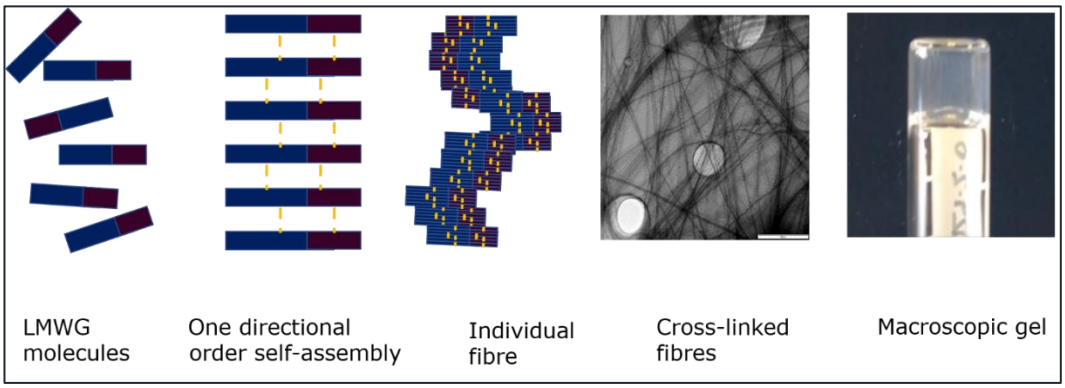


Figure 1-9 Schematic representation of LMWG self-assembly. Non-covalent bonding of single molecules into hierarchical assemblies as their primary structure followed by fibre formation and their entanglement into macroscopic form of a gel. Blue-purple area presents often diverse gelator structure (polar and non-polar regions) and yellow lines present non-covalent bonding between the molecules.

Self-assembly is governed by weak physical interactions and certain functional groups are found to support formation of fibres and their association. The amides and ureas can connect through hydrogen bonding; long alkane chains create van der Waals forces and/or hydrophobic interactions while nucleobases and carbohydrates have a predisposition for H-bonding[94]. Furthermore, there are distinct molecule types reported as LMW gelators such as steroidal, cholesterol, fatty acid, sugar, nucleoside, di/tri peptide and urea derivatives. They are thoroughly discussed by Skilling *et al.* in the latest review on LMWGs[95], herein examples will be presented on their application in cancer drug delivery.

LMWGs in cancer therapy are increasingly reported over the last decade. For instance, DOX was physically entrapped in oligopeptide (H2N-Gly-Ala-Ile-Leu-COOH (peptide 1) and H2N-Gly-Phe-Ile-Leu-COOH (peptide 2)) type of hydrogel and slowly released up to 85-90% in first 45 h. Additionally, these gels remained stable at lower pH, typical of the interstitial tumour environment and exhibited a similar release profile (75-80% release after 35 h)[96]. Cheetham *et al.* reported another way of obtaining anticancer-LMW gel where a prodrug is the gelator[97]. In fact, the anticancer drug camptothecin was conjugated to a β-sheet-forming peptide through a linker, where the peptide multi-functionality allowed conjugation of 1, 2 or 4 camptothecin molecules. Release studies revealed slow release of camptothecin without a burst effect. Systems with 2 or 4 camptothecin molecules showed higher stability to hydrolysis in presence of glutathione. They also confirmed *in vitro* efficacy in a human MCF-7 breast cancer cells. It is important to point out the main advantage of this type of formulation is high drug loading of 38%. Wang *et al.* reported Taxol conjugate with Gly-Tyr-Lys tripeptide with even higher drug loading (49%)[98]. They also introduced a folic acid ligand hypothesising its role as a targeting moiety. Two clinically used peptides, Lanreotide (Somatuline®) and Degarelix for hormone therapy are in the form of gels. Somatuline®, a synthetic cyclical octapeptide, is produced in a pre-filled syringe and is given by deep subcutaneous injection. It is used to control the symptoms such as acromegaly by reducing growth hormone (GH) and insulin growth factor-1 in prostate cancer patients with an inadequate response that cannot be treated with surgery and/or radiotherapy. Its antiproliferative activity is also being tested (phase III clinical trial) in patients with metastatic or locally inoperable, well-differentiated (grade 1) midgut neuroendocrine tumours[99]. Similarly, Degarelix (Firmagon®), a gonadotropin-releasing hormone (GnRH) receptor antagonist, forms a depot upon subcutaneous

administration. The acetate salt of the decapeptide amide binds reversibly to the pituitary GnRH receptors, reducing the release of gonadotropins and consequently testosterone in treatment of patients with prostate cancer[100].

1.5.1.3 *Gel-nanoparticle composite*

Systems in which a gel is in any way associated or contains any of nanoparticulate systems is defined as a gel nanocomposite[101]. One of the first applications of gel nanocomposite formulations was the use of inorganic nanoparticles to adsorb or attach to polymer chains evoking crosslinking of hydrogels. Besides that, NPs would bring mechanical strength by being entrapped in the hydrogel network, replacing traditional chemical crosslinkers. Such examples are silicate NPs for crosslinking hydrogels made of PEO and chitosan[102]; N,N'-methylenebis(acrylamide)[103]; PVA[104]; poly(dimethylacrylamide) (PDMA)[105] and amongst others, the recently published clay – polyacrylamide nanocomposites[106]. Also, there are examples of polymeric gel networks used for stabilisation of nanoparticles. Gold and silver nanoparticles tend to aggregate and polymeric networks formed by poly(2- vinyl pyridine)[107], poly(sodium acrylate)[108], or with a LMW gelator such as tryptophan-containing peptide amphiphile[109] are reported to stabilise them[110].

Our focus is on composite formulations for localised and cancer delivery, therefore some examples are listed in table 1-4.

Table 1-4 Examples of gel-NPs for localised drug delivery

Nanocarrier	***Gel***	***Drug***	***Application***	***Ref.***
PEG-b-PLA NPs	HPMC	NA (Dye)	Local delivery	[111]
Eudragit NCs	Chitosan	NA (Dye)	Vaginal delivery	[112]
PLA-PEO NPs	Chitosan phosphatidylcholine	PCX	Ovarian cancer	[113]
PCEC NPs	Pluronic F127	Honokiol	Local delivery	[114]
Chitosan NPs	Chitosan	GEM	Bladder cancer	[115]
Liposomes	PEG	Camptothecin	Breast cancer	[116]

As shown in the Table 1-4, polymeric over supramolecular gel-NPs composites are predominant. NPs and the gelator characteristics and their amounts influence the properties of gel-NPs formulation. In the recent publication by the Langer group, hydroxypropyl methylcellulose derivatives (HPMC-x) were formulated with poly(ethylene glycol)-block-poly(-lactic acid) (PEG-b-PLA) NPs in a NP-gel system for local delivery. Firstly, commercial styrene NPs were used and particles > 100 nm failed to produce the gel. Moreover, they showed that the number of particles is a critical parameter that facilitates gel formation. Swapping styrene particles for polymeric (PEG-b-PLA) NPs increased the number of interactions with the polymer when HPMC is functionalised with C_{12} moiety, resulting in stronger adhesion and a significant increase in storage modulus. These gels exhibited shear-thinning injectable properties with full recovery after the remove of stress[111]. Common features that local drug delivery can benefit from nanocomposite gel formulations are altered drug release profile and improved gel

strength. Contri *et al.* designed composite formulations of a chitosan gel in association with Eudragit polymeric NCs containing Nile Red (NR) as a model drug for local vaginal delivery. The presence of NCs brought a higher viscosity of the gel, prolonged mucoadhesion and increased penetration in vaginal delivery[112].

Grant *et al.* also tested in vivo release of PCX from gel-NPs composite. They produced chitosan phosphatidylcholine stabilised hydrogels in which PCX loaded PLA-PEO nanoparticles were dispersed[113]. *In vitro* release of PCX from chitosan films was evaluated in presence of ovarian SKOV-3 cancer cells and has exhibited a zero-order release profile. Also, a sustained without burst effect release profile was modelled from drug excretion data in an *in vivo* i.p. administered implant in healthy mice over 2 weeks. Furthermore, they demonstrated suitability of this composite for local delivery by absence of inflammation and infection at and adjacent to implantation site.

For localised cancer delivery, depot formation after injection into the tumour is important. Honokiol, a hydrophobic drug with antitumour activity was loaded into poly(ε-caprolactone)- poly(ethylene glycol)-poly(ε-caprolactone) (PCEC) nanoparticles which were then incorporated into thermo-sensitive Pluronic F127 hydrogel[114]. This formulation showed slight retardation in its drug release profile compared to release from NP alone. However most importantly, the gel-NPs system exhibited gel-depot formation upon s.c. injection in mice.

Bernkop-Shnürch *et al.* designed a composite formulation for bladder cancer and compared composite and NCs formulation in terms of drug release and gelling properties. Bioadhesive thiolated chitosan NPs were dispersed in a chitosan gel and rheological frequency measurements showed very poor and weak gel characteristics. However, after 4 h, more than 50% of GEM is released from the NPs

while the gel exhibited release in a more controlled manner with only 30% of GEM released. Additionally, the gel formulation retained its gelling properties in artificial urine[115]. Similarly, camptothecin loaded liposomes physically entrapped into PEG gels were reported by Lallo *et al.*[116]. While almost complete release of the camptothecin from the liposome or gel only was observed in the first 24 h, the liposome-gel composite formulation reduced the release of camptothecin to only 20% in the same timeframe. Additionally, efficacy was tested upon s.c. injection in a mouse breast cancer model and the composite formulation achieved a notable reduction in the tumour growth compared to untreated control. However, this reduction was not significantly different from the efficacy of drug solution alone.

The synergistic effect of gel-NP composites, in terms of gel strength, slower release and subsequently better stability at the administration site, is certain. More composite formulations of polymeric gels and NPs are discussed in 4.1. However, LMWGs-NPs for cancer drug delivery have not been reported to the best of our knowledge.

1.6 Gemcitabine

Gemcitabine is cytidine analogue (2',2'-difluoro-2'-deoxycytidine - dFdC) and its hydrochloride form is known under the name Gemzar® (Eli Lilly and Company). Gemcitabine hydrochloride (GEM-HCl) is water soluble and intravenously administered alone or in combination with other anticancer drugs in the therapy of several cancers.

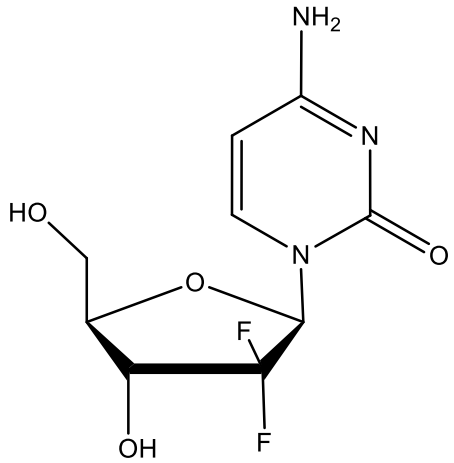


Figure 1-10 The chemical structure of gemcitabine.

In 1996 it was approved by the FDA as a first line treatment of non-resectable (Stage II or Stage III) or metastatic (Stage IV) adenocarcinoma of the pancreas. It is also indicated as second-line therapy for patients who have previously been treated with 5-fluorouracil. In the same year, it started to be used in combination with cisplatin for the first-line treatment of patients with inoperable, locally advanced or metastatic NSCLC. Later in 2004, gemcitabine in combination with paclitaxel was adopted for first-line treatment of patients with metastatic breast cancer after the failure of prior anthracycline-containing adjuvant chemotherapy. Additionally, in combination with carboplatin gemcitabine is used for the treatment of patients with advanced ovarian cancer after completion of platinum-based therapy[117]. It can also be used for bladder cancer, Hodgkin's lymphomas, cervical and bone cancer[118].

1.6.1 **Uptake and mechanism of action**

Considering gemcitabine's hydrophilic nature, diffusion into the cell at effective doses is not possible, hence its uptake relies on the presence of transporters responsible for nucleoside internalisation. These transporters are proteins at the cell surface and are: human equilibrative nucleoside transporters (hENT) or concentrative (hCNT) transporters. Gemcitabine is taken up by hENT1 and hENT2 and

hCNT1, hCNT2 and hCNT3 transporters. The hENTs seem to be extensively found in various cell types, while the hCNTs appear to be more specialised to e.g. intestinal and renal epithelia, liver and leukemic cells[119–121].

Cell uptake is not a guarantee for dFdC action as it first has to be transformed to its phosphorylated active form. As the deoxycytidine analogue, phosphorylation to monophosphate form (dFdCMP) is done by deoxycytidine kinase (dCK), while active di and triphosphate forms of gemcitabine (dFdCDP and dFdCTP, respectively) are obtained by other mono (UMP-CMP) and diphosphate pyrimidine kinase (DPK)[122].

dFdC is metabolised by cytidine deaminase (CDA) to 2',2'-difluorodeoxyuridine (dFdU) with reduced activity[123]. Gemcitabine monophosphate is deaminated by deoxycytidylate deaminase (DCTD) into 2',2' -difluorodeoxyuridine monophosphate (dFdUMP)[124]. Additionally, 5'-nucleotidase (5'-NT) catalyses the hydrolysis of phosphates therefore converts dFdCTP into dFdCDP and dFdCDP into dFdCMP. As a result, dFdCMP is reduced to the inactive form of gemcitabine[125].

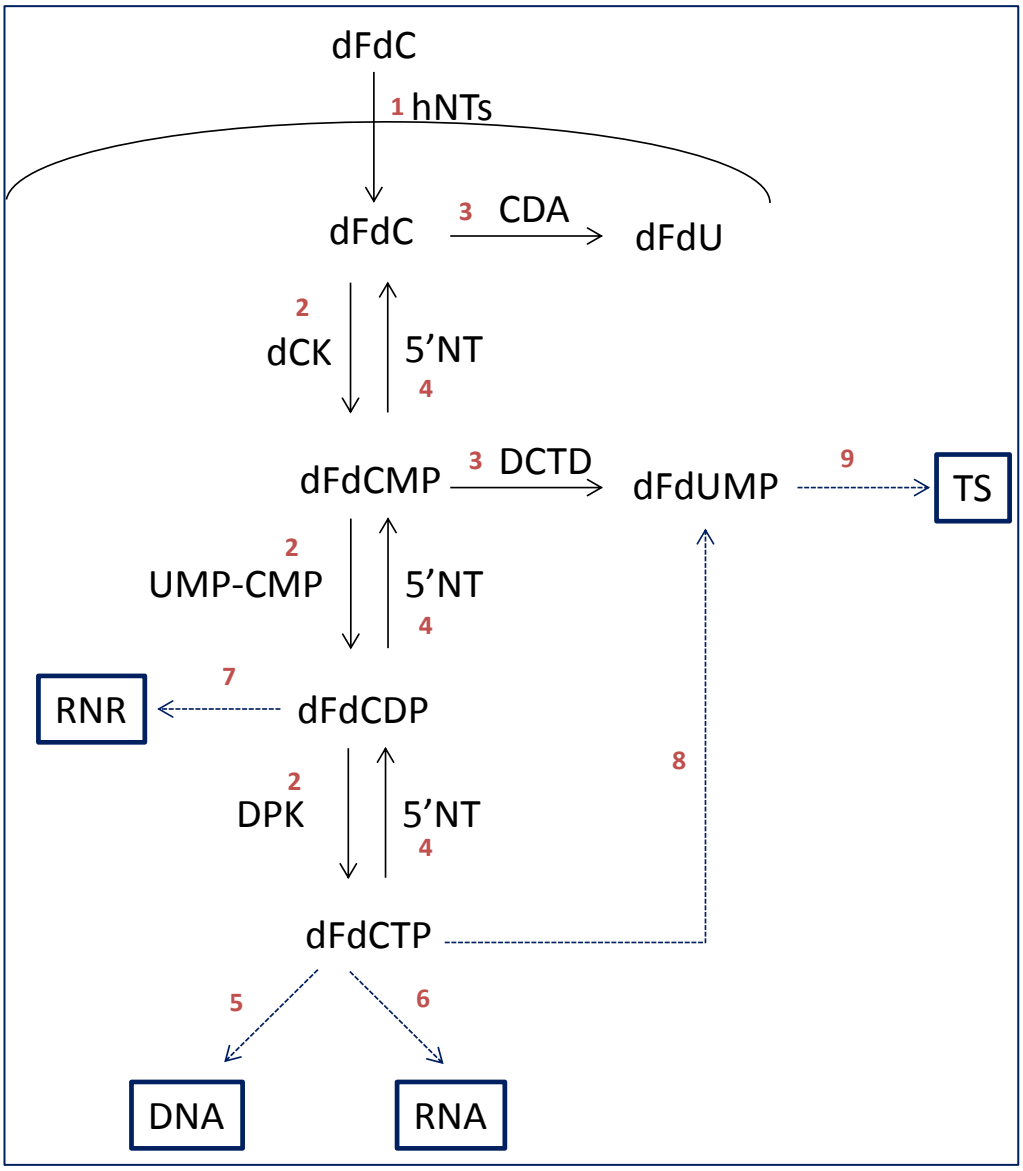


Figure 1-11 Schematic representation of gemcitabine uptake, cellular and mechanism of action. 1) Internalisation of gemcitabine (dFdC) by human nucleoside transporters (hNTs). 2) Gemcitabine phosphorylation to gemcitabine monophosphate (dFdCMP) by deoxycytidine kinase (dCK); phosphorylation of dFdCMP by monophosphate pyrimidine kinase (UMP-CMP) to gemcitabine diphosphate (dFdCDP) and its subsequent phosphorylation to gemcitabine triphosphate (dFdCTP) by di phosphate pyrimidine kinase (DPK). 2) Deamination of dFdC and dFdCMP by cytidine deaminase (CDA) and deoxycytidylate deaminase (DCTD) respectively. 4) Dephosphorylation with 5'-nucleotidase (5'-NT). Mechanisms of action are indicated by blue dashed lines: 5) incorporation into DNA; 6) incorporation into RNA; 7) inactivation of ribonucletide reductase (RNR); 8) inhibition of deoxycytidine monophosphate deaminase (DCTD); 9) inhibition of thymidylate synthase (TS).

The mechanism by which gemcitabine induces apoptosis is by its incorporation into DNA. dFdCTP acts as a nucleoside analogue of deoxycytidine triphosphate (dCTP) which promotes its incorporation into the DNA helix during replication. Only one more deoxycytidine is able to be incorporated when masked-chain termination occurs. The advantage of masked chain termination is that after gemcitabine incorporation, any additional nucleoside that is added allows gemcitabine to bypass DNA repair enzymes[126]. Although far less studied gemcitabine incorporation in RNA was reported by Ruiz van Haperen *et al.*[127].

Gemcitabine diphosphate also acts as an inhibitor of ribonucleotide reductase (RNR). The RNR is an enzyme that controls the transformation of ribonucleotides into deoxyribonucleotides. Obtained deoxyribonucleotides are used in DNA synthesis and repair, hence inactivation of RNR by dFdCDP influences DNA replication rate[128]. Additionally, DCTD is directly inhibited by dFdCTP resulting in dFdCTP higher intracellular concentration. These are known as self-potentiating mechanisms of gemcitabine[129]. Another potential mechanism is inhibition of thymidylate synthase (TS). The dFdUMP is a product of dFdCMP deamination and can be an analogue of 2' – deoxyuridine monophosphate (dUMP) which is a natural substrate of TS. Incorporation of a gemcitabine derivate instead of dUMP can cause DNA damage[130].

1.6.2 **Gemcitabine resistance**

Gemcitabine is administered i.v. and usually at very high doses (single injection of ~1000 mg/m^2). The high activity of CDA in the liver and the spleen is responsible for the short half-life of gemcitabine (<70 minutes in patients)[131]. Therefore, administration of high doses is required which is effective at the beginning of the treatment but eventually leads to tumour resistance. Complex and

multiple mechanisms of gemcitabine (GEM) action give an opportunity for abnormalities to take place; therefore, resistance to GEM can be developed *via* different mechanisms. For instance, it was shown *in vitro* that cells that lack nucleoside transporters are resistant to GEM[132]. Additionally, confirmed clinically, patients with detected hENT1 showed a prolonged survival of 13 months compared to 4 months survival in patients that lacked these transporters[133]. In a similar manner, this was shown for levels of deoxycytidine kinase (dCK) which is enzyme needed to phosphorylate gemcitabine to its active form. Investigated on various tumour models in mice, it was shown that ovarian tumours with highest dCK enzymatic activity of 18 nmol/h/mg protein had lowest relative tumour volume (0.02) compared with head and neck (HNX-22B) where dCK activity was 3.3 and a relative tumour volume 0.98[134]. Relative tumour volume is expressed as maximal T/C (tumour volume treated mice/tumour volume control mice).

Also, it was shown that elevated level of enzymes that are usually responsible for the elimination of GEM, such as CDA, can also be responsible for its resistance[135]. For example, Fujita *et al.* showed on 2 pancreatic cancer cell lines (SUIT-2 and Capan-1) that the CDA level was significantly increased in their gemcitabine resistant parental cells.

1.6.3 **Gemcitabine prodrugs**

One of the ways to improve GEM efficacy in the presence of such resistance mechanisms is its modification to prodrugs. Potential, and the most explored sites for modification are the 4-(*N)* position of cytosine and the 5’ position of the ribose molecule.

Modification at the 4-(*N)* position protects gemcitabine from deamination as the first step of its elimination. Recent work of Khare *et al*. reported 4-(*N)* tocopherol poly (ethylene glycol) succinate

(TPGS) modified GEM as a molecule designed to self-assemble into a micelle formulation. In pancreatic cancer cell line (BxPC-3) native GEM and TPGS-GEM micelles showed similar IC_{50} values of 2.4 and 1.6 μM respectively. However, when nucleoside transporters were blocked, IC_{50} value for GEM was 5 times higher, while TPGS-GEM micelles did not express any significant change in IC_{50} value showing that they are not dependent on NTs to cross the membrane. Additionally, the micellar formulation showed *in vitro* stability against CDA with 90% of gemcitabine present after 30 minutes while only 10% of GEM remained, in the presence of CDA in the medium, in the same timeframe[136]. Similarly, further prodrugs with PEG[137], PEG active targeting conjugates[138], triterpenes[139] have shown improved efficacy of GEM towards resistance. Furthermore, one of the GEM prodrugs with valproic acid conjugate at 4-(*N)* position, LY2334737, reached clinical trials. The low rate of *in vitro* hydrolysis <14% over a 6 h incubation period resulted in a prolonged circulation of gemcitabine. However, dFdU is still shown to be major metabolite *in vivo* in mice and dogs[140]. In combination with other oral prodrugs, LY2334737 has reached phase 1b clinical trial for the treatment of solid tumours[141].

Lipophilic side chains are conjugated at the 5’ position in order that GEM can be internalised independently of hNTs by passive diffusion across the cell membrane. This found was useful for tumours with low expression of these transporters, as confirmed with eladic acid (CP-4126)[142] and cardiopilin (NEO6002)[143] derivatives of GEM. Modification at 5’ site could mean that 4-(*N)* position stays unprotected against cytidine deaminase and that these prodrugs are less promising. However, Qi *et al.* showed that 5’ modification can have the same or better potency than the previously described LY2334737 (4-(*N)* valproic gemcitabine derivative). They conjugated a C18 chain to monophosphate ester at the 5’ position of GEM and showed IC_{50} values of 39.7, 567, 30 and 284 nM compared to IC_{50}

values of LY2334737 of 1350, $>10^4$, $>10^4$ and 4284 nM respectively for NSCLC, pancreatic, prostate and colon cancer cell lines [144]. As well as being designed for intracellular delivery, the 5' modifications of monophosphate form of gemcitabine also ensures that activity will be independent of kinase expression[145].

1.7 The proposed platform

The main aim of cancer drug delivery systems currently under research is to target cancer cells avoiding healthy tissue and provide prolonged release, consequently reducing the frequency of chemotherapy. Hydrogels are ideal systems for local cancer delivery since they have the potential for prolonged residence time at the injection/implantation site. However, drugs loaded directly into hydrogels often result in relatively rapid drug release, due to the high-water content and large pore sizes of hydrogels. On the other hand, nanocarriers, as alternative for more controlled release, are usually prepared in a liquid form and difficult to maintain at the site of the disease on their own as can be quickly processed by body systems. However, as it was shown they often bring strength that soft injectable gels sometimes lack. Their association could result in a synergistic effect, implying that gel would localise longer in a body providing higher local retention of drug loaded nanocarriers.

1.7.1 Aim of the project

In this research project, a new injectable drug delivery platform for cancer therapy is proposed and investigated. Such platform is based on the incorporation of polymeric nanocapsules (NCs) into a gel network. This platform design is primarily relevant for inoperable cancers, but the gel-NCs formulation could also be injected into tumour resection sites.

The proposed platform should confer injectable properties that can be easily used in patients with late tumour stages that are too weak to undergo surgery. Due to usually late diagnosis, one such inoperable tumour is pancreatic cancer; therefore, gemcitabine was chosen as a model drug to explore. Additionally, considering drawbacks that gemcitabine faces (short half-life and acquired resistance) its modified form, *N*4-myristoyl gemcitabine, was selected. This hydrophobic modification on gemcitabine further allowed its encapsulation in the lipid core of NCs.

Considering that tumours in late stage can be bigger than 5 cm and are often spread to nearby lymph nodes, distribution of anticancer drugs further from the injection/resection site is needed. Hence, using very small nanocapsules to ensure penetration deeper through the whole tumour and possible trafficking to the lymphatics would be important to achieve. Finally, the introduction of the gel structure should ensure localised drug delivery over many cell cycles.

Objectives of this PhD thesis are:

- Production of small NCs (<100 nm) (Chapter 2).
- Maintained activity of GEM C14 - loaded NCs in cancer cells *in vitro* (Chapter 3).
- Production of injectable gel-NCs composite formulation.
- Use of LMW gelators in the nanocomposite gel formulation, as its use with NCs for cancer delivery has not been previously explored (Chapter 4).

2 Development of polymeric nanocapsules

Nanocapsules are normally defined as colloids composed of a lipid core surrounded by a polymer shell[39,146,147]. The polymer can define the targeting characteristics of the nanocapsules whilst the lipid core can be used as a reservoir for drugs especially with low water solubility. The encapsulation of drug in the lipid core of nanocapusles can also protect the drug from either chemical or enzymatic degradation. However, drugs can also be attached to the polymeric shell[148–150].

Depending on the application, nanocapsules with various characteristics have been manufactured. Physico-chemical characteristics that can be modified include size, surface charge, shape, and the release rate of the drug.

This thesis is focused on the design, development and characterization of nanocarriers for cancer therapy. In fact, in nanocarrier targeting in cancer therapy, it is both the tumour biology (abnormal vasculature, extracellular matrix, blood flow, permeability), and physicochemical properties of nanocarrier (shape, size, surface chemistry and charge) that affect the uptake and the retention of nanoparticles at tumour sites[151–156]. For instance, Liu *et al*. studied the biodistribution of liposomes ranging from 30 to 400 nm and the results of the study indicated that liposomes ranging from 100 to 200 nm were 4-fold more concentrated in tumours compared to liposomes below 70 and above 200 nm. Indeed, 20% of injected dose (ID) of 200 nm liposomes were taken up by the spleen which further increased with size whereas 70% of the ID of particles below 50 nm were taken up by the liver[157]. When it comes to nanoparticles smaller than 100 nm, the work of Lee *et al.* on block copolymer micelles showed faster clearance of micelles with

diameter of 25 nm from breast cancer xenografts compared to 60 nm micelles. In the same study functionalisation of 25 nm micelles with epidermal growth factor showed delayed clearance to the level of uncoated 60 nm micelles[158]. Similarly, Jiang *et al*.[159] showed the importance of size on *in vitro* internalisation. Their gold nanoparticles (2-100 nm in size) coated with the antibody (Herceptin) showed significant increase in uptake when incubated with ErbB2-overexpressing human breast cancer SK-BR-3 cells, compared with unmodified nanoparticles. Moreover, internalisation of antibody-coated nanoparticles was highly dependent on size, with the most efficient uptake occurring within the 25–50 nm size range. Although it is difficult to generalise on the optimum size range for penetration within tumours, it is evident however that nanocarriers <100 nm are beneficial.

So far polymeric nanocapsules (NCs) have been generally produced with an average size between 100 and 200 nm[160], while the production of NCs <100 nm could only be achieved through the use of high temperatures[161]. A great variety of NCs have been produced by Alonso and co-workers [162–164], using different polymer shells, i.e. chitosan[149,165], polyarginine[166], protamine[167] and more recently polyglutamic acid-polyethylene glycol (PGA-PEG)[168]. Plitidepsine-loaded PGA-PEG NCs of approximately 190 nm in size led to an increase (2.5-fold) in the maximum tolerated dose (MTD) and a significant reduction in tumour growth (xenograft human renal carcinoma, MRI-H-121) when compared with the control plitidepsin formulation (Cremophor® EL solution)[169]. In addition, PGA-PEG NCs were found to be drained into lymph nodes faster than the 200 nm NCs of the same composition. Moreover, when loaded with docetaxel these NCs were able to significantly reduce lymphatic metastases and substantially improve the survival rate when tested on an adapted orthotopic lung metastasic cancer model[168]. More recently, Teijeiro C. and Cadete *et al*. showed in their PhD theses the

production of 100 nm HA NCs and their ability to target docetaxel in an A549 orthotropic lung tumour model.

In conclusion, there is significant information regarding the production of a large array of polymeric NCs with a size equal to or larger than 100 nm. Considering the advantage of small nanoparticles in terms of enhanced internalisation and biodistribution into the tumour, we concluded that it was important to produce polymeric NCs smaller than 100 nm. Hence, the main objective of the work described herein has been to produce NCs with an oily core and a polymeric shell and to evaluate their potential for the delivery of anticancer drugs. Docetaxel and a lipophilic derivative of gemcitabine -*N*4-myristoyl gemcitabine (GEM C14) were chosen as model drugs which could potentially benefit from the defined nanotechnology.

Aim:

Design, development and characterization of anticancer drug-loaded polymeric NCs smaller than 100 nm for intra-tumoural drug delivery are explored in this chapter.

Hypothesis:

The adequate choice of the formulation and processing parameters can lead to a formulation of polymeric NCs with a size smaller than 100 nm.

Objectives:

1. To determine the influence of the surfactant and the amount of oil on the size of nanoemulsions, as precursors of nanocapsules.
2. To produce nanocapsules with a polymer shell.
3. To define the influence of the chemical structure of the oil on the size of NCs.
4. To encapsulate anticancer drugs into the NCs.
5. To evaluate the physical stability of NCs.
6. To evaluate *the in vitro* release of an anticancer drug.

2.1 Materials and methods

2.1.1 Self-emulsification method

There are a variety of techniques reported for the production of polymeric NCs. The basic principle for their formation involves the dispersion of an oil into an aqueous phase with the aid of high energy sources (sonication, ultrasound, heat) or low energy sources (simple mixing), which rely on the use of solvents and/or high amounts of surfactants[40]. Some authors[160,170] divided these techniques into two categories: solvent-free and solvent displacement techniques. However, in order to emphasise the importance of energy consumption, here the production of NCs will be differentiated according to high or low energy sources used.

High-energy methods include the use of rotor/stator devices, ultrasound or high-pressure homogenisers (HPH). Depending on the method used and the formulation parameters it is possible to modulate the size of the nanoparticles. For instance, changing HPH pressure and the number of passes through the HPH, particles of 135 nm can be obtained[171]. Recently, using ultrasound curcumin-loaded polymer double layered (chitosan and carboxymethylcellulose) NCs of approximately 150 nm were produced[172]. The size of the NCs prepared by the solvent displacement could be modified by adjusting the amount of the different ingredients forming the NCs, as well as the nature of the solvent and its elimination rate[173–175]. Chorny *et al*. reported tyrphostin loaded nanospheres formed of poly(D,L-lactide) and Pluronic F-68 with a size <100 nm using a nanoprecipitation technique where polymer content was key parameter in controlling the size. The technique based on the phase transition temperature (PIT)[176,177] has also been shown to lead to the formation of lipid NCs (no polymer shell) with a size of <100 nm[161,178]. However, in this

case, the temperature had to be increased up to 80ºC in order to produce these small NCs.

A goal of this project was to produce NCs <100 nm using a low energy, solvent-free and, thus, environmentally friendly technique. For this we chose the self-emulsification technique. Such a technique can be easily scalable and, therefore, attractive for further development of the formulation presented here.

Initially, self-emulsification was mainly used as a way of preparing oral lipid-based drug delivery systems in order to improve oral bioavailability of poorly water soluble drugs. These systems include lipid depots (oils and (co)emulsifiers) containing drug which after oral administration rapidly disperse (self-emulsify) in gastrointestinal fluids producing micro- or nano- emulsions, thereby augmenting its absorption, preventing precipitation and increasing bioavailability of the drugs. Various drugs have been incorporated in self-emulsified drug delivery systems (SEDDS) such as cyclosporine[179], danazol[180], diazepam and novel anti-depressant drugs[181,182], vitamin E[183], and ubiquinone[184]. Some of these formulations have progressed to marketed commercial formulations [185,186].

The explanation for spontaneous emulsification dates back to 1972 when Ruschak and Miller showed models of super-saturation between two immiscible phases and subsequent diffusion between them, as a mechanism responsible for formation and growth of droplets[187]. More recent literature has confirmed that the mechanism for self-emulsification lies in the presence of surfactants at very high concentrations (≥30-60%)[188]. The surfactant molecules are localised at the oil-water surface of the emulsion droplet and reduce the interfacial free energy, thereby resulting in a thermodynamically spontaneous dispersion[184,189]. Although not thoroughly investigated, it has been suggested that the self-emulsification mechanism goes

through several steps from formation of an interphase between oil-water by addition of surfactants; water penetration through the interphase leading to solubilisation within the oil phase and finally dispersion of droplets in the form of liquid crystals. Gentle agitation (for instance mild magnetic stirring), induces faster water penetration which leads to interface disruption and the droplet formation.

In addition to the formation of SEDDS, the self-emulsification technique has also been reported for the production of nanoemulsions[190–192].

With all these benefits that self-emulsification technique has, it should still be borne in mind that one of the major disadvantages of this technique is the need for surfactants at high levels, a fact that may lead to toxicity of the formulation. Although this is not such a concern for our localised cancer delivery application i.e. intratumoural drug delivery. For other drug delivery applications, further purification of the nanocapsules and partially elimination of the surfactants would need to be considered.

A few antitumoural drugs have been formulated in SEDDS with the final goal of using them for oral administration[193–195]. For instance, a self-microemulsifying drug delivery system (SMEDDS) formulation of doxorubicin (size ~200 nm) administered orally to mice bearing fibrosarcoma tumours exhibited comparable efficacy and significantly lower toxicity than DOX administered i.v.[196]. Similarly, Yang *et al.* prepared SMEDDS (2 nm microemulsions) containing paclitaxel and showed a higher bioavailability than the commercially available form of paclitaxel (Taxol®) [194]. In a similar manner, Seo *et al.* showed the increased bioavailability of a self-nanoemulsifying drug delivery system (SNEDDS) formulation containing docetaxel as compared to the free docetaxel. The same formulation was administered intravenously and the anti-tumour efficacy was found

to be very similar to the one achieved following oral administration[195].

Cadete *et al*. pioneered the development of HA NCs using a self-emulsification technique. These original nanocapsules, which were loaded with the antitumoural drug docetaxel, had a size of approximately 140 nm. Taking this work as a reference, the goal of this project was to reduce the size of the nanocapsules below 100 nm. For this, a number of formulation parameters were defined (amount of surfactants and oil, type of oil, amount of cationic surfactant and type of polymer) and their influence on physico-chemical characteristics of NCs was analysed.

2.1.2 Materials used for production of nanoemulsions and nanocapsules

Chemicals used for production of nanoemulsions:

Oils: Miglyol® 812N oil which contains caprylic/capric acid triglyceride - medium chain triglyceride (MCT) was kindly donated by CREMER OLEO GmbH & Co. and Maizine® 35-1 (glyceryl linoleate) by Gattefosse, France.

Surfactants: Kolliphor® HS 15 (PEG-660-12 hydroxystearate) was kindly donated by BASF ChemTrade GmbH; Tween® 80-polyoxyethylene sorbitan monooleate and hexadecyltrimethylammonium bromide (CTAB) were purchased from Sigma.

In addition to materials used for the production of nanoemulsions following chemicals were needed for production of NCs:

Polymers: Sodium hyaluronate 50kDa (HA, LifeCore biomedical); poly-L-glutamic acid sodium salt 5kDa - (PGA, Sigma).

Cytotoxic drugs: Docetaxel (DCX, from Fluka); *N*4 myristoyl gemcitabine (GEM C14) was synthesised by Kathryn Skilling, PhD student at School of Pharmacy, University of Nottingham, UK.

For the HPLC analysis Centripure P10 columns were purchased from EmpBiotech, Germany and AMSbio, UK and solvents of HPLC grade were purchased from commercial suppliers and used without further purification. Ultra-pure water used throughout the experiments.

2.1.3 Preparation and optimisation of NCs

Polymeric NCs were produced by a self-emulsifying method. This is a very simple and mild technique where fine oil-in-water emulsions are spontaneously produced when an oil phase is added to aqueous phase under gentle agitation. Blending the oil and surfactant in appropriate ratios at low heat (40-50 °C) until all solubilised and dispersing them directly in water which was at room temperature (RT) produces a nanoemulsion, or NCs in presence of polymer in the aqueous phase. The influences of different formulation parameters on the physicochemical properties of the NCs were investigated. In a first step, the experimental conditions for the production of nanoemulsions with a droplet size less than 100 nm were identified. In a second step, a polymer coating around the nanodroplets was formed by simple addition of the polymer into the external aqueous phase.

Figure 2-1 schematically presents the steps of the process and the formulation variables investigated using a systematic approach. Firstly, non-ionic nanoemulsions were produced (Fig. 2-1, i), where oil phase consisted only of Kolliphor® HS 15 and Tween® 80 as a non-ionic surfactants and as aqueous phase only pure deionised water (Mili-Q) was used. In case of cationic nanoemulsions' production (ii) the oil phase contained the cationic surfactant (CTAB) in addition to non-ionic surfactants from step (i). In the next step,

the addition of the anionic polymer coating (HA or PGA) to the aqueous phase led to the formation of NCs (Fig. 2-1, iii). Finally, a hydrophobic drug (DCX or GEM C14) was dissolved in the oil phase in the presence of the surfactants and stirred at low temperature overnight. Addition of this mixture into polymeric aqueous phase resulted in the production of drug loaded polymeric NCs (Fig. 2-1, iv).

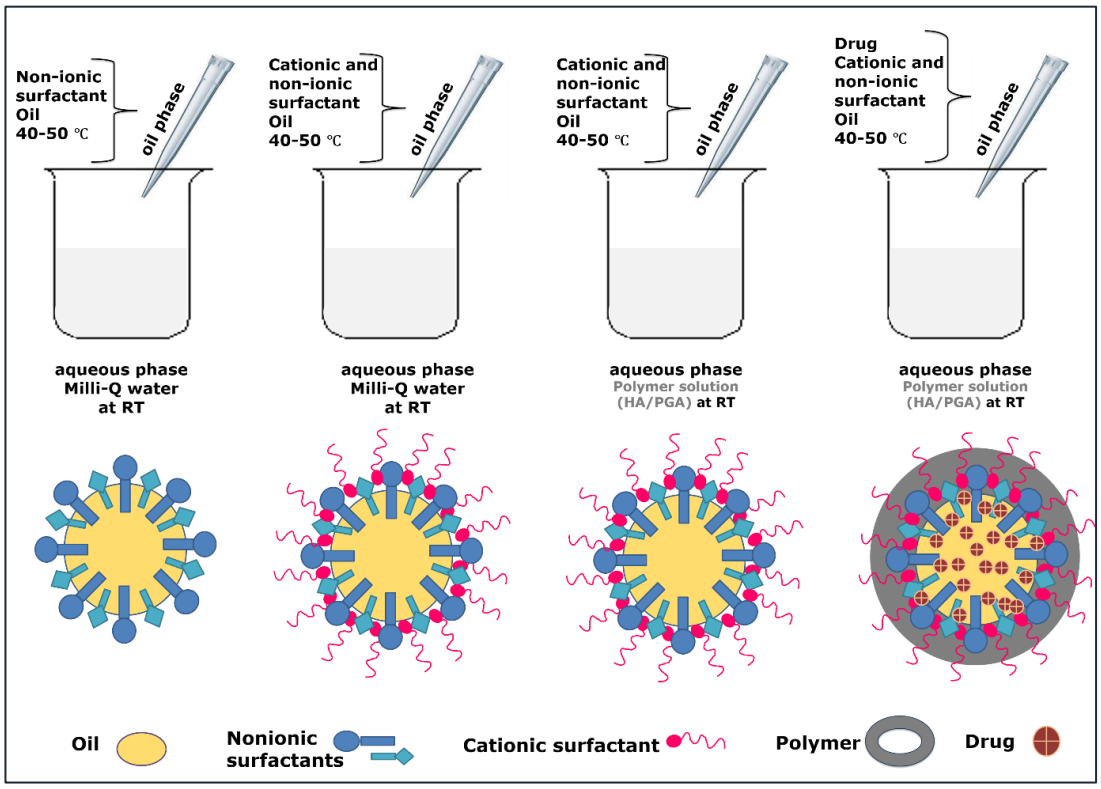


Figure 2-1 Schematic representation of nanocapsule's formulation development. From left to right i) non-ionic emulsion preparation; ii) cationic nanoemulsion preparation; iii) polymeric nanocapsules formulation; iv) drug loaded polymeric nanocapsules formulation preparation.

2.1.3.1 *Optimisation of nanoemulsions*

In the first step of nanoemulsions' development the following parameters were investigated:

- **(1) ratios between non-ionic surfactants (Tween® 80 and Kolliphor® HS 15).** The following ratios Tween® 80:

Kolliphor® were used: 1:5, 1:2, 1:1, 1:1.5, 1.5:1, 2:1, 3:1, 5:1, 24:1 w/w. For this analysis, the total weight of the surfactants in each batch was fixed at 105 mg and the amount of oil (Miglyol® 812N) was 55 mg.

- **(2) total amount of surfactants.** The total amount of surfactants varied from 105, 90, 85, 75, 60 and 55 mg. The amount of oil was fixed at 55 mg and the ratio Tween® 80: Kolliphor® was fixed at 1:1.
- **(3) oil content.** The amount of surfactants was fixed at 90 mg and their ratio was 1:1, while the oil amount varied from 55 mg to 70 and 90 mg.

Oil and aqueous phase ratio of 1:8 was kept constant.

2.1.3.2 *Influence of oil nature on physico-chemical characteristics of nanoemulsions*

Once the experimental conditions for the formation of the nanoemulsions were fixed, the influence of oil nature on the size of the nanoemulsions was evaluated. Mygliol® (caprilic/capric medium chain triglycerides with HLB value 5)[197] and Maizine® (glycerol monolinoleate with HLB=4 (http://www.alfa-chemicals.co.uk/pharma/products/maisine-35-1) were compared. These oils, despite their similar required hydrophilic-lipophilic balance (HLB) values, have a very different hydrophobic chain, a fact that can influence their interaction with the surfactants and the subsequent formation of the oily droplets. Indeed, while Maizine® has linoleic acid, that is a carboxylic acid with an 18-carbon chain and two double bonds attached on glycerol, Miglyol® 812N has

mixture of in this case saturated capric and caprylic acids, which are shorter (C10 and C8) than linoleic acid. Such variabilities can make a difference in interaction with surfactants resulting in change in NC size. The total amount of surfactants was 90 mg and the amount of oil was 70 mg. Additionally, the ratios Tween® 80: Kolliphor® HS 15 investigated were 1:2, 1:3, 1:4, 1:5, 1:8, 1:10.

2.1.3.3 *Preparation of cationic nanoemulsions and polymer introduction*

As a way to attract polymer onto the surface of the nanoemulsions, a cationic surfactant was introduced into the system as a base for subsequent electrostatic interaction with the anionic polymer. The following variables were investigated:

- **(1) concentration of the cationic surfactant.** The amount of CTAB varied in oil phase was 0.25, 0.5 or 1 mg. The amounts of oil (Miglyol® 812N) and surfactants (Tween® 80: Kolliphor® HS 15) were fixed at 70 mg and 90 mg (ratio 1:1) respectively.
- **(2) type of polymer was investigated.** Sodium hyaluronate or poly-L- glutamic acid were used as the polymer. Poly-glutamic acid is a polymer of amino glutamic acid, while HA is a polysaccharide composed of repeating disaccharide units of glucuronate and N-acetyl glucosamine (Figure 2-2). The amounts of these polymers were fixed at 2 mg/mL.

Oil and aqueous phase ratio of 1:8 in the final volume of 1.5 mL was used.

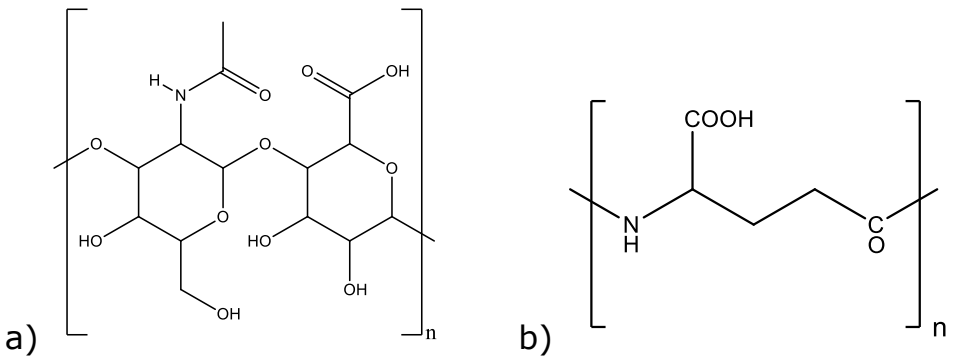


Figure 2-2 Structural representation of a) hyaluronic acid and b) poly-L-glutamic acid.

2.1.3.4 ***Drug encapsulation***

Two different drugs were encapsulated into the optimised NCs: DCX and GEM C14. Following the report from A. Cadete, 2 mg of DCX were solubilised in 1 mL of Miglyol® oil that was used for preparation of oil phase as previously described.

Similarly, *N*4-myristoyl gemcitabine (GEM C14) was solubilised in the selected oil (Miglyol®) at concentrations of 2, 3, 4 and 5 mg/mL of oil. Surfactants were added in the oil phase in order to help the solubilisation of the drug.

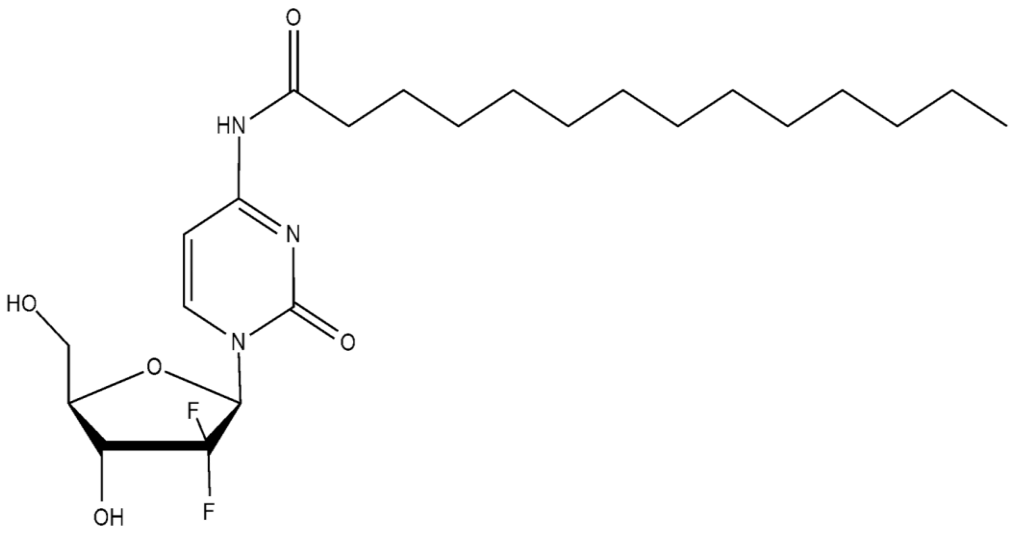


Figure 2-3 The chemical structure of GEM C14.

2.1.3.5 *In vitro drug release*

Release of GEM C14 was assessed from HA 40 and HA 80 nm NCs. The procedure for release involved incubation of 0.5 mL GEM C14 loaded NCs with 37.5 mL of release medium in water bath at 37 °C. Firstly the release of GEM C14 from HA 80 nm NCs was assessed both in PBS buffer (pH 7.4) and in addition with 0.1% SDS (pH=6.8). Solubility of GEM C14 of 0.456 mg/mL in PBS (0.1% SDS) was obtained by Mohammed Masar a PhD student at School of Pharmacy, University of Nottingham. Considering that concentration of GEM C14 in NCs is approximately 100 µg/mL, upon incubation with PBS if all the drug was released it would yield a concentration 0.0013 mg/mL of GEM C14 i.e 350 times the saturated solubility and hence ensuring sink conditions. Since the presence of SDS did not affect the release of GEM C14 (Appendix 1), *in vitro* drug release was evaluated using PBS (pH=7.4). Also, most importantly further dilution was not possible due to the drug detection limit. At predetermined time intervals sample of 1 mL was taken out and isolated by size exclusion chromatography columns (SEC) in order to separate free drug from the NCs. The sample was replaced with 1 mL of PBS.

By taking asample the amount released at various times is calculated using standard calibration curve. The actual amount of drug released cumulatively is calculated by adding the amount discarded each time with removing sample and replacing it with PBS to the amount in the medium at certain time point. The released amount is calculated by indirect method using following equation for percentage of cumulative release:

$$\%\ cumulative\ release = \frac{Xi - Xt}{Xi} \times 100$$

where Xi is the amount initially loaded into NCs and Xt the amount that is in NCs at time point t.

2.1.4 Methods of characterisation

To evaluate the size and charge of NCs, morphology, encapsulation efficiency and stability in *in vitro* cell culture media and upon storage of the NCs, the methods of characterisation used are described below.

2.1.4.1 *Physicochemical characterisation of NCs*

The average diameter and polydispersity index (PDI) of nanocapsules were characterised by dynamic light scattering after diluting the samples 3:100 with Milli-Q water. Zeta potential was determined by Laser Doppler Micro-electrophoresis after 5:100 sample dilution with Milli-Q water. The measurements were performed on a Malvern ZetaNano ZS, UK.

2.1.4.2 *Isolation of nanocapsules and quantification of the drug loading*

All formulations were isolated using size exclusion chromatography columns (SEC) – Zetadex 25M, CentriPure P10. Columns were prepared according to the manufacture's protocol. Non-isolated formulation (1 mL) was transferred into the column and eluted with water. Elutions of 200 µl were collected and their size, PDI and attenuator factor were noted. The first 400 µl eluted from the column were discarded and the following 1.6 mL were collected as they contained the purified NCs.

Encapsulation efficiency was calculated as percentage of the drug in isolated NCs compared to the total amount of the drug in NCs before the isolation. Drug amount was quantified using HPLC.

Drug loading was calculated as percentage of the drug amount in the total amount of lipid phase of NCs.

For DCX NCs, the system was dissolved in acetonitrile and an aliquot was injected in Agilent Zorbax eclipse XDB C8 HPLC column followed by isocratic elution (55% Milli-Q water (containing 0.1% ortho phosphoric acid), 45% acetonitrile) at 30 °C and UV detection at 227 nm.

In the case of GEM-C14-loaded NCs, they were dissolved in methanol and then, an aliquot was injected in the C18 HPLC column followed by isocratic elution (80% methanol, 20% pure water) at 30°C and UV detection at 248 nm.

The standard calibration curves of DCX and GEM C14 were linear (R^2>0.999) in the range of concentrations between 0.2 and 5 µg/mL and 0.5 and 50 µg/mL for DCX and GEM C14 respectively.

2.1.4.3 *Morphological analysis by transmission electron microscopy - TEM*

Preparation of NCs for TEM imaging involved pipetting approximately 10-20 µl of formulation on to a carbon-coated copper grid. Samples were then subjected to plunge freezing into slushed liquid nitrogen. TEM was performed at 100 kV using a Tecnai 12 D1287 BioTwin equipped with a Gatan 626 cryoholder. Images were acquired using a MegaView III camera.

2.1.4.4 *Freeze drying of NCs*

One mL of NCs was pre-frozen in liquid nitrogen and then placed in Biopharma freeze dryer for 48 hours or until a dried sample was obtained. Calculated concentration of NCs was 83±13 and 78±5 mg/mL for 80 nm and 40 nm NCs respectively. In chapter 4 different concentrations of NCs are used and NCs with this initial concentration are labelled as 8% w/v NCs.

2.1.4.5 *Stability of the nanocapusules*

Colloidal stability of GEM C14 loaded NCs was assessed upon storage at room temperature (RT) or in the fridge (8 °C) for up to 4 weeks.

Also, colloidal stability was also assessed upon incubation in PBS as well as in the cell culture medium (RPMI 1460) used in the *in vitro* cell culture studies. The dilution factor in these studies was 1:10 (v/v).

2.1.4.6 *Statistical analysis*

Unless it is stated differently, all experiments were performed in triplicate (n=3±s.d.), where n is number of independent replicates. Statistical evaluation of data was performed using one-way analysis of variance (ANOVA) comparison using GraphPad prism 7.01 GraphPad Software, UK.

2.2 Results and discussion

2.2.1 Development and characterisation of nanoemulsions

As previously indicated, nanoemulsions were prepared using a self-emulsifying technique following the steps presented in Figure 2-1. The effect of a number of formulation factors (amount of surfactant and their ratio as well as oil amount) that were investigated are presented in Table 2-1.

Table 2-1 Influence of surfactants amount and their ratio as well as oil amount on size of nanoemulsions. The oil:water ratio was kept constant at 1:8. Mean values (n=3) are shown, error bars represent standard deviation of the mean, where n is number of independent trials.

Ratio of Tween® 80:Kolliphor® HS 15	Amount of surfactants (mg)	Amount of Miglyol® 812N (mg)
1:5	105	55
1:2		
1:1		
1:1.5		
1.5:1		
2:1		
3:1		
5:1		
24:1		

Ratio of Tween® 80:Kolliphor® HS 15	Amount of surfactants (mg)	Amount of Miglyol® 812N (mg)
1:1	**55** **60** **75** **80** **90** **105**	55
1:1	90	**55** **70** **90**

2.2.1.1 *Ratios between non-ionic surfactants (Tween® 80 and Kolliphor® HS 15)*

The results in Figure 2-4 indicate the size of the nanoemulsion droplets increases when the amount of Tween® 80 becomes greater than that of Kolliphor® HS 15. Nanoemulsions >50 nm were obtained when the ratio Tween® 80:Kolliphor® HS 15 is 5:1 and 24:1 with average size of 48±9 and 127±9 nm respectively. When the amount of these two surfactants in the oil phase is the same, or the amount of Kolliphor® HS 15 is greater than that of Tween® 80, the average size of nanoemulsions decreases notably to 28±1 nm. The influence

of Kolliphor® HS 15 on the size of nanoemulsion droplets has already been reported[161]. However, in this previous study the nanoemulsion was prepared using the "phase transition temperature method". In another more recent study, a number of surfactants and oils with surfactant properties were investigated for the formulation of glipizidein in SEDDS. The results indicated that the concentration of Solutol® HS 15, which is a different brand name of Kolliphor® HS 15, was critical in order to reduce the size of the emulsion droplets[198].

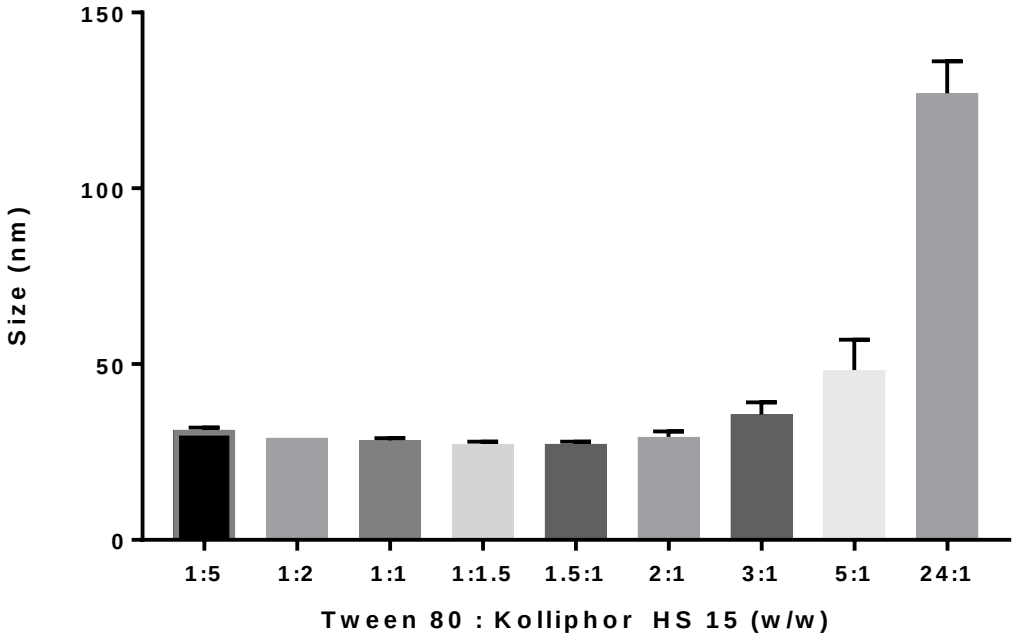


Figure 2-4 Influence of ratio of non-ionic surfactants in oil phase on size of nanoemulsions. Total amount of surfactants is 105 mg where ratio of Tween 80 and Kolliphor HS 15 varies 1:5, 1:2, 1:1, 1:1.5, 1.5:1, 2:1, 3:1, 5:1, 24:1 w/w. Amount of Miglyol 812N oil used was 55 mg and oil:water ratio was kept constant at 1:8. Mean values (n=3) are shown, error bars represent standard deviation of the mean, where n is number of independent trials.

For all tested ratios of Tween® 80:Kolliphor® HS15 between 1:5 and 3:1, the size of the nanoemulsions was ≤ 40 nm. It is important to remind that all surfactants were solubilised in oil phase. Komaiko *et al.* showed the importance of having the surfactant present in the oil

phase for obtaining significantly smaller sizes of nanoemulsions as compared to when surfactant is present in the aqueous phase[190]. This is in accordance with work in this project where all surfactants are melted and blended altogether in the oil phase.

The presence of Tween® 80 in high concentrations may have a positive impact in terms of the interaction of the nanoemulsions with cells. In fact, it has been shown that Tween® 80 affects the fluidity of the CaCo-2 monolayer and inhibits the P-glycoprotein (P-gp) in cells as an effect of modulation of membrane fluidity[199,200]. Moreover, this effect has also been shown to be important for significantly higher uptake of Tween® 80-coated nanoparticles by epithelial human brain cells when compared with non-coated nanoparticles[201].

Whilst, in 1991, it was shown that Kolliphor® HS 15 can reverse MDR in human epidermoid carcinoma cells *in vitro* at concentrations 10-fold lower than the toxic concentration[202]. Also, Cornaire *et al.* screened a wide range of surfactants investigating their ability to increase the absorption of P-gp substrate drugs by inhibiting P-gp activity. When examining effect of excipients on digoxin transfer across the intestinal mucosa in the rat everted gut sac model, they noted 2.2-fold higher uptake with Solutol® HS 15 present[203].

Considering these advantages of Tween® 80 and Kolliphor® HS 15 which could potentially help to overcome multidrug resistance and increase uptake by cancer cells, it was decided that the Tween® 80 and Kolliphor® HS 15 as 1:1 ratio should be used in the subsequent optimisation of nanoemulsions.

It is important to highlight that for all the nanoemulsions, whose size is shown in Figure 2-4, the PDI values were ≤ 0.2, which indicates that the globule population is homogenous.

2.2.1.2 *Total amount of surfactants*

Once the ratio Tween® 80:Kolliphor® HS 15 was fixed on 1:1, the formulation parameter investigated was the total amount of surfactants, which varied from 105 mg to 50 mg, while the rest of the excipients, including the oil and aqueous phase ratio (1:8) was kept constant. As expected, Figure 2-5 indicates that as the amount of surfactant increases the size of the nanoemulsion decreases. For instance, for the highest (105 mg) and lowest (50 mg) amount of surfactants, the size of the nanoemulsions was 28±1 and 125±4 nm, respectively. This agrees with the results of previous reports on the formulation of nanoemulsions or NCs [190,195].

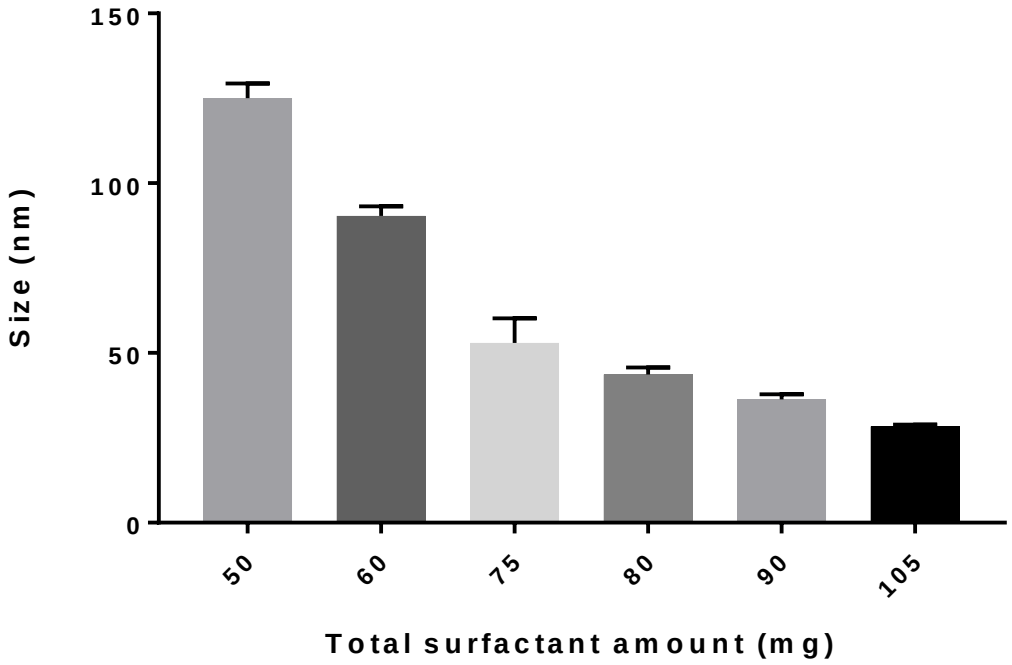


Figure 2-5 Effect of total surfactant amount on size of nanoemulsions. The total amount of surfactants was varied from 105, 90, 85, 75, 60 and 55 mg. The amount of Miglyol 812N was 55 mg with constant ratio of Tween® 80:Kolliphor® HS 15 as 1:1. The oil:water ratio was kept constant at 1:8. Mean values (n=3) are shown, error bars represent standard deviation of the mean, where n is number of independent trials.

Based on these data, and in order to keep the size of nanoemulsions below 50 nm with the lowest amount of surfactants, we selected the 90 mg of surfactants (45 mg each of surfactant) for further optimisation of the nanoemulsions.

2.2.1.3 *Oil content*

Once the amount of surfactants was fixed at 90 mg, the influence of the amount of oil on nanoemulsions' particle size was investigated. For this purpose, formulations with 55, 70 or 90 mg of oil were prepared. This effect is of high importance, as a higher amount of oil would allow the incorporation of a greater amount of drug.

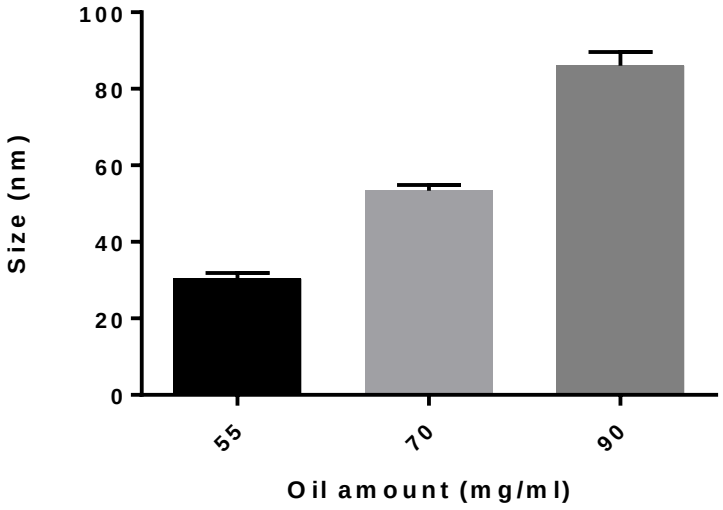


Figure 2-6 Effect of the amount of oil (55 mg to 70 and 90 mg) on the size of nanoemulsions. Amount of surfactants (Tween 80 and Kolliphor HS 15) has kept constant (45 mg of each), as well as the lipid-aqueous phase ratio at 1:8. Mean values (n=3) are shown, error bars represent standard deviation of the mean, where n is number of independent trials.

As expected, increasing the amount of oil led to the formation of nanoemulsions with larger droplets. As the interest of the study was to produce nanoemulsions with a size less than 50 nm, the maximum amount of oil was fixed at 70 mg.

Based on the formulation screening, it was decided that the experimental conditions for the production of NCs would be the ones presented in Table 2-2.

Table 2-2 Composition and physico-chemical characteristics of 2 nanoemulsion systems that are chosen from wide range of sizes for progression. Amount of surfactants and oil is provided below, while the oil:water ratio used was 1:8. Mean values (n=3) are shown, error bars represent standard deviation of the mean, where n is number of independent trials.

Formulation name	***Kolliphor® HS 15 (mg)***	***Tween® 80 (mg)***	***Miglyol® 812N (mg)***	***Size (nm)***	***PDI***	***ZP (mV)***
A	45	45	70	60 ± 5	0.2	-5
B	53	53	53	30 ± 6	0.1	-4

2.2.1.4 *Influence of the type of oil on size of nanocapsules*

Using the same amount of surfactants and oil, as well as maintaining the same ratio of lipid and aqueous phase, the influence of the nature of oil on the physico-chemical characteristics of nanoemulsions was investigated. For this, Miglyol® (medium chain triglyceride oil) was compared to Maizine® 35-1 (glycerolmonolinoleate) as two oils of the similar HLB values but with different chemical structures. The following formulation parameters were used in both cases: 70 mg of oil, 90 mg of surfactants (Tween® 80: Kolliphor® HS 15= 1:1) and an aqueous:lipid ratio of 1:8.

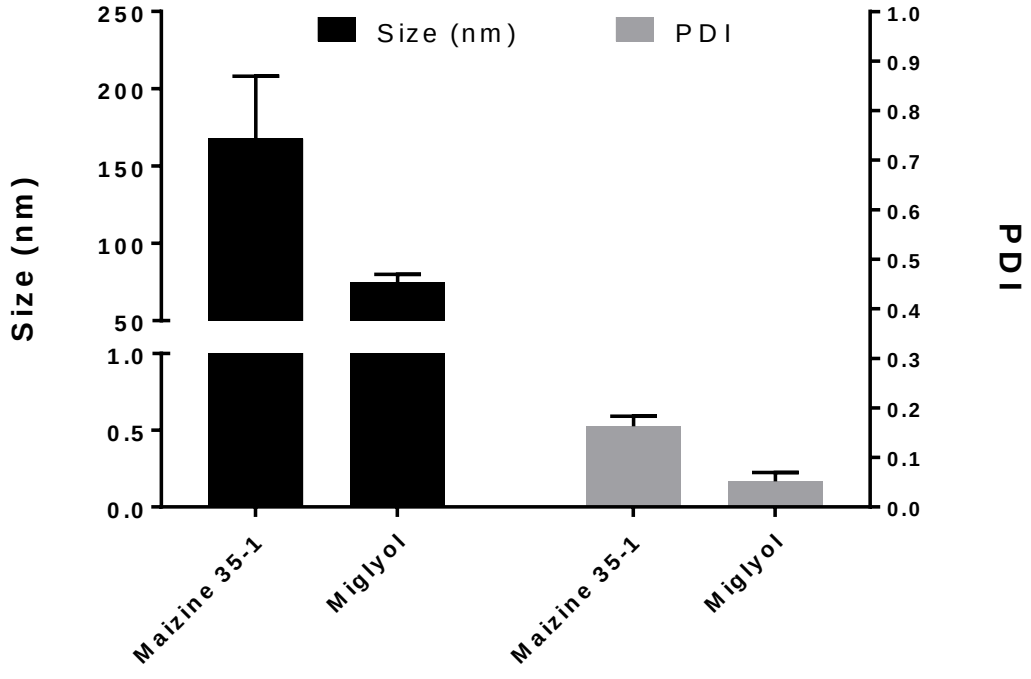


Figure 2-7 Effect of oils with different chemical structure on physico-chemical characteristics of nanoemulsions. Amount of Miglyol 812N and Maizine 35-1 was 70 mg while the total amount of surfactants was 90 mg and the oil:water ratio

was 1:8. Mean values (n=3) are shown, error bars represent standard deviation of the mean, where n is number of independent trials.

The results in Figure 2-7 indicate that replacing Miglyol® with Maizine® failed to obtain nanoemulsions smaller than 100 nm. An explanation for this observation could be that Maizine® is a monolinooleate derivative of glycerol, while Miglyol® is a medium chain triglyceride oil with a combination of capric and caprilic acid attached to glycerol backbone. Also, linoleic acid is a carboxylic polyunsaturated acid with an 18-carbon chain and two double bonds, while caprylic and capric are saturated acid with shorter chain containing 8 and 10 carbons respectively. The difference in structure of glycerol derivatives of these two oils and their interaction with surfactants could have played a significant role in achieving the desired size of nanoemulsions. Although there is not an exact theory on how oil structure influences the physico-chemical characteristics; alignment of surfactants and oil at the interface of oil/water can impact features of nanoemulsions[204]. Wang *et al.* used 4 different oils which all had HLB values of approximately 11 but differed in chemical structure. They demonstrated that, methyl decanoate, with straight saturated C12 chain gave the largest size, while smaller sizes were obtained when the oils (methyl oleate and ethyl oleate) with a double bond in the carbon chain were used. The smallest nanoemulsion size was obtained with isopropyl myristate that has a short branch in the ester structure[205]. They suggest that oils with unsaturated chains favour smaller droplets which was not the case with data reported here for the unsaturated C18 chain of Maizine 35-1 oil and Miglyol 812N with saturated medium chain length molecules. On the other hand, Habib Ali *et al.* investigated lipid geometry in liposome formation and suggested that molecules with increased alkyl chain formed more condensed structures, while asymmetric lipids formed less condensed monolayers[206]. The interaction

between chains will dictate how closely molecule pack themselves at interface. In our case, due to the unsaturated bonds in the 18 carbon chain, the increase in intermolecular distance reduces interactions between hydrophobic regions inhibiting effective packing despite longer chain in Maizine 35-1 compared to Miglyol 812N. It is probably that unsaturated structure of Maizine 34-1 chain imposes fluidity of interfacial film which favours the formation of smaller curvature resulting in larger size of NEs compared to the shorter and saturated chain of Miglyol 812N.

As previously shown, in section 2.2.1.1, the presence of a high amount of Kolliphor® HS 15 was essential for the production of small size nanoemulsions. Non-ionic surfactants used in this work, Tween® 80 and Kolliphor® HS 15, have HLB values around 15 and present a good choice in order to obtain an o/w NE. Hence, in this study using Maizine® as the oil, the influence of the increasing amount of Kolliphor® HS 15 in the lipid phase, was investigated. The total amount of surfactants was 90 mg and oil amount was 70 mg.

Table 2-3 Influence of Tween® 80: Kolliphor® HS 15 ratio on size of nanoemulsions when Maizine® 35-1 was used as the oil. The total amount of surfactants was 90 mg and oil amount 70 mg while the oil:water ratio was kept constant at 1:8. The number of independent trials was n=2.

Tween® 80:Kolliphor® HS 15 ratio (w:w)	***1:2***	***1:3***	***1:4***	***1:5***	***1:8***
Size (nm)	146 ± 8	159 ± 9	192 ± 1	189 ± 11	224 ± 21
PDI	0.27	0.26	0.27	0.3	0.3

The results in Table 2-3 show that increasing amount of Kolliphor® HS 15 did not bring any decrease in size as it was the case when Miglyol® was used as an oil instead of Maizine®. Moreover, PDI

values were always above 0.2. Once more this has demonstrated the importance of oil and surfactant structure no matter what their ratio is.

2.2.2 Production of polymeric NCs from cationic nanoemulsions

The nanoemulsions described above were obtained with non-ionic surfactants and, consequently, their surface charge was neutral. However, in order to form the shell with the anionic polymer (either PGA or HA), cationic surfactants are used as a interphase link between the oil phase and polymer [207]. The resulting positive surface charge favours the electrostatic interaction with a negatively charged polymer and, hence, the formation of the polymeric NCs.

Hexadecyltrimethylammonium bromide (CTAB) was used as the cationic surfactant. CTAB is a highly toxic surfactant, that is a characteristic of cationic surfactants in general, and it is known to induce damage of mitochondria and apoptosis[208]. However, in the context of this work, where the formulation is intended for intratumoural delivery of cytotoxic drugs, the use of this surfactant might be considered acceptable. This might justify the use of this surfactant for the production of NCs, keeping in mind the need to reduce its amount to a minimum[207,209,210]. However, it is has been shown *in vitro* that blank NCs (with no loaded cytotoxic drug) exhibit very low toxicity[211–213].

Following the incorporation of the cationic surfactant into formulation, two different anionic polymers were selected for the formation of the NC shell: sodium hyaluronate (HA) or poly-L-glutamic acid sodium salt (PGA). The physicochemical properties of the formulations containing increasing amounts of CTAB (0.25; 0.5 and 1 mg/formulation) and a fixed amount of either HA or PGA

(2 mg/mL) were prepared. The rest of the components of the formulation are those as indicated in Table 2-4.

Table 2-4 Physicochemical characteristics of polymeric NCs and their primary cationic nanoemulsions. First two rows present non-ionic nanoemulsions prepared as shown in Table 2-2 where the primary nanoemulsion (A) is 60-70 nm in size, while primary nanoemulsions (B) are smaller in size approximately between 30-40 nm. Cationic surfactant, CTAB, is added in order to get cationic nanoemulsions, followed by addition of polymer coating (hyaluronic acid or poly-L-glutamic acid) to form polymeric NCs. All amounts are expressed in mg per formulation, where final formulation volume is 1.5 mL.

Primary emulsion (Table 2-2)	***CTAB (mg)***	***HA (mg)***	***PGA (mg)***	***Size (nm)***	***PDI***	***ZP (mV)***
A	-	-	-	60 ± 5	0.2	-5 ± 2
B	-	-	-	30 ± 6	0.1	-4 ± 1
A	0.25	-	-	70 ± 5	0.2	+7 ± 1
B	0.25	-	-	30 ± 2	0.1	+3 ± 1
A	0.25	2	-	79 ± 6	0.2	-19 ± 1
A	0.5	2	-	76 ± 2	0.3	-18 ± 5
A	1	2	-	agglomerates		
A	0.25	-	2	79 ± 5	0.2	-10 ± 1
A	0.5	-	2	66 ± 9	0.2	-8 ± 1
A	1	-	2	70 ± 6	0.2	-3 ± 2
B	0.25	2	-	40 ± 2	0.2	-9 ± 1
B	0.5	2	-	41 ± 1	0.2	-11 ± 1
B	1	2	-	agglomerates		
B	0.25	-	2	34 ± 2	0.1	-4 ± 1
B	0.5	-	2	32 ± 1	0.1	-3 ± 1
B	1	-	2	33 ± 1	0.1	-4 ± 1

The results in Table 2-4 indicate that the formulations with composition "A" (Table 2-2) exhibit a size of 70 to 80 nm, and zeta

potential of -5 mV, 7 mV and -19/-10mV for non-ionic NE, cationic NE and polymeric NCs (with either HA or PGA polymer) respectively, while formulations with composition "B" (Table 2-2) exhibit a size of 30 to 40 nm size and zeta potential values of -4 mV, 3 mV and -9/-4 mV for non-ionic NE, cationic NE and polymeric NCs, respectively. However, the incorporation of increasing amounts of CTAB in the formulation did not bring any significant increase in zeta potential. Therefore, to avoid using high amounts of toxic surfactant, 0.25 mg of CTAB was selected for the final formulations. It should be noted that the negative charge of the NCs comes from the fact that the polymer is surrounding the CTAB due to their ionic interaction. This effect is illustrated in Figure 2-8, where it can be noted that the zeta potential values switch from neutral (non-ionic nanoemulsion) to positive (CTAB nanoemulsion) and, finally to negative, due to the presence of the negatively charged polymer.

These changes in the zeta potential (ZP) values are lower than those reported for HA NCs produced using solvent displacement technique[207], where the ZP value shifted from +30 mV, for the nanoemulsion, to -40 mV, for the NCs. However, in the work reported in Cadete A. thesis, where NCs were produced by the self-emulsification technique, cationic NE had maximum charge +10 mV which changed to -20 mV when HA NCs were formulated. The lower charge of NCs produced by self-emulsification could be a result of higher non-ionic surfactant content.

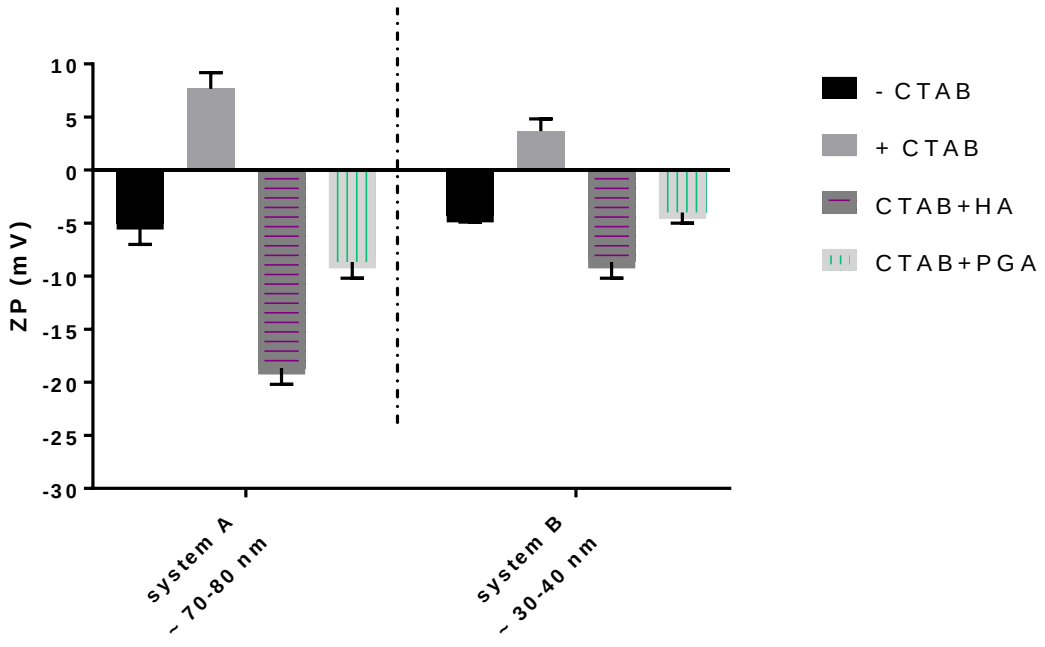


Figure 2-8 Change in charge of nanoemulsions (system A and B) with the addition of cationic surfactant (CTAB) and subsequent polymer coating (HA or PGA). The amount of CTAB used was 0.25 mg. The amounts of polymers were 2 mg/mL, while the oil aqueous phase ratio was 1:8 and the final volume of 1.5 mL was used. Mean values (n=3) are shown, error bars represent standard deviation of the mean, where n is number of independent trials.

It should also be noted that the ZP values were also influenced by the amount of non-ionic surfactants (the higher the amount, the lower the ZP and the smaller the size) and by the type of polymer coating. The use of PGA led to the formation of NCs with lower ZP values (-10 mV), as compared to those obtained for HA (-20 mV). This may be due to the higher number of carboxylic and hydroxyl groups in the HA molecule (Figure 2-2) which contributes to negative charge compared to PGA.

Based on the collected information, the NCs selected for subsequent experiments are those, whose characteristics are shown in Table 2-5.

Table 2-5 Characterisation of final systems that are going to be used in future experiments. The compositions of NCs are the ones highlighted in orange from Table 2-4.

Sample name	Size (nm)	PDI	ZP (mV)
HA 80 nm NCs	79 ± 6	0.2	-19 ± 1
PGA 80 nm NCs	79 ± 5	0.2	-10 ± 1
HA 40 nm NCs	40 ± 2	0.2	-9 ± 1
PGA 40 nm NCs	34 ± 2	0.1	-4 ± 1

From now on the abbreviated name of the formulations will be:

HA 80 nm NCs	*Hyaluronic acid coated NCs in size of 80 nm*
PGA 80 nm NCs	Poly-L-glutamic acid coated NCs in size of 80 nm
HA 40 nm NCs	Hyaluronic acid coated NCs in size of 40 nm
PGA 40 nm NCs	Poly-L-glutamic acid coated NCs in size of 40 nm

2.2.2.1 *TEM characterisation of polymeric NCs*

Samples for TEM imaging were prepared as described in 2.1.4.3. Sample preparation is very important step since, during drying or under the vacuum of an electron microscope, shrinkage or rearrangement of the sample can happen. In the case of NCs, there is an oil phase dispersed in an aqueous phase and during the drying process, the elimination of water might lead to the destabilisation of the system. To avoid that process, in this study the fixation of the samples was done in cryogenic conditions. In Figure 2-9 HA NCs in size of 40 and 80 nm are prepared and imaged on the day of preparation using cryo-TEM. These TEM images confirm regular, spherical structure of nanocapsules showing as well a fairly uniform size distribution.

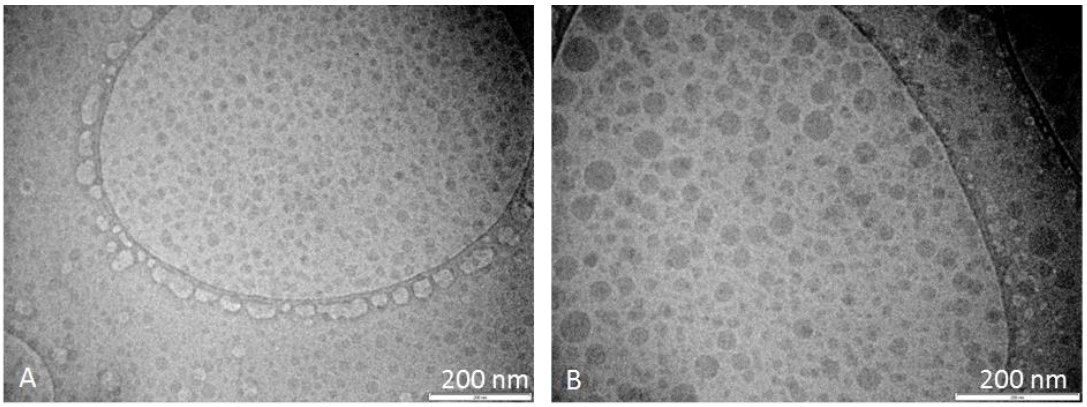


Figure 2-9 TEM images of A) HA 40 nm and B) HA 80 nm NCs imaged under cryo conditions. Scale bars are 200 nm.

When compared with DLS measurement it can be confirmed that both NCs systems are <100 nm in size. There is a difference in size between samples in image A as compared to the image B (A is ~ half the size of B). This is in line with DLS measurement, although it seems that TEM images show even smaller size of NCs. This may be due to fundamental principles of the techniques used[214]. In order for average size obtained by DLS to be comparable with other techniques sample has to be monomodal (i.e. only one peak), spherical, monodisperse (i.e. very narrow width of distribution) and diluted in a suitable dispersant. Additionally, during DLS measurements, the sample is in a hydrated state and the size obtained includes any molecules that are associated with nanocaspules. These can be either molecules of solvent or surfactant or polymer which will appear larger by DLS, while they might not be detected by TEM due to poor contrast. On the other hand, the difference might be in part because of oil droplets shrinkage upon freezing, during sample preparation for TEM, which together with limitations as described above of the DLS technique could serve as an explanation for this slight difference in size between these two techniques[214,215].

2.2.3 Encapsulation of anticancer drugs and purification of NCs

The selected compositions of NCs were loaded with DCX or GEM C14 according to the method described in 2.1.3.4. Although GEM is a first line drug treatment for advanced pancreatic cancer, it has a short half life and its uptake relies on the presence of human nucleoside transporters (hNT) (see chapter 1.6.1 section). Therefore, GEM was modified by conjugation of a myristic acid chain on the N^4 position on the pyrimidine ring to give *N*4-myristoyl gemcitabine. Myristic chain brings, both, possible protection of the drug from deamination and introduces hydrophobicity to the drug which is needed for its incorporation into the oil phase of NCs.

The physicochemical characteristics of the loaded NCs and the encapsulation efficiency values are shown in Table 2-6. The encapsulation efficiency values were calculated as described in 2.1.4.2. For the determination of this parameter NCs were isolated as described below.

Prior to the determination of the drug loading and in order to minimise the amount of surfactants in the NCs suspension, it was important to establish an adequate isolation procedure. So far, the most common methods used for the separation of colloids have been ultra-centrifugation, size exclusion chromatography (SEC) membrane filtration[216]. The ultra-centrifugation technique is based on the fact that particles of different sizes move with different velocities making particles separate according to a density gradient. Unfortunately, in the case of ultra-small low density particles, as it is the case of the NCs, the quality of separation is poor. Hence, as described in 2.1.4.2. size exclusion

chromatography (SEC) was elected as a method for the purification of the NCs.

For the visual representation of NCs' separation through the SEC column, a very lipophilic dye Sudan III is incorporated in HA 80 nm NCs. Subsequently elutions of 200 µl with water were run through the column and collected in eppendorfs. An image of elutions collected through SEC column can be found in Appendix 2. Between elutions 2 and 10, gradient of pink colour is present showing where the NCs formulation is eluted. In other elutions colour is fading away or is absent. This observation is in line with size measurement data presented in Figure 2-10. Elutions with the pink colour that are collected from SEC column also show the size of desired formulation (~ 80 nm and PDI of 0.2)

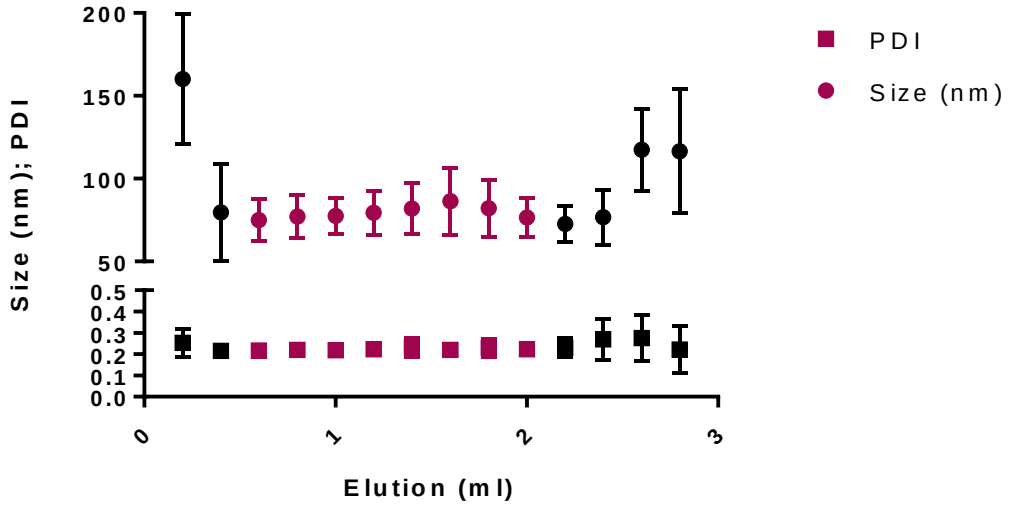


Figure 2-10 Physico-chemical characteristics of elutions after HA 80 nm NCs loaded with a lipophilic dye is run through the SEC column. Mean values (n=3) are shown, error bars represent standard deviation of the mean, where n is number of independent trials.

An additional parameter that was considered for the identification of the NCs-containing sample was attenuation from the DLS

measurement which is the parameter related to the particle concentration in the sample. Its normal value for these polymeric NCs is between 6 and 7. In order not to dilute isolated formulation too much, elutions with attenuation above 7 were discarded. The final isolated formulation was collected between 0.4 and 2 mL, as shown in pink in Figure 2-10.

Finally, Table 2-6 shows characteristics of loaded NCs. A slight increase in size of the NCs, due to the loading of the drug into their core, is noted. The surface charge and polydispersity index remained the same as in the case of the non-loaded NCs. Overall, the encapsulation efficiency values for both, for DCX and GEM C14, were around 90% for an initial drug loading of 0.1% (w/w). An increase in initial theoretical loading of GEM C14 into the oil did not result in any significant increase in the final drug loading. This could be due to the limited solubility of the drug in the oil. Therefore, it was concluded that the saturation of the oily phase was achieved with the original amount.

Table 2-6 Physico-chemical characteristics of NCs loaded with either DCX or GEM C14. HA 80, HA 40, PGA 80 and PGA 40 nm NCs loaded with DCX or GEM C14 (0.1% w/w). Mean values (n=3) are shown, error bars represent standard deviation of the mean, where n is number of independent trials.

System	Drug	Size (nm)	PDI	ZP (mV)	EE (%)
HA 80 nm	DCX	71 ± 5	0.2	-21 ± 1	96 ± 2
PGA 80 nm	DCX	61 ± 2	0.2	-8 ± 1	93 ± 3
HA 40 nm	DCX	39 ± 1	0.2	-18 ± 1	89 ± 15
PGA 40 m	DCX	32 ± 4	0.2	-8 ± 2	94 ± 4
HA 80 nm	GEM C14	80 ± 7	0.2	-19 ± 5	95 ± 8
PGA 80 nm	GEM C14	78 ± 2	0.2	-3 ± 1	90 ± 5
HA 40 nm	GEM C14	46 ± 3	0.2	-23 ± 2	92 ± 7
PGA 40 m	GEM C14	36 ± 3	0.2	-3 ± 2	90 ± 5

It should now be considered as to whether this drug loading is sufficient for intratumoural delivery. The best example to benchmark our data against is that of Lee *et al.,* where a polymeric film designed for treatment of gastrointestinal cancer contained 150 μg of GEM per implant and showed appropriate loading as it induced complete regression of CT-26 colon carcinoma s.c. model in mice[217]. With a drug loading of 0.1% (w/w) or 100 μg/mL of drug we can achieve only 10 μg per tumour (max volume that can be injected is typically 100 μl). Hence, NC drug loading should probably be increased in order to optimise the formulation for future *in vivo* experiments.

2.2.4 Stability of the NCs upon storage, in PBS and in cell culture medium

Stability of the NCs upon storage

From an industrial and translational perspective, it is important to obtain systems that are stabile upon storage. Also, from the physiological perspective, it was important to investigate the stability of the NCs in PBS, pH=7.4 and in the cell culture medium RPMI, as described in section 2.1.4.5. GEM C14 drug loaded NCs were used for this experiment without separation of free drug by SEC.

In Figures 2-11 and 2-12, the physico-chemical stability of the NCs under storage conditions at either RT or 8 ºC is presented.

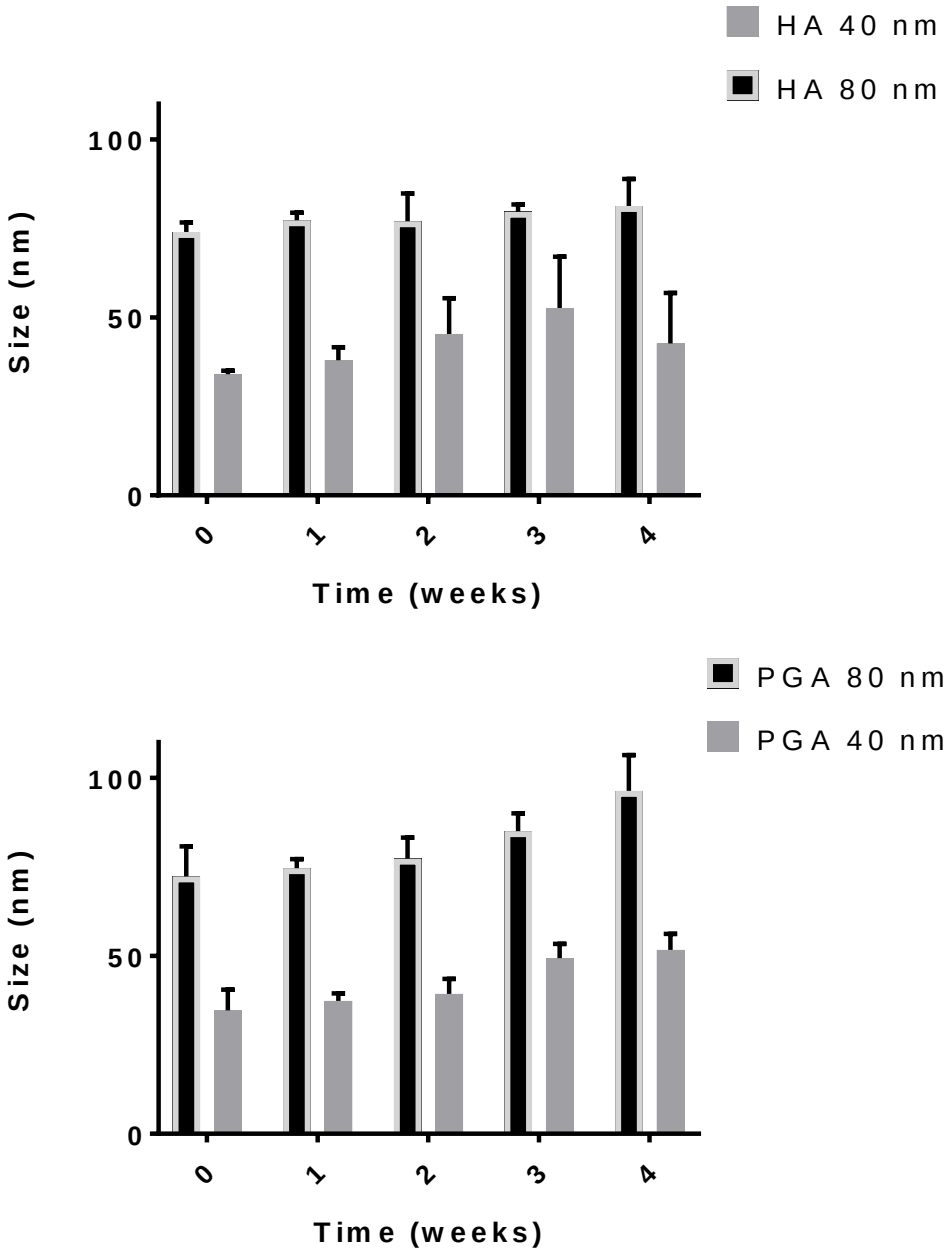


Figure 2-11 Stability of NCs upon the storage at room temperature and its influence on size of NCs. HA 80, HA 40, PGA 80 and PGA 40 nm NCs were stored in a cupboard at RT and size was evaluated weekly. Mean values (n=3) are shown, error bars represent standard deviation of the mean, where n is number of independent trials.

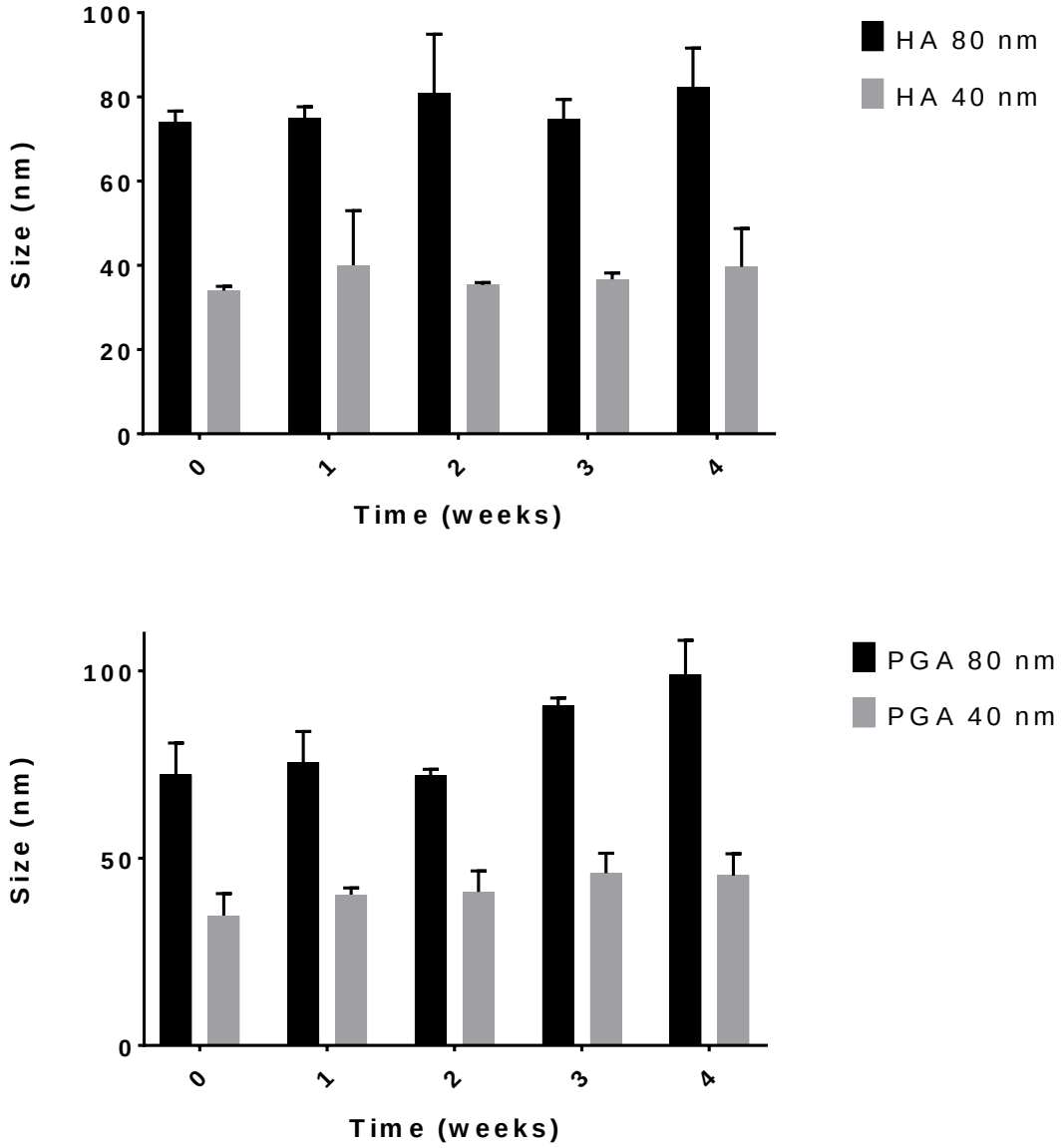


Figure 2-12 Stability of NCs upon storage in fridge at temperature of 8 °C and its influence on size of NCs. HA 80, HA 40, PGA 80 and PGA 40 nm NCs were stored in the fridge and size was evaluated weekly. Mean values (n=3) are shown, error bars represent standard deviation of the mean, where n is number of independent trials.

In the stability study, no aggregation or precipitation of nanoparticles was observed during storage for up to 1 month. This good colloidal stability profile, which could be attributed to the electrostatic repulsion between the negatively charged

nanocapsules is in line with the stability data reported for other polymeric based NCs[174,218–220]. Additionally, changes in particle size of the nanoparticles throughout the entire course of the study were minimal. In Figure 2-13 a comparison of the size of NCs after 4 weeks storage in the fridge or at RT is shown. Formulations with HA exhibited an increase in size of <10 nm, while PGA NCs, independent on size, show increases in size of 10 to 30 nm after 4 weeks storage in the fridge or at RT. It is important to note that PGA formulations showed significant (1 way ANOVA, $p<0.05$) increase in size after 4 weeks storage in fridge for PGA 80 nm NCs and at RT for both PGA 40 and 80 nm NCs. As explained in section 2.2.2., the reason for this could be the lower negative charge of the PGA NCs. When sedimentation, aggregation and flocculation are not present in the system, increase in size in nanoemulsions is explained as a consequence of coalescence and/or Oswald ripening. Coalescence is process in which two droplets merge into a larger one because of film thinning between them. Whilst, Ostwald ripening is caused by the diffusion of molecules of the dispersed phase through the continuous medium. In this case, not only drug is moving but small drops that have large area per volume, they lose material, disappear and bigger drops grow in size. The driving force for this process is concentration gradient of the solute molecules between smaller and bigger droplets (solute describes material contained within the droplets i.e. the dispersed phase of an emulsion)[40,221]. Since PGA coated NCs exhibited a bigger increase in size it can be speculated that lower polymer coverage (assessed by ZP) led to weak repulsive forces between PGA NCs compared to HA NCs system. This resulted into film thinning and NCs coalescence. Both mechanisms (coalescence and/or Ostwald ripening) lead to an increase in average size and measuring size in a time dependence manner cannot distinguish between these two mechanisms of destabilisation.

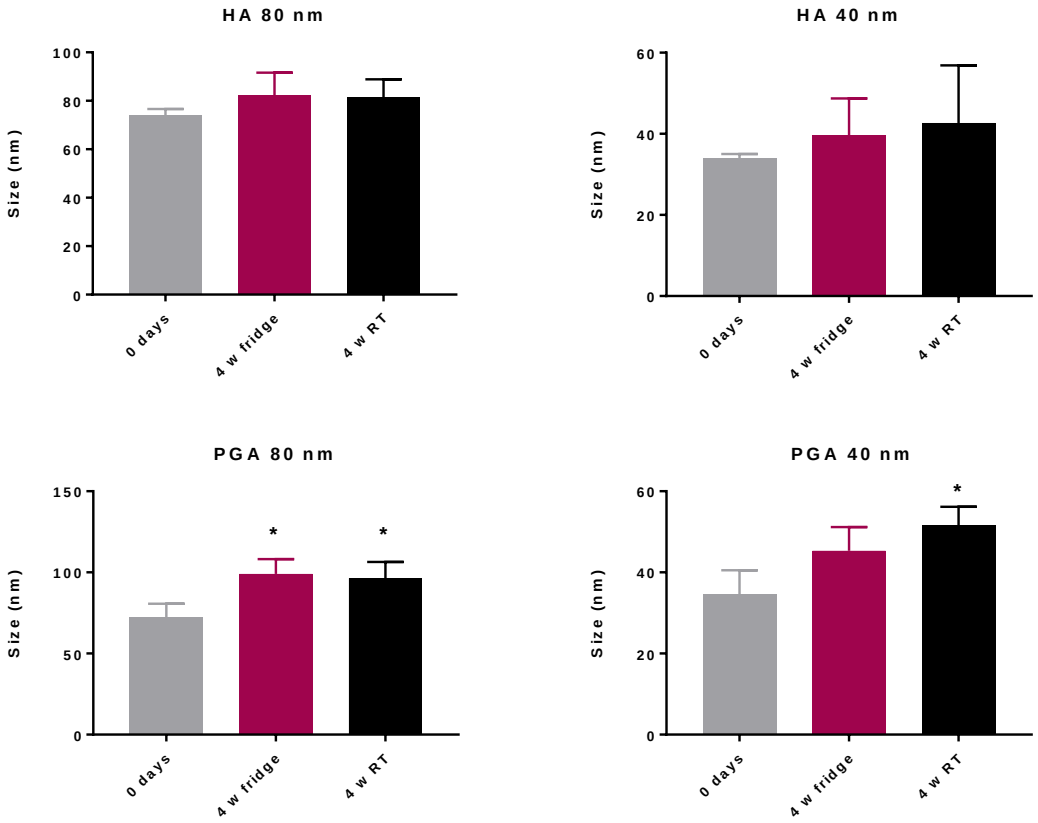


*Figure 2-13 Influence of the storage conditions (room or fridge temperature) on the size of NCs after 4 weeks. Size of HA 80, HA 40, PGA 80 and PGA 40 nm NCs was assessed after storage in a cupboard at RT or in the fridge at 8 °C. Mean values (n=3) are shown, error bars represent standard deviation of the mean, where n is number of independent trials. 1 way ANOVA Dunnett's multiple comparison test, size of NCs after 4w storage compared with initial size at day 0. *($p<0.05$).*

2.2.5 **Stability of the NCs in PBS and in cell culture medium**

A critical aspect for the physiological relevance of the formulations is their stability in bio-relevant media. In fact, it is known that stability in biological media is the barrier in the development of many nanoformulations[222]. Therefore, the stability of NCs in PBS

and RPMI medium supplemented with 10% of foetal bovine serum was investigated.

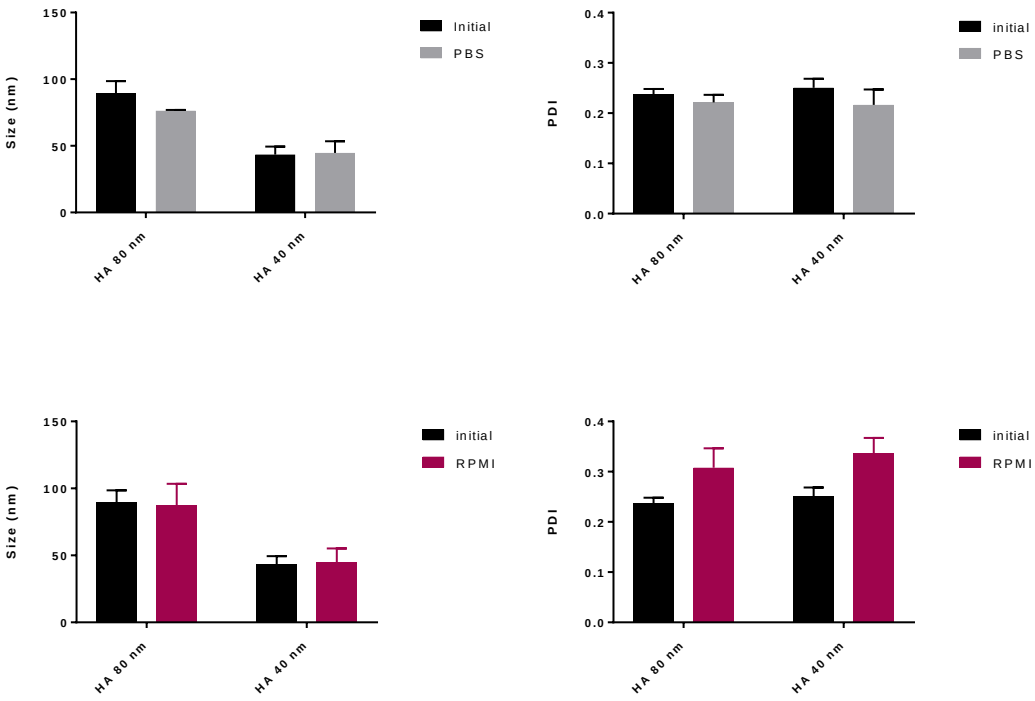


Figure 2-14 Physico-chemical characteristics (size and PDI) of HA 80 and HA 40 nm NCs after incubation with PBS and RPMI medium. Measurements were performed on the day of the incubation at RT. Mean values (n=3) are shown, error bars represent standard deviation of the mean, where n is number of independent trials.

As can be seen in Figure 2-14, the size and polydispersity index of HA 80 and HA 40 nm NCs did not change significantly ($p>0.05$ for both NCs formulations, paired t-test) after incubation in PBS. Although not significant, a slight increase in the PDI value was observed upon incubation of the NCs in RPMI medium. This could be due to higher salt content (2x potassium ions) in the RPMI medium and is more likely due to the potential interaction of the proteins, from RPMI and FBS serum, with the NCs. Presence of polymers and other molecules on the surface of particles is well known approach for establishing electrostatic and steric

stabilisation to NCs[222–224]. Besides the polymer coating, the effect of PEG groups in terms of preventing the steric repulsion of proteins and the consequences in the biodistribution of nanocarriers is well known. For instance, in a recent study by Matteis *et al*. it was shown that the stability of NCs in biological media was dependent on polymer coating. When chitosan NCs were PEG grafted, the size of NCs in biological media remained the same, while for NCs coated only with chitosan an increase in size from 100 to 400 nm was observed. In NCs explored in this chapter, presence of Kolliphor® HS 15 - surfactant with hydrophilic PEG chains part (polyglycol mono- and di-esters of 12-hydroxystearic acid) probably together with the polymeric shell contributes to the NCs stability in the medium. Given that there is no change in mean size, NCs appear appropriately stable for intra-tumoural injection *in vivo*.

2.2.6 *In vitro* release of GEM C14 from NCs

In vitro drug release assay represents a key study in drug development and the release profile can serve as a quality control parameter to differentiate between various formulations. Souza *et al.* reviewed methods used for the *in vitro* release assessment from nanosized formulation[225]. Three most commonly used methods are sample and separate (SS), use of dialysis membranes (DM) and continuous flow (CF) or combinations of these. In theory, the selection of appropriate release method should consider the one that mimics *in vivo* conditions the best. In this review, the authors stress the importance of the composition of the medium and temperature used, and suggest the use of physiological parameters (pH=7.4, 37 °C). However, correlation between *in vitro* and *in vivo* data cannot be easily established. Some of the differences between the *in vivo* and *in*

vitro release conditions are related to presence of enzymes, proteins and cells in addition to the shear forces due to the blood circulation and/or a consequence of the low volumes used in the *in vitro* studies[226].

In theory, *in vitro* studies should be designed as close as possible to simulate *in vivo* conditions. However, in practical terms this is not feasible due to analytical reasons. In any case, in an attempt to obtain information that could be useful in the design of nanocarriers, researchers have followed different experimental conditions, some of which are indicated in Table 2-7. Polymeric NCs in combination with gel and systems containing GEM are of higher interest because of the relevance to this project. Since the lipophilic derivative of gemcitabine is used in our experiments other systems that show release of hydrophobic drugs are also of interest. It can be seen that for the most of the formulations, independent of route of administration or type of nanomaterial, PBS (pH=7.4) is used as a release medium. Sometimes for compounds with low solubility in water, small amounts of surfactants or solvents are added to maintain sink conditions. As for the method of release, SS and DM are mainly used. Volume of release medium used differs between methods of release. While for DM higher volumes are reported, in SS method ratio of formulation to medium is rarely above 1:5.

Table 2-7 Conditions of in vitro *drug release evaluation from nanocarriers that are described in the literature. Abbreviations: PTX - paclitaxel; ACSF - artificial cerebrospinal fluid; BSA – Bovine Serum Albumin; OR – oil red; DW – deionised water; SC – subcutaneous; *several formulations variations were tested; i.c. – intracavitary; DOX – doxorubicin; DCX – docetaxel; n.a.- in some papers the ratio of formulation to release medium is not provided.*

Type of nanosystem	***Drug***	***Method of release***	***Release medium***	***Formulation to medium ratio***	***% Released (time)***	***Route of Administration***	***Ref.***
NPs	GEM C14	SS	PBS, 7.4	2 mg + 3 mL	50% (24 h)	i.v.	[227]
Micelles	PTX	DM	PBS, 7.4 + 10% PEG 400	n.a.	55% (192 h)	-	[228]
Liposomes*	GEM	DM	PBS, 7.4	1 mL + 50 mL	10-90% (24h)	-	[229]
NCs	DCX	SS	PBS, 7	sink cond.	~35% (24 h)	sc.	[174]
NCs	DCX	SS	PBS, 5	sink cond.	50% (8 h)	-	[230]
NPs	GEM	SS	PBS, 7.4	2 mg + 1 mL	~70% (30 d)	n.a.	[231]
NPs ***Gel-NPs***	GEM	DM	PBS, 6.4	5 mL + 100 mL	~40% (24 h) ~20% (24 h)	i.c.	[115]
NCs	Curcumin	DM	W/P80/EtOH (80:2:20 v/v)	1 mL + 200 mL	35% (72 h)	i.p.	[220]

Type of nanosystem	*Drug*	*Method of release*	*Release medium*	*Formulation to medium ratio*	*% Released (time)*	*Route of Administration*	*Ref.*
NPs	DOX	SS	PBS, 4	n.a.	5% (48 h)	-	[165]
NCs	plitidepsin	SS	PBS, 7.4	sink cond.	80% (1 h)	i.v.	[169]
LMWO gel	Pyrazineamide	SS	W/+ p- toluene sulfonic acid.	1:1	50% (24 h) 60% (24h)	-	[232]
LMWO gel	Niclosamide	SS	W	Xerogel + 150 mL	~50% (48 h)	-	[233]
LMWO gel	1. ibuprofen 2.indomethacin	DM+CF	1. PBS, 7.4 2. EtOH	Sink	1. 50% (24 h) 2. 20% (24 h)	skin	[234]
Hydrogel	GEM C12	SS	ACSF, 7.35	200 µl +300 µl	57% (48 h)	i.t.	[235]
Gel-NPs	BSA OR	SS	DW	200 µl + 1.5 mL	~40% (48 h) ~10% (48 h)	sc.	[111]

2.2.6.1 *Release of GEM C14 from HA NCs*

A 0.5 mL of NCs sample containing approximately 100 µg/mL GEM C14 was incubated with 37.5 mL of PBS (7.4). GEM C14 is a poorly water soluble drug and high medium volumes are needed in order to ensure sink conditions. The buffer volumes used were higher than reported for lipophilic derivatives (Table 2-7 ref. [227,235]).

In Figure 2-15 release of GEM C14 from HA 40 and HA 80 nm NCs is shown. Initially there was burst release of 20% of the drug which is usually attributed to the release of the drug that is adsorbed on the surface of NCs. The presence of non-ionic surfactants which tend to migrate to the oil water interface can solubilise some drug and is the possible reason for burst release[236]. After the initial burst release, slow release of GEM C14 from the NC was reached over 1 month with 63 ± 8 and 66 ± 10 % released from HA 40 and HA 80 nm NCs respectively. This observation is a result of low solubility of GEM C14 in the aqueous phase.

Nanoparticle size can influence the drug dissolution rate due to different surface areas as previously reported[237]. However, the drug release plots of 40 and 80 nm NCs are almost overlapping with minor differences in percentage of drug released. Lamprecht *et al.* showed that lipid NCs of various diameters (25-100 nm) exhibit only slight differences in release where these smaller particles release lipophilic drug amiodarone only slightly slower than bigger ones[238]. They attributed this behaviour to packing density of the surfactant molecules, which hinder the diffusion of the drug from the interface and thus delay the release. Considering that NCs presented in this thesis have higher amount of surfactant than oil and that difference is greater for smaller NCs, the increased compactness of surfactant at the interface of the smaller particles can hinder release from

smaller NCs to the same extent as the larger NCs, even with a larger surface area available for diffusion.

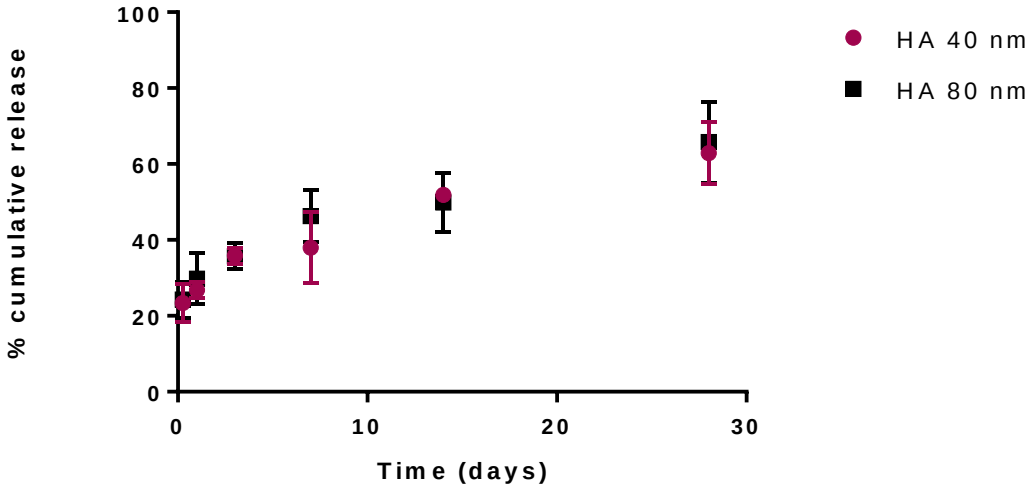


Figure 2-15 Release of GEM C14 from HA 80 and HA 40 NCs with drug loading of 0.1%. Volume of NCs formulation used was 0.5 mL with 37.5 mL of PBS (pH=7.4). Experiments were performed at 37 °C. Mean values (n=3) are shown, error bars represent standard deviation of the mean, where n is number of independent trials.

Kinetics of the release were fitted with to Ritger-Peppas model. Diffusional release is described with following equation:

$$\frac{M_t}{M_\infty} = K \times t^n$$

Where M_t presents mass of the drug released at time t, M_∞ is the mass of the drug that formulation contained initially, hence M_t/M_∞ presents the fraction of drug released at time t, K is the constant of the release rate. An indicator of the mechanism of drug release is diffusion coefficient, n, which for spherical carriers if $n \leq 0.43$ indicates Fickian diffusion. If $0.43 \leq n \leq 0.85$ is a characteristic of a non- Fickian transport and $n \geq 0.85$, a zero order drug release mechanism is prevalent[229]. The approximation is valid for the first 60% total released drug[239,240].

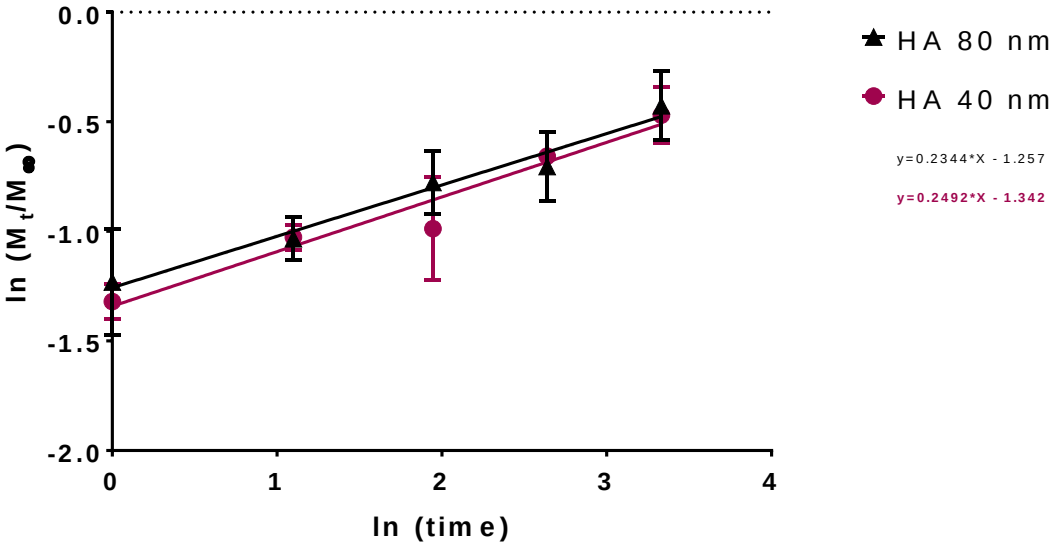


Figure 2-16 Fitting the release data indicating that GEM C14 is released from NCs by Fickian diffusion. Mean values (n=3) are shown, error bars represent standard deviation of the mean, where n is number of independent trials.

Table 2-8 Release exponent (n) and correlation coefficient (R) by fitting the GEM C14 release profiles for HA 40 and HA 80 nm NCs.

	HA 40 nm NCs	***HA 80 nm NCs***
n	0.2492 ± 0.0327	0.2344 ± 0.02116
R²	0.9508	0.9761

The release data was highly correlated to the Ritger-Peppas model (> 0.95). Diffusion exponent values obtained by fitting the release data of GEM C14 are 0.25 and 0.23 for HA 40 and HA 80 nm NCs respectively. When n<0.43, release is governed by Fickian diffusion.

Antonov *et al*. used this model for release of desonidine (corticosteroid) from polymeric NCs. Depending on method of release used i.e. dialysis bag or Franz diffusion cell they report non-Fickian (anomalous) with n=0.47 ± 0.03 and Fickian release, respectively[241]. Similarly, Jäger *et al.* used this model for release of indomethacin from NCs. However, they obtained a non-Fickian (n=0.5-0.7) release mechanism. These NCs had a substantially

larger size range (250 – 390 nm) which also did not result in differences in the drug releases mechanism[242]. Indeed, the release profile and the mechanism is not only influenced by the type of the NCs and their size but also by the drug release method used, making it difficult to compare the systems.

2.3 Summary

Developed here are new small polymeric NCs with a size of approximately 40 nm with potential applications in cancer drug delivery. These nanocapsules are composed of an oily core and a polymeric shell consisting of HA or PGA. The optimisation of the NC formulation gave the ability to tune the size of the NCs from 30 to 150 nm with different surface charges depending on the nature of the polymeric coating and showed the importance of the oil and surfactant selection in achieving the small size.

The two structurally diverse anti-cancer drugs selected in this study were docetaxel, a hydrophobic drug, and a prodrug of gemcitabine modified at the N^4 position on the pyrimidine ring with a myristic acid chain (GEM C14). Both were incorporated with high encapsulation efficiency into the polymeric NCs without changing their physico-chemical characteristics. Functionalisation on the pyrimidine ring of gemcitabine introduces the hydrophobicity required to solubilise the drug within the hydrophobic core and achieve high encapsulation efficiency (90%). Solubility of GEM C14 in oil phase, without using any solvents, allowed a final loading of 0.1 % which corresponded to 100 µg of GEM C14 per mL of HA 80 nm NCs. Additionally, GEM C14 exhibited slow release from the NCs over 1 month.

Importantly, these systems are produced using very mild, solvent free technique with low environmental impact, and that is suitable for industrial use.

These small NCs were stable in simulated biological conditions in different media and showed a good stability upon storage. Hence, they were further investigated for their ability to inhibit cancer growth in *in vitro* and were then co-formulated in association with a hydrogel. This work will be presented in Chapters 3 and 4 respectively.

3 *In vitro* activity of drug loaded nanocapsules in cancer cells

Nanocarriers have the ultimate goal to deliver a cytotoxic drug to the site of the disease and minimise toxicity elsewhere in the body. Many nanocarriers successfully deliver drug to the tumour and elicit antitumour activity greater than the drug alone (see section 1.3.7).

Since the NCs formulation reported in this thesis are loaded with GEM, pancreatic carcinoma cell lines were selected as the focus for these *in vitro* studies. Apart from that, use of HA and PGA polymer coatings of NCs could be beneficial as nanoparticles coated with various polymers are used to target tumours that express specific receptors. For example, overexpression of CD44 receptors on pancreatic cancer cell lines has been widely reported[243–245]. Furthermore, pancreatic cancer cells acquire GEM resistance after a few cycles of administration. Hong *et al.* investigated possible mechanisms involved and suggested that CD44 positive cells might be responsible for GEM resistance[243]. They carried out experiments for markers present on cancer stem cells and concluded that CD44 was significantly more highly expressed in GEM resistant cells, while other two markers were unchanged or decreased. Indeed, CD44 is a receptor for HA. Therefore, using a HA polymer coating on the nanocapsules could be a means of targeting to CD44 positive cells and overcoming drug resistance. Similarly, Dalla, E. *et al.* designed GEM prodrug-loaded liposomes coated with HA which showed increased uptake in MIA PaCa-2 cell line that highly expressed CD44 receptors while the cells that did not express CD44 receptors (VIT 1) showed similar uptake to non-coated liposomes and free drug[246]. In addition, it has been reported that the molecular weight of HA influences its binding affinity towards CD44 receptors. More

precisely, it has been suggested that the HA chain should be composed of at least 6 sugar units for an efficient occupation of HA binding site on CD44[247] and that the affinity increases for higher molecular weight HA[248].

Another natural and biodegradable polymer, PGA, that was used in the preparation of NCs, has previously shown potential in overcoming the barriers that malignant disease brings[249,250]. In recently published work of Liu *et al.* improved *in vivo* efficacy of combretastatin in conjugation with PGA is demonstrated[251]. Actually, tested in a murine colon C26 tumour, PGA conjugate of combretastatin, resulted in significantly higher tumour suppression rate of 74% compared to 24% tumour suppression rate demonstrated by the combretastatin alone. Another PGA nanocarrier, micelles, showed excellent progress in an *in vivo* treatment of pancreatic tumours in mice. Indeed, pegylated PGA micelles loaded with oxaliplatin restricted tumour growth, reduced metastasis and immensely extended overall survival of 80%, after 100 days of treatment with micelles formulation. Only 20% of overall survival was reported for the group treated with oxaliplatin only. Additionally, the penetration and retention within the tumour, authors attributed to the PEG shield and very small size of nanoparticles (30 nm)[252]. The targeting properties of PGA-nanocarriers can further be enhanced by attaching other targeting moieties such as antibodies. Docetaxel was encapsulated in a chitosan-PGA matrix to which anti EGFR antibody was conjugated and tested in two colorectal cell lines: HT-29 cells that express EGFR and IEC-6 cells that do not express EGFR. A two-fold increase in cellular uptake was shown in HT-29 cell line *in vitro*. *In vivo*, there was no significant difference in biodistribution when the carrier was conjugated to the antibody, while cetuximab docetaxel particles had better elimination time compared to non-coated particles[253].

Xu and co-workers loaded PGA -doxorubicin conjugate (PGA-Dox) into non-porous silicon particles which demonstrated slow release of pDox and subsequent internalisation by breast cancer cells (MDA-MB-231) *in vitro*. In an *in vivo* murine model, Dox was cleared quickly regardless of the formulation (Dox; PGA-Dox, silica-pDox), while toxicity-wise PGA-Dox and silica formulation did not cause high accumulation in the heart, Dox alone led to severe cardiac damage in mice. Additional tests showed that silica PGA-Dox nanoparticles are able to overcome MDR with specific distribution ability to tumours which have metastasised to lung and liver[254].

It can be concluded that nanocarriers coated with HA or PGA show targeting activity towards pancreatic and colon cancer cell lines, therefore GEM C14 loaded HA or PGA NCs were tested in colorectal (HCT 116) and pancreatic (MIA PaCa-2 and Panc-1) carcinoma cell lines. Ability of NCs to overcome drug resistance was tested on GEM resistant Panc-1 cell line and importance of overcoming drug resistance in cancer is further discussed below.

3.1 Material and methods

GEM C14-loaded NCs as reported in Chapter 2 were assessed for *in vitro* activity on cancer cell lines. Eight formulations (HA 80, HA 40, PGA 80 and PGA 40 nm NCs blank or loaded with GEM C14) were tested and compared with GEM C14 and GEM hydrochloride (GEM-HCl).

NCs were prepared as per 2.1. The initial concentration of GEM C14 in NCs was approximately 25 μM. Blank NCs did not contain drug.

GEM C14 was obtained as explained in 2.1.2. and GEM hydrochloride (GEM-HCl) was purchased from Sigma.

Reagents:

Cell culture medium-RPMI 1640, phosphate buffer serum (PBS), foetal bovine serum (FBS, F7524); trypsin; 3-(4,5-dimethylthiazol-2-yl)-2,5-diphenyltetrazolium bromide – MTT and methylene blue were purchased from Sigma and solvents DMSO and methanol were purchased from commercial suppliers and used without further purification.

3.1.1 **Cell lines used:**

Colorectal cancer cell line:

- HCT 116
- Vincristine (VC)-resistant colorectal cancer cell line: HCT 116 VR

Pancreatic cancer cell lines:

- MiaPaCa-2
- Panc-1

- GEM-resistant Panc-1

Human carcinoma cell lines (HCT 116, MIA Paca-2 and Panc-1) were all sourced from the American Type Culture Collection (ATCC) and GEM-resistant Panc-1 was donated by Lodewijk Dekker.

General cell culture:

Cells were serially sub-cultured in 25 cm^2 tissue culture flasks (Costar) incubated at 37 ºC in a humidified atmosphere of 95% air and 5% CO_2. Cells were grown in RPMI 1640 medium supplemented with 10% v/v FBS. Once cells had reached approximately 70% confluence they were sub-cultured. Medium was aspirated and 1 mL trypsin-EDTA added to detach cells. Cells were re-suspended in 5 mL fresh medium, and 0.5 to 1 mL transferred to a new flask containing 7 mL fresh, complete medium. Cultures at approximately 70% confluence were used for the experiments.

**It was ensured that cells are mycoplasma-free using Alonzo test. Additionally, bulked up stocks of cells were preserved in liquid nitrogen in 1 mL aliquots stored in cryovials. This was all done in order to ensure minimal genotypic/phenotypic drift.

3.1.2 **Assays:**

3.1.2.1 ***Growth inhibition assay:***

The MTT assay was used for mitochondrial activity evaluation, a surrogate marker for viable cell number. Briefly, cells were seeded into 96-well plates at a density of $3x10^3$ cells/well in 180 µl of culture medium. An extra plate was prepared containing cells from each cell line in order to carry out an MTT assay at the time the cells were

treated. This allows the initial optical density (OD) to be determined. After 24 h, cells were treated with drug alone (GEM C14), blank NCs and GEM C14 loaded NCs starting with GEM concentration from 25 μM followed by serial dilutions where each one was 10 times lower than previous. Four wells were used for each condition. Control cells were treated just with medium. Following 72 h incubation time, 50 μl of 2 mg/mL MTT solution were added to each well. Cells were incubated for a further 2.5 h to allow formazan production. The aqueous medium was then aspirated and the formazan product solubilised in DMSO (150 μl/well). Absorbance at 570 nm (optical density - OD_{570}) was read using an EnVision 2104 Multilabel Reader.

Data Analysis

Estimated concentrations of each test agent were calculated that could inhibit cell proliferation by 50% (GI_{50}). The OD_{570} value for the GI_{50} was calculated using the following formula:

$$OD_{570} \text{ at } GI_{50} = \frac{Control\ OD_{570} - Initial\ OD_{570}}{2} + Initial\ OD_{570}$$

where Control OD_{570} represents the absorbance of non treated cells in the end of the treatment and Initial OD_{570} stands for absorbance of untreated cell at the time when cells were initially treated. The concentrations at which cell growth is inhibited by 50% (GI_{50}) were calculated from the dose-response curves estimated by linear interpolation between two closest values after taking into account the initial optical density acquired at the time of treatment. MTT assays were carried out on three separate occasions with at least three repeats and mean GI_{50} values were calculated.

3.1.2.2 *Colony formation assay*

The clonogenic cell survival assay was used in order to evaluate the ability of colorectal and pancreatic cancer cells to produce colonies after brief treatment with GEM, GEM C14 and blank and GEM C14 containing NC systems. Briefly, cells were seeded at low concentrations (300-400/well) in 6-well plates and cultured for 24 hours. Cells were exposed to free GEM, GEM C14 GEM C14 NCs in concentration of 10, 100 and 500 nM and blank NCs for 24 hours. The gemcitabine-containing culture medium was replaced by a drug-free medium. Surviving cells were incubated at 37 ^{o}C for 7 and 14 days for HCT 116 and MIA PaCa-2 cells respectively, to allow formation of colonies. When colonies in control wells contained > 50 cells colonies were fixed, stained and counted. Colonies were fixed in 100% MeOH for 10 min, followed by staining with 0.05% methylene blue in 1:1 d.$H_2$0:MeOH forl 10 min. Methylene blue was rinsed with tap water, colonies were air-dried and counted.

Plating efficiency represents the percentage of colonies formed in control wells, compared to the number of cells seeded. This parameter varied between 40 and 60% for both HCT 116 and MIA PaCa-2 cell line.

After colonies were counted, IC_{50} values were calculated. IC_{50} value represents the concentration where the number of colonies in treated wells is reduced to 50% compared to control. First, the number of colonies was expressed as a fraction of control and then IC_{50} was calculated from dose response parameters by interpolation between 2 closest values. At least three independent survival experiments with one repeat were performed for each cell line. Groups were compared with one-way analysis of variance where groups were greater than two.

3.2 Effect of NCs on cancer cell lines

Two human tumour cell lines: colon – HCT 116 and pancreatic – MiaPaCa-2, were used to assess the *in vitro* activity of NCs. All four NC systems whose formulations are presented in Chapter 2 (HA 80; HA 40; PGA 80 and PGA 40) were tested blank or loaded with GEM C14 and compared with activity of GEM C14 prodrug and GEM-HCl. Growth inhibition and colony formation of cancer cells after the treatment with NCs has been assessed.

3.2.1 Growth inhibition of HCT 116 and MiaPaCa-2

Human colorectal and pancreatic carcinoma cells were exposed to serial dilutions of NCs (blank or loaded with the drug) and to drug alone for 72 h. Subsequently, MTT assay as described in 3.1.2.1. was carried out to assess cell viability. Examples of dose-response curves are shown in Figure 3-1.

It can be seen that the HCT 116 cell line is sensitive to all tested formulations with concentration-dependent profiles. However, a difference between the cytotoxicity profiles for blank, loaded NCs and the free drug could be observed. While blank NCs evoke sensitivity only at the two highest concentrations, loaded NCs as well as free drugs show higher potency against cancer cells.

Similar growth inhibitory profiles are noted for the MiaPaca-2 cell line (Figure 3-1B). Nevertheless, it should be noted that the growth curve of HA 80 nm NCs loaded with GEM C14 is almost overlapping with the

growth inhibitory curve of drug alone (GEM C14), showing that these two systems have similar activity in MiaPaCa-2 cells.

Growth curves of all blank NCs were very similar, with no significant difference between the profiles of NCs which are coated with the different polymers. Additionally, the reduction in size of NCs from 80 to 40 nm did not bring any different effects on either cancer cell line. GEM C14-loaded NCs also exhibit similar profiles independent of polymer coating or size of NCs. These individual growth curves are available in Appendix 3. In work of Elbaz *et al*. similar effects were reported. Doxorubicin (DOX) Ag-NPs were coated with 3 different polymers. Use of polyvinyl alcohol (PVA), polyethylene glycol (PEG) or polyvinyl pyrrolidone (PVP) as a polymer coating of DOX-Ag-NPs did not cause any significant difference on the percentage of viable breast cancer (MCF-7) cells[211].

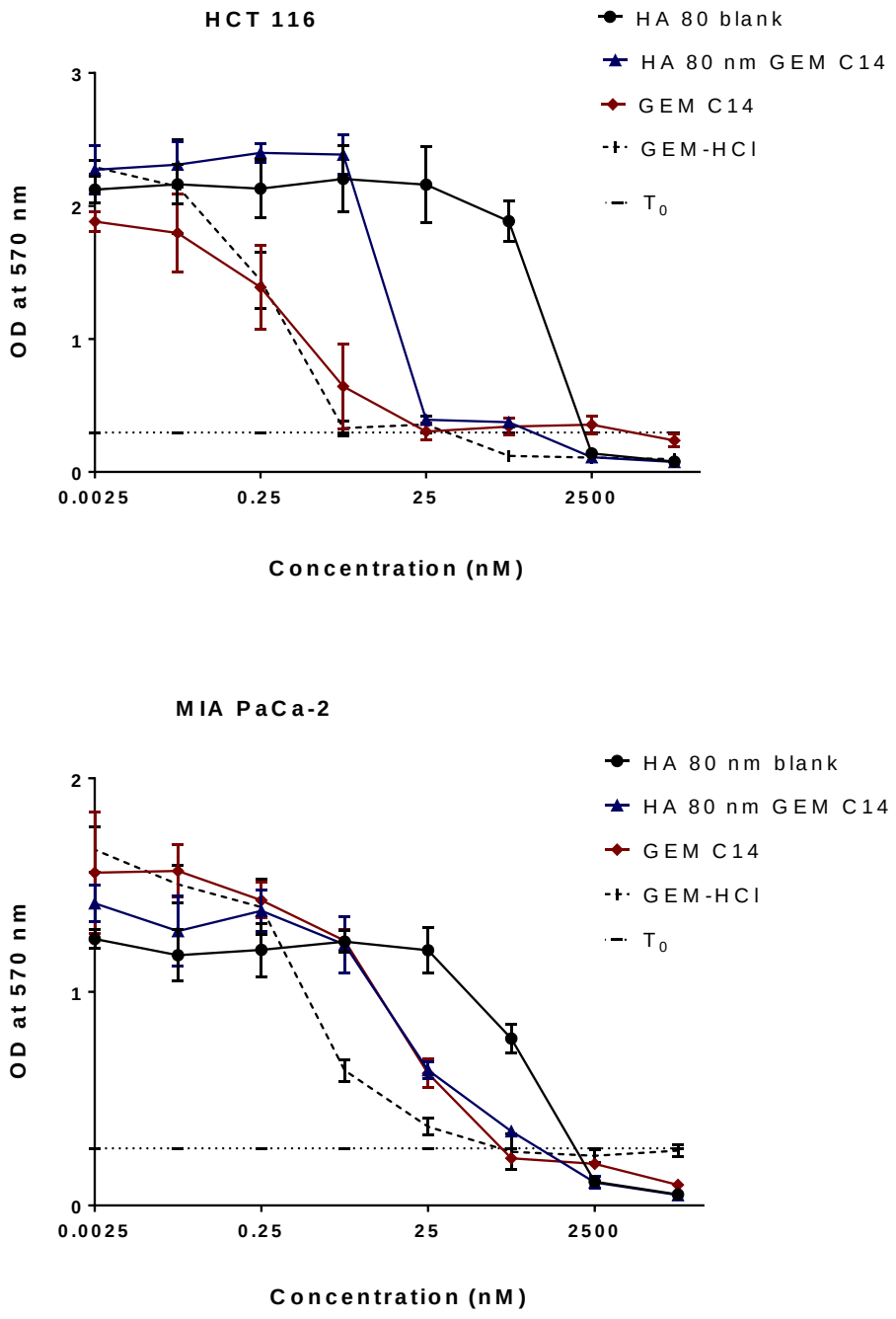


Figure 3-1 Example dose-response curves generated from 72 h MTT assay data for (top) HCT 116 and (bottom) MiaPaCa-2 cells treated with HA 80 nm NCs (blank or loaded with GEM C14), GEM C14 and GEM-HCl. Blank NCs do not contain drug and are diluted in the same way as loaded NCs in order to match amount of NCs.

In order to highlight differences between the systems investigated, GI_{50} values are presented in Table 3-1. Additionally, in Figures 3-2 and 3-3 statistical differences are illustrated.

Table 3-1 Mean GI_{50} values (nM) ± s.d. of tumour cell lines following 72 h treatment, with all types of blank or GEM C14 loaded NCs and with GEM-HCl or modified GEM alone, generated by MTT cell viability assay.

System/cell line	HCT 116	MIA PaCa - 2
HA 80 nm GEM C14	15 ± 6	10 ± 9
PGA 80 nm GEM C14	8 ± 1	11 ± 6
HA 40 nm GEM C14	8 ± 3	14 ± 10
PGA 40 nm GEM C14	10 ± 8	11 ± 3
HA 80 nm blank	1203 ± 460	250 ± 43
PGA 80 nm blank	702 ± 234	374 ± 263
HA 40 nm blank	820 ± 413	439 ± 250
PGA 40 nm blank	596 ± 173	254 ± 132
GEM C14	2 ± 1	20 ± 1
GEM HCl	1 ± 1	6 ± 4

GEM C14, GEM-HCl and all NCs loaded with GEM C14 evoke sub-µM GI_{50} values in both cancer cell lines, which can be interpreted as a very good potency. The GI_{50} values of all systems containing drug fall within an order of magnitude of each other, demonstrating a narrow range. On the other hand, the results showed a 10 to 100-fold difference in cytotoxicity when blank NCs were compared to the drug-containing NCs.

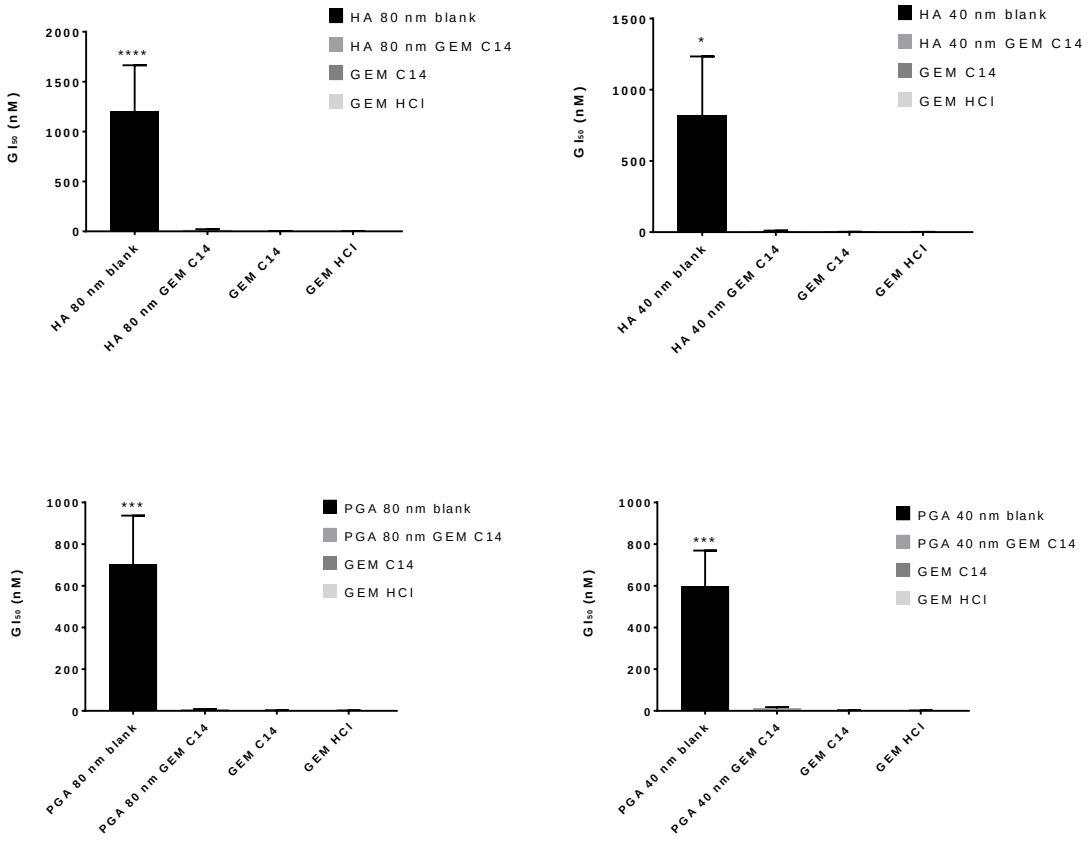


*Figure 3-2 Growth inhibition studies on all blank and loaded NCs compared to drugs alone on HCT 116 cell line. One-way ANOVA Tukey's multiple comparisons test ****(p<0.0001); ***(p<0.001); **(p<0.01); *(p<0.05). Mean values (n=3) are shown, error bars represent standard deviation of the mean, where n is number of independent trials.*

Groups from Table 3-1 were compared with one-way analysis of variance with Tukey correction and after the treatment of HCT 116 cells, no significant difference is noted among blank nor among loaded NCs (data not shown). However, there is a significant difference between loaded and blank NCs ($p<0.05$; Figure 3-2). These results imply that the growth inhibition of colorectal cancer cells is mainly due to drug activity. GI_{50} values of GEM C14 and GEM-HCl were not significantly different from GI_{50} values of loaded NCs, but they were significantly

different from blank NCs. Moreover, similar statistical analyses results are obtained for the MiaPaCa-2 cell line (Figure 3-3).

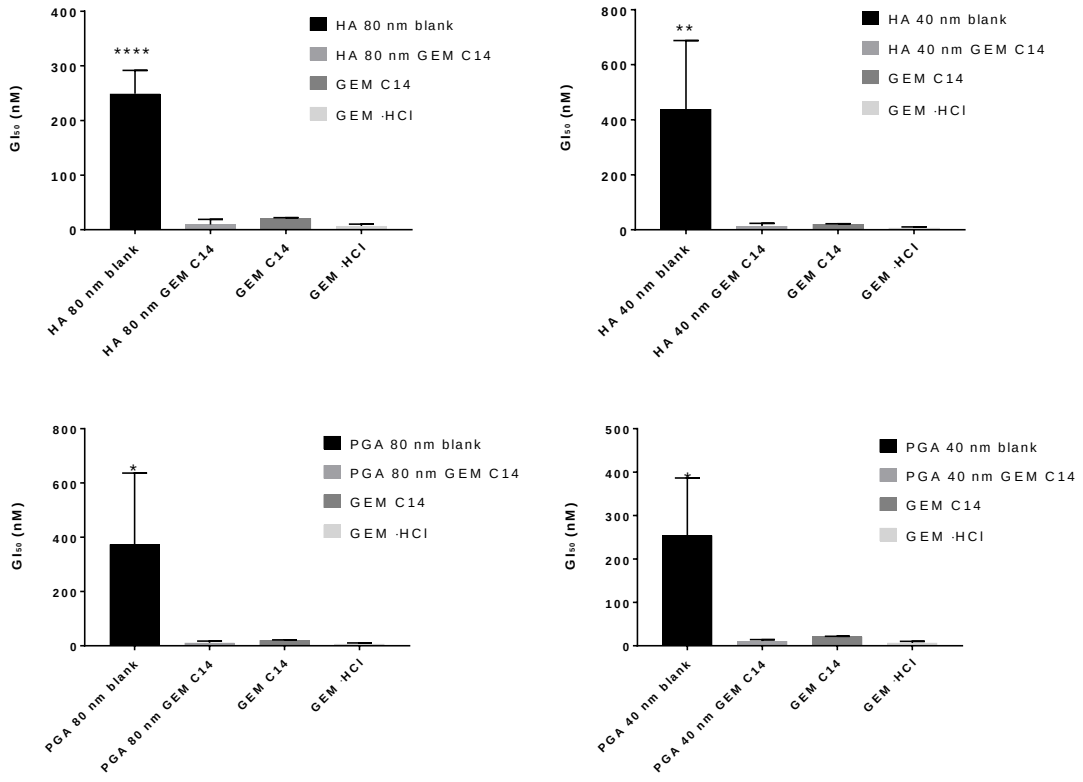


*Figure 3-3 Growth inhibition studies on all blank and loaded NCs compared to drugs alone on MiaPaCA-2 cell line. One-way ANOVA Tukey's multiple comparisons test ****(p<0.0001); ***(p<0.001); **(p<0.01); *(p<0.05). Mean values (n=3) are shown, error bars represent standard deviation of the mean, where n is number of independent trials.*

Interestingly, GEM C14 and GEM-HCl showed similar growth inhibitory profiles, indicating that modification of GEM on *N*-terminal did not influence drug potency. On the other hand, this modification enabled the encapsulation of GEM into the lipid core of NCs. In already mentioned work of E. Dalla Pozza *et al*. it was also shown that commercially available and modified (C12 chain) GEM have similar *in vitro* effects on MiaPaCa-2 and VIT1 pancreatic cell lines. Additionally,

their previous studies showed that modified GEM has a longer half-life in plasma and higher *in vitro* toxicity compared to the free drug. In the work of Yu. *et al.* the equivalent toxicity of C14 modified GEM to non-modified GEM on BxPC-3 cell line was also reported[227].

Although not statistically significant, a slightly lower GI_{50} value of GEM C14-loaded NCs (10 to 14 nm) over the one of the GEM C14 free drug (20 nm) was observed for MIA PaCa -2 cell line. The explanation could the related to the different cellular uptake mechanisms of the free and encapsulated drug. This was hypothesised by Bastianchic *et al.,* investigating cytotoxicity of GEM-C12 prodrug loaded into lipid NCs on glioma U 87 cancer cells. IC_{50} values of their GEM-C12-loaded NCs and free GEM C12 prodrug were in micromolar region (0.18 and 0.56 μM respectively)[235] which is higher than what we report for similar GEM C14 prodrug although against different cancer cell line. Similarly, higher activity of drug loaded into NCs compared to free drug was reported by L.R. Jaidev *et al*. Indeed, GEM loaded into PLGA nanospheres gave 45% and 54% lower IC_{50} values than free drug when tested *in vitro* on MiaPaCa-2 and ASPC-1 pancreatic cell lines. Interestingly, this effect was not confirmed in PANC-1 cells, where the IC_{50} value was 29% higher for GEM-loaded nanospheres compared to free GEM. Their work supports the thesis that nanospheres may use other uptake mechanisms, such as endocytosis, which contributed to toxicity of the polymeric nanospheres[231]. Additionally, Yu *et al.* reported no significant difference in toxicity between GEM, GEM C14 and albumin-GEM nanoparticles, as a result of *in vitro* cytotoxicity assays on the BxPC-3 pancreatic cancer cell line. However, in an *in vivo* tumour model, significantly slow tumour growth was monitored in albumin nanoparticles treated mice compared to mice treated with GEM or GEM-C14 alone[227].

Considering that GEM in its mechanism of action replaces one of the building blocks of nucleic acids during DNA replication for which it has to enter the cell, we can speculate from this data that GEM-C14-loaded NCs can enter the cancer cells and deliver the drug into the cytosol, from where the drug may diffuse into the nuclei. Further discussion on the mechanism of internalisation is not possible without performing additional assays. Assays that could elucidate this mechanism better include tritiated thymidine incorporation assays which together with cell counts can determine whether DNA is replicating; flow cytometry assays to determine cell cycling; gamma-H2AX to determine DNA double strand break damage.

Overall, it can be concluded that polymeric NCs managed to successfully deliver the loaded GEM prodrug and lead to the expected growth inhibitory effects on colorectal and pancreatic cancer cells.

3.3 Colony formation after the treatment with NCs

The ability of the cancer cells to form colonies after 24 h exposure to NCs (blank or loaded) and the free drugs was assessed. The experimental procedure for this test is described in 3.1.2.2. The concentration of free drug or drug in NCs used in this experiment ranged between 10 and 500 nM. These concentrations were derived from GI_{50} values obtained by MTT assay and this wide range was taken so that GI_{50} values of all formulations would be included in the clonogenic assays. Although, it should be noted that while the number of cells initially seeded in MTT assays was 10^3, for clonogenic assay only 300-400 cells were seeded prior to the treatment. However, the 2 assays examine different phenomena. The MTT assay was designed to examine the ability of drug to inhibit growth / proliferation of cells

undergoing continuous exposure to the drug. The principle of the clonogenic cell survival assay is to determine the ability of a cell to survive brief challenge (24 h) with the test agent and retain proliferative capacity, thereby maintaining its reproductive ability to form a colony, or re-populate a tumour.

3.3.1 The clonogenic cell survival of HCT 116 and MIA PaCa-2 cancer cells

The number of colonies formed (colony forming units – CFU) upon the treatment of HCT 116 cells with all 4 types of blank NCs as well as their paired GEM C14 loaded NCs are shown in figures 3-4 and 3-5. The ability of cells to survive exposure and proliferate after treatment is compared with control, untreated cells 'capacity to form colonies un-impeded by any test agent. Blank NCs do not contain drug and are diluted in the same way as loaded NCs. Therefore, the x-axis in Figure 3-4 is labelled with equivalent concentration although there is no drug present.

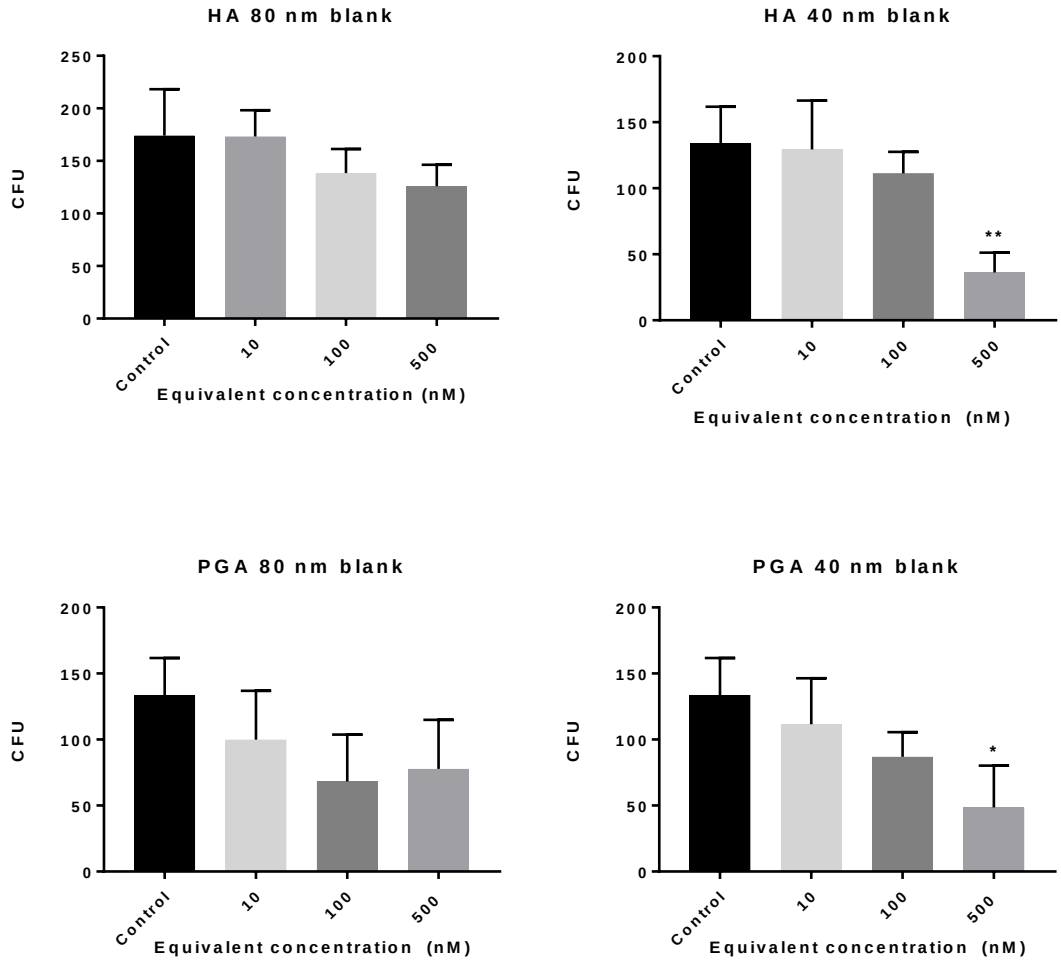


*Figure 3-4 Influence of NC concentration on number of colonies formed after the treatment of HCT 116 cells with the blank NCs. Blank NCs do not contain drug but they are diluted in the same way as loaded ones. 1 way ANOVA Dunnett's multiple comparison test, NCs compared with number of colonies in control *($p<0.05$); **($p<0.01$).*

It can be seen that blank NCs diluted in a way that they match the amount of loaded NCs in concentration of 10 and 100 nM, negligibly impact number of colonies formed. However, for 500 nM blank NCs number of colonies is slightly reduced especially for the NCs with the smaller size (HA 40 nm and PGA 40 nm) which were statistically different from the control ($p<0.05$). Smaller NCs have lower oil and

higher surfactant content than the larger ones. It is possible that elevated surfactant concentration can influence the toxicity of the system and cause the reduction in the number of colonies formed. Oyarzun-Ampuero *et al.* also reported toxicity of blank NCs in the presence of cationic surfactant (CTAB or benzalkonium chloride) at higher concentrations[162]. They drew their conclusion from cell viability data and not from a clonogenic assay. Nevertheless, as already discussed, considering local delivery of anticancer drug to the tumour, slight toxicity as a consequence of surfactant amount should not be prohibitive for this application.

In the case of GEM C14-loaded NCs (Figure 3-5) 100 and 500 nM GEM C14 concentrations caused significant reduction in the number of colonies, while for 10 nM treatment the number of colonies remained similar to the control (~150 colonies).

The effect of free drug (GEM C14 and GEM-HCl) on HCT 116 cell colony formation is presented in Figure 3-6. After treatment with 100 and 500 nM of these drugs almost no colonies formed. The lowest concentration (10 nM) of either GEM C14 or GEM-HCl decreased the number of colonies at least 2-fold compared to the number of colonies in control.

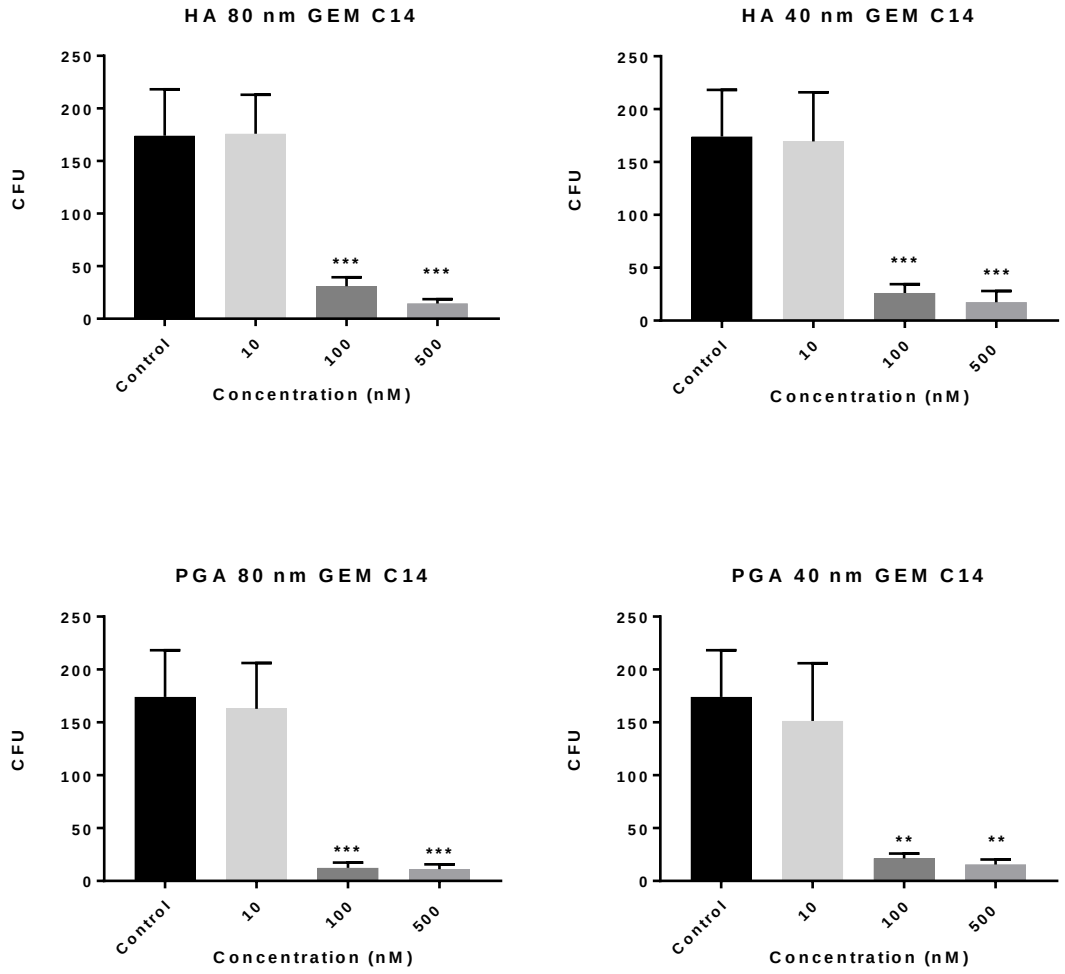


*Figure 3-5 Influence of GEM C14 concentration on number of colonies formed after the treatment of HCT 116 cells with the loaded NCs. Control presents number of colonies for non-treated cells. 1 way ANOVA Dunnett's multiple comparison test, NCs compared with number of colonies in control. ***(p<0.001); **(p<0.01).*

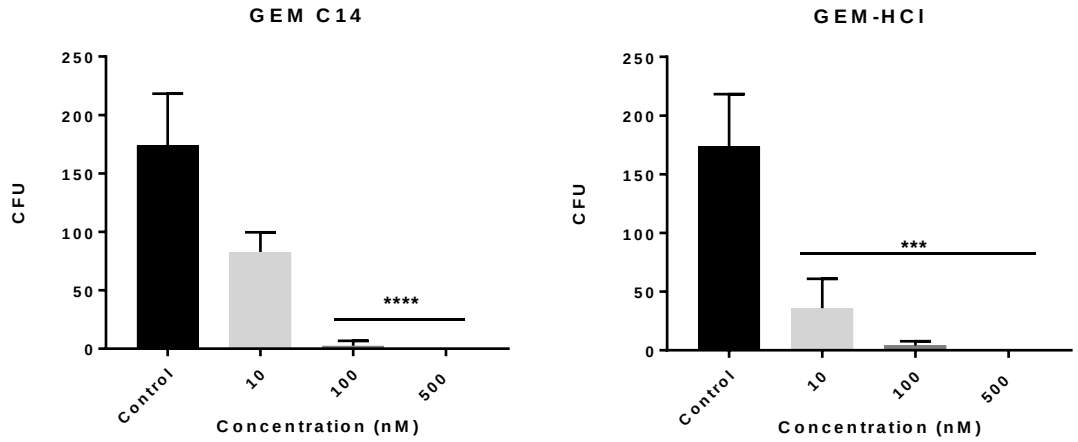


*Figure 3-6 Influence of GEM C14 versus GEM-HCl concentration on number of colonies formed after the 24h treatment of HCT 116 cells with drug alone. 1 way ANOVA Dunnett's multiple comparison test, NCs compared with number of colonies in control. ****(p<0.0001); ***(p<0.001).*

The clonogenic cell survival assay was also performed in MIA PaCa-2 cells. Examination of the effect of blank NCs on the number of colonies (Figure 3-7) revealed concentration-dependent decrease in colony formation. The highest amount of blank NCs (500 nM) reduced the number of colonies from 174±44 (control) to 50±39 (HA 80 blank).

As expected, an even greater reduction in the number of colonies was detected when MIA PaCA-2 cells were briefly exposed to GEM C14-loaded NCs, where the highest concentration of GEM C14 (500 nm) reduced the number of colonies from 174±44 (control) to 1±1 (HA 80 nm) (see Figure 3-8). Neither polymer coating nor NC size confer distinctions in survival among blank and loaded NCs. Free and unmodified drug seem to cause similar effects as drug-loaded NCs (Figure 3-9).

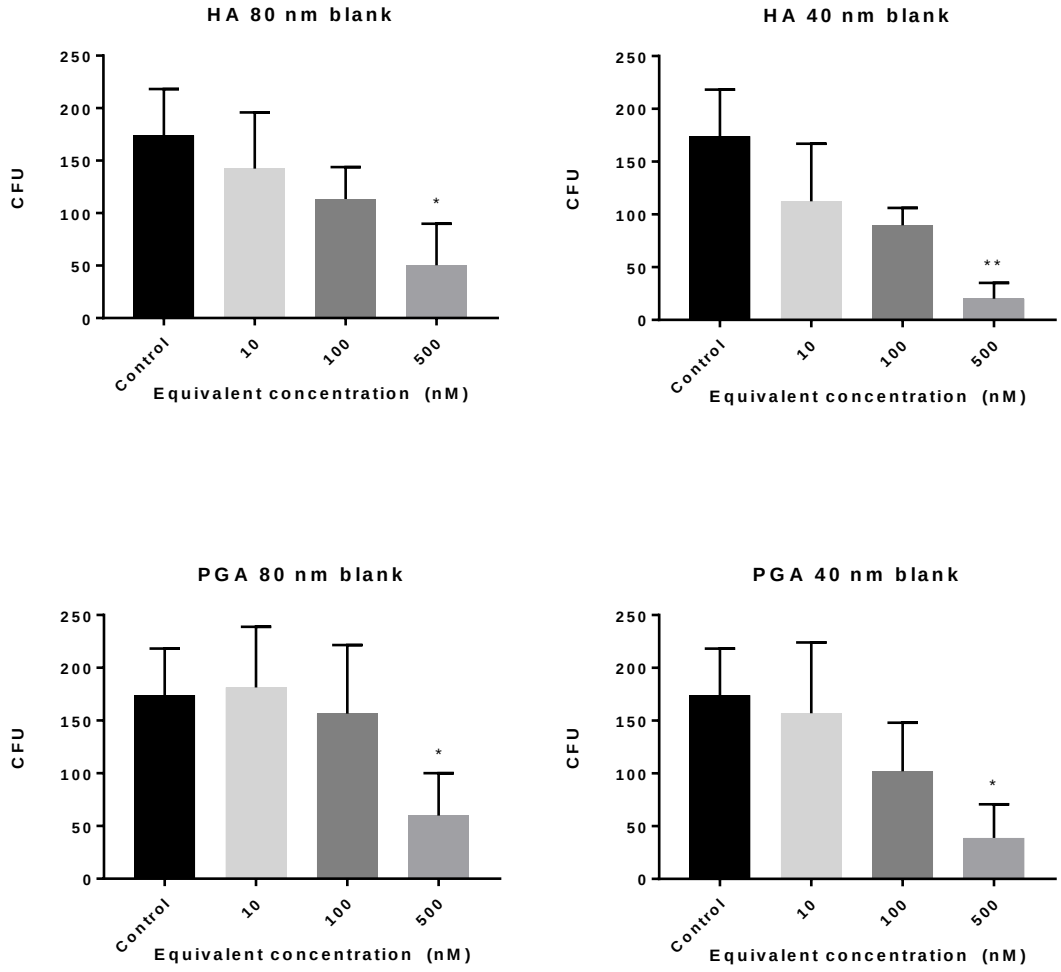


*Figure 3-7 Influence of NCs' concentration on number of colonies formed after the treatment of MIA PaCa-2 cell line with the blank NCs. 1 way ANOVA Dunnett's multiple comparison test, NCs compared with number of colonies in control. *($p<0.05$); **($p<0.01$).*

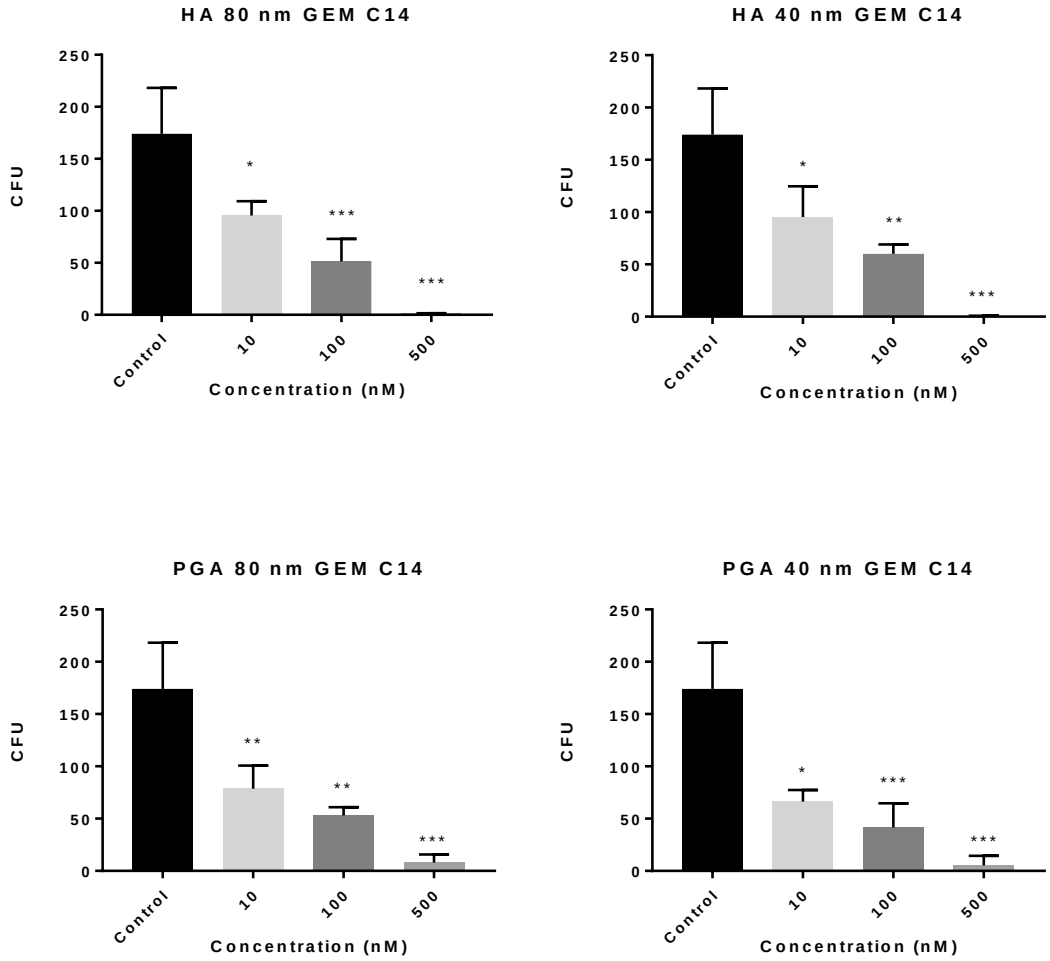


*Figure 3-8 Influence of GEM C14 concentration on number of colonies formed after the treatment of MIA-PaCa-2 cell line with the loaded NCs. Control presents number of colonies for non-treated cells. 1 way ANOVA Dunnett's multiple comparison test, NCs compared with number of colonies in control. *($p<0.05$) ***($p<0.001$); **($p<0.01$).*

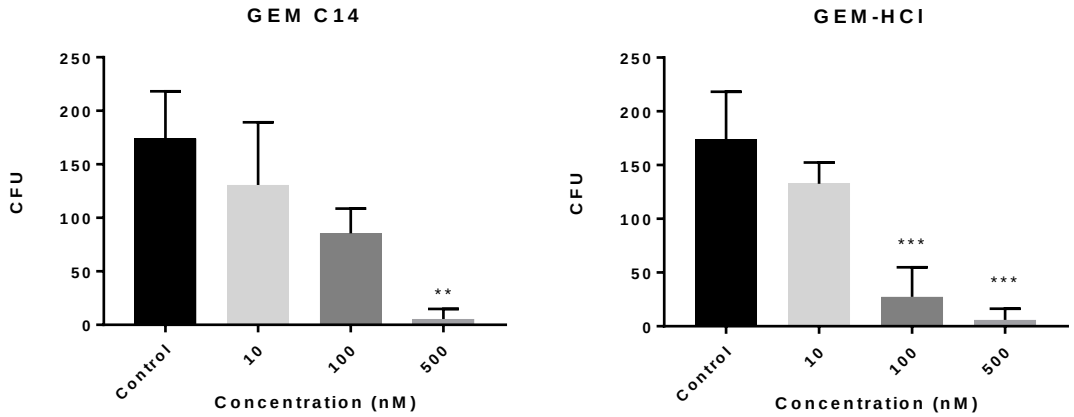


*Figure 3-9 Influence of GEM C14 versus GEM-HCl concentration on number of colonies formed after the 24h treatment of MIA PaCA-2 cells with drug alone. 1 way ANOVA Dunnett's multiple comparison test, NCs compared with number of colonies in control. ***(p<0.001); **(p<0.01).*

3.3.2 IC_{50} values

In order to better detect differences between blank and loaded NCs, and compare their effect with free drugs on colony formation in pancreatic and colorectal cancer cells, IC_{50} values were calculated as described in 3.1.2.2. and compared using one-way analysis of variance with Tukey correction. Calculated IC_{50} values for all systems in both cell lines (HCT 116 and MIA PaCA-2) are presented in Table 3-2. Summaries detailing significantly different IC_{50} values are presented in Figures 3-10 and 3-11.

Table 3-2 IC_{50} values (nM) of all blank and loaded NCs on colorectal and pancreatic cancer cell line.

System/Cell line	***HCT 116***	***MiaPaCa-2***
HA 80 nm blank NCs	485 ± 135	352 ± 7
HA 40 nm blank NCs	365 ± 100	247 ± 95
PGA 80 nm blank NCs	380 ± 149	362 ± 123
PGA 40 nm blank NCs	367 ± 126	291 ± 122
HA 80 nm GEM C14 NCs	87 ± 15	127 ± 25
HA 40 nm GEM C14 NCs	86 ± 20	88 ± 54
PGA 80 nm GEM C14 NCs	73 ± 10	89 ± 25
PGA 40 nm GEM C14 NCs	80 ± 20	98 ± 43
GEM C14	37 ± 7	161 ± 29
GEM-HCl	11 ± 7	83 ± 20

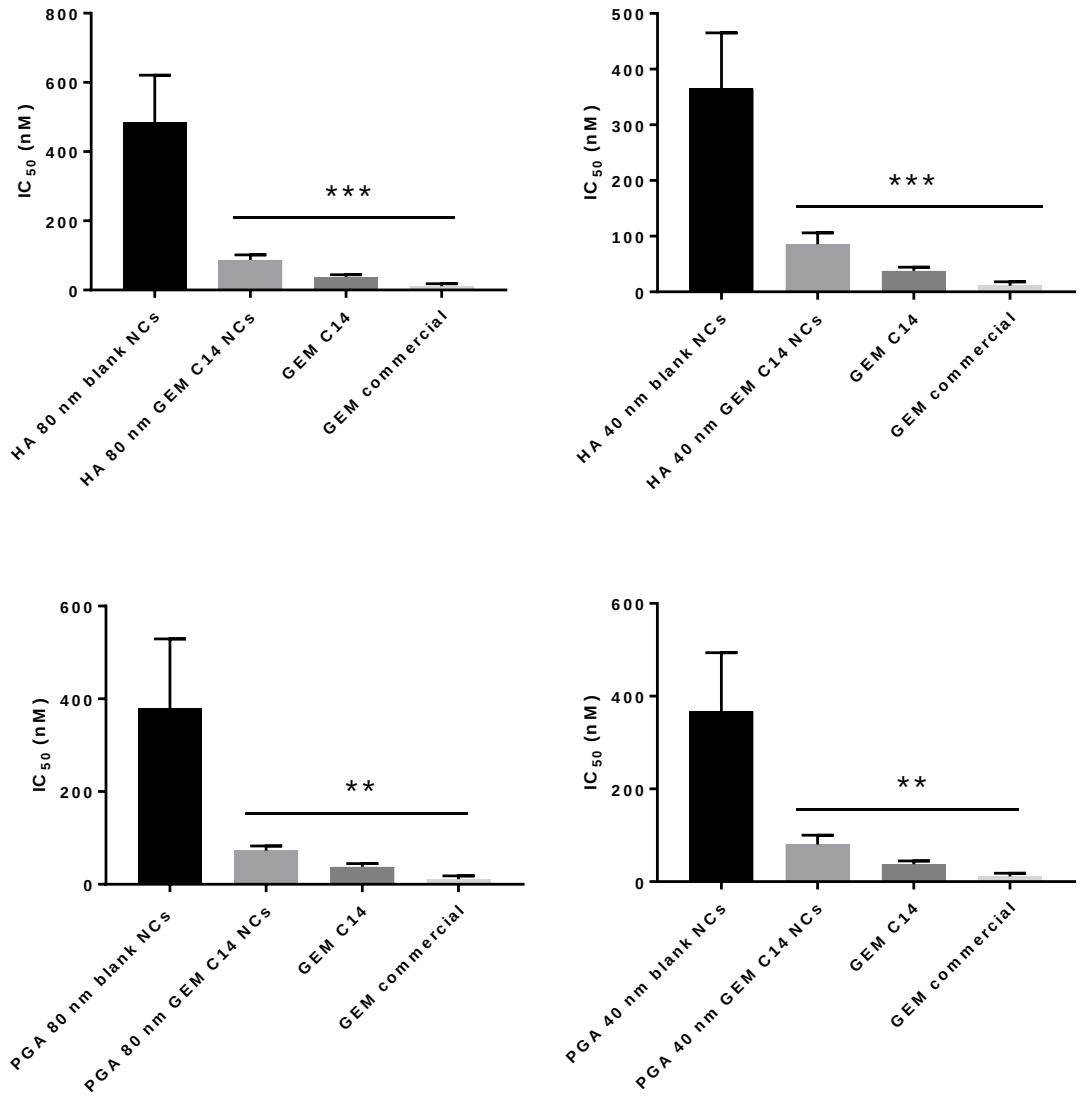


*Figure 3-10 IC_{50} values for all systems of blank, loaded NCs and non-encapsulated drug on HCT 116 cell line calculated from clonogenic assay data. ***($p<0.001$); **($p<0.01$).*

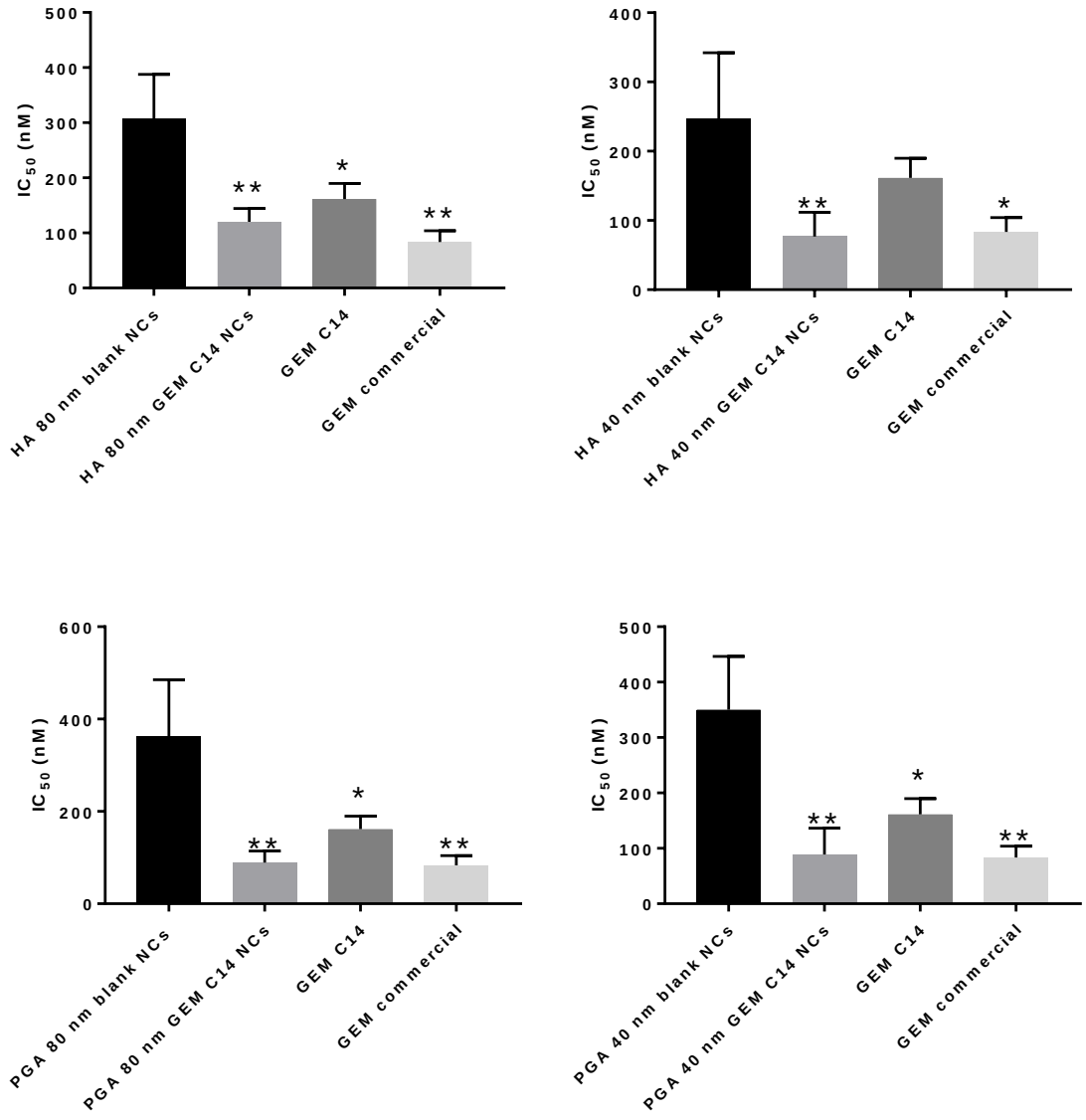


*Figure 3-11 IC_{50} values for all systems of blank, loaded NCs and non-encapsulated drug on MIA-PaCa-2 cell line calculated from clonogenic assay data. **(p<0.01); *(p<0.05).*

IC_{50} values for the colorectal cell line show a significant difference between blank NCs and their GEM C14-loaded pair. Similarly, blank NCs have significantly higher IC_{50} value than free drug, while there is no significant difference between loaded NCs and free drug (Fig. 3-10).

A quite similar statistical analysis is obtained for the MIA PaCa-2 cell line. IC_{50} values of blank NCs are statistically different from loaded NCs and free drug, with p values slightly higher than for HCT 116 cells (Fig. 3-11). These results concur with conclusion drawn from growth inhibitory (MTT) assays, hence supporting literature described above (3.2.1.).

Interestingly, if IC_{50} values of the same system are compared between two cell lines (HCT 116 and MiaPaCa-2), no significant difference can be found. For instance, IC_{50} values of HA 80 blank NCs in HCT 116 cells is not significantly different from IC_{50} values of the same systems in MIA PaCa -2 cells. However, there is a significant difference when IC_{50} values of GEM C14 are compared between these two cell lines. The same conclusion stands for GEM-HCl. This may be a consequence of variable cancer cell line sensitivity to GEM. GEM sensitivity was screened in a wide range of pancreatic cell lines by Iwamoto *et al.* Pancreatic cancer cell lines, such as MIAPaCa-2, Panc-1, BxPC-3, were very sensitive to GEM and showed low IC_{50} values (6.81, 8.07, 6.67 μg/mL). On the other hand, PK45p and PK59 cell lines exhibited IC_{50} values that are 30-50 times higher (417 and 295 μg/mL), and are characterised as gemcitabine-resistant cancer cell lines[255]. Overall, there is distinctive toxicity of loaded NCs when compared to blank NCs and ability of NCs to deliver the drug to cancer cells is shown.

3.4 Can NCs overcome drug resistance?

Treatment of human cancers very often includes chemotherapy. Unfortunately, this type of therapy is frequently limited because of inherent or acquired resistance to the drugs used. After prolonged treatment, the chemotherapy becomes ineffective as cancer cells

develop resistance to more than one agent i.e. multi drug resistance (MDR). Various mechanisms involved in drug resistance include: drug elimination, detoxification, increased DNA repair activity, reduced uptake due to lack of receptors/transporters, defective apoptotic pathways, over expression of drug efflux pumps and many others[256]. Increased expression of transporter proteins (efflux pumps) that lowers drug concentration inside the cell is one of mechanisms majorly reported to contribute to MDR[257]. More than 200 proteins that participate in molecules' transport through the cell are members of ABC (ATP-binding cassette) family. Most of the efflux pumps involved in cancer drug resistance belong to this ABC family of proteins and include permeability glycoprotein (P-gp; MDR1 protein), followed by multidrug resistance associated proteins (MRP1-MRP9), and breast cancer resistance protein (BCRP)[258]. P-gp protein is widely explored and highly expressed on colon, kidney, pancreas and liver carcinoma and lower P-gp levels are expressed in breast, ovary, lung, oesophagus, stomach, lymphomas and confer acquired resistance[259]. Some of the drugs that are affected by presence of efflux pumps are vinblastine, vincristine, doxorubicin, daunorubicin, actinomycin, paclitaxel[260]. A protein that does not belong to ABC family and it is often included in discussion on MDR is lung resistance protein (LRP) situated in cytoplasm in ribonucleoprotein particles. It has been reported that this protein is responsible for hindering the access of drugs to their intracellular targets[261].

Approaches to overcome drug resistance include the synthesis of prodrugs which under enzymatic or chemical transformation improve delivery and release of drug[142], as well as the conjugation with ligands (peptides, antibodies, growth factors etc.) and adoption of a stimulus-responsive concept[253,262,263]. Additionally, targeting efflux transporter

proteins by combination therapy with chemosensitisers, or use of small interfering RNA to down regulate MDR related proteins to secure access for chemotherapeutic agents or nanocarriers, has been explored[264–267]. An alternative and straight-forward approach involves the drug encapsulation into nanocarriers[257,268,269].

3.4.1 Are vincristine (VC) resistant cells resistant to gemcitabine?

Here activity of polymeric NCs on an MDR cell line was evaluated. A colon cancer cell line (HCT 116) resistant to vincristine was developed by Vijay Raja. HCT 116 cells were exposed to stepwise incremental concentrations of VC and after 6 months, stable acquired resistance was developed; cells survived and were routinely maintained in nutrient medium spiked with 2 μM VC. It was established that these cells expressed P-gp[270].

Firstly, we examined whether HCT 116 VR cells demonstrated resistance towards naked drugs i.e. GEM-HCl and GEM C14.

GI_{50} values of GEM C14 or GEM-HCl, obtained from MTT assays performed in the HCT 116 VR cell line, were 8 ± 10 and 6 ± 10 nM respectively. These nanomolar values demonstrate the sensitivity of HCT 116 VR cells towards GEM, therefore, they are unsuitable for testing the hypothesis that NCs may overcome drug resistance. Dose response curves illustrating GEM activity on the HCT 116 VR cell line are available in Appendix 4. The reason for the absence of resistance to GEM on VC resistant cell line might be GEM is not a P-gp substrate. Moreover, resistance to GEM is developed *via* different mechanisms, such as alterations in nucleoside transporters, high levels of cytidine

deaminase, mutation on the p53 gene, overexpression of ribonucleotide reductase and thymidylate synthase, as discussed in Chapter 1.

3.4.2 **GEM resistant cell line**

A pancreatic GEM resistant cell line was obtained by continuous culture of parental Panc-1 cells in gemcitabine and maintained with gemcitabine at a dose of 1 μM. This cell line was developed and kindly donated by Lodewijk Dekker. Thus, was offered the possibility of testing the activity of free drug and drug-loaded NCs on both sensitive and GEM-resistant pancreatic cancer cells (GEM R Panc-1).

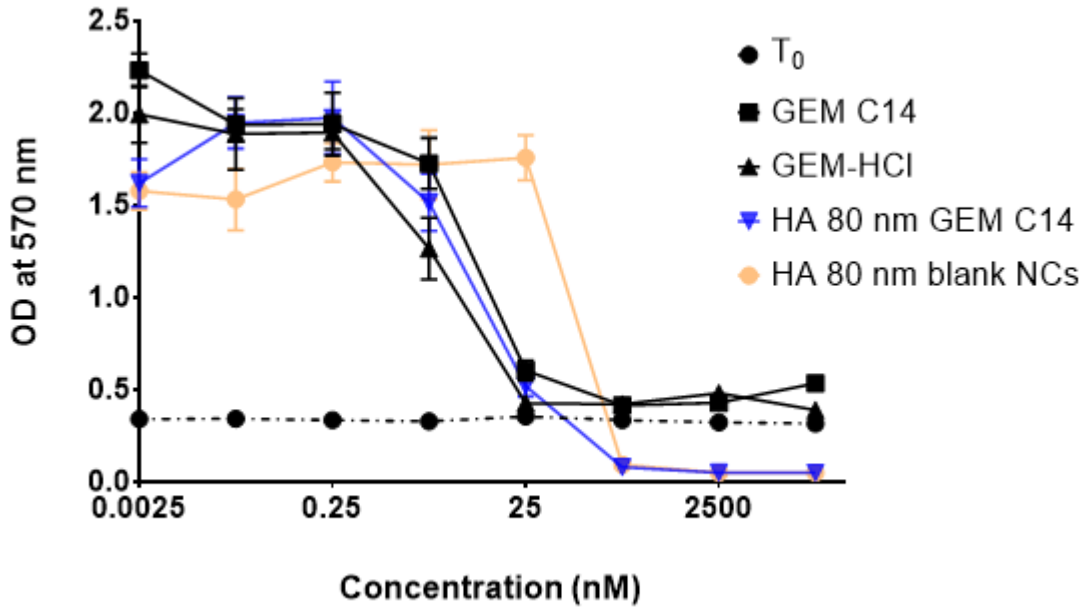


Figure 3-12 Growth inhibitory profiles of HA 80 nm NCs blank or loaded with GEM C14 and for GEM-HCl or modified GEM on Panc-1 cell line.

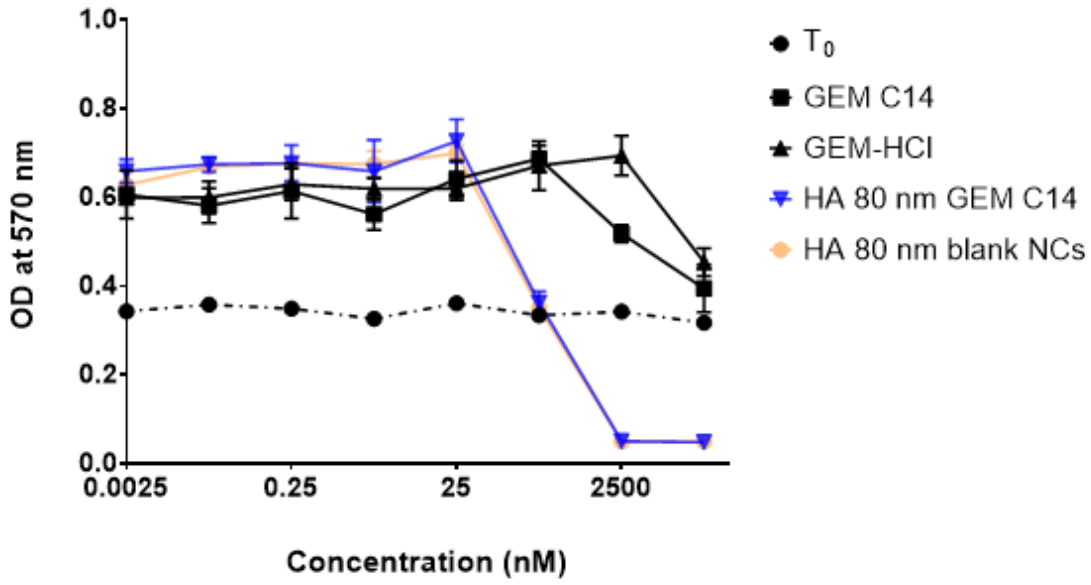


Figure 3-13 Growth inhibitory profiles of HA 80 nm NCs blank or loaded with GEM C14 and for GEM-HCl or modified GEM on GEM resistant Panc-1 cell line.

Example dose-response curves generated from 72 h MTT assay data for Panc-1 and GEM resistant Panc-1 cell lines treated with HA 80 nm blank or NCs loaded with GEM C14 and with commercial or modified GEM are presented in Figures 3-12 and 3-13.

Figure 3-12 shows similar dose response curves to that of MIA PaCa-2 and HCT 116, blank NCs show reduced activity against Panc-1 cell line, while loaded NCs and free drug exert higher growth inhibitory activity revealing similar profiles. In contrast, in the GEM resistant Panc-1 cell line (Fig. 3-13) the free drug in the form of either GEM C14 or GEM-HCl exhibited negligible growth inhibitory effects except at the highest concentration (25 μM). NCs, either blank or loaded with GEM showed a much higher potency with no significant difference between blank and loaded NCs suggesting that the empty NCs give activity. Calculated GI_{50} values are presented in Table 3-3.

Table 3-3 Mean GI_{50} values (nM) ± s.d. in tumour cell lines following 72 h treatment, with HA 80 nm NCs blank or loaded with GEM C14 and for GEM-HCl or modified GEM, generated by MTT cell viability assay. Resistance factor (Rf) is ratio of GI_{50} values of the same system compared between sensitive and resistant cell lines.

GI_{50} (nM)	***Panc-1***	***Panc-1 GEM Resistant***	***Rf***
HA 80 nm blank	293 ± 50	760 ± 246	2.6
HA 80 nm GEM C14	13 ± 3	410 ± 463	31.5
GEM C14	14 ± 1	8300 ± 5523	592.9
GEM-HCl	7 ± 3	20124 ± 4521	2857.1

On the other hand, the GI_{50} values observed in the Panc-1 and MIA PaCa-2 cell lines were very similar, as shown in Table 3-1. In that case, blank NCs exhibited a significantly lower toxicity compared to the loaded NCs and free drug ($p<0.001$, ANOVA), while no significant difference was observed among the drug-loaded NCs and the free drugs.

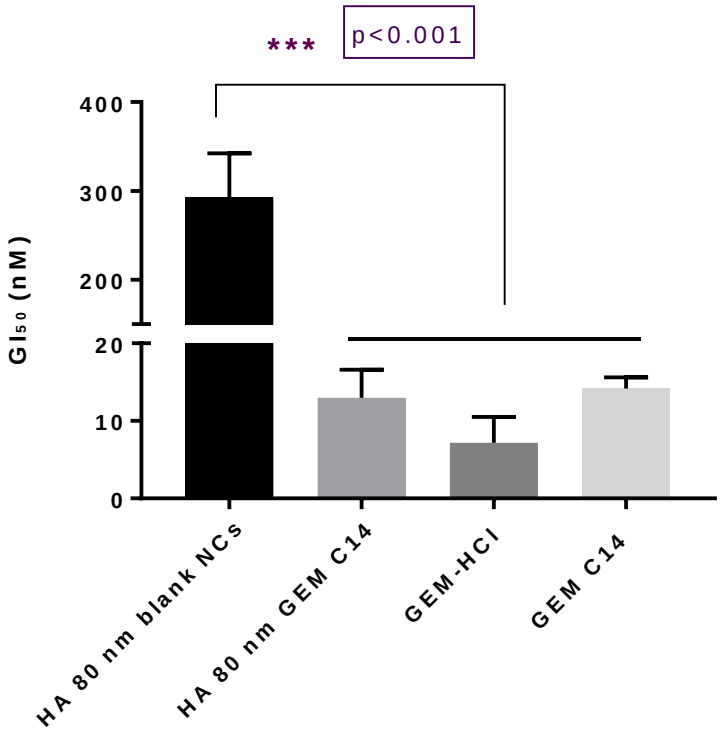


Figure 3-14 Mean GI_{50} values (nM) ± s.d. of Panc-1 cell line following 72 h treatment, with HA 80 nm NCs blank or loaded with GEM C14 and for GEM-HCl or GEM C14.

On the contrary, very high GI_{50} values (low potency) of free drug (GEM-HCl and GEM C14) on GEM resistant Panc-1 cell line are significantly different than GI_{50} values of loaded NCs. Nevertheless, loaded NCs did not totally reverse/overcome drug resistance i.e. HA GEM C14 loaded NCs did not achieve GI_{50} value in the same order of magnitude on Panc-1 and GEM R Panc-1. However, it is important to note that also the GI_{50} value of blank NCs is significantly lower than the GI_{50} value of free drug in GEM R Panc-1 cell line (Fig. 3-15).

The interaction between NPs and cells can be surfactant-dependent. Among many surfactants that showed influence, CTAB has shown major role as a chemosensitiser in reversing MDR[268,271]. The presence of CTAB

in blank NCs can possibly explain similar toxicity as of loaded NCs on GEM R pancreatic cell line.

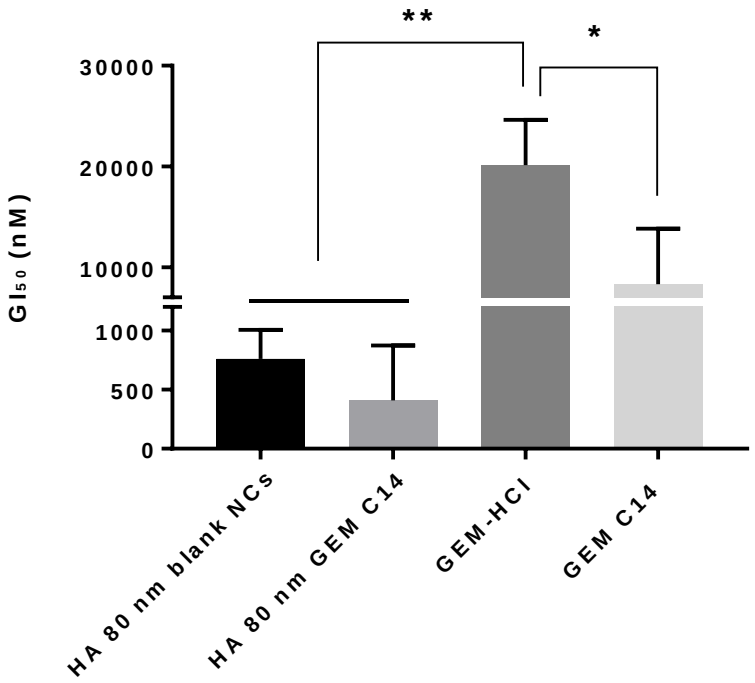


*Figure 3-15 Mean GI_{50} values (μM) ± s.d. of GEM resistant Panc-1 cell line following 72 h treatment, with HA 80 nm NCs blank or loaded with GEM C14 and for GEM-HCl or modified GEM. 1-way ANOVA: *(p<0.05); **(p< 0.005).*

Researchers are trying to develop systems that will circumvent MDR. One of the methods is an actual modification on the drug itself. A thorough review detailing promising modifications on gemcitabine was given by Moysan *et al*. Nevertheless, as it can be seen from Fig. 3-15 Panc-1 GEM resistant cells has acquired resistance for C14 modified GEM as well.

A resistance factor which compares the ratio of IC_{50} values for resistant and drug sensitive cell line is often used to describe the ability of a system to circumvent the resistance by comparing resistant factors of

free drug and nanocapsulated system. In the work of Kievit *et al.* resistance factor for free drug was 56 ± 2.3 and for loaded NPs this factor was 3.3 ± 0.1[272]. For free cisplatin, Krieger *et al.*, report resistance factor of 4.46 between cisplatin resistant and sensitive cell line, while for a liposomal formulation this factor was around 1[273]. The ratio between resistance factors of free and encapsulated drug in these two papers is 4 and 10 respectively.

In our work resistance factors for GEM-HCl, GEM C14 and GEM C14-loaded NCs are calculated by comparing GI_{50} values of these systems in Panc-1 sensitive and Panc-1 GEM resistant cell lines, the values are presented in Table 3-3. The ratio between resistance factor of free GEM C14 and encapsulated drug is 20, while for GEM-HCl it rises to 90. Compared with already reported literature data, these differences are significant. Moreover, we have shown that polymeric NCs represent a promising system in overcoming MDR taking into account that blank NCs also show activity probably due to the high surfactant content.

3.5 Summary

Here we report *in vitro* activity of polymeric NCs loaded with modified GEM in comparison with that of the free drug itself against two human cancer cell lines (HCT 116 and MIA PaCa-2). Additionally, the activity of polymeric NCs was assessed in pancreatic (Panc-1) cell lines: parent GEM-sensitive and its derivative GEM-resistant phenotype.

Antiproliferative assays revealed that GEM C14 and GEM C14-loaded NCs significantly inhibited growth and colony formation in human cancer cell lines.

The significant difference between loaded and blank NCs implies that the growth inhibition of cancer cells is mainly due to drug activity. GEM C14 and commercially GEM-HCl show similar growth inhibitory profiles, indicating that modification of GEM on N-terminal did not influence drug potency.

Comparing IC_{50} values derived from clonogenic cell survival assays, no significant difference can be found among NC formulations. However, HCT 116 and MIA PaCA-2 cell lines seem to show different sensitivity towards free drugs (GEM C14 and GEM-HCl).

The activity of NCs in Panc-1 cells is similar to that in HCT 116 and MIA PaCa-2 cell lines. GEM-resistant Panc-1 cells confers resistance towards modified GEM as well, while the situation is different for polymeric NCs. Resistance factors for GEM C14-loaded NCs, GEM C14 itself and GEM-HCl are 31.5, 592.9, and 2857.1 respectively, showing that NCs are far less susceptible to drug resistance than free drug. Although polymeric NCs are widely reported to deliver cytotoxic drug there is little information on their ability to overcome drug resistance. This study implies the use of NCs as a promising system for overcoming limitations

of acquired resistance in cancer cells. However, further examination should consider the effect of blank NCs in resistant cancer cell lines.

4 Gel-nanocapsule composites for localised cancer therapy

4.1 Systems designed for localised cancer therapy

The main aim of local drug delivery systems is to provide prolonged release at the tumour site improving efficacy and consequently reducing the systemic toxicity. Numerous drug delivery systems for local cancer delivery have been investigated so far including systems such as nanoparticles[274], microparticles[275], microspheres[70], fibers[276,277], films[75], cubes[278], gels[279–282].

The focus of this chapter is the association of NCs with a gel designed for the local intratumoural injection. Hydrogel composite formulations containing micelles, microparticles, liposomes have been designed for local delivery in various types of cancers[68,116,283,284]. These formulations exhibited a slower drug release profile, longer retention in the tumour and greater tumour mass reduction than fromulations without a gel. For example, Yeon, D. *et al.* reported a composite formulation of DOX-loaded microcapsules and a 5-fluorouracil loaded hydrogel designed to gel at body temperature. This composite inhibited tumour growth more effectively than gel or microparticles alone and both drugs were retained in the B16F10 melanoma tumour for 18 days, without distribution of the drugs to normal tissues[285].

PLGA microspheres are often used in gel composite systems for local delivery of anti-cancer drugs. For instance, paclitaxel-loaded PLGA

microspheres uniformly distributed in alginate gel beads significantly decreased the tumour volume compared to Taxol® when injected into a glioma tumour model in mice[286]. In another study, PLGA microspheres loaded with camptothecin (CPT) or vincristine (VCR) in association with a thermoresponsive gel were reported to increase the mean survival time compared with non-treated rats. In addition, 2/6 animals treated with VCR loaded composite exhibited long-term survival (>60 days) with complete remission of the tumour[287]. Besides microparticles, nanoparticles embedded into gel matrices have shown to drastically decrease the mean number and weight of tumour nodules and significantly increase the median survival time in a colorectal cancer model in mice[288]. Furthermore, siRNA carrying oligopeptide-terminated poly(β-aminoester) nanoparticles embedded in polyamidoamine-dextran hydrogels improved transfection efficiency in breast cancer *in vivo* when compared to the commercial reagents, INTERFERin® and Lipofectamine® [289].

4.1.1 **Chitosan gels**

Chitosan hydrogels have been extensively reported as formulations for localised drug delivery[290–292]. Beyond that, several more composite systems consisting of chitosan gel and NPs have been reported[115,293,294]. For instance, GEM loaded chitosan – thioglycolic acid NPs dispersed in a chitosan gel were designed for bladder cancer therapy and exhibited *in vitro* release in a more controlled manner compared to NPs. Furthermore, the gel formulation remained as gel n artificial urine. Likewise, camphotecin loaded chitosan nanocolloids were loaded into a chitosan gel and it remained as a gel (partially degraded) 7 days after subcutaneous injection into the flank of mice[294].

Nonetheless, a composite of chitosan gel and polymeric NCs have not been reported to the best of our knowledge. Additionally, considering the anionic nature of hyaluronic acid coating of NCs and its ability to form complexes with chitosan as a polycation[295,296], it made chitosan an attractive material for composite formation of chitosan gel containing HA NCs, as described in this thesis.

4.1.2 **LMWGs for localised cancer delivery**

LMWGs have gained attention in the last few decades for drug delivery applications and there have been a few systems specifically designed for local cancer delivery. For instance, a Taxol derivative (succinic acid - glutathione) self-assembles into an injectable hydrogel and when injected in breast tumour model in mice hinders tumour growth by two-fold compared to an i.v. injection of Taxol® at same concentration. Furthermore, the Taxol hydrogel was able to prevent metastasis[67]. In another example, DOX was physically entrapped in a gel made of L-alanine hydrazide gelator and reported to reduce tumour burden by 40% as compared to an untreated control when injected into a breast tumour model in mice. DOX alone at an equivalent concentration had a negligible effect upon injection[66]. The LMW hydrogels have been reviewed for cancer therapy by Tian *et al.*[297]. They presented a review on numerous Taxol® prodrug based hydrogels and their inhibition of tumour growth. In the same paper, peptide self-assembled fibres and LMWGs with physically incorporated drugs are reviewed in terms of drug release and tumour efficacy. Alternatively, nanocomposites of supramolecular gels have been reported mainly with inorganic particles Ag, Au, Si and metal NPs as described in 1.5.1.3. section.

The closest reported studies to our idea is the work of Moysan *et al.* that showed the ability of a drug to influence gel formation. In

particular, 4-(*N*)-lauroyl gemcitabine (GEM C12) encapsulated in lipid nanocapsules at a certain concentration (>5% w/w GEM C12/oil) formed a waxy gel. Below this drug concentration, no gelation occurred. The gel showed the ability to reform after being dispensed from a syringe through a needle[298]. Bastiancich *et al.* used this gel system for assessing local delivery in a subcutaneous glioblastoma tumour model[235]. The prodrug alone caused a slight increase in the size of tumour while only the gel formulation induced a significant reduction in size. Furthermore, after 8 days the gel was still present at the injection site.

However, supramolecular gel-NCs have not been previously reported particularly in the scope of local cancer delivery, to the best of our knowledge.

The chemistry-driven approach to discovery of self-assembled gelators for drug delivery employed by the Skilling *et al.*[299] led to the synthesis of the LMW gelator- *N*4-octanoyl-2'-deoxycytidine that forms a gel in water without the presence of any solvents. This gelator was of particular interest for association with NCs, due its biocompatibility.

Hence, this chapter is devoted to the formation and characterisation of composite formulations, which encompass nanocapsules and polymeric or LMWGs. Using oscillatory rheology, the mechanical properties of composite formulation were investigated with a focus on the effect of the NCs on gel formation. Gel-NCs structure was confirmed by TEM. Specifically, considering its application, the injectability and ability to control release of nanocapsules was also assessed.

Aim

Development and characterisation of polymeric or supramolecular gels containing drug loaded polymeric NCs.

Hypothesis:

Physico-chemical characteristics of NCs (size and polymer coating) as well as their amount, together with gelator concentration can influence the type and number of interactions between gel and NCs defining gel formation and its characteristics.

Objectives:

1. Association of chitosan- hyaluronic acid gels with hyaluronic acid polymeric NCs.
2. Use of polymeric (HA or PGA) NCs loaded with GEM C14 (see chapter 2) as a medium for supramolecular gel formation using *N*4-octanoyl-2'-deoxycytidine gelator. Investigation of rheological properties of the gel as a function of the following factors:
    - type of NCs (size and polymer coating)
    - concentration of NCs
    - concentration of gelator
3. Examination of gel-NCs morphology using imaging techniques.
4. Release studies of fluorescent dyes from NCs and release from the gel
5. Injectability of the gel-NCs formulation

4.2 Materials and Methods

4.2.1 Materials used for manufacture of gels and gel-NCs associated formulations

Chemicals used for manufacture of gels:

Polymers:

- Hyaluronic acid streptococcus sodium salt, 1500-1800 kDa – hyaluronic acid of medium molecular weight (HA MMW), Sigma;
- Chitosan, 210-310 kDa (CS) Sigma.

Low molecular weight gelator:

- *N*4-octanoyl-2'-deoxycytidine, was synthesized by Kathryn Skilling, PhD student at School of Pharmacy, University of Nottingham, UK.

Fluorescent dyes:

- 9-Diethylamino-5H-benzo[a]phenoxazine-5-one - (Nile Red), MP Biomedical;
- 4,4',4'',4'''-(Porphine-5,10,15,20-tetrayl) tetrakis(benzoic acid) - (Porphyrin), Sigma.

For preparation of the release medium, phosphate buffered saline (PBS) in the form of tablets was purchased from Sigma. One tablet dissolved in 200 mL of deionized water yielded 0.01 M phosphate buffer, 0.0027 M potassium chloride and 0.137 M sodium chloride, pH 7.4, at 25 °C.

Solvents of HPLC grade (acetic acid) were purchased from commercial suppliers and used without further purification. Ultra-pure water was used throughout the experiments.

In addition to the materials already listed, to produce gel-NC composites the following NCs were used:

- HA 80 nm NCs
- HA 40 nm NCs
- PGA 80 nm NCs
- PGA 40 nm NCs

The NCs were loaded with GEM C14 and formulated as described in Chapter 2.

For preparation of polymeric gels double barrel syringe 5 mL 1:1 (K-system MIXPAC, Sulzur Ltd) was used.

4.2.2 Preparation of gels and gel-NCs composites

4.2.2.1 *Preparation of polymeric gels*

Polymeric gels were prepared by mixing solutions of two oppositely charged polymers using either a double barrel syringe or simple magnetic mixing. In the first case polymer solutions are loaded in the separate barrels of the double barrel syringe. Content is simultaneously discharged into the vial through a mixing tip, where it has a static mixing element. An image of the double barrel syringe is shown in Figure 4-1.



Figure 4-1 Photographed image of double barrel syringe

Another way of gel preparation included the addition of one polymer into the vial that contained another oppositely charged polymer, under magnetic stirring. The anionic polymer was HA MMW and cationic polymer was CS. HA MMW was dissolved in pure water, while CS needed a small percentage (3.4% (v/v)) of acetic acid to be solubilised. Due to high viscosity, the maximum concentration of HA MMW evaluated was 5 mg/mL. CS was also used at a concentration of 5 mg/mL.

A gel-NCs composite was prepared in the same way i.e. using double barrel syringe or magnetic stirring. The way of introducing NCs into the gel system was using the nanocapsule formulation as a dissolution medium for HA MMW instead of pure water. HA 80 nm and HA 40 nm NCs at concentration of 8% w/v were used in this experiment. Polymer concentrations, HA MMW of 5 mg/mL and for gels formed using magnetic stirring two additional concentrations of CS, 10 and 30 mg/mL were also evaluated.

4.2.2.2 ***Preparation of hydrogels from LMW gelators***

*N*4-octanoyl-2'-deoxycytidine was used as LMW gelator. It was synthesized by Kathryn Skilling and reported to gel in water[299]. A heat-cooling method was used to produce the gels. As follows, a defined

amount of gelator was added to water and heated in a water bath up to 60 °C until the compound completely dissolved. The sample was then allowed to cool down to a room temperature for approximately 30 minutes.

For the preparation of gel-NCs composite, the procedure was the same except that the gelator was dissolved in NCs formulation instead in pure water. Following concentrations of LMW gelator were used: 0.5, 1, 1.5, 2, 2.5, 3, 3.5 and 4% (w/v).

All four NCs formulations were tested (HA 80, HA 40, PGA 80 and PGA 40 nm NCs). HA 80 nm NCs were tested at concentrations of 8; 4 and 2% w/v. For the comparison among different NCs, all NCs formulations at a concentration of 4% w/v were formulated with 2% w/v gelator concentration.

4.2.3 Encapsulation and quantification of fluorescent dye

Two fluorescent dyes, Nile red (NR) and porphyrin, were encapsulated into nanocapsules. Ethanol solution containing either NR or porphyrin was added into the oil phase. As previously explained in chapter 2, oil phase was composed of surfactants (Tween 80, Kolliphor HS 15 and CTAB), oil (Miglyol) and drug (GEM C14). After blending all components together, oil phase plus dye, was stirred for few hours at 80 °C to ensure that all ethanol is evaporated. NCs were formulated, as described in previously (see 2.2.2.), by dispersing oil phase into polymer solution under magnetic stirring. Final theoretical dye concentration in NCs was approximately 10 µg/mL.

4.2.4 Characterisation of NCs loaded with fluorescent dye

Size of NCs loaded with dye was determined using the Zeta sizer as described in 2.1.4.1.

Fluorescent dyes were quantified using plate reader SPARK® 10M, Tecan. Excitation/emission wavelengths used are 553/636 and 430/655 nm, for NR and porphyrin respectively.

Calibration curve for NR was made from NCs formulation as a stock and lower concentrations were obtained by diluting NCs stock with PBS. Solvatochromism[300] of NR is phenomenon already described in the literature and we found as well that the same theoretical concentration of NR in different medium (oil, PBS, MeOH) gives different fluorescence signals. To avoid any inconsistency in the data, calibration curve for NR is made from NR loaded HA 80 nm NCs, where dilutions are made with PBS – the same that was used as for release medium.

Such a phenomenon was not noted for porphyrin, however in order to keep consistency, the calibration curve for porphyrin was obtained from porphyrin loaded HA 80 nm NCs.

The standard calibration curves of both dyes were linear (R^2>0.97) in the range of concentrations between 0.2 and 5 µg/mL, see Appendix 5.

4.2.5 *In vitro* release experiment procedure

4.2.5.1 *Release of fluorescent dyes from NCs*

Procedure for release of compounds from NCs involved incubation of dye loaded NCs with release medium at a defined ratio and in a water bath at 37 °C. As a release medium, PBS of pH 7.4 was used. The ratio of the volume NCs to volume of release medium was maintained at 1:5

for NR and 1:25 for porphyrin. At predetermined time intervals, a sample of 1 mL was withdrawn and isolated by SEC to separate free dye from NCs. The taken sample was replaced with fresh 1 mL of PBS.

By taking a sample the amount, released at various timepoints, was calculated using a standard calibration curve. The cumulative amount of the dye released was calculated by adding the amount discarded each time with removing the sample and replacing it with fresh PBS to the amount in the medium at certain time point. The amount of unreleased dye was determined by isolating the nanocapsules using SEC column. Hence, the amount that is released is calculated by an indirect method using following equation for percentage of cumulative release:

$$\%\ \text{cumulative release} = \frac{\mathrm{Xi} - \mathrm{Xt}}{\mathrm{Xi}} \times 100$$

where Xi is the amount of dye initially loaded into NCs and Xt is the amount that is not released from NCs at time point t plus the amounts that were removed with previous sampling.

4.2.5.2 *Release from the gel-NCs formulation*

Release of NR and porphyrin from gel system was performed in the similar way as from NCs. Formulations containing 2% w/v gelator in following NR loaded NCs were evaluated:

- 8% w/v HA 80 nm NCs;
- 4% w/v HA 80 nm NCs;
- 4% w/v HA 40 nm NCs.

A release of porphyrin from 2% w/v gel- 4% w/v HA 80 nm NCs formulation was also assessed.

Gels were formulated with 0.5 mL of NCs a day before the experiment and then topped up with 12.5 mL of release medium (PBS, pH 7.4). Samples were stored at 37 °C in a water bath.

Initially a ratio of 1:5 was chosen after a literature review on release conditions from NCs and gel formulations (see table 2-7). However, this volume of buffer was found to be too low for the release assessment from gels, since whole release medium gelled during the release experiment. Therefore, 12.5 mL was added to 2% w/v gel prepared in 0.5 mL NCs amount of gel and no gelling occurred and hence was used for further release experiments.

At predetermined time points a sample was taken from medium above the gel, the amount of NR released from the gel was quantified and cumulative release was calculated. At this point, there was no separation step as it was shown that NR was not released from NCs or if it was so it was in low percentage (20% released after 72h).

To evaluate the integrity of NCs after gel formation, both NCs alone and gel-NC composite were heated to 60 °C. At this temperature, the gelator is expected to dissolve, liberating the NCs. A sample was collected before the gel restructures, and the size was determined as per 2.1.4.1.

4.2.6 **Injectability of the Gel-NC system**

After dissolution of the gelator in NR HA 80 nm NCs at 60 °C, while still in liquid form, the formulation was loaded into a syringe and allowed to cool to RT (~30 minutes). When the gel had formed, the content of syringe was dispensed through a needle (25G).

Injectability was tested as well by mimicking *in vivo* procedure for local tumour delivery. Chicken thigh was used as model in which a hole was

bored and the gel was dispensed using a syringe. The tissue was resected and shape of gel was imaged.

4.2.7 Methods for gel characterisation

4.2.7.1 *Vial inversion*

Vial or test tube inversion is a simple test for detecting if gels are formed. Turning the vial, containing the formulation, upside down and taking a note if the formulation flows or not is the basis of this test. If no flow is observed from the formulation under its own weight, it is assumed that sample is gel like. To obtain more quantitative information on gel structure, further experiments should be performed as will be described below.

4.2.7.2 *Measurment of storage and loss modulus*

Oscillatory rheology was carried out using an Anton Paar MCR302 Modular Compact Rheometer using a cup and vane geometry. Two millilitres of gel sample was placed in a disposable measuring Cup EMB-Z4 (Anton Paar) which was set into lower part of the rheometer (cup). The upper part of the rheometer (vane) was positioned into the centre of the gel at a depth of 2 mm. All gel samples were prepared a day before the rheological measurement. Oscillatory amplitude sweep measurements were carried out at strain varying between 0.05 – 100 %. The G’ and G’’ (storage modulus and loss modulus, respectively) were measured at a constant angular frequency of 10 rad/s. The temperature was set to 37 °C to mimic physiological conditions.

4.2.7.3 *Transmission Electron Microscopy (TEM)*

TEM of gels that do not contain NCs were carried out by pipetting a small amount of gel (5-10 µl) onto a carbon-coated copper grid (Holey Carbon on 300 Cu mesh). Excess sample was blotted with Whatman 50 filter paper. The grid was subjected to high vacuum in a Gatan dry pumping station (model 655) prior to inserting into the machine and imaging at an accelerated voltage of 100 kV.

The gel-NCs formulation was imaged in cryogenic conditions. Sample preparation for cryo-TEM imaging involved pipetting approximately 5-10 µl of formulation onto a carbon-coated copper grid. Samples were then subjected to plunge freezing into liquid ethane in a Gatan CP3 Cryoplunge system. Imaging was performed at a current density measured at 10pA/cm2 for no sample on the fluorescent screen at 20000x magnification, TEM - JEOL 2100F equipped with a Gatan Orius camera, operating at 100kV, Sample holder - Gatan 914 Cryo-tomography holder.

4.3 Results and discussion

4.3.1 Hyaluronic acid - chitosan gels

HA and CS gels were prepared by using a double barrel syringe. The anionic and the cationic polymer solutions are loaded in the separate barrels of the double barrel syringe and dispensed simultaneously through the static mixer connected at the front into an empty vial. Oppositely charged polymers used in appropriate concentrations interact through electrostatic attraction and can result in gel formation. This electrostatically-driven liquid-liquid phase separation i.e. complex coacervation results in what are also called polyelectrolyte complexes (PEC)[301]. Sometimes gel formation can be impeded by strong ionic interactions and precipitates are formed[302].

Barrel A was filled with a solution of HA MMW and a barrel B with CS at a concentration of 5 mg/mL. Previously, HA MMW was dissolved in a pure water, while CS needed 3.4% v/v of acetic acid in water and mild heating over 2-3 hours. Solutions were simultaneously dispensed through the static mixer into the vial. Figure 4-2 shows the formation of a diffuse gel floating in the remaining fluid in the vial. It seems the polymers were enriched in one of the separating phases as chitosan-HA complexes seem to be a more compact and precipitated.



Figure 4-2 CS – HA gel produced by a double barrel syringe, CS and HA were used in concentration of 5 mg/mL. Gel is shown with an arrow.

The use of a double barrel syringe for a preparation of gels has been widely reported in the literature[303–305]. Likewise, chitosan and hyaluronic acid hydrogels have received particular attention[306–308]. Nonetheless, most of these systems employed chemical crosslinkers[309] or used polymers in order to generate reactive groups for hydrogel formation[305,307]. An example of chitosan and hyaluronic acid gel formed by complexation without use of any linkers or polymer modifications was reported by Florczyk *et al.* They have designed a polymeric porous scaffold mimicking the microenvironment of glioblastoma. This scaffold was a compact complex, in the form of disc, with an average pore size of 77.31 μm[296].

As already described, our goal was to assemble nanocapsules in a gel network and use the resulting composite gel as a local drug delivery system. In next subchapter, the association of polymeric NCs with HA-CS gels is reported.

4.3.2 **Hyaluronic acid – chitosan gels with nanocapsules**

HA 80 nm or HA 40 nm NCs were introduced into CS-HA MMW polymeric gels. For this, HA-MMW was dissolved in HA nanocapsules with size of 80 or 40 nm (Fig. 4-3. b and c). The resulting suspension was incorporated into barrel A, whereas the barrel B was loaded with an aqueous CS solution as indicated in 4.3.1. Polymer concentrations, both for HA MMW and CS, were 5 mg/mL. Nanocapsules were loaded with a lipophilic dye NR for visual tracking. In Fig. 4-3, b) and c) a diffuse gel was formed. The pink colour concentrated in the gel suggests the presence of nanocapsules in the gel. Shortly (5 min.) after the gel-nanocapsules preparation the remaining liquid around gel was transparent or lightly pink and its colour intensified with time as the nanocapsules were released from the gel. Three to four hours after the gel formation, most of the nanocapsules were released based on the colour of the gel which was almost translucent. The fast release was expected if the gel's pore size is considered. For this particular system, the pore size was not investigated however according to previously published reports, the pore size of CS-HA hydrogel systems are usually in micrometre range[296,310,311]. For example, Florzcyk *et al.* reported a PEC CS-HA composite with a pore size of 77 μm, Tan *et al.* also reported a pore size of 10–100 μm for their succinic CS – aldehyde HA[307], and a pore size of approximately 5 μm was reported for CH-PNIPAAm-HA hydrogels by Fang *et al.*[310]. Considering the nanometric size of NCs and micrometric pore size of the gel scaffold it can be speculated that NCs diffused from the gel network. The reason for this could be that NCs were just physically entrapped in the gel without any physical bonds between the gel and NCs.

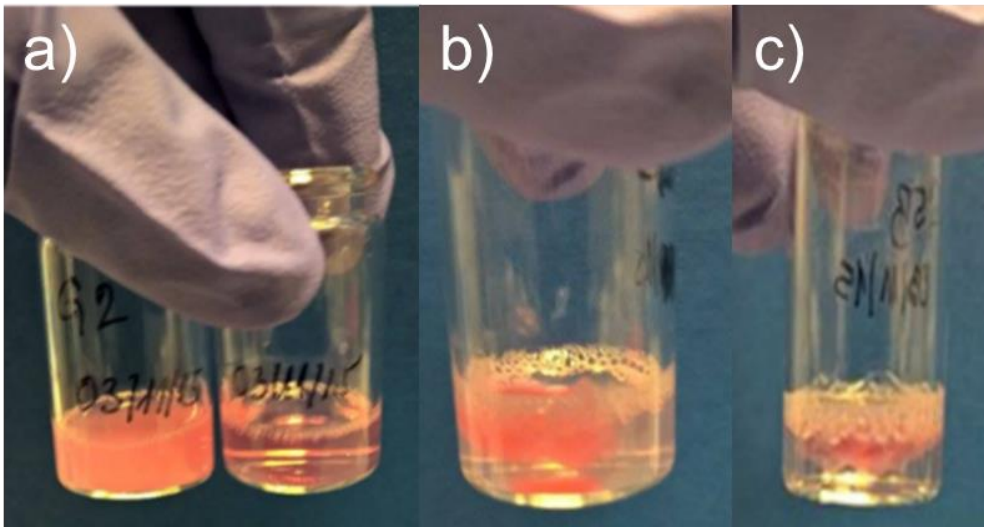


Figure 4-3 Polymeric gels produced by a double barrel syringe. a) CS - NCs HA 80 nm/ HA 40 nm b) CS - NCs HA 80 nm - HA MMW; c) CS - NCs HA 40 nm - HA MMW. In case a) barrel A contains only HA NCs 80 or 40 nm NCs and barrel B contains a solution of CS; while in b and c) barrel A contains HA polymer of medium molecular weight dissolved in nanocapsules (HA NCs 80 and 40 nm), barrel B contains a solution of CS. Concentrations of both polymers are 5 mg/mL and HA 40 or HA 80 nm NCs were used at a concentration of 8% w/v. Gels were imaged in the same hour of the preparation.

Figure 4-3 a) shows the gel-NCs system when barrel A contained only nanocapsules (NCs HA 80 nm or HA 40 nm) without HA MMW polymer. The barrel B contained only CS solution as in all previous cases. In this experiment, gelation did not occur. It is shown that the presence of the hyaluronic acid polymer of a higher molecular weight, than one present as a coating of nanocapsules, is essential for the gelation process. The molecular weight of hyaluronic acid streptococcus (HA MMW) used for polymer interaction in gel was 1500-1800 kDa and for the nanocapsules preparation sodium hyaluronate (HA) of 41-65 kDa. The hydrogel formation is exclusive to the presence of both polymers HA MMW and CS, regardless of the presence of HA NCs.

It was observed that the shape of gel is inconsistent in each preparation because of manual intervention in operating the double barrel syringe. To better control this process, a modification in process of preparation was evaluated. The solution of CS was added into the vial containing HA MMW or HA MMW+NCs under magnetic stirring (Fig. 4-4). As in experiments where the double barrel syringe was used, two different gels were prepared: 1) gels through mixing two polymers alone and 2) gel-NCs composite. The same polymer materials and NCs were used as in experiments with double barrel syringe. The highest concentration of HA MMW used in the experiment, before becoming too viscous was 5 mg/mL. Additionally, CS was tested at various concentrations of 5, 10, 30 mg/mL. It can be noticed that the volume of gel formed is greater compared with ones prepared by a double barrel syringe. Higher concentrations of CS influence the gel appearance and 30 mg/mL (Fig. 4-4 c) creates very viscous gels. The presence or absence of the nanocapsules does not seem to influence the amount of gel formed.

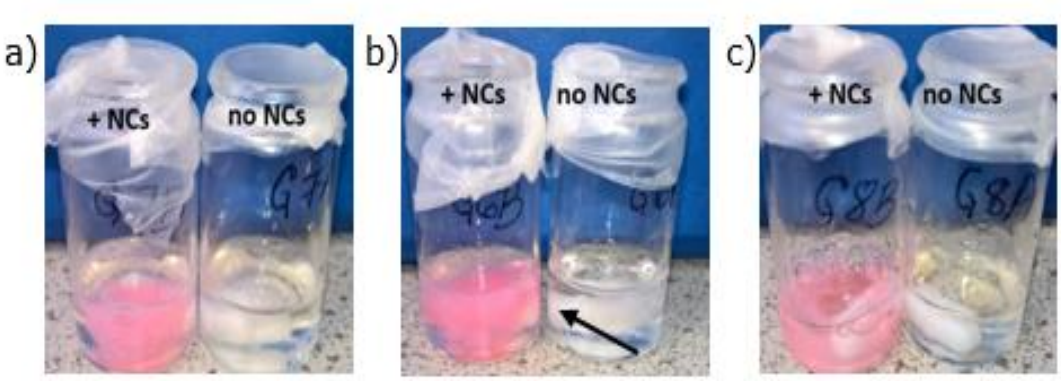


Figure 4-4 Polymeric gels formed by magnetic stirring of chitosan in various concentrations and hyaluronic acid at concentrations of 5 mg/mL with and without NCs HA 80 nm. Concentrations of Chitosan used are: a) 5 mg/mL; b) 10 mg/mL; c) 30 mg/mL. White object marked with an arrow is a magnetic bar, while gel is wrapped around it.

Here we showed the association of NCs with CS-HA gel and how polymer concentration and method of gel production influenced the amount and appearance of the gel.

4.4 Low molecular weight organic gels - LMWGs

Preparation of polymeric gels using the double barrel syringe showed some disadvantages including the fast release of NCs from the gel (Fig. 4-3 c), difficulty in manipulation and dependency on manual dexterity to create the gel. Alternatively, LMWGs are produced using more simplistic methods such as heat-cooling cycles or pH switch. In order to get simpler and more reproducible process of manufacture, LMW gelators were chosen for gel-NC composite.

To the best of our knowledge nanocomposite formulation that combines polymeric NCs and LMWGs has not yet been published. However, an addition of polymers to LMW hydrogels has shown superior characteristics than supramolecular gels alone in terms of strength and gelation time. For example, a small amount of HA (0.3 wt%) in succinated taxol gels, resulted in higher G' values and a more fibrillar network with a presence of bundles compared to supramolecular gels alone[312]. Similarly the addition of poly(acrylic acid) to pyridine-based gelators gave a significant decrease in the critical gel concentration[313]. Contrarily, in some cases, as reported by Adams and co-workers, the presence of polymer (dextran) does not enhance the properties to the LMW hydrogel (dipeptide type gel)[314]. In this case, gels with dextran exhibited a lower G' as compared to those in the absence of dextran, and spherulitic structures and entanglement that are usually observed in gels were less in the presence of dextran. These studies revealed that structure and nature of the polymer affects the gel properties due

to specific adsorption of the polymer on to the fibers which can not be generalised.

4.4.1 **LMW hydrogels - *N*4-octanoyl-2'-deoxycytidine gelator**

A nucleoside type of gelator with an octanoyl modification on the *N*4 position of deoxycytidine (Fig. 4-5) was synthesised by Kathryn Skilling and reported to gel after solubilisation in water only[299].

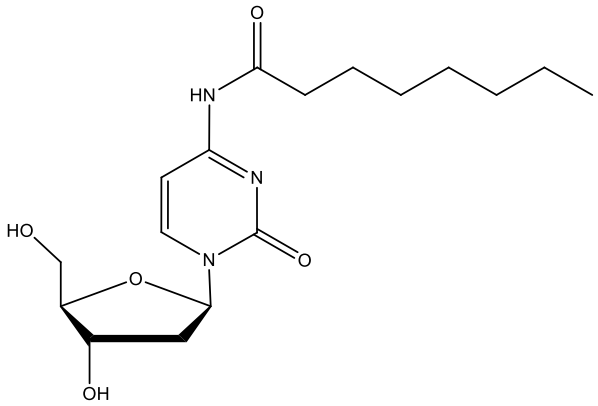


Figure 4-5 The structural formula of N4-octanoyl-2'-deoxycytidine gelator

Manufacture of this gel involved solubilising the gelator in water by heating to 60°C, while gelation occurred after cooling down the gelator solution to room temperature. A preliminary screening of the gelation process was done by a simple test of vial inversion; when no flow was present the gel was formed. The range of gelator concentrations between 0.5 and 2.5% w/v were tested and results of the vial inversion test are shown in Fig. 4-6. The increase in turbidity, as well as presence of small precipitates or tiny fibres were noted as the concentration of gelator increases.

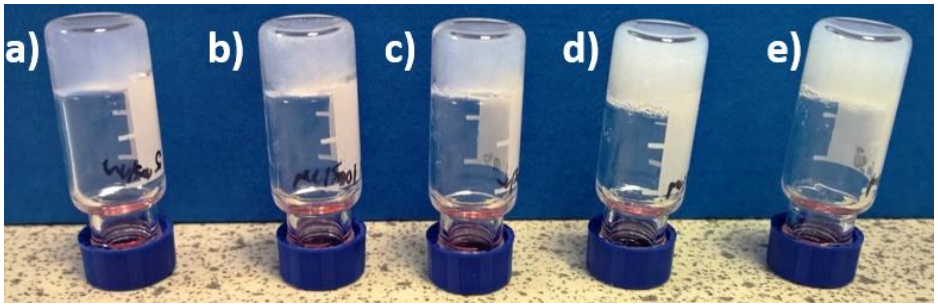


Figure 4-6 Vial inversion of N4-octanoyl-2'-deoxycytidine gelator in water. Final component concentration in % w/v is a) 0.5; b) 1; c) 1.5; d) 2; e) 2.5.

A quantitative way of characterising gels is to use rheological measurements to get an insight of mechanical strength of the system. The mechanical behaviour of soft materials such as hydrogels lie between an elastic solid and viscous liquid. It is possible to quantify both the viscous-like and the elastic-like properties of a material using oscillatory rheology. During oscillatory tests, the measuring geometry oscillates around the rotation axis instead of moving constantly in one direction. Therefore, the measured values show not only the viscous behaviour but also the stiffness (elasticity) of the sample. Amplitude and frequency sweeps are among the most used tests.

During an amplitude sweep, the amplitude of the shear stress - is varied, while the frequency is kept constant. The amplitude is the maximum strain during oscillatory motion. For the analysis, the storage – G' (solid like modulus) and the loss – G'' (liquid like modulus) are plotted against the strain (deformation). At low deformation G' and G'' are mainly constant and it is characteristic of an undisturbed sample. This region is called linear-viscoelastic region (LVE). As soon as the moduli start to decrease, the structure is disturbed and the end of the LVE-region is reached. The ratio of the two moduli gives information about the characteristics of the sample. When the storage modulus is larger than the loss modulus, the sample behaves as a viscoelastic

solid. In the opposite case - G'' > G' in the LVE-region - the sample has the properties of a viscoelastic fluid. In order to have a solid-gel like structure, a long LVE region and G’ of at least one order of magnitude higher than the G’’ value should be observed.

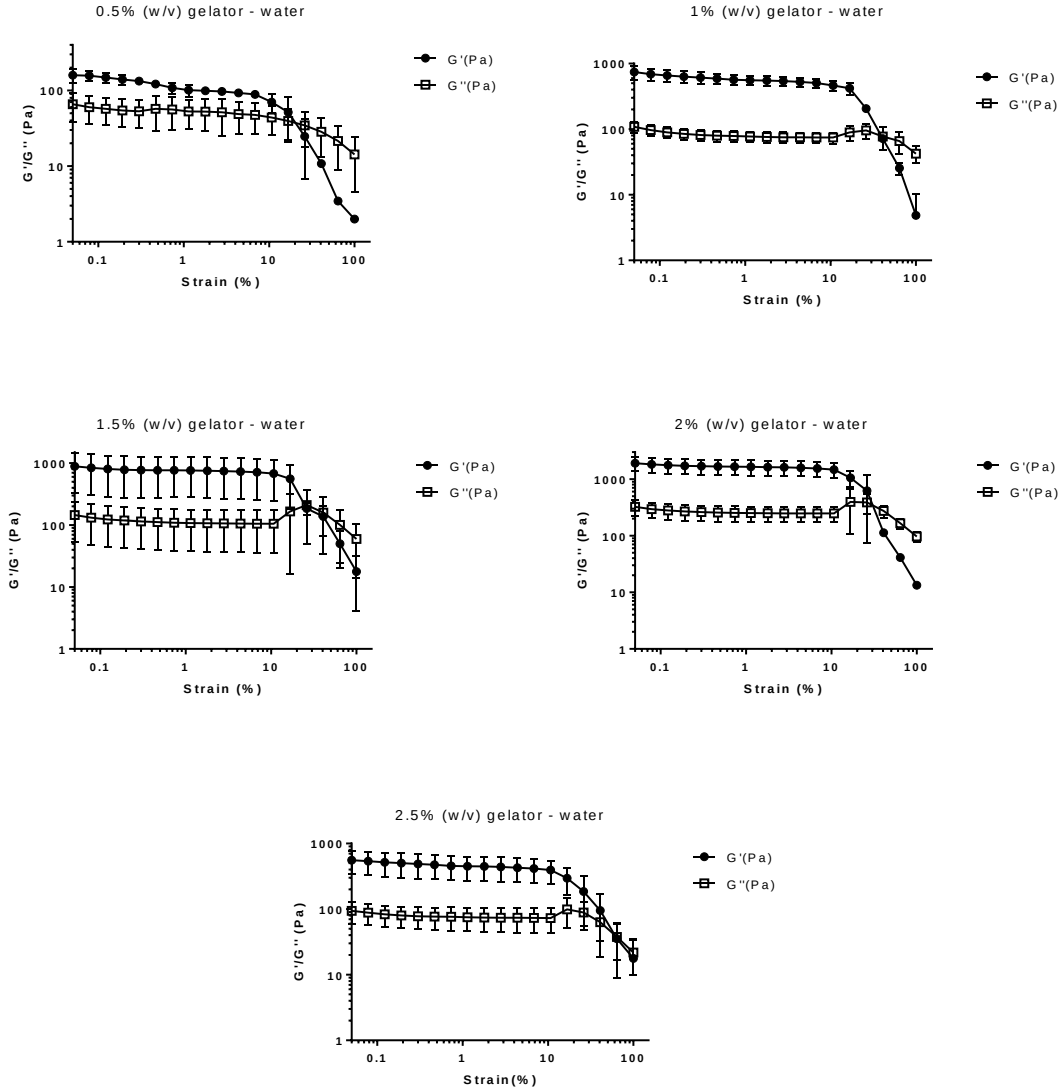


Figure 4-7 Rheological data for N4-octanoyl-2’-deoxycytidine gelator in water. Gelation time was ≤ 30 minutes. Testing was performed a day after gel preparation. Amplitude sweeps (G’ and G’’) of 0.5, 1, 1.5, 2 and 2.5% w/v, at 37 °C, γ= 0.05 – 100% and ω=10 rad/s. Mean values (n=3) are shown, error bars represent standard deviation of the mean, where n is number of independent trials.

The results derived from amplitude sweep rheology indicated that concentration of gelator is a variable that can influence the gel strength and as shown in Fig. 4-7, the lowest concentration of 0.5% w/v gave a very small difference between G' and G'' (148 Pa and 57 Pa), while for 1% w/v gelator concentration, these values are 657 Pa and 89 Pa and for 2% increased to 1760 Pa and 279 Pa respectively. The length of LVE region for these concentrations (0.5, 1, 2% w/v) also increases from 0.1 to 1.833 and 2.29, respectively. LVE region was calculated using Rheoplus Anton Paar software where deviation from linearity was <3%. In LVE region, for each gel, G' was always greater than G'', suggesting the presence of an elastic three-dimensional network in the gel[315].

In Fig. 4-8 it can be clearly seen that G' and G'' values increase when the concentration goes from 0.5 – 2% w/v. For the highest concentration (2.5% w/v), the value of elastic modulus dropped to 517 Pa. This may be due to the presence of the precipitate that disturbs the structure and reduces the strength of the gel.

The influence of the gelator concentration on the value of elastic module has been reported elsewhere. For example, Mohmeyer *et al.* reported sorbitol based LMWGs where the elastic modulus increased with concentrations reaching a plateau at the two highest concentrations[316]. A different behaviour was observed for gelator 14 aroyl L-cystine where decrease in G' values was observed above the concentration of 5 mM. As an explanation they suggested that with the higher gelator concentration, gelation process was almost instant which resulted in shorter fibres and consequently reduced the elasticity of the system[317]. In our study, the presence of the precipitate at the highest concentration can be the reason for decreased G' values. Considering that gelation process lies between solubilisation and crystallisation, at

a certain concentration it is possible to still have gel like system with some precipitates that diminishes the elastic modulus of the gel.

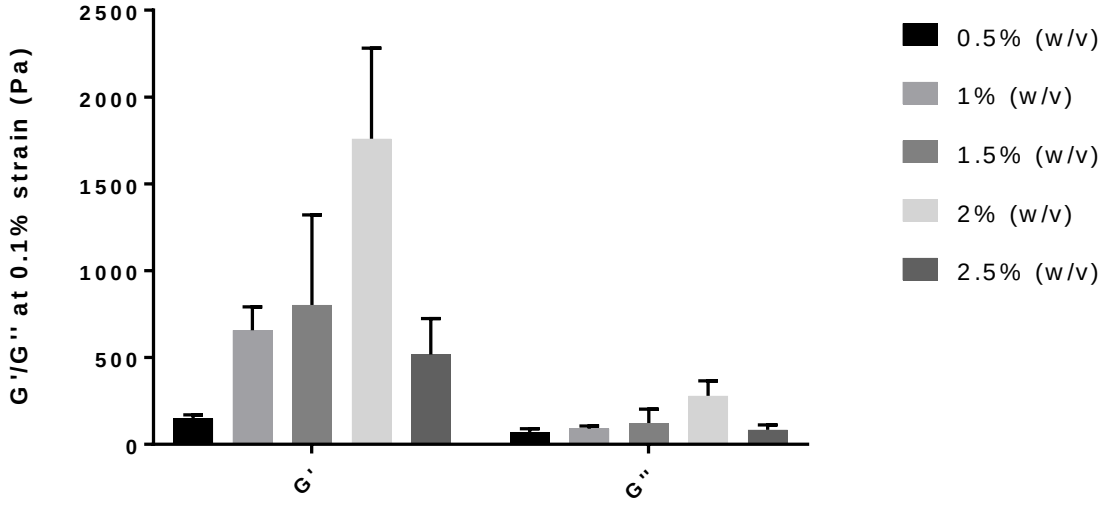


Figure 4-8 Influence of concentration of N4-octanoyl-2'-deoxycytidine gelator on gel strength (G') in gel-water systems. Measurements were performed at 37 °C, γ= 0.05 – 100% and ω=10 rad/s and G values derived from LVE region at 0.1% strain. Mean values (n=3) are shown, error bars represent standard deviation of the mean, where n is number of independent trials.

As described in 4.1.2. of this chapter, LMWGs have already demonstrated to be suitable platforms for drug delivery and especially for intratumoural drug delivery. Besides their design to undergo controllable and sustained release of drugs, they have been shown to be retained at the site of the tumour injection which is directly related to the network structure. A comparison of the elastic moduli values of different gels reported led to the conclusion that they range from ~300 Pa for a curcumin loaded dipeptide self-assembled hydrogel[318] to 1000 Pa for a Taxol-SA-GSSG gel[67] and Ferrocenyl di-cholesterol gelator[319], and for derivatives of Fmoc gels[320,321] which exhibited G' values up to 10^5 Pa as was similarly found for DOX[66] loaded carboxamide and hydrazide alanine gels. For the nucleoside type LMW gelator presented

here, assessment by the vial inversion and amplitude sweep assay, show that these gels have good mechanical properties (G'= 500 – 2000 Pa). Absence of any solvent in the gelation process presents a great advantage making it suitable for association with nanocapsules.

4.4.2 LMWGs -NCs composites

Gel associated nanocapsules systems were produced in the same way as gel-water systems (4.4.1.). Gelator was weighed into a vial and topped up with the suspension of nanocapsules, heated up to 60°C for half an hour and left at room temperature to cool down and to gel. Vial inversion tests were done after 1h, while rheological measurements were performed the following day.

4.4.2.1 *Gels with 80 nm nanocapsules coated with hyaluronic acid*

HA 80 nm NCs were used as prepared initially as explained in chapter 2. Briefly, approximately 175 µl of the oil phase was solubilised in the aqueous phase up to 1.5 mL total volume of NCs. After water elimination (freeze-drying), the mass of this NCs was calculated as 8% (w/v) and as such the nanocapsules were subsequently labelled as 8% HA 80 nm NCs. From this concentration by dilution with pure water other lower amounts of NCs were prepared and used for association with the gel.

Gelator, *N*4-octanoyl-2'-deoxycytidine, in concentrations of 0.5 and 1% w/v failed to gel in the presence of (8% w/v) nanocapsules although gelation occurred in water as previously shown (Fig. 4-6). However, increasing the gelator concentration to 2% and higher (2.5, 3, 3.5 and

4% w/v) no flow was noticed in vial inversion 30 minutes after gelator solubilisation and hence demonstrating the formation of gels.

4.4.2.1.1 Rheological studies

Amplitude sweeps were carried out for these gel-NCs formulations and are presented in Fig. 4-9. Comparing with gel-water formulations, the gel-NCs formulations have both moduli which start to decrease earlier implying a shorter LVE region. For the determination of LVE region using Rheoplus software, deviation from linearity had to be increased to 5-9%. However, increases in gelator concentration resulted in increased G' values (Fig. 4-10) and also in the length of LVE. G' values taken from LVE region are 870, 1566, 4096, 4553, 10160 Pa for concentrations 2, 2.5, 3, 3.5 and 4% w/v respectively. Comparing the strength of gel in water formulations with the gel-NCs formulation at the same concentration (2% w/v), the G' values (1760 and 870 Pa respectively) indicates that the gel without nanocapsules is stronger. It can be concluded that 2% of gelator in the presence of 8% of NCs is not enough to generate strong gels. Contrarily, higher gelator concentration (2.5% w/v) results in a drop of G' for the gel-water system to 517 Pa, while presence of the NCs in the gel system results in a three times higher G' of 1566 Pa. Considering that gelator is an amphiphilic compound, some of it might accumulate at the interface of oil-water of NCs. Similarly Moysan *et al.* confirmed, by surface tension measurement, that their amphiphilic drug (GEM C12) sits at the water-oil interface since surface tension decreases with higher drug content[298]. Furthermore, they report an increase in storage modulus of 100, 2000 and 8000 Pa with drug concentration in lipid NCs for 5, 7.5 and 10% w/w respectively (Drug percentage is reported in respect to the amount of oil). More importantly, gel formation did not occur when

drug concentration was <5%. The data are in accordance with what we report here.

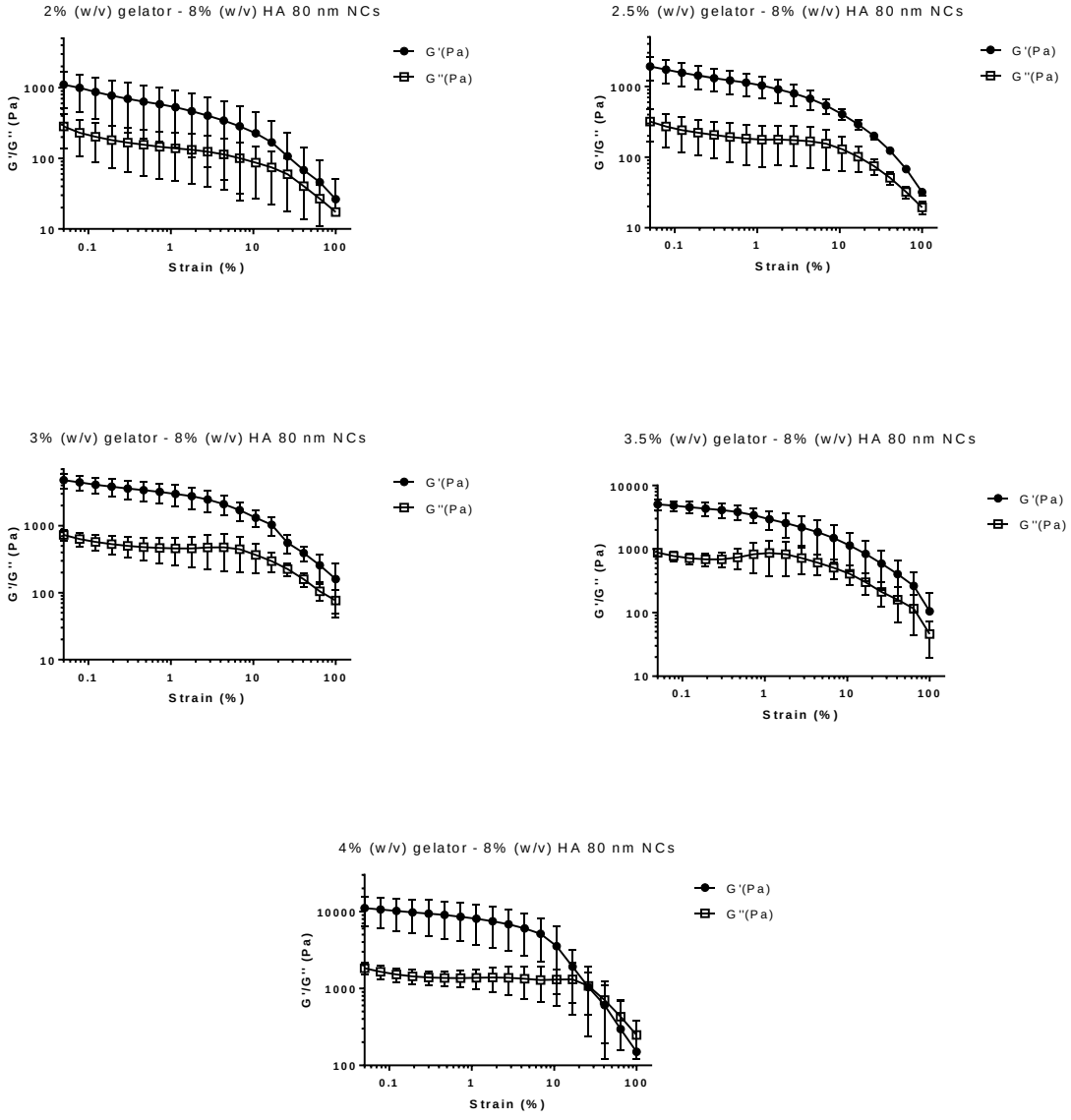


Figure 4-9 Rheological data for N4-octanoyl-2'-deoxycytidine gelator in 8% w/v HA 80 nm NCs. Gelation time was ≤ 30 minutes. Test was performed a day after gel preparation. Amplitude sweeps (G' and G'') of 2, 2.5, 3, 3.5 and 4% w/v, at 37 °C, γ= 0.05 – 100% and ω=10 rad/s. Mean values (n=3) are shown, error bars represent standard deviation of the mean, where n is number of independent trials.

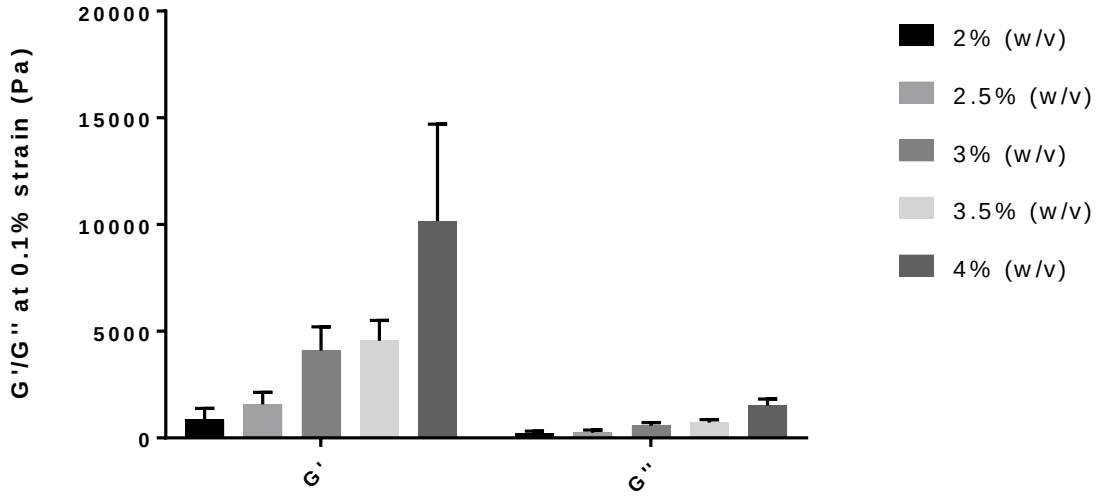


Figure 4-10 Influence of concentration of gelator on gel strength (G') in gel-8% w/v HA 80 nm NCs systems. Test was performed a day after gel preparation at 37 °C, γ= 0.05 – 100% and ω=10 rad/s and G values derived from LVE region at 0.1% strain. Mean values (n=3) are shown, error bars represent standard deviation of the mean, where n is the number of independent trials.

4.4.2.1.2 Influence of amount of NCs on characteristics of gel-NCs

It was shown that increased gelator concentration resulted in stronger gels, while 0.5 and 1% w/v of gelator was not enough to gel 8% HA 80 nm NCs. One explanation previously described was the accumulation of gelator at the interface of NCs o/w phase (Figure 4-22). Accordingly, lower amounts of NCs would reduce the surface area of the interface for amphiphilic gelator to accumulate and hence would be available to form the 3D fibre structure instead. To test this hypothesis, we examined the influence of the amount of NCs on gelation. In next experiments 4 and 2% w/v of HA 80 nm NCs were used instead of 8% w/v. However, it should be borne in mind that often, the therapeutic effect requires a higher amount of NCs. Hence, a balance between gel strength and the amount of NCs needs to be established.

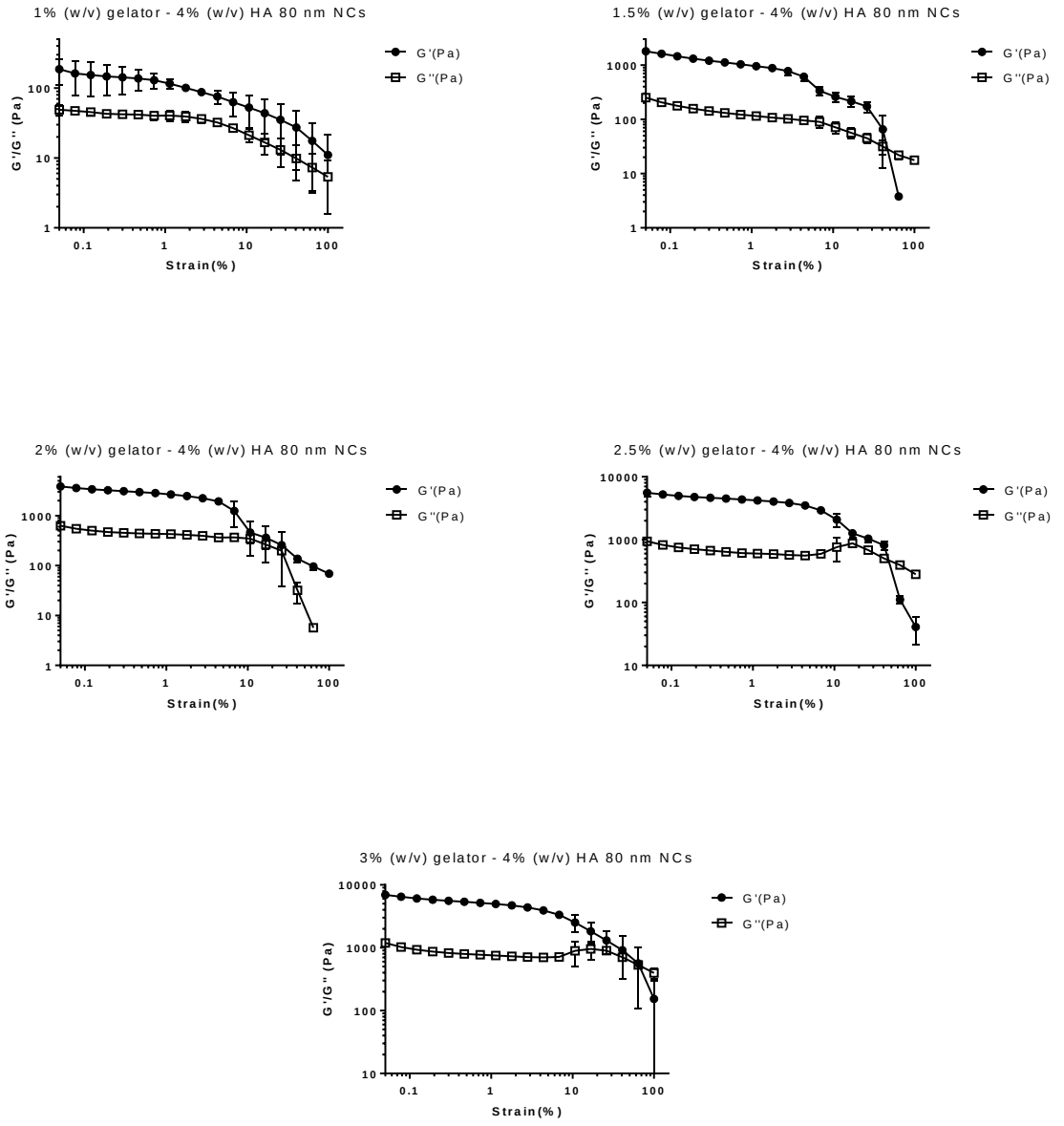


Figure 4-11 Rheological data for N4-octanoyl-2'-deoxycytidine gelator in 4% w/v HA 80 nm NCs. Gelation time was ≤ 30 minutes. Test was performed a day after gel preparation. Amplitude sweeps (G' and G'') of 1, 1.5, 2, 2.5, 3, w/v, at 37 °C, γ= 0.05 – 100% and ω=10 rad/s. Mean values (n=3) are shown, error bars represent standard deviation of the mean, where n is number of independent trials.

Firstly, 1% w/v of gelator was enough to form a gel with 4 and 2% of NCs (Fig. 4-11 and 4-12 top left graph) which was not the case with 8% of NCs where at least 2% of gelator was needed. Although for a concentration 1% w/v of gelator, the amplitude sweeps gave a small LVER (155 and 676 Pa for 4 and 2% w/v of NCs respectively). However, with increased concentration LVER had good linearity and length was extended. For the highest gelator concentration (3%) G' values taken from LVE region were 5370 and 21380 Pa, for 4 and 2% w/v of NCs respectively. As expected, G' value increased with the gelator concentration in both systems containing 4% or 2% of NCs as shown in Figure 4-13. As explained above (4.4.1.) concentration of gelator influences gel characteristics. In addition, the influence of gelator concentration on strength of LMW gel-NPs composite has been assessed by Song *et al.* where they have reported an increase in G' from 119 to 1000 Pa with a concentration increase of pyridine derivative gelator from 4 to 7% and where the clay nanoparticles concentration remained constant during this assessment. They also showed that presence of small amount of NPs (1%) results in 7 times greater G' values[322].

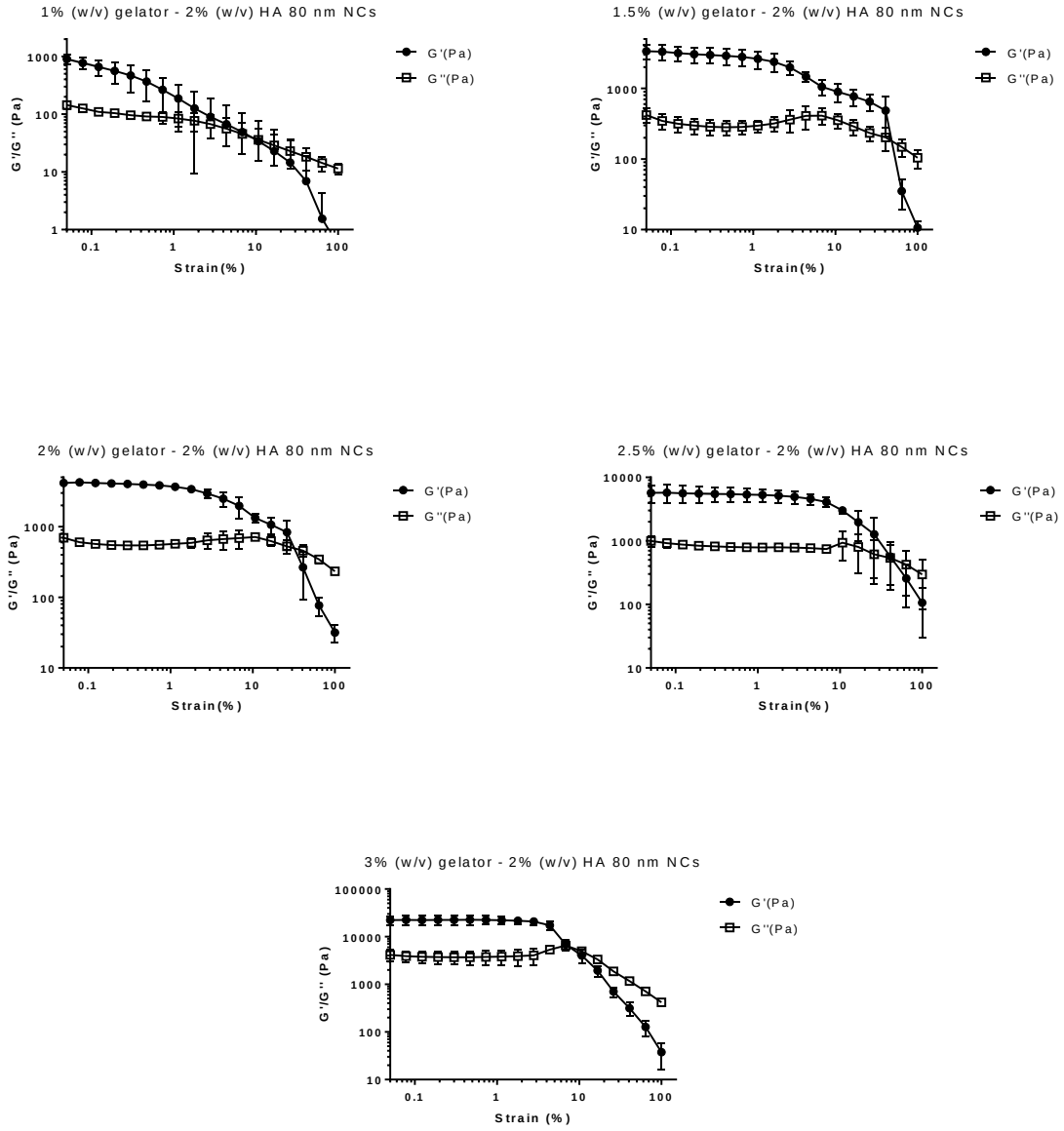


Figure 4-12 Rheological data for N4-octanoyl-2'-deoxycytidine gelator in 2% w/v HA 80 nm NCs. Gelation time was ≤ 30 minutes. Test was performed a day after gel preparation. Amplitude sweeps (G' and G'') of 1, 1.5, 2, 2.5, 3% w/v, at 37 °C, γ= 0.05 – 100% and ω=10 rad/s. Mean values (n=3) are shown, error bars represent standard deviation of the mean, where n is number of independent trials.

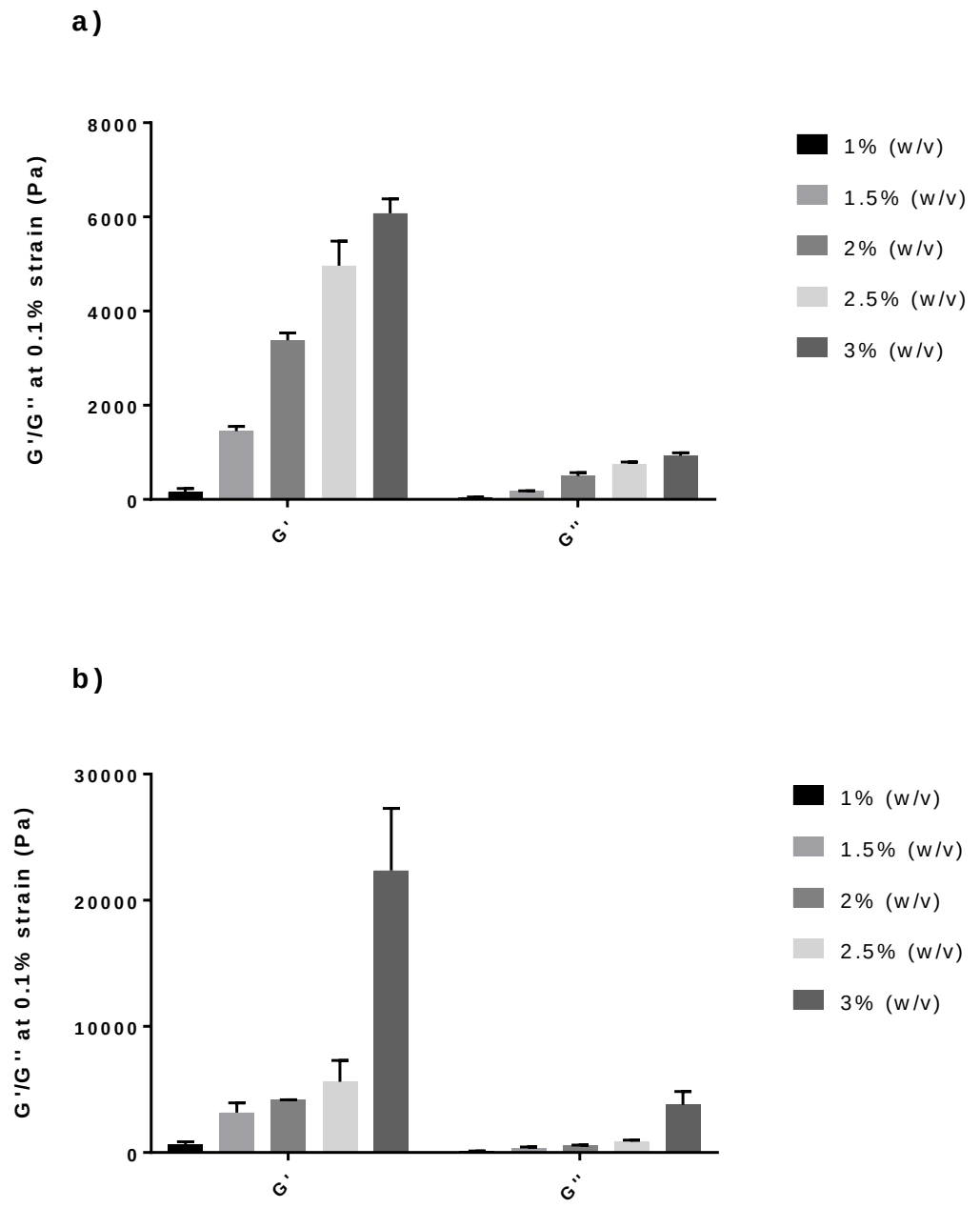


Figure 4-13 Influence of concentration of gelator on gel strength in a) gel-4% w/v HA 80 nm NCs and b) gel-2% w/v HA 80 nm NCs systems. Gelation time was ≤ 30 minutes. Test was performed a day after gel preparation at 37 °C, γ= 0.05 – 100% and ω=10 rad/s and G values derived from LVE region at 0.1% strain. Mean values (n=3) are shown, error bars represent standard deviation of the mean, where n is number of independent trials.

The influence of the amount of NCs on gel strength is summarised in Figure 4-14. The results indicated that an increase in the amount of NCs led to a reduction of the G' values. In that instance, G' values of the system where 8% NCs formulation was used are drastically lower, while the values in case of 2% and 4% NCs are closer to each other. An explanation for this behaviour could lie in the affinity of the amphiphilic gelator to collect at the oil-water interface of NCs. As the amount of NCs increased, the number of gelator molecules at the interface also increased resulting in the formation of a gel with a weaker structure (Figure 4-22). However, in work of Basrur *et al*., the opposite has been shown. The increase in concentration of Si NPs from 0.5 to 1% increased the modulus of LMWGs with smaller enhancements with further increases in NP concentrations [315]. Similar results were reported by Cheng *et al*. where stronger oligopeptide gels were obtained with increasing concentrations of gold NPs[323]. Unfortunately, the gel-NCs system described in this chapter cannot be compared with their work since Si or Au NPs and polymeric NCs differ much in chemical surface composition and the work on the similar topics could not be found in the literature. The closest example to our system is the one reported by Moysan *et al.* which was described above (see 4.4.2.1.). They showed a decrease of G' values with the dilution of LNCs, which is the opposite from what we obtained. However, in this case the gelator was the drug included in the nanocapsules and thus the dilution of the NCs implies reduction of gelator amount. Therefore, to conclude our data showing a decrease in G' values with an increase in NCs concentration supports our hypothesis about the accumulation of the gelator at the interface and a subsequent decrease of the gelator involvement in the formation of gel network (Figure 4-22).

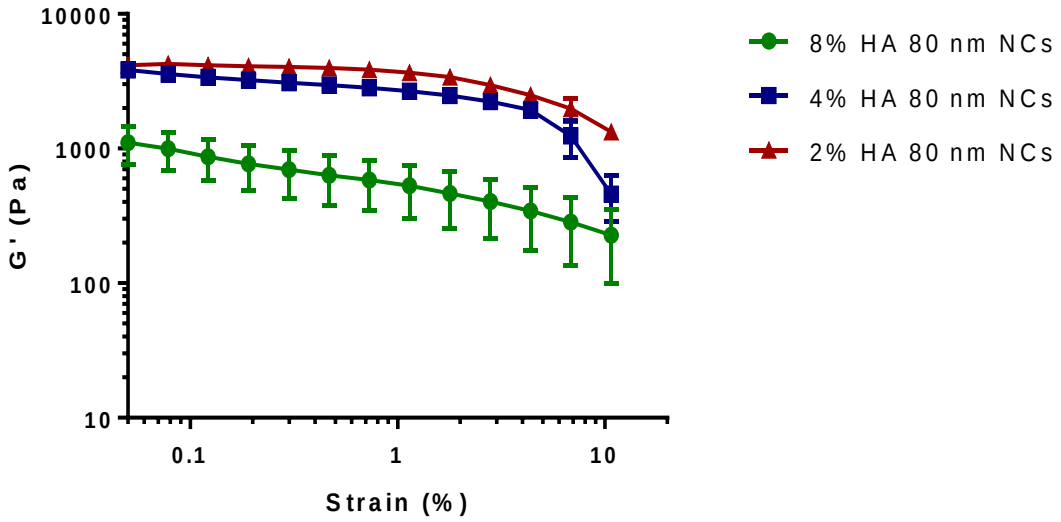


Figure 4-14 Influence of concentration of nanocapsules on gel strength (G') in gel-HA 80 nm NCs systems, where gelator concentration is constant at 2% w/v, while concentration of nanocapsules varies from 2, 4 and 8% w/v. Gelation time was ≤ 30 minutes. Test was performed a day after gel preparation at 37 °C, γ= 0.05 – 100% and ω=10 rad/s. Mean values (n=3) are shown, error bars represent standard deviation of the mean, where n is number of independent trials.

The highest gelator concentration used (3% w/v) and lowest NCs concentration (2% w/v) gives exceptionally high G' values and is something that would probably be the best system to choose in terms of gel strength. However, a low amount of NCs means a low amount of the drug loaded. Hence, for drug delivery purposes, an imperative would be to use systems containing minimum of 4% of NCs. Based on this we selected 4% w/v and 8% w/v as targeted concentrations of NCs. Reported G' of LMWGs have already been described in 4.4.1. and their values range compare with ones reported here. Apart from LMWG formulations, injectable polymeric gels report G' values of 500 Pa for liposome-hydrogel[324] and NP-hydrogel composites[111] which is well below the values obtained for 8% NC -gel formulation.

4.4.2.2 *Comparison of gel strength between different nanocapsules*

As previously shown, HA 80 nm NCs in the concentration of 4% w/v with 2% w/v of gelator gave optimal system. Here we investigate if NCs different size and with a different polymer coating have an influence on gel characteristics.

For that purpose, the following nanocapsules loaded with GEM C14 were used:

- HA 40 nm
- PGA 80 nm
- PGA 40 nm

Gels were formulated as previously explained (4.2.2.2.) using 2% w/v gelator concentration and 4% w/v NC.

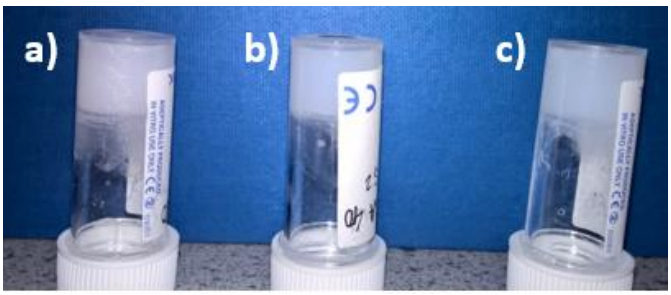


Figure 4-15 Vial inversion of N4-octanoyl-2'-deoxycytidine gelator in presence of NCs: a) PGA 80 nm; b) PGA 40 nm; c) HA 40 nm. Final gelator component concentration in all systems is 2 % w/v; and amount of NCs used is 4 % w/v. Gelation time was ≤ 30 minutes.

As shown in Figure 4-15. upon vial inversion, no flow was noted in any of the vials enabling us to proceed with rheological measurements. As with previous samples, amplitude sweeps were carried out, at 37°C and varying the strain from 0.05-100%. All three types of NCs showed

similar behaviour. When compared with HA 80 nm NCs in the same conditions, it can be seen that curves are almost overlapping (Fig. 4-16 d.). The same was confirmed using 1 way ANOVA – Tukey's multiple comparison test on G' values derived from LVE region (0.1% strain). P values > 0.05 were obtained. This data showed that the difference in size of NCs from ~40 nm to 80 nm had no significant difference on gel strength. Moysan *et al.* reported similar gel properties that were independent of the size of lipid NCs, comparing NCs of 29 nm and 55 nm[298].

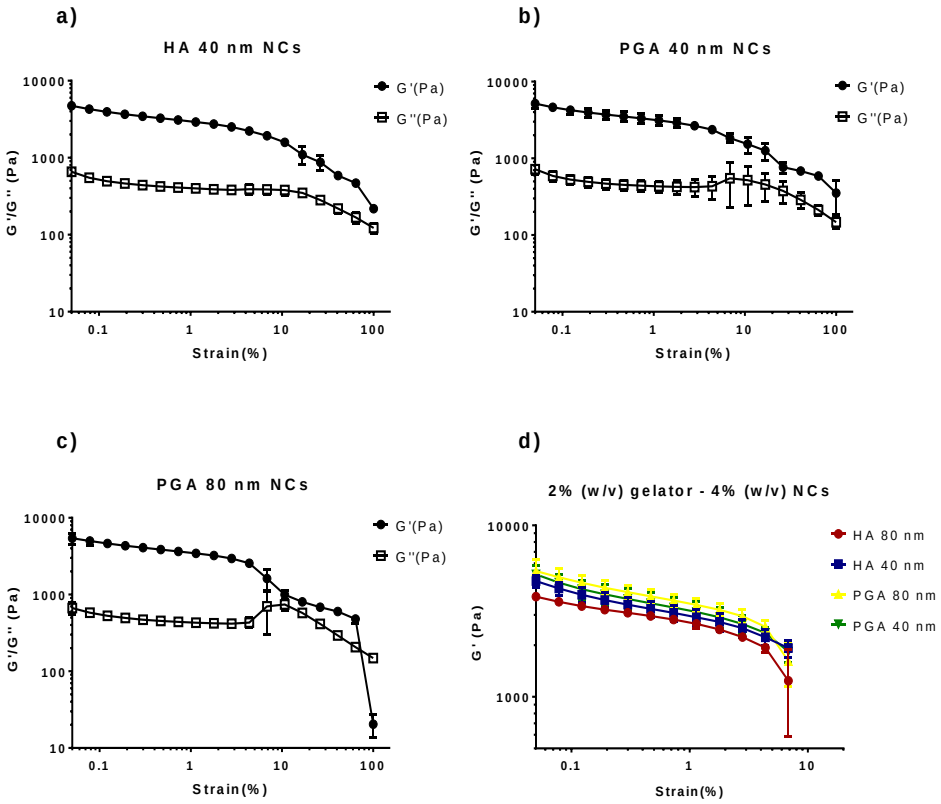


Figure 4-16 Effect of different NCs on gel strength. NCs of 40 or 80 nm in size coated with either hyaluronic acid or polyglutamic acid were used in these experiments. Concentration of gelator and NCs are constant, where N4-octanoyl-2'-deoxycytidine gelator a concentration was 2% w/v with 4% w/v NCs. Amplitude sweeps (G' and G'') at 37 °C, γ= 0.05 – 100% and ω=10 rad/s. Mean values (n=2) are shown where n is a number of independent trials. Gelation time was ≤ 30 minutes.

4.4.3 **Fate of the nanocapsules at 60 ˚C**

Gel manufacture involves solubilisation of the gelator in the aqueous environment of NCs by heating at 60 °C for half an hour where also elevated temperature can influence the characteristics of NCs. Hence in Figure 4-17 effect of temperature on NCs with and without gelator is shown where black bars present size of NCs (40 or 80 nm) initially obtained; bars with grey lines belong to NCs heated at 60 °C and solid light grey bars to gel-NCs formulation heated at 60 °C.

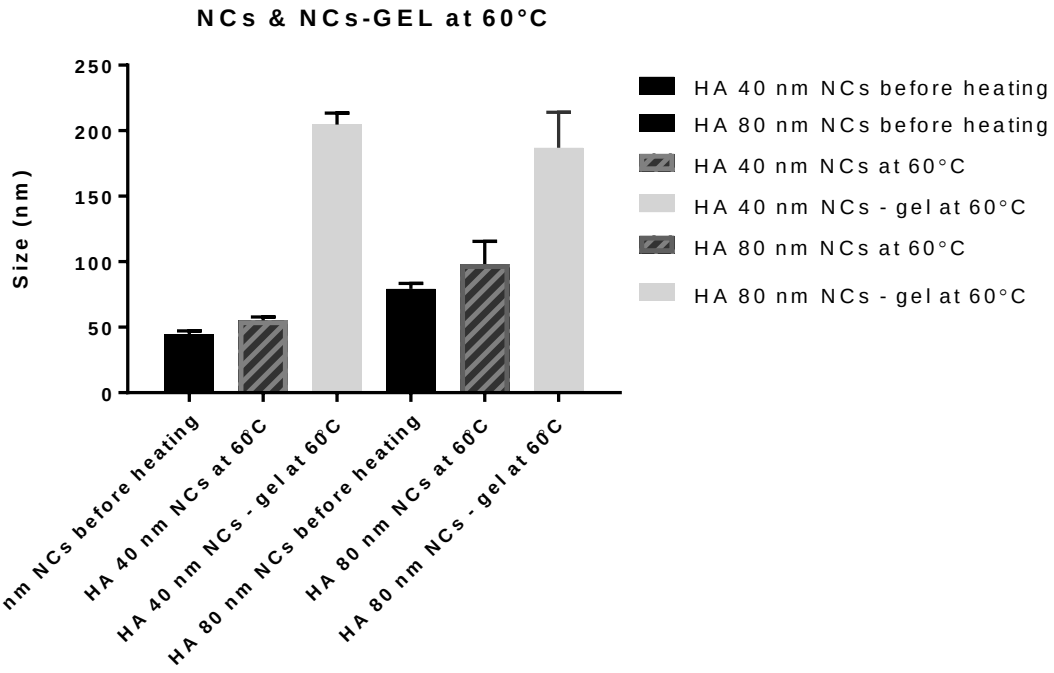


Figure 4-17 Size (nm) of HA 40 or HA 80 nm NCs at 60°C with and without gelator. Black bars present size of nanocapsules before heating or mixing with gelator at room temperature. Black bars with grey lines present size of nanocapsules exposed to heat at 60-70˚C ***without*** *presence of gelator. Grey bars present size of the nanocapsules-gel system* ***together****, when heated/dissolved at 60-70˚C. Mean values (n=3) are shown, error bars represent standard deviation of the mean, where n is number of independent trials.*

NCs heated to 60 °C exhibited only a slight increase in size to 55±3 and 98±17 nm for HA 40 and HA 80 nm systems respectively. However, in the presence of the gelator, the size of NC for both systems, increased up to ~200 nm. It seems that it is not the temperature that causes increase in size of NCs, but presence of gelator around NCs. PDI values for all samples were ≤0.2 suggesting that no aggregation occurred.

4.5 Analysing the microscopic behaviour

Microscopic techniques are used to image gel morphology, its structure and nature of fibres. The most widely used are electron microscopy techniques (scanning and transmission; SEM and TEM respectively). In order to elucidate better gel morphology in presence of capsules in nanometre range, TEM was used over SEM.

4.5.1 Nano structure determination by electron microscopy studies

Morphology of gels and NCs-gel system was assessed using electron microscopy technique and it is performed as per 4.2.6.3. Vacuum drying sample preparation for TEM imaging is more commonly performed, since the preparation of the sample and imaging per se are simpler and less costly, compared to cryo-TEM procedure. Gel in water (Figure 4-18 a.) was imaged using that procedure, while gel-NCs formulation required to be imaged in cryo state in order to preserve its structure. Gel-NCs composite was imaged on the day of the preparation.

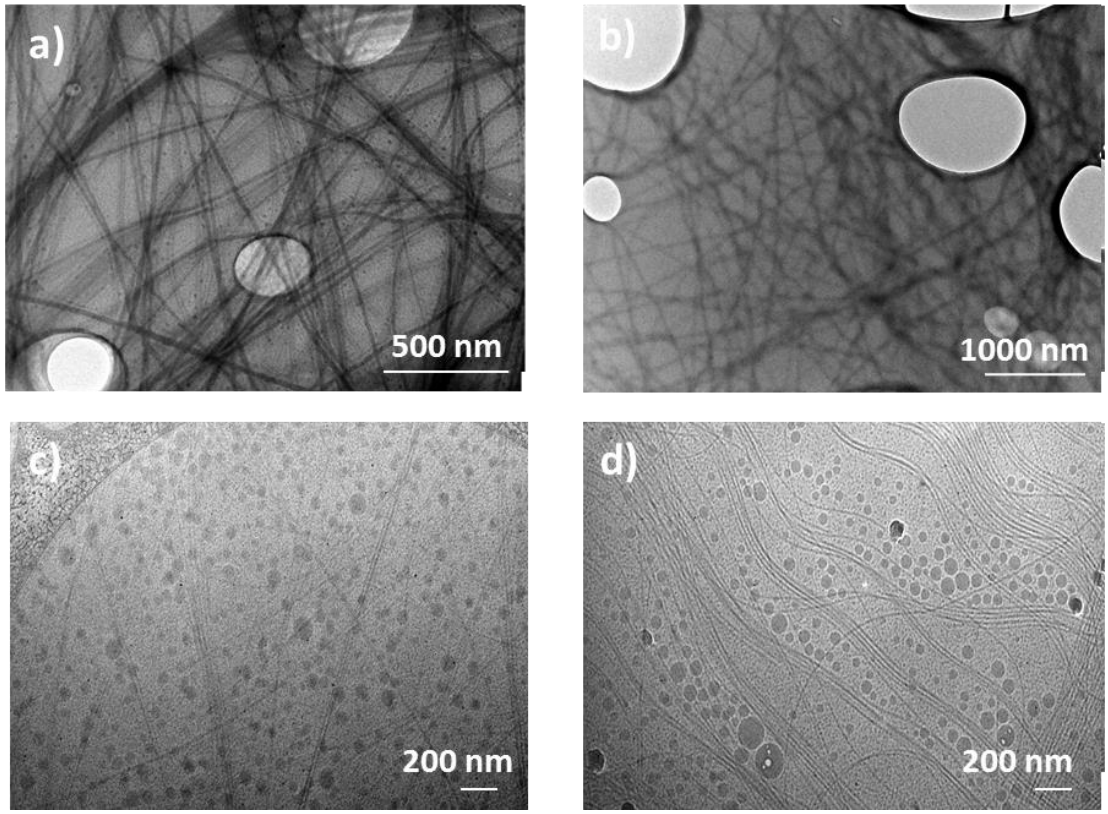


Figure 4-18 TEM images of N4-octanoyl-2'-deoxycytidinegelator in a) water 2% w/v; scale bar is 500 nm; b) HA 80 nm NCs (2% w/v gelator – 8% w/v NCs); scale bar is 1000 nm. Samples were vacuum dried before imaging. c) and d) cryo-TEM imaging of 2% w/v gelator – 8% w/v HA 80 nm NCs.

The image in Figure 4-18 a) presents the structure of the hydrogelator without NCs. A dense structure of relatively straight interconnected fibres that are longer than 2 μm and approximately 10 nm in diameter is characteristic of this hydrogelator (2% w/v *N*4-octanoyl-2'-deoxycytidine in water)[299]. Vacuum drying as a process of sample preparation gives an image of the gel in the dehydrated state i.e. a xerogel and can sometimes can result in formulations collapsing as discussed in 2.2.2.1. This was the case with the gel-NCs formulation (Fig. 4-18 b). The image showed a crosslinked nanofibre structure but no NCs were observed on the sample. However, cryo-TEM was used instead to image the sample allowing analysis of the sample in its

hydrated state. Cryo-TEM image of the gel-NCs associated system is shown in Figure 4-18 c. and d. The presence of fibrous network is clearly seen with homogenous distribution of spheroid particles in between fibres. This indicates that gel formation is not caused by agglomeration. Furthermore, the NCs actually participated in the gel network formation, and they appear to be physically entrapped in the gel network (Figure 4-18. d.). The size of the NCs on the image c) suggests that NCs retained their size <100 nm, while on d) NCs with some larger diameters were observed (<200 nm). Increases in size of the NC to 200 nm as measured by zeta sizer (Figure 4-17), in comparison with data here, suggests that the particles are not aggregating but that the nanofibres are associated with the nanocapsules.

4.6 *In vitro* release of fluorescent dyes from NCs and gel-NCs system

Production of gel-NCs composite, as previously stated, was intended for intratumoural administration. The aim was to produce a gel system that will slowly release NCs loaded with cytotoxic drug to facilitate its delivery through the tumour. In order to investigate the biodistribution of nanocapsules upon injection into an animal, *in vivo* imaging system (IVIS) is commonly used. IVIS often requires introduction of a fluorescent molecular probe that emits in the near infra-red region. This is because animal tissue absorbs visible light, which prevents it from reaching deeper structures. Additionally, high autofluorescence from biological tissue at visible wavelengths (≤650 nm) leads to poor signal-to-background ratios and thus limits the detection[325].

Therefore, two fluorescent dyes were incorporated in NCs: NR and porphyrin. Besides them, encapsulation of DiD and Lumogen IR dyes were attempted, but poor solubility (Lumogen IR) or change in characteristics of the dye (DiD) after incorporation in the lipid phase occurred. Addition of Tween 80 into the oil phase containing DiD transformed its colour from blue-green to yellow-brown where the specific interaction between DiD and Tween 80 masked its colour (see Appendix 6). Hence these formulations were not progressed further.

NR is a hydrophobic dye which emits light below IR where signal could not be separated from the background autofluorescence therefore is not suitable for IVIS imaging. However, due to its lipophilicity and long retention in NCs it is often used to follow the release of NCs from gels[298].

On the other hand, porphyrins, due to their ring structure, absorbs photons efficiently and are one of the compounds most used in photodynamic therapy and for fluorescence diagnosis of cancer[326,327]. It has also been reported elsewhere in encapsulated form in a hydrogel [328,329] for *in vivo* tracking upon intratumoural injection or designed for tracking NPs[330].

For the initial evaluation of the system PBS of 7.4 was chosen. After evaluation of methods of release as discussed in Chapter 2 (Table 2-7) a sample separate method was used for *in vitro* release experiments.

4.6.1 **Release of Nile Red**

Lipophilic dye NR was loaded into polymeric NCs as described in 5.1.2. Size of NCs did not change with loading of NR (Table 4-1).

Table 4-1 Size (nm) and polydispersity (PDI) index of the HA 80 nm NCs after encapsulation of Nile Red. Mean values (n=3±SD), where n is a number of independent trials, are shown.

Sample	***Size (nm)***	***PDI***
HA 80	79 ± 4	0.2
HA 40	44 ± 3	0.2

To investigate the release of the dye from NCs, the HA 80 nm formulation loaded with NR, was incubated with PBS (1:5). SEC columns were used to separate the released free drug from drug still retained in the NCs. Figure 4-19 a. confirms that SEC can be used to separate the nanocapsules from the NR due to small size of NR molecules they are retained in the column, while dye encapsulated in NCs is eluted in the first 2 mL. Figure 4-19 b. shows release of the NR from NCs over 72 hours. Release of NR is very slow with a maximum of 21% released after 3 days, which was expected considering that NR is a hydrophobic compound with higher affinity towards the oil core of NCs compared to the release medium.

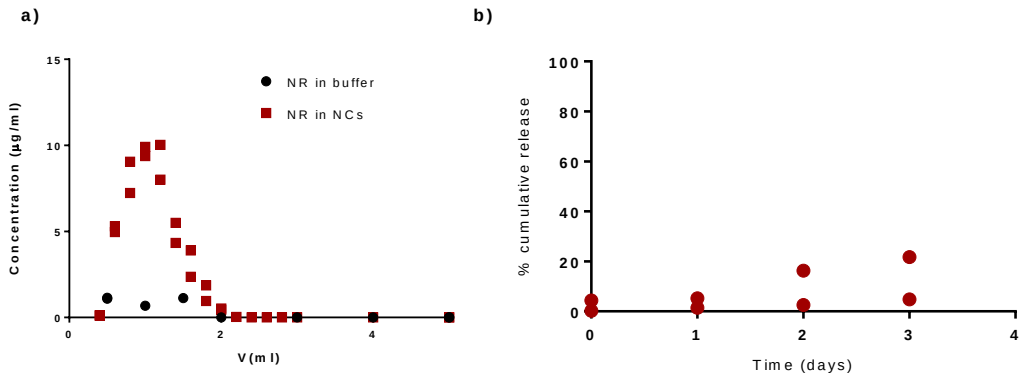


Figure 4-19 Encapsulated NR separation from free dye by SEC columns using PBS buffer as eluent. b) Release of NR from HA 80 nm NCs over 72h, where 1 mL of NCs was incubated with 4 mL of PBS. Mean values (n=2) are shown where n is number of independent trials.

4.6.1.1 ***Release of NCs from the LMW hydrogel***

Drug release from NCs is described in 2.2.6.1. and a very high dilution (0.5 mL of NC with 37.5 mL of buffer) of the NCs in the release medium was used in order to maintain sink conditions. Results showed very slow release of GEM C14 from NCs in buffer (~60% after 30 days). In case of polymer hydrogels, a much lower dilution is commonly reported in the literature and is usually not higher than 1:5[111,232,235]. Indeed, it would not be plausible to follow drug release from the gel at that such low dilutions as sink conditions would not be maintained. On the other hand, if a very high volume of medium was used to follow the release from the gel it would have a significant impact on dissolution of the gel and the nanocapsules could be released instaneously. Therefore, it was decided to follow the release only of NCs from the gel to get an insight into the network between the gel and NCs.

Slow release of NR from NCs, indicated the possibility of understanding the release of NCs from the gel by following the release of NR from the

gel. Hence, 2% w/v gels prepared in 0.5 mL of NR NCs as described in 4.2.5.2. were incubated with 1.25, 2.5 or 5 mL of PBS. NCs formulations were also loaded with GEM C14. Release studies were performed as per 4.2.4.1. With the time, loss of initial gels' mass was noticed. However, after 10 hours, the release medium contained more viscous structures. After 24 h, complete gelation of the release medium occurred (Figure 4-20) independent of the volume buffer added to the gel. This can be explained by gel disassembly in contact with water and reassembly of fibres once the gelator was distributed in the medium. Hence, NC-gels formed with 2% w/v gelator concentration need a higher volume of medium to investigate the NCs' release.

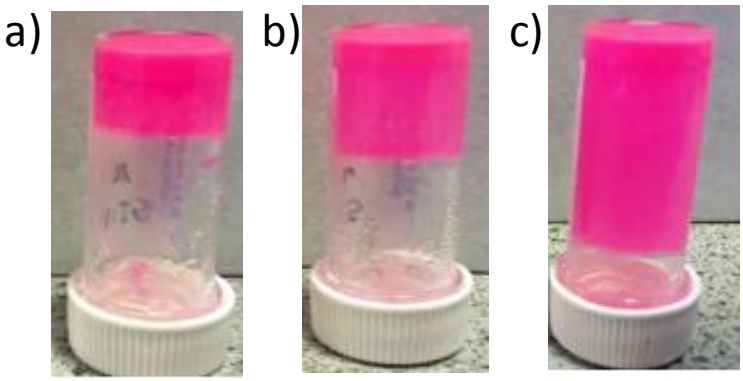


Figure 4-20 2% (w/v) gel - 8% HA 80 NCs system gelled release medium after 24h incubation in water bath (37 °C). PBS, pH=7.4, was used as a release medium. Gels were prepared in 0.5 mL of NCs and toped up with a) 1.25; b) 2.5; c) 5 mL of PBS.

Finally, release of the NCs from gel was followed in PBS with 12.5 mL of buffer added to 0.5 volume of gel. No macroscopic gelling of the medium was observed during the time of the experiment (72 h) and moreover slow gel disassemble was noticed. Different size of NCs and different amounts of NCs were compared (Figure 4-21). Release plots show similar profiles. The gel containing 8% of NCs released NR slightly quicker compared to gel with 4% of NCs. Although not significant, gels containing 80 nm NC showed faster release than from gels containing

smaller 40 nm NCs. Similar was reported for lipid NCs where GEM C12 plays a role as a gelator where NCs of 29 and 55 nm showed negligible difference (10-20%) in release from their gel[298].

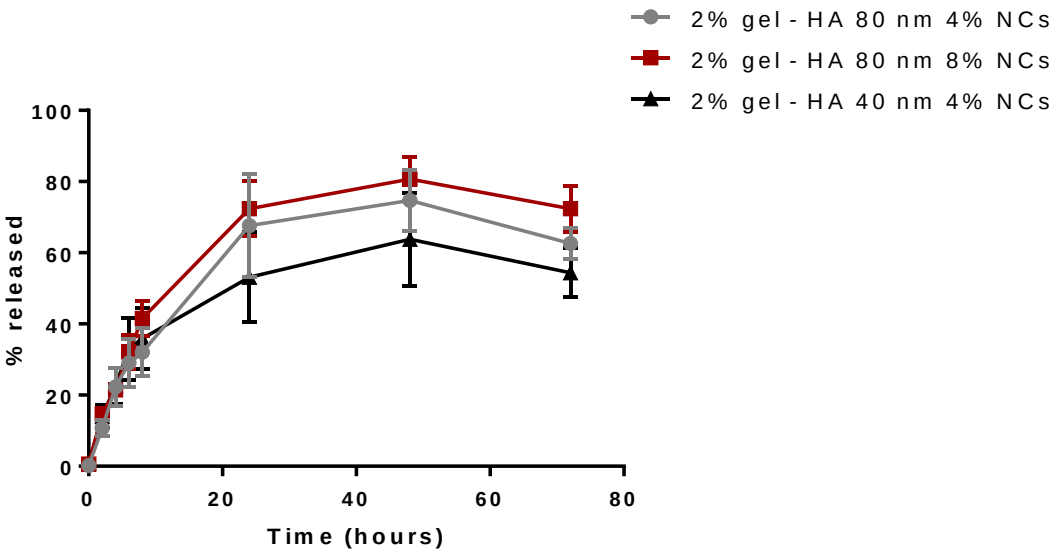


Figure 4-21 Cumulative release of Nile Red/NCs from gel-NCs system at 37°C in PBS medium, pH=7.4. Concentration of gelator in all systems is 2% w/v and NCs used in this experiment are: HA 80 nm NCs of 4 and 8% w/v and HA 40 nm NCs in concentration of 4% w/v. Gels were prepared with 0.5 mL volume of NCs and gel was incubated with 12.5 mL of PBS. Mean values (n=3) are shown, error bars represent standard deviation of the mean, where n is number of independent trials.

Following the release of NCs from the gel, size of the NCs released in the medium was examined as well (Figure 4-23). Released NCs of <200 nm were observed, but much larger than initial size of NCs. Interaction between gelator and NCs is certain, as TEM imaging of gel-NCs system (4.5.1.) also showed presence of fibres and NCs mainly <200 nm. He *et al.* also reported an increase in size of NCs in a thermoresponsive gel formulation compared to NCs alone, where increase in the amount of crosslinker ($CaCl_2$), in organogels made of 12-HSA, increased the size of the beta-lactoglobulin coated lipid particles from 175 to 205 nm[331]. However, they do not provide more details and it is not possible to

compare systems or have a hypothesis on the potential interactions between gel and NPs. It was already hypothesised that drug incorporated in molecular gels can connect to fibres through hydrogen bonds, for example in case of hydrophobic curcumin[318] and camptothecin[321] in peptide hydrogels.

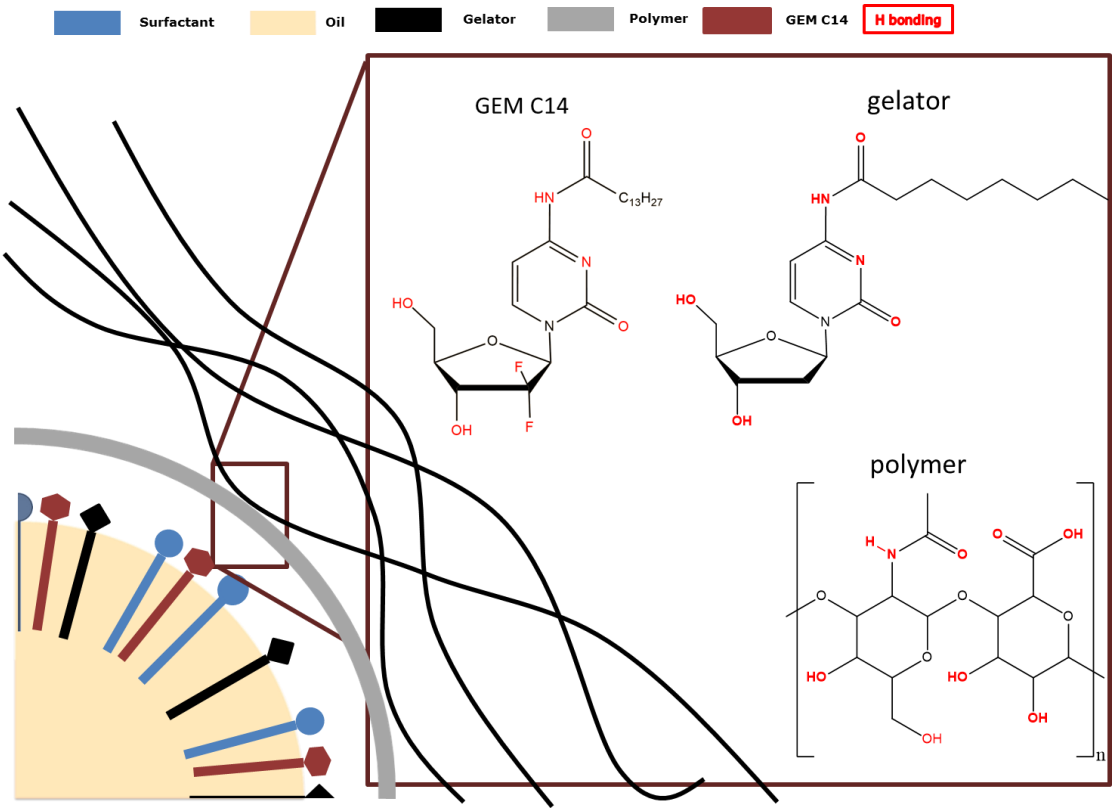


Figure 4-22 Schematical representation of gelator participation in gel-NCs composite. Apart from gelator self-assembly into fibers, it can hypothetically participate at oil-water interface due to its amphiphilic structure. Additionally, connection between gelator and polymer coating (HA) of NCs is presented in red rectangle through hydrogen bonds. Chemical groups with potential for hydrogen bonding are presented in red.

Using FTIR, Nagahama *et al.* suggested that laponite (Si) particles connect with micelles though hydrogen bonds with PEG from the surface of micelles. Similarly Nanda *et al.* assumed that hydrogen bonds are reason for interaction between different ligands of Ag NPs

and peptide gelators[332]. The pyrimidine of *N*4-octanoyl-2'-deoxycytidine, used in our work, has hydrogen bond donors and acceptors that were reported to contribute in self-assembly[333]. Besides the intermolecular hydrogen bonds that provides the basis for self-assembly of the gelator[299], hydrogen bonds could also be the reason for interaction between gelator molecules and polymers from the surface of NCs (Figure 4-22).

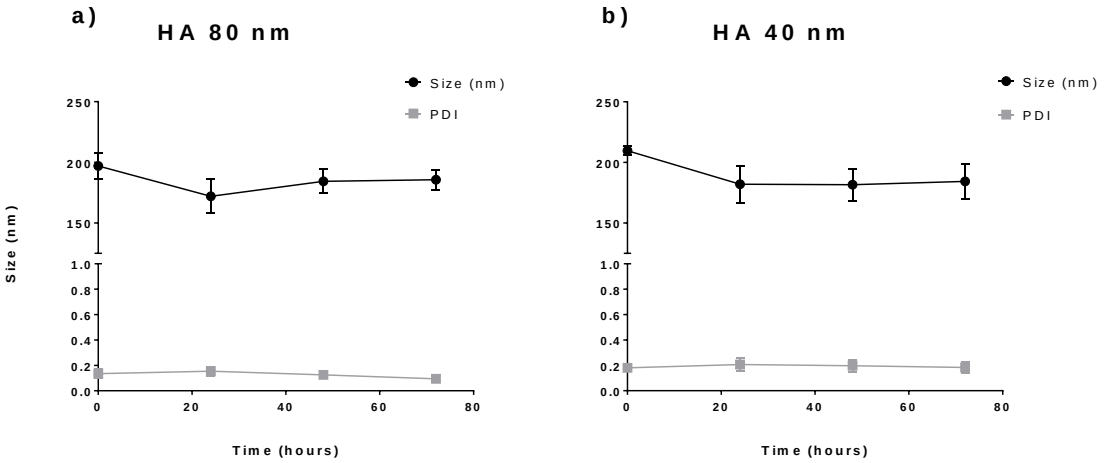


Figure 4-23 Size (nm) and PDI of the sample taken from the release medium over 72h of the experiment. a) 2% gel- 4% HA 80 nm system and b) 2% gel- 4% HA 40 nm system. Mean values (n=3) are shown, error bars represent standard deviation of the mean, where n is number of independent trials.

4.6.2 **Release of porphyrin**

Porphyrin was loaded into HA 80 NCs as described in 4.2.3. Encapsulation efficiency was ~60%, and size 93±9 nm (PDI=0.2). NCs were separated from free porphyrin using SEC columns and as for NR, free dye was retained in the column longer than NCs making SEC suitable for their separation (4-24 a). In Figure 4-24 b. release of porphyrin from NCs and gel are shown. Burst release of the porphyrin from NCs of 80% occurred after just 2 hours and then no further

porphyrin was released within 24 hours. Presence of gelator in the system slowed porphyrin release in a manner that same percentage (~80%) was released after 24 hours. Indeed, gel-nanocomposite formulations have been previously shown to improve release kinetics. For example, Lallo *et al.* showed that while topotecan was completely released from liposome or hydrogel in less than 24 hours, a composite formulations of liposomes and hydrogel slowed down the release to 20% in the same time frame[116]. Significantly ($p<0.05$) slower release of docetaxel in presence of a pluronic gel was also reported from peptide NPs[288].

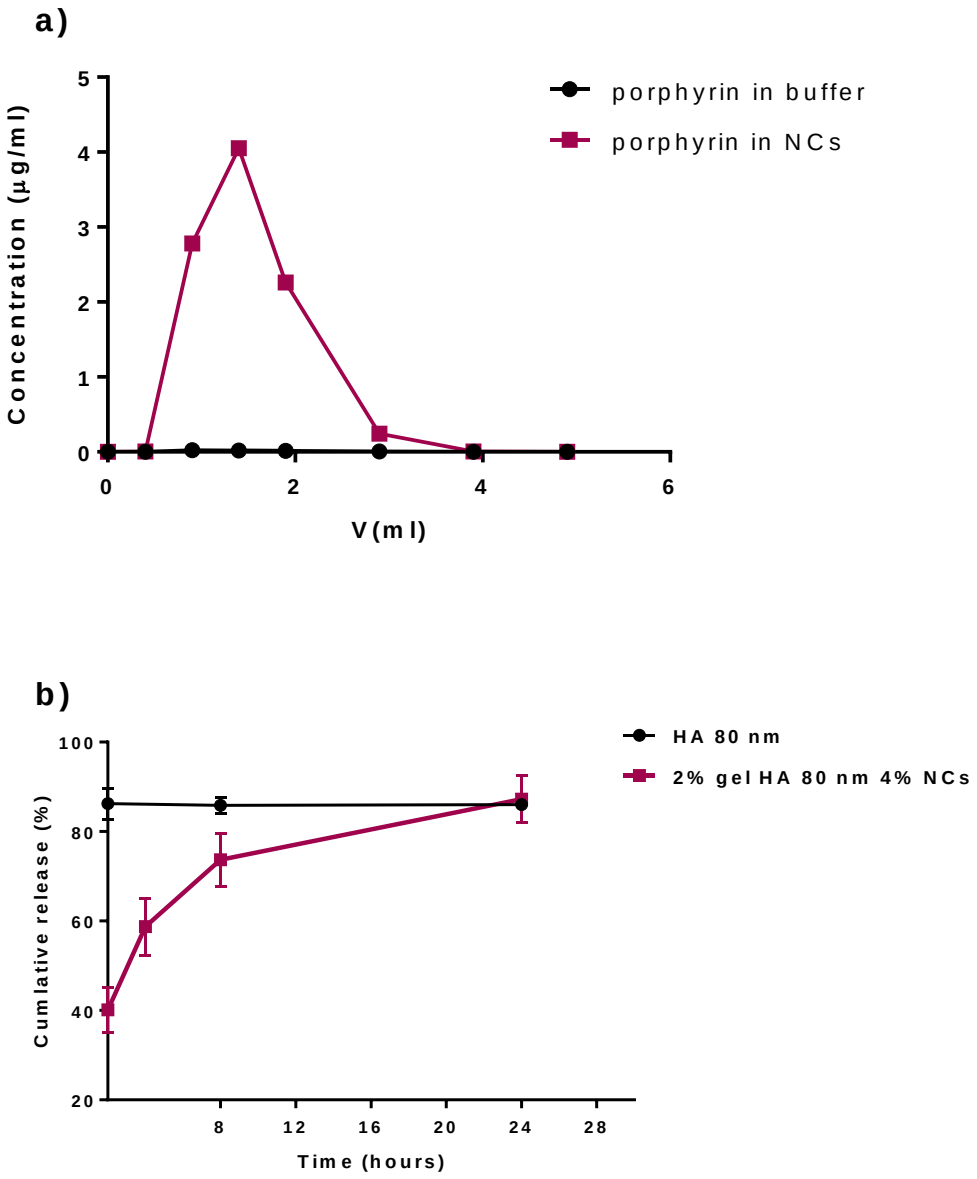


Figure 4-24 a) Encapsulated porphyrin separation from free dye by SEC columns using PBS buffer as eluent. b) Release of porphyrin from HA 80 nm NCs and gel system over 24 h, where formulation to PBS ratio is 1:25. Mean values (n=3) are shown, error bars represent standard deviation of the mean, where n is number of independent trials.

4.6.2.1 *IVIS imaging*

In collaboration with Phil Clarke from Faculty of Medicine & Health Sciences, University of Nottingham, porphyrin formulations were screened using IVIS Image software (4.3.1, Perkin Elmer). It was concluded that porphyrin containing formulations emit light at near infra-red wavelengths (680 nm) with good signal /background ratios at low concentrations (~10 μg/mL).

In conclusion, there are two major requirements for a fluorescent probe to be used for *in vivo* imaging of nanocapsules:

- to have NIR emission that gives a good signal to noise ratio
- to be retained in nanocapsule during the time of imaging,

Unfortunately, porphyrin incorporated in NCs, did not fulfill completely both requirements. The porphyrin formulation has appropriate emission in NIR, but its quick release from the nanocapsules does not allow tracking of the nanocapsule release from the gel. Since, porphyrin delivery is not aligned to the goal of the PhD this was not progressed further.

4.6.3 Injectability of the NC-gels

When considering a formulation for direct intratumoural delivery, injectability of the system is a crucial characteristic to evaluate. In Figure 4-25 syringes loaded with gel formulation with and without NCs are shown and their appearance after dispensing them through the needle is shown at the bottom picture. After dispensing them into the vial, the gel formulation with NCs remained in a gel form. The gel formulation without NCs did not reform into the gel instantly, but only

after some time (30 minutes to 1 h). However, the concentrations of gelator in systems with and without NCs are not comparable, as described earlier in 4.4.2.1.1. rheological studies.

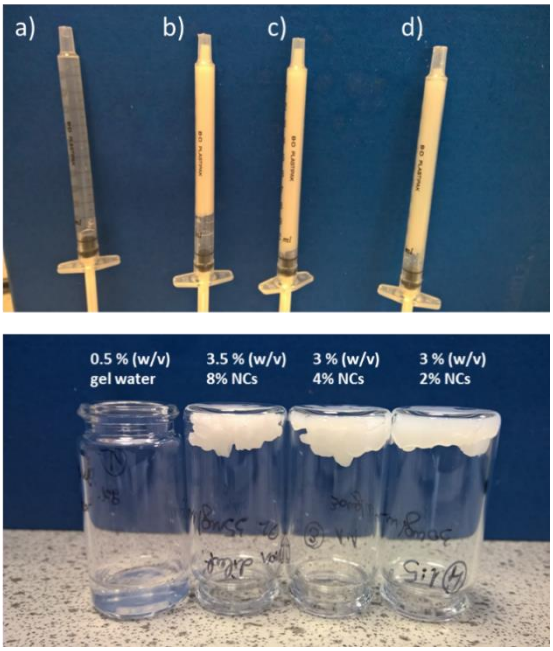


Figure 4-25 Gel formulations dispensed through the syringe (top picture) using needle (25G) into the vial (bottom picture). Formulation used are: a) 0.5% (w/v) gelator-water; b) 3.5% (w/v) gelator – 8% NCs; c) 3% (w/v) gelator – 4% NCS; d) 3% (w/v) gelator – 2% NCs.

Indeed, from the rheological assessment 2% w/v gelator and NC formulations had sufficient mechanical strength for tissue retention and hence for a controlled release depot. Therefore, their ability to be placed in tissue was tested and is presented in Figure 4-26. Formulations with same gelator concentration (2% w/v) but different amount of NCs (8 and 4% w/v) are compared in terms of injectability. While the gel containing 4% w/v NCs retained its structure, the gel containing 8% w/v NCs did not reform after dispensing through a syringe. To mimic a resection site and intratumoural delivery, we bored out a hole in chicken thigh and used a syringe (without needle) to place

the gel inside and observed the shape of the gel. Bottom picture in Figure 4-26 showed the ability of the gel – 4% w/v NCs to retain its gel structure in the tissue, while the gel with 8% of NCs did not.

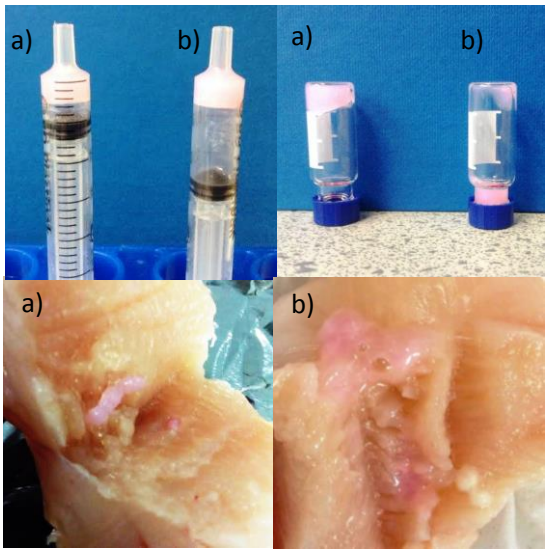


Figure 4-26 Images of 2% w/v gelator in a) 4% w/v HA 80 nm NCs or b) 8% w/v HA 80 nm NCs. Gels formed after dissolution at 60°C were stored in the syringe for 1 hour and dispensed into a vial or in a chicken muscle tissue. Images were taken 5-10 minutes after dispensing gels in into a vial/chicken tissue.

Gels and gel-nanocomposite formulations that reform after intratumoural injection have already been discussed in 4.1.2. Recovery sweep rheology is often carried to mimic the conditions that would be encountered during injection into a tumour site. The measurements are performed by varying the strain between stable condition (as quantified by the LVE region found during the amplitude sweep) and at strain upon which the gel would undergo complete deformation. By monitoring the recovery between these strains gel behaviour upon injection could be predicted. Several LMWG formulations[52,55,70,71] and gel-NPs composite[86,336] showed ability to recover to or near to initial strength. Moysan *et al.* reported concentration dependant recovery with significantly lower G' values after dispensing a gel (5% gelator) through a syringe, while higher concentrations almost fully recovered gel

strength[298]. Skilling *et al.* reported 70% recovery, after time dependant test, for gelator used in this work[299]. We have shown here that appropriate gelator and NCs concentration gives characteristics of a gel that is able to reform after injection.

4.7 Summary

Using hyaluronic acid and chitosan polymers in association with polymeric nanocapsules, gives gels with an observed difference in viscosity when different concentrations of chitosan were used. Further investigation, in terms of gel strength and structure, would be needed for this system to be considered as a drug delivery system.

To obtain optimal gel-NCs composite with use of LMWG the following variables were tested:

- Gelator concentration
- NCs concentration
- Type of nanocapsules

It was concluded that for gel-NCs associated formulations, gel formation is dependent on gelator concentration. Gel mechanical strength increased with increase in gelator concentration, until precipitates were formed which disrupted gel structure. Additionally, an amount of NCs was found to be crucial for gel strength, since too high amount inhibited the LMW gelator from forming the dense cross-linked fibre structures around NCs. Varying concentration of both components, optimal values of 4% w/v NCs and 2% w/v gelator were obtained. The presence of nanocapsules in a nanofibre network was confirmed by TEM imaging.

Changing NCs' size (40 or 80 nm) or polymeric coating (hyaluronic acid or poly-glutamic acid) did not have a significant impact on gel strength.

In conclusion, the amount of NCs and gelator concentration in the formulation were dominant controlling parameters, affecting the rheological properties of the gel-NCs system.

Nanocapsules were slowly released from gel in first 24 hours (~60%), after which an equilibrium was reached. Also, the change in size of NCs (to 172 ± 24 nm) was observed after their release from gel.

Additionally, gel-NCs system exhibited an ability to reform after being dispensed through a syringe.

Compared with previous studies on injectable polymer gel - nanocomposites, data for this gel-NCs formulation suggests that it has promise for applications in drug delivery.

5 Conclusions and future perspectives

Using polymeric NCs and LMWGs, a novel injectable composite was designed for intratumoural application providing a slow delivery of anticancer agent. The composite formulation was developed, characterised and tested for *in vitro* efficacy, injectability and stability in a physiological environment. In this chapter achievements obtained from its development are described. However, there is always room for further improvement and it is discussed below.

5.1.1 **Development of polymeric nanocapsules < 100 nm**

The production of HA or PGA NCs, using a simple and environmentally friendly self-emulsification method, is described in Chapter 2. Polymeric NCs of this size have not been reported before using this method. The optimisation of the composition in terms of non-ionic surfactants and oil lead to the development of NCs <100 nm. In the optimisation process it was found as expected that with the increase in the amount of oil (Miglyol 812N), the size of the nanoemulsion increased. Also, the higher the total amount of surfactants (Tween® 80 and Kolliphor® HS 15) the smaller the size of nanoemulsion. When the amount of Tween® 80 was greater than that of Kolliphor® HS 15 the size of the nanoemulsion droplets increased. Under the same conditions, but using a different oil influenced the size of nanoemulsions where replacing Miglyol® 812N with Maizine® 35-1 resulted in a size increase from <100 to >150 nm.

In order to produce polymeric NCs, the presence of CTAB on the surface of the nanoemulsion droplets facilitated the formation of the polymer

shell of the nanocapsules as confirmed by the switch of the zeta potential from positive to negative values. It was shown that the charge of NCs is influenced by the amount of non-ionic surfactants and by the type of the polymer forming the shell. Increasing the amount of non-ionic surfactant resulted in less negative charge (less negative ZP values). On the other hand, a polymer coating with a higher number of negative groups (HA *versus* PGA) led to NCs with more negative ZP values.

The physical characteristics including the spherical structure of NCs and size < 100 nm were confirmed by TEM imaging. Additionally, NCs did not show any significant change in size upon incubation in simulated biological media (PBS and RPMI). The same was obtained at storage conditions of 8 ºC and RT over a period of 1 month.

For the purpose of final application, anticancer drugs, DCX and GEM C14, were encapsulated with high EE (90%). The final drug loading of the formulations developed was 0.1% (w/w). *In vitro* release experiments showed slow release of GEM C14 from NCs with 60% released during 1 month.

5.1.2 *In vitro* activity of nanocapsules in cancer cells

In chapter 3, the activity of NCs against cancer cell lines was explored and following nanomolar potency of GEM C14 loaded NCs against colorectal - HCT 116 and pancreatic - MIA PaCa-2 and Panc-1 cancer cell lines was concluded. Furthermore, it was shown that the potency of GEM C14 loaded NCs was independent of the polymer coating or the size of the NCs. The non-encapsulated prodrug of gemcitabine and GEM-HCl showed similar GI_{50} values suggesting that modification on *N*-terminal did not influence the drug potency. Potential contribution of surfactants to activity in cancer cells was noted. In the clonogenic

assay, brief exposure of a small number of cancer cells to blank NCs showed that blank NCs with higher surfactant content induced statistically lower number of colonies formed when compared to the control.

Activity of prodrug and NCs against anticancer drug resistant cell lines was also assessed. While GEM showed sensitivity towards vincristine resistant HCT 116 cancer cell line, in Panc-1 cell line with developed resistance to GEM, negligible activity of GEM C14 was observed. The resistance of Panc-1 cells to GEM C14 was significantly reduced, in terms of GI_{50} value, when GEM C14 was loaded into the NCs. However, GI_{50} values of blank and drug loaded NCs were not significantly different in GEM R Panc-1 cell line.

5.1.3 Gel-nanocapsules associated system for localised cancer therapy

In chapter 4 a gel-NCs formulation was designed for local cancer therapy. Composites of NCs and gels were formed. The work was mainly focused on LMWGs, however NCs associated with polymeric gels were screened initially. Polymeric gels of CS-HA were formulated with HA 80 and HA 40 nm NCs using a double-barrel syringe or mixing with magnetic stirring where the later procedure yielded a greater volume of gel with better observable consistency. It was also shown that an increased concentration of CS resulted in formation of more viscous gels. These gels were not studied in detail as difficulties in keeping the consistency between independent repeats occurred. In addition, quick release of NCs from gel was observed.

*N*4-octanoyl-2'-deoxycytidine, a LMW gelator, formed gels by a heat-cooling cycle in a suspension of NCs. Both gelator and NC

concentrations influenced the gel strength. A low gelator concentration (0.5 and 1% w/v) did not gel with 8% HA 80 nm NCs whilst reducing the amount of NCs to 4 and 2% resulted in the production of gels. When the gelator concentration increased, the mechanical strength of the gels increased as measured by oscillatory rheology. Specifically, values of storage and loss moduli (G' and G''), as well as the difference between them and the length of LVE region increased in both gel-water and gel-NCs formulations. Also, the gel strength was independent of the nature of the polymer coating (HA versus PGA) or the size of NCs.

The release of NCs from the gel was followed incorporating NR into the NCs. Upon exposure of the LMWG gel-NCs formulation to large volumes of PBS, it was shown that gel can retain NCs as approximately 30% of the NCs were released in the first 8h and 63% at 72h for 2% gel - 4% HA 80 nm NCs formulation. The size or concentration of NCs did not influence the release profile significantly.

Structure of this novel LMWG-NCs formulation was confirmed by TEM where the presence of fibers >2 μm in length and 10 nm in diameter and NCs approximately 100 nm in diameter were observed in the same sample.

As a final perspective of this formulation for local cancer delivery, 3% w/v gel with 8, 4 or 2% w/v NCs formulations reformed instantly their gel structure upon being dispensed through a needle. In addition, formulation with gelator concentration 2% w/v and 4% w/v of NCs retained its structure, after being placed by a syringe (without needle) in a hole of chicken thigh mimicking retention in tissue.

5.2 Future work

5.2.1 Further optimization of NCs formulation

The objective to produce NCs <100 nm as a carrier for anticancer drugs is achieved. However, very small NCs (~30-40 nm) were produced at the expense of a decrease in the amount of oil. Although, the potential of NCs as a carrier for anticancer drugs was demonstrated through high encapsulation efficiency, a drawback was low drug loading (0.1%) of the formulations developed. Hence, screening of additional oils and surfactants that can accommodate more drug, while retaining small size, would be beneficial. This is important in order to ensure drug amounts at a therapeutic level.

Although NCs yielded good stability in PBS and RPMI, these simulated biological media are far from *in vivo* conditions. The physicochemical characterisation of the NCs incubated in human blood plasma and the analysis of the potential protein corona around the NCs would give a better insight on what would happen to NCs in the body.

5.2.2 NCs on cellular level

The activity of NCs in wild type cancer cell lines (HCT 116, MIA PaCa-2 and Panc-1) is shown and the activity of GEM C14 was not compromised during the encapsulation process. Additionally, blank NCs were not toxic at GI_{50} concentrations against the same cell lines. Contrarily, although GEM C14 loaded NCs showed significantly lower GI_{50} values compared to those of the drug alone towards a GEM resistant cell line, surprisingly, both, blank and GEM-loaded NCs, showed similar activity. Therefore, it would be important to elucidate the impact of all NCs components on these cancer cells. For instance, the effect of especially

the cationic surfactant, as a potential chemosensitiser, on cancer cells could explain similar activity of blank and loaded NCs. Furthermore, assessment of NEs' activity (NCs without polymer coating) would help to understand if polymer coating brings any targeting properties towards receptors on these cancer cells.

In order to elucidate mechanism of GEM C14 and GEM C14 loaded NCs on cancer cells future experiments should also involve confocal imaging of fluorescently labeled NCs in order to confirm their uptake, identification of transporters on the cell surface and their influence on drug and NCs uptake, as well as, experiments which would explore mechanisms by which apoptosis is induced. Finally, selectivity of NCs towards non-cancerous cells (e.g. human fibroblast) also remains unexplored.

5.2.3 Localisation of gel-NCs formulation upon intratumoural injection

5.2.3.1 *Polymeric gel-NCs composite*

HA 80 or 40 nm NCs associated with HA-CS polymer network were characterised mainly by visual appearance. Although increase in viscosity was noted with polymer concentration, rheological evaluation is needed to have an insight on gel strength. Furthermore, future experiments should involve TEM imaging in order to elucidate gel-NC structure.

Apparently, HA-CS gel containing NCs left in unreacted liquid showed a relatively fast release of the NCs. However, this analysis was simply based on visual qualification and a more rigorous analysis of this process would be necessary. In brief, release experiments of NCs and

drug from various polymeric gel-NCs formulation should be done in order to optimise the formulation further.

5.2.3.2 *LMW gel-NCs composite*

It was confirmed that *N*4-octanoyl-2'-deoxycytidine gelator formed fibrous structure around spherical NCs, however additional analysis is needed to further analyze the type of interaction between gel and NCs network. For example, it is possible that imaging of the samples from release medium would give some more information on what is happening in this complex system i.e. if NCs are diffused through gel structure or fibre disassembly also occurred. Additionally, considering the amphiphilic structure of both, the gelator and the modified drug, surface tension measurements would be important to confirm whether they have the potential to sit at the oil water interface of the NCs and contribute to the connection between NCs and fibres.

Incubation of NCs with gel increased the size of NCs which was concluded to be probably due to the effect of gelator presence around NCs and not elevated temperature. However, a method of gel-NCs preparation can involve some improvements. Indeed, during gel-NCs preparation, solubilisation of gelator in NCs at elevated temperatures (60-70 °C) had to be monitored since these conditions could be destructive. Perhaps another way of their association could be explored. For instance, in future experiments, the gelator could be first solubilised in water and then mixed with NCs, in order to minimize the exposure to heat.

Conditions under which release from the gel is followed are extreme in terms of volume used, compared to similar systems available in the literature. This implies similar or superior behavior of gel retention at the injection site *in vivo*. Therefore, *in vivo* imaging of the fluorescent

labelled nanocapsules upon their injection to a tumour xenograft model has to be examined. Explored fluorescent labels, NR and porphyrin, did not fully satisfy requirements for IVIS imaging, hence another fluorescent label has to be considered.

Overall, the achievements of this project brought for the first-time development of the very small NCs with nanomolar potency against cancer cells and progress towards tackling chemoresistance *in vitro*. Another novelty is NCs composite formulation with LMWGs with the slow release of the anticancer agent. The observed retained gel properties after the stress of being dispensed through the syringe makes this formulation attractive for the local delivery of anti-cancer drugs. The next big question that these data leave is if this formulation can make an impact *in vivo* as well?

References

1. Hanahan, D. & Weinberg, R. A. Review Hallmarks of Cancer : The Next Generation. *Cell* **144,** 646–674 (2011).
2. Cancer Research UK. www.cancerresearchuk.org. Available at: https://www.cancerresearchuk.org/. (Accessed: 11th December 2017)
3. Home - Macmillan Cancer Support. Available at: https://www.macmillan.org.uk/. (Accessed: 28th August 2017)
4. Noppen, M. & Rabe, K. F. Place of cryotherapy, brachytherapy and photodynamic therapy in therapeutic bronchoscopy of lung cancers. *Eur. Respir. J.* **28,** 200–218 (2006).
5. Durante, M. & Loeffler, J. S. Charged particles in radiation oncology. *Nat. Rev. Clin. Oncol.* **7,** 37–43 (2009).
6. Verellen, D., Ridder, M. De & Storme, G. A (short) history of image-guided radiotherapy. *Radiother. Oncol.* **86,** 4–13 (2008).
7. Kong, F.-M. *et al.* High-dose radiation improved local tumor control and overall survival in patients with inoperable/unresectable non–small-cell lung cancer: Long-term results of a radiation dose escalation study. *Int. J. Radiat. Oncol. Biol. Phys.* **63,** 324–333 (2005).
8. Barlesi, F. *et al.* Pemetrexed and cisplatin as first-line chemotherapy for advanced non-small-cell lung cancer (NSCLC) with asymptomatic inoperable brain metastases: A multicenter phase II trial (GFPC 07-01). *Ann. Oncol.* **22,** 2466–2470 (2011).
9. Adam, R. *et al.* Rescue Surgery for Unresectable Colorectal Liver Metastases Downstaged by Chemotherapy. *Meet. Am. Surg.*

Assoc. **CXXII,** 242–256 (2004).

10. Alsop, B. R. & Sharma, P. Esophageal Cancer. *Gastroenterol. Clin. North Am.* **45,** 399–412 (2016).
11. Strasser, J., Fung, L., Saltzman, W. M. & Fung, L. K. Distribution of 1,3-bis(2-Chloroethyl)-1-Nitrosourea and tracers in the Rabbit Brain After Interstitial and Tracers Delivery by Biodegradable polymer implants. *J. Pharmacol. Exp. Ther.* **275,** 1647–1655 (1995).
12. Lu, D. S. K., Reber, H. a, Krasny, R. M., Kadell, B. M. & Sayre, J. Local Staging of Pancreatic Cancer: Criteria for Unresectability of Major Vessels as Revealed by Pancreatic-Phase, Thin-Section Helical CT David. *Am. J. Radiol.* **168,** 1439–1443 (1997).
13. *European Medical Research Councils (EMRC) Forward Look on Nanomedicine report*. (2004).
14. Strebhardt, K. & Ullrich, A. Paul Ehrlich ' s magic bullet concept : 100 years of progress. *Nat. Rev. Cancer* **8,** 473–480 (2008).
15. Bangham, A. D. & Horne, R. W. Negative Staining of Phospholipids and their Structural Modification by Surface-active agents as observed in electron microscope. *J. Mol. Biol.* **8,** 660–668, IN2–IN10 (1964).
16. Lee D. Lesserman, Jacques Barbert, F. K. Targeting to cells of fluorescent liposomes covalently coupled with monoclonal antibody or protein A. *Nature* **288,** 602–604 (1980).
17. Hervella, P. Nanomedicine: new challenges and opportunities in cancer therapy. *J. Biomed. …* **4,** (2008).
18. Shi, J., Kantoff, P. W., Wooster, R. & Farokhzad, O. C. Cancer nanomedicine : progress , challenges and opportunities. *Nat. Publ.*

Gr. **17,** 20–37 (2016).

19. Samad, A., Sultana, Y. & Aqil, M. Liposomal Drug Delivery Systems : An Update Review. *Curr. Drug Deliv.* **4,** 297–305 (2007).

20. Allen, T. M. & Cullis, P. R. Liposomal drug delivery systems : From concept to clinical applications. *Adv. Drug Deliv. Rev.* **65,** 36–48 (2013).

21. Immordino, M. L. & Cattel, L. Stealth Liposomes : Review of the Basic Science, Rationale, and Clinical Applications, Existing and Potential. *Int. J. Nanomedicine* **3,** 297–315 (2006).

22. Noble, G. T., Stefanick, J. F., Ashley, J. D., Kiziltepe, T. & Bilgicer, B. Ligand-targeted liposome design : challenges and fundamental considerations. *Trends Biotechnol.* **32,** 32–45 (2014).

23. Sercombe, L. *et al.* Advances and challenges of liposome assisted drug delivery. *Front. Pharmacol.* **6,** 1–13 (2015).

24. Li, C. Poly(L-glutamic acid)--anticancer drug conjugates. *Adv. Drug Deliv. Rev.* **54,** 695–713 (2002).

25. Duncan, R. Development of HPMA copolymer-anticancer conjugates: Clinical experience and lessons learnt. *Adv. Drug Deliv. Rev.* **61,** 1131–1148 (2009).

26. Banerjee, S. S., Aher, N., Patil, R. & Khandare, J. Poly (ethylene glycol) -Prodrug Conjugates : Concept , Design and Applications. *J. Drug Deliv.* 1–17 (2012). doi:doi:10.1155/2012/103973

27. Hamley, I. W. PEG – Peptide Conjugates. *Biomacromolecules* **15,** 1543–1559 (2014).

28. Duncan, R. Polymer conjugates as anticancer nanomedicines. *Nat. Rev.* **6,** 688–701 (2006).

29. Cheng, Y., Zhao, L., Li, Y. & Xu, T. Design of biocompatible dendrimers for cancer diagnosis and therapy: current status and future perspectives. *Chem. Soc. Rev.* **40,** 2673–2703 (2011).

30. Kronberg, B. Current Opinion in Colloid & Interface Science The hydrophobic effect. *Curr. Opin. Colloid Interface Sci.* **22,** 14–22 (2016).

31. Biswas, S., Kumari, P., Lakhani, P. M. & Ghosh, B. European Journal of Pharmaceutical Sciences Recent advances in polymeric micelles for anti-cancer drug delivery. *Eur. J. Pharm. Sci.* **83,** 184–202 (2015).

32. Ren, J., Fang, Z., Yao, L., Zohra, F. & Yin, L. A micelle-like structure of poloxamer – methotrexate conjugates as nanocarrier for methotrexate delivery. *Int. J. Pharm.* **487,** 177–186 (2015).

33. Pouton, C. W. & Akhtarb, S. Biosynthetic polyhydroxyalkanoates and their potential in drug delivery. *Adv. Drug Deliv. Rev.* **18,** 133–162 (1996).

34. Sharma, S., Parmar, A., Kori, S. & Sandhir, R. PLGA-based nanoparticles : A new paradigm in biomedical applications. *Trends Anal. Chem.* **80,** 30–40 (2016).

35. Dan, G., Mihai, A., Bejenaru, C. & Everard, L. Polymeric protective agents for nanoparticles in drug delivery and targeting. *Int. J. Pharm.* **510,** 419–429 (2016).

36. Atilla, A. H. & Bilensoy, E. Amphiphilic cyclodextrin nanoparticles. *Int. J. Pharm.* (2017). doi:10.1016/j.ijpharm.2017.06.010

37. Masood, F. Polymeric nanoparticles for targeted drug delivery system for cancer therapy. *Mater. Sci. Eng. C* **60,** 569–578 (2016).

38. Yurgel, V., Collares, T. & Seixas, F. Developments in the use of nanocapsules in oncology. **46,** 486–501 (2013).

39. Huynh, N. T., Passirani, C., Saulnier, P. & Benoit, J. P. Lipid nanocapsules: a new platform for nanomedicine. *Int. J. Pharm.* **379,** 201–9 (2009).

40. Anton, N., Benoit, J.-P. & Saulnier, P. Design and production of nanoparticles formulated from nano-emulsion templates-a review. *J. Control. Release* **128,** 185–99 (2008).

41. Barenholz, Y. C. Doxil ® — The fi rst FDA-approved nano-drug : Lessons learned. *J. Control. Release* **160,** 117–134 (2012).

42. Batist, G., Barton, J., Chaikin, P. & Swenson, C. Myocet (liposome-encapsulated doxorubicin citrate): a new approach in breast cancer therapy. *Drug Eval.* **3,** 1739–1751 (2002).

43. Krown, S. E., Northfelt, D. W., Osoba, D. & Stewart, J. S. Use of Liposomal Anthracyclines in Kaposi ' s Sarcoma. *Oncology* **13,** 36–52 (2004).

44. Silverman, J. A. & Deitcher, S. R. Marqibo Ò (vincristine sulfate liposome injection) improves the pharmacokinetics and pharmacodynamics of vincristine. 555–564 (2013). doi:10.1007/s00280-012-2042-4

45. Jr, F. C. P., Grapsa, D., Syrigos, K. N. & Wasif, M. The safety and efficacy of Onivyde (irinotecan liposome injection) for the treatment of metastatic pancreatic cancer following gemcitabine-based therapy. *Expert Rev. Anticancer Ther.* **7140,** (2016).

46. Nardin, A., Lefebvre, M., Labroquère, K., Faure, O. & Abastado, J. Liposomal Muramyl Tripeptide Phosphatidylethanolamine : Targeting and Activating Macrophages for Adjuvant Treatment of

Osteosarcoma. *Curr. Cancer Drug Targets* **6,** 123–133 (2006).

47. P.M. Anderson, MD, PhD, P. Meyers, MD, E. Kleinerman, MD, K. Venkatakrishnan, PhD, D.P. Hughes, MD, PhD, C. Herzog, MD, W. Huh, MD, R. Sutphin, MD, Y. M. Vyas, MD, PhD, V. Shen, MD, A. Warwick, MD, N. Yeager, MD, C. Oliva, MD, B. Wang, PhD, Y. & Liu, PhD, and A. Chou, M. Mifamurtide in Metastatic and Recurrent Osteosarcoma: A Patient Access Study with Pharmacokinetic, Pharmacodynamic, and Safety Assessments. *Pediatr Blood Cancer.* **61,** 238–244 (2015).

48. FDA Approval for Paclitaxel Albumin-stabilized Nanoparticle Formulation - National Cancer Institute. (2013). Available at: https://www.cancer.gov/about-cancer/treatment/drugs/fda-nanoparticle-paclitaxel. (Accessed: 30th June 2017)

49. Pillai, G. Nanomedicines for Cancer Therapy : An Update of FDA Approved and Those under Various Stages of Development. *SOJ Pharm Pharm Sci* **1,** 1–13 (2014).

50. Verma, Jyoti, Sumit Lal, and C. J. V. N. Nanoparticles for hyperthermic therapy : synthesis strategies and applications in glioblastoma. *Int. J. Nanomedicine* **9,** 2863–2877 (2014).

51. Patricia Anne Dinndorf, Joseph Gootenberg, Martin H. Cohen, Patricia Keegan, R. P. FDA Drug Approval Summary: Pegaspargase (Oncaspar) for the First-Line Treatment of Children with Acute Lymphoblastic Leukemia (ALL). *Oncologist* **12,** 991–998 (2007).

52. Ishii, H. *et al.* A Phase I Study of Hepatic Arterial Infusion Chemotherapy with Zinostatin Stimalamer Alone for Hepatocellular Carcinoma. **33,** 570–573 (2003).

53. Kyung, H., Minkyu, A., Sun, J. & Sym, J. A phase II trial of

Cremorphor EL - free paclitaxel (Genexol - PM) and gemcitabine in patients with advanced non - small cell lung cancer. *Cancer Chemother Pharmacol* **8,** 277–282 (2014).

54. Miller, K. *et al.* HERMIONE : a randomized Phase 2 trial of MM-302 plus trastuzumab versus chemotherapy of physician ' s choice plus trastuzumab in patients with previously locally advanced / metastatic breast cancer. *BMC Cancer* **16,** 1–11 (2016).

55. Merrimack Stops the Phase 2 HERMIONE Trial of MM-302 in HER2-Positive Metastatic Breast Cancer. Available at: http://www.prnewswire.com/news-releases/merrimack-stops-the-phase-2-hermione-trial-of-mm-302-in-her2-positive-metastatic-breast-cancer-patients-300382177.html. (Accessed: 30th June 2017)

56. Senzer, N. N. *et al.* Abstract C36: MBP-426, a novel liposome-encapsulated oxaliplatin, in combination with 5-FU/leucovorin (LV): Phase I results of a Phase I/II study in gastro-esophageal adenocarcinoma, with pharmacokinetics. *Mol. Cancer Ther.* **8,** C36–C36 (2009).

57. Shirao, K., Shimada, Y., Nakahama, H. & Matsumura, Y. A phase I and pharmacokinetic study of NK105 , a paclitaxel- incorporating micellar nanoparticle formulation Clinical Studies. *Br. J. Cancer* **97,** 170–176 (2007).

58. Kesharwani, P., Iyer, A. K. & Biomaterials, U. Recent advances in dendrimer-based nanovectors for tumor- targeted drug and gene delivery. *Drug Discov. Today* **20,** 536–547 (2016).

59. Shirao, K., Shimada, Y., Nakahama, H. & Matsumura, Y. A phase I and pharmacokinetic study of NK105 , a paclitaxel- incorporating micellar nanoparticle formulation Clinical Studies. *Br. J. Cancer*

97, 170–176 (2007).

60. Senzer, N. *et al.* Phase I Study of a Systemically Delivered p53 Nanoparticle in Advanced Solid Tumors. *Mol. Ther.* **21,** 1096–1103 (2013).

61. Strumberg, D. *et al.* Phase I clinical development of Atu027 , a siRNA formulation targeting PKN3 in patients with advanced solid tumors. *ternational J. Clin. Pharmacol. Ther.* **50,** 76–78 (2012).

62. Ramanathan, R. K., Hamburg, S. I., Halfdanarson, T. R. & Borad, M. J. A Phase I / II Dose Escalation Study of TKM-080301 , a RNAi Therapeutic Directed Against PLK1 , in Patients with Advanced Solid Tumors , with an Expansion Cohort of Patients with NET or ACC. 80301

63. Bora, R. S. & Gupta, D. RNA interference therapeutics for cancer : Challenges and opportunities (Review). *Mol. Med. Rep.* **6,** 9–15 (2012).

64. Venditto, V. J. & Jr, F. C. S. Cancer nanomedicines : So many papers and so few drugs! *Adv. Drug Deliv. Rev.* **65,** 80–88 (2013).

65. Lammers, T. *et al.* Effect of Intratumoral Injection on the Biodistribution, the Therapeutic Potential of HPMA Copolymer-Based Drug Delivery Systems. *Neoplasia* **8,** 788–795 (2006).

66. Singh, M. *et al.* Injectable small molecule hydrogel as a potential nanocarrier for localized and sustained in vivo delivery of doxorubicin. *Nanoscale* **6,** 12849–12855 (2014).

67. Wang, H. *et al.* The inhibition of tumor growth and metastasis by self-assembled nano fi bers of taxol. *Biomaterials* **33,** 5848–5853 (2012).

68. Yang, Y., Wang, J., Zhang, X., Lu, W. & Zhang, Q. A novel mixed

micelle gel with thermo-sensitive property for the local delivery of docetaxel. *J. Control. Release* **135,** 175–82 (2009).

69. Lee, A. L. Z., Ng, V. W. L., Gao, S., Hedrick, J. L. & Yang, Y. Y. Injectable biodegradable hydrogels from vitamin D-functionalized polycarbonates for the delivery of Avastin with enhanced therapeutic efficiency against metastatic colorectal cancer. *Biomacromolecules* **16,** 465–475 (2015).

70. Emerich, D. F. *et al.* Sustained Release Chemotherapeutic Microspheres Provide Superior Efficacy over Systemic Therapy and Local Bolus Infusions. *Pharm. Res.* **19,** 1052–1060 (2002).

71. Attenello, F. J. *et al.* Use of Gliadel (BCNU) Wafer in the Surgical Treatment of Malignant Glioma: A 10-Year Institutional Experience. *Ann. Surg. Oncol.* **15,** 2887–2893 (2008).

72. Harper, E., Dang, W., Lapidus, R. G. & Garver, R. I. Enhanced efficacy of a novel controlled release paclitaxel formulation (PACLIMER delivery system) for local-regional therapy of lung cancer tumor nodules in mice. *Clin. Cancer Res.* **5,** 4242–4248 (1999).

73. Armstrong, D. K., Fleming, G. F., Markman, M. & Bailey, H. H. A phase I trial of intraperitoneal sustained-release paclitaxel microspheres (Paclimer ®) in recurrent ovarian cancer : A Gynecologic Oncology Group study. *Gynecol. Oncol.* **103,** 391–396 (2006).

74. Weinberg, B. D., Ai, H., Blanco, E., Anderson, J. M. & Gao, J. Antitumor efficacy and local distribution of doxorubicin via intratumoral delivery from polymer millirods. *J. Biomed. Mater. Res.* **A,** 161–170 (2006).

75. Liu, R. *et al.* Prevention of Local Tumor Recurrence Following

Surgery Using Low-Dose Chemotherapeutic Polymer Films. *Ann. Surg. Oncol.* **17,** 1203–1213 (2010).

76. Elstad, N. L. & Fowers, K. D. OncoGel (ReGel / paclitaxel) — Clinical applications for a novel paclitaxel delivery system ☆. *Adv. Drug Deliv. Rev.* **61,** 785–794 (2009).

77. Fleming, A. B. & Saltzman, W. M. Pharmacokinetics of the carmustine implant. *Clin. Pharmacokinet.* **41,** 403–419 (2002).

78. Lee, J., Park, H., Ju, E., Kwark, Y. & Yong, K. Colloids and Surfaces B : Biointerfaces Tuning the sphere-to-rod transition in the self-assembly of thermoresponsive polymer hybrids. **136,** 612–617 (2015).

79. Graham, T., Trans, P. & Lond, R. S. Liquid Diffusion Applied to Analysis. *Phil. Trans. R. Soc. Lond.* **151,** 183–224 (1861).

80. Ferry, J. D. *Viscoelastic properties of polymers*. (Wiley, 1980).

81. Almdal, K., Dyre, J. & Hvidt, S. Towards a Phenomenological Definition of the Term â€™ Gel ’. *Polym. Gels Networks* **1,** 5–17 (1993).

82. Tomasini, C. & Castellucci, N. Peptides and peptidomimetics that behave as low molecular weight gelators. *Chem. Soc. Rev.* **42,** 156–172 (2013).

83. Gibas, I. & Janik, H. Review : Synthetic Polymer Hydrogels for Biomedical. *Chem. Technol.* **4,** 297–304 (2010).

84. Hellio, D. & Djabourov, M. Physically and chemically crosslinked gelatin gels. *Macromol. Symp.* **241,** 23–27 (2006).

85. Vintiloiu, A. & Leroux, J.-C. Organogels and their use in drug delivery--a review. *J. Control. Release* **125,** 179–92 (2008).

86. Appel, E. a., del Barrio, J., Loh, X. J. & Scherman, O. a.

Supramolecular polymeric hydrogels. *Chem. Soc. Rev.* **41,** 6195 (2012).

87. Berger, J. *et al.* Structure and interactions in covalently and ionically crosslinked chitosan hydrogels for biomedical applications. *Eur. J. Pharm. Biopharm.* **57,** 19–34 (2004).

88. Gupta, P., Vermani, K. & Garg, S. Hydrogels: From controlled release to pH-responsive drug delivery. *Drug Discov. Today* **7,** 569–579 (2002).

89. Dewitt, J. M. *et al.* EUS-guided paclitaxel injection as an adjunctive therapy to systemic chemotherapy and concurrent external beam radiation before surgery for localized or locoregional esophageal cancer : a multicenter prospective randomized trial. *Gastrointest. Endosc.* 1–10 (2016). doi:10.1016/j.gie.2016.11.017

90. BioSyntech. Available at: https://www.bdc.ca/en/bdc-capital/venture-capital/portfolio/pages/biosyntech.aspx. (Accessed: 9th August 2017)

91. Berrada, M. *et al.* A novel non-toxic camptothecin formulation for cancer chemotherapy. *Biomaterials* **26,** 2115–2120 (2005).

92. Sangeetha, N. M. & Maitra, U. Supramolecular gels : Functions and uses. *Chem. Soc. Rev.* **34,** 821–836 (2005).

93. Editor, G., Amabilino, D. & Smith, D. K. Lost in translation? Chirality effects in the self-assembly of nanostructured gel-phase materials. *Nanoscale* **38,** 684–694 (2009).

94. Dastidar, P. Supramolecular gelling agents: can they be designed? *Chem. Soc. Rev.* **37,** 2699 (2008).

95. Skilling, K. J. *et al.* Insights into low molecular mass organic gelators: a focus on drug delivery and tissue engineering

applications. *Soft Matter* **10,** 237–256 (2014).

96. Naskar, J., Palui, G. & Banerjee, A. Tetrapeptide-based hydrogels: For encapsulation and slow release of an anticancer drug at physiological ph. *J. Phys. Chem. B* **113,** 11787–11792 (2009).

97. Cheetham, A. G., Zhang, P., Lin, Y., Lock, L. L. & Cui, H. Supramolecular Nanostructures Formed by Anticancer Drug Assembly. *J. Am. Chem. Soc.* **135,** 2907−2910 (2013).

98. Wang, H. *et al.* Self-assembled nanospheres as a novel delivery system for taxol: a molecular hydrogel with nanosphere morphology. *Chem. Commun.* **47,** 4439 (2011).

99. Pokuri, V. K., Fong, M. K. & Iyer, R. Octreotide and Lanreotide in Gastroenteropancreatic Neuroendocrine Tumors. *Curr. Oncol. Rep.* **18,** 1–9 (2016).

100. Klotz, L. *et al.* The efficacy and safety of degarelix: A 12-month, comparative, randomized, open-label, parallel-group phase III study in patients with prostate cancer. *BJU Int.* **102,** 1531–1538 (2008).

101. Schexnailder, P. & Schmidt, G. Nanocomposite polymer hydrogels. *Colloid Polym. Sci.* **287,** 1–11 (2009).

102. Jin, Q., Schexnailder, P., Gaharwar, A. K. & Schmidt, G. Silicate cross-linked bio-nanocomposite hydrogels from PEO and chitosan. *Macromol. Biosci.* **9,** 1028–1038 (2009).

103. Okay, O. *et al.* Polyacrylamide - Clay Nanocomposite Hydrogels : Rheological and Light Scattering Characterization. *Macromolecules* **40,** 3378–3387 (2007).

104. Kokabi, M. & Hassan, Z. M. POLYMER PVA – clay nanocomposite hydrogels for wound dressing. **43,** 773–781 (2007).

105. Rose, S. *et al.* Nanoparticle solutions as adhesives for gels and biological tissues. *Nature* **505,** 382–5 (2014).

106. Hu, Z., Haruna, M., Gao, H., Nourafkan, E. & Wen, D. Rheological Properties of Partially Hydrolyzed Polyacrylamide Seeded by Nanoparticles. *Ind. Eng. Chem. Res.* (2017). doi:10.1021/acs.iecr.6b05036

107. Tokarev, B. I., Tokareva, I. & Minko, S. Gold-Nanoparticle-Enhanced Plasmonic Effects in a Responsive Polymer Gel. *Adv. Mater.* **20,** 2730–2734 (2008).

108. Loo, S. *et al.* Superabsorbent Cryogels Decorated with Silver Nanoparticles as a Novel Water Technology for Point-of-Use Disinfection. *Environ. Sci. Technol. 2013,* **47,** 9363−9371 (2013).

109. Mitra, R. N. & Das, P. K. In situ Preparation of Gold Nanoparticles of Varying Shape in Molecular Hydrogel of Peptide Amphiphiles. *J. Phys. Chem. C* **112,** 8159–8166 (2008).

110. Kudaibergenov, S. E. Polymer Protected and Gel Immobilized Gold and Silver Nanoparticles in Catalysis. *J. Inorg. Organomet. Polym. Mater.* **26,** 1198–1211 (2016).

111. Appel, E. A. *et al.* polymer – nanoparticle interactions. *Nat. Commun.* **6,** 1–9 (2015).

112. Contri, R. V *et al.* Chitosan gel containing polymeric nanocapsules : a new formulation for vaginal drug delivery. *Int. J. Nanomedicine* **9,** 3151–3161 (2014).

113. Grant, J., Blicker, M. & Allen, C. Hybrid Films from Blends of Chitosan and Egg Phosphatidylcholine for Localized Delivery of Paclitaxel. *J. Pharm. Sci.* **94,** 1512–1527 (2005).

114. Gou, M. *et al.* Pharmaceutical Nanotechnology A novel injectable

local hydrophobic drug delivery system : Biodegradable nanoparticles in thermo-sensitive hydrogel . **359,** 228–233 (2008).

115. Bernkop-schnürch, A. Design and evaluation of an intravesical delivery system for superficial bladder cancer : preparation of gemcitabine HCl-loaded chitosan – thioglycolic acid nanoparticles and comparison of chitosan / poloxamer gels as carriers. *Int. J. Nanomedicine* **10,** 6493–6507 (2015).

116. Lalloo, A., Chao, P., Hu, P., Stein, S. & Sinko, P. J. Pharmacokinetic and pharmacodynamic evaluation of a novel in situ forming poly (ethylene glycol) -based hydrogel for the controlled delivery of the camptothecins. **112,** 333–342 (2006).

117. FDA Approval for Gemcitabine Hydrochloride - National Cancer Institute. (2013). Available at: https://www.cancer.gov/about-cancer/treatment/drugs/fda-gemcitabine-hydrochloride. (Accessed: 28th June 2017)

118. Gemcitabine-Gemzar®. Available at: https://find.cancerresearchuk.org/?xss-q=gemcitabine&p=1. (Accessed: 28th June 2017)

119. Mackey2, J. R. *et al.* Functional Nucleoside Transporters Are Required for Gemcitabine Influx and Manifestation of Toxicity in Cancer Cell Lines. *Cancer Res.* **58,** 4349–4357 (1998).

120. García-Manteiga, J., Molina-Arcas, M., Casado, F. J., Mazo, A. & Pastor-Anglada, M. Nucleoside transporter profiles in human pancreatic cancer cells: role of hCNT1 in 2',2'-difluorodeoxycytidine- induced cytotoxicity. *Clin. Cancer Res.* **9,** 5000–8 (2003).

121. Damaraju, V. L. *et al.* Nucleoside anticancer drugs: the role of

nucleoside transporters in resistance to cancer chemotherapy. *Oncogene* **22,** 7524–7536 (2003).

122. Hsu, C.-H., Liou, J.-Y., Dutschman, G. E. & Cheng, Y.-C. Phosphorylation of Cytidine, Deoxycytidine, and Their Analog Monophosphates by Human UMP/CMP Kinase Is Differentially Regulated by ATP and Magnesium. *Mol. Pharmacol.* **67,** 806–14 (2005).

123. Bouffard, D. Y., Laliberté, J. & Momparler, R. L. Kinetic studies on 2′,2′-difluorodeoxycytidine (gemcitabine) with purified human deoxycytidine kinase and cytidine deaminase. *Biochem. Pharmacol.* **45,** 1857–1861 (1993).

124. Gilbert, J. a. *et al.* Gemcitabine pharmacogenomics: Cytidine deaminase and deoxycytidylate deaminase gene resequencing and functional genomics. *Clin. Cancer Res.* **12,** 1794–1803 (2006).

125. Mini, E., Nobili, S., Caciagli, B., Landini, I. & Mazzei, T. Cellular pharmacology of gemcitabine. *Ann. Oncol.* **17,** 7–12 (2006).

126. Heinemann, V. *et al.* Cellular Elimination of 2′,2′-Difluorodeoxycytidine 5′-Triphosphate: A Mechanism of Self-Potentiation. *Cancer Res.* **52,** 533–539 (1992).

127. Ruiz van Haperen, V. W. T., Veerman, G., Vermorken, J. B. & Peters, G. J. 2′,2′-Difluoro-deoxycytidine (gemcitabine) incorporation into RNA and DNA of tumour cell lines. *Biochem. Pharmacol.* **46,** 762–766 (1993).

128. Cerqueira, N. M. F. S. a., Fernandes, P. a. & Ramos, M. J. Understanding ribonucleotide reductase inactivation by gemcitabine. *Chem. - A Eur. J.* **13,** 8507–8515 (2007).

129. Abbruzzese, J. L. New applications of gemcitabine and future directions in the management of pancreatic cancer. *Cancer* **95,** 941–945 (2002).

130. Honeywell, R. J., Ruiz Van Haperen, V. W. T., Veerman, G., Smid, K. & Peters, G. J. Inhibition of thymidylate synthase by 2',2' difluoro-2' deoxycytidine (Gemcitabine) and its metabolite 2',2'-difluoro-2'-deoxyuridine. *Int. J. Biochem. Cell Biol.* **60,** 73–81 (2015).

131. Leaflet, G. (GEMCITABINE HCl) FOR INJECTION. *B1.0 NL 4063 AMP* 1–23

132. Mackey2, J. R. *et al.* Functional Nucleoside Transporters Are Required for Gemcitabine Influx and Manifestation of Toxicity in Cancer Cell Lines1. *Cancer Res.* **58,** 4349–4357 (1998).

133. Spratlin, J. *et al.* The Absence of Human Equilibrative Nucleoside Transporter 1 Is Associated with Reduced Survival in Patients With Gemcitabine- Treated Pancreas Adenocarcinoma. *Clin. Cancer Res.* **10,** 6956–6961 (2004).

134. Kroep, J. R. *et al.* Pretreatment deoxycytidine kinase levels predict in vivo gemcitabine sensitivity. *Mol. Cancer Ther.* **1,** 371–376 (2002).

135. Weizman, N. *et al.* Macrophages mediate gemcitabine resistance of pancreatic adenocarcinoma by upregulating cytidine deaminase. *Oncogene* **33,** 3812–3819 (2014).

136. Khare, V., Sakarchi, W. A., Gupta, P. N., Curtis, A. D. M. & Hoskins, C. Synthesis and characterization of TPGS–gemcitabine prodrug micelles for pancreatic cancer therapy. *RSC Adv.* **6,** 60126–60137 (2016).

137. Vandana, M. & Sahoo, S. K. Long circulation and cytotoxicity of PEGylated gemcitabine and its potential for the treatment of pancreatic cancer. *Biomaterials* **31,** 9340–9356 (2010).

138. Pasut, G. *et al.* Antitumoral activity of PEG-gemcitabine prodrugs targeted by folic acid. *J. Control. Release* **127,** 239–248 (2008).

139. Reddy, L. H. *et al.* A new nanomedicine of gemcitabine displays enhanced anticancer activity in sensitive and resistant leukemia types. *J. Control. Release* **124,** 20–27 (2007).

140. Wickremsinhe, E. *et al.* Preclinical absorption, distribution, metabolism, and excretion of an oral amide prodrug of gemcitabine designed to deliver prolonged systemic exposure. *Pharmaceutics* **5,** 261–276 (2013).

141. Infante, J. R. *et al.* Phase 1b study of the oral gemcitabine 'Pro-drug' LY2334737 in combination with capecitabine in patients with advanced solid tumors. *Invest. New Drugs* **33,** 432–439 (2015).

142. Venugopal, B. *et al.* A first-in-human phase i and pharmacokinetic study of CP-4126 (CO-101), a nucleoside analogue, in patients with advanced solid tumours. *Cancer Chemother. Pharmacol.* **76,** 785–792 (2015).

143. Ali, S. M. *et al.* Synthesis and biological evaluation of gemcitabine-lipid conjugate (NEO6002). *Bioorganic Med. Chem. Lett.* **15,** 2571–2574 (2005).

144. Qi, H. *et al.* Enhanced Antitumor Activity of Monophosphate Ester Prodrugs of Gemcitabine: In Vitro and In Vivo Evaluation. *J. Pharm. Sci.* **105,** 2966–2973 (2016).

145. Wu, W., Sigmond, J., Peters, G. J. & Borch, R. F. Synthesis and biological activity of a gemcitabine phosphoramidate prodrug. *J.*

Med. Chem. **50,** 3743–3746 (2007).

146. Kamaly, N., Xiao, Z., Valencia, P. M., Radovic-Moreno, A. F. & Farokhzad, O. C. Targeted polymeric therapeutic nanoparticles: design, development and clinical translation. *Chem. Soc. Rev.* **41,** 2971 (2012).

147. Damge, C., Michel, C., Aprahamian, M. & Couvreur, P. New approach for oral administration of insulin with polyalkylcyanoacrylate nanocapsules as drug carrier. *Diabetes* **37,** 246–251 (1988).

148. Kirpotin, D. B. *et al.* Antibody targeting of long-circulating lipidic nanoparticles does not increase tumor localization but does increase internalization in animal models. *Cancer Res.* **66,** 6732–40 (2006).

149. Torrecilla, D. *et al.* Anti-tumor efficacy of chitosan-g-poly(ethylene glycol) nanocapsules containing docetaxel: anti-TMEFF-2 functionalized nanocapsules vs. non-functionalized nanocapsules. *Eur. J. Pharm. Biopharm.* **83,** 330–7 (2013).

150. Cirstoiu-Hapca, a. *et al.* Benefit of anti-HER2-coated paclitaxel-loaded immuno-nanoparticles in the treatment of disseminated ovarian cancer: Therapeutic efficacy and biodistribution in mice. *J. Control. Release* **144,** 324–331 (2010).

151. He, C., Hu, Y., Yin, L., Tang, C. & Yin, C. Effects of particle size and surface charge on cellular uptake and biodistribution of polymeric nanoparticles. *Biomaterials* **31,** 3657–66 (2010).

152. Luo, G. *et al.* LyP-1-conjugated nanoparticles for targeting drug delivery to lymphatic metastatic tumors. *Int. J. Pharm.* **385,** 150–6 (2010).

153. Young, K. *et al.* Biomaterials Self-assembled hyaluronic acid nanoparticles for active tumor targeting OH OH OH OH OH OH. *Biomaterials* **31,** 106–114 (2010).

154. Kim, K. *et al.* Self-assembled hyaluronic acid nanoparticles as a potential drug carrier for cancer therapy : synthesis , characterization , and in vivo biodistribution. *J. Mater. Chem.* **19,** 4029–4280 (2009).

155. Gratton, S. E. a *et al.* The effect of particle design on cellular internalization pathways. *Proc. Natl. Acad. Sci. U. S. A.* **105,** 11613–8 (2008).

156. Ernsting, M. J., Murakami, M., Roy, A. & Li, S.-D. Factors controlling the pharmacokinetics, biodistribution and intratumoral penetration of nanoparticles. *J. Control. Release* **172,** 782–794 (2013).

157. Liu, D., Mori, A. & Huang, L. Role of liposome size and RES blockade in controlling biodistribution and tumor uptake of GM , -containing liposomes *. *Biochim. Biophys. Acta* **1104,** 95–101 (1992).

158. Lee, H., Fonge, H., Hoang, B., Reilly, R. M. & Allen, C. articles The Effects of Particle Size and Molecular Targeting on the Intratumoral and Subcellular Distribution of Polymeric Nanoparticles. **7,** 1195–1208 (2010).

159. Jiang, W., Kim, B. Y. S., Rutka, J. T. & Chan, W. C. W. Nanoparticle-mediated cellular response is size-dependent. *Nat. Nanotechnol.* **3,** 145–150 (2008).

160. Mora-Huertas, C. E., Fessi, H. & Elaissari, a. Polymer-based nanocapsules for drug delivery. *Int. J. Pharm.* **385,** 113–42 (2010).

161. Heurtault, B. *et al.* The influence of lipid nanocapsule composition on their size distribution. *Eur. J. Pharm. Sci.* **18,** 55–61 (2003).

162. Oyarzun-Ampuero, F. a., Rivera-Rodriguez, G. R., Alonso, M. J. & Torres, D. Hyaluronan nanocapsules as a new vehicle for intracellular drug delivery. *Eur. J. Pharm. Sci.* **49,** 483–490 (2013).

163. Rivera-Rodriguez, G. R. *et al.* In vivo evaluation of poly-l-asparagine nanocapsules as carriers for anti-cancer drug delivery. *Int. J. Pharm.* **458,** 83–89 (2013).

164. Lollo, G. *et al.* Enhanced in vivo therapeutic efficacy of plitidepsin-loaded nanocapsules decorated with a new poly-aminoacid-PEG derivative. *Int. J. Pharm.* **483,** 212–219 (2015).

165. Janes, K. A., Fresneau, M. P., Marazuela, A., Fabra, A. & Alonso, M. J. Chitosan nanoparticles as delivery systems for doxorubicin. *J. Control. Release* **73,** 255–267 (2001).

166. Rivera-Rodriguez, G. R. *et al.* In vivo evaluation of poly-l-asparagine nanocapsules as carriers for anti-cancer drug delivery. *Int. J. Pharm.* **458,** 83–89 (2013).

167. Gonz??lez-Aramundiz, J. V. *et al.* Rational design of protamine nanocapsules as antigen delivery carriers. *J. Control. Release* **245,** 62–69 (2017).

168. Borrajo, E. *et al.* Docetaxel-loaded Polyglutamic acid-PEG Nanocapsules for the Treatment of Metastatic Cancer. *Submitt. to J. Control. Release* **238,** 263–271 (2016).

169. Lollo, G. *et al.* Enhanced in vivo therapeutic efficacy of plitidepsin-loaded nanocapsules decorated with a new poly-aminoacid-PEG derivative. *Int. J. Pharm.* **483,** 212–219 (2015).

170. Ezhilarasi, P. N., Karthik, P., Chhanwal, N. & Anandharamakrishnan, C. Nanoencapsulation Techniques for Food Bioactive Components: A Review. *Food Bioprocess Technol.* **6,** 628–647 (2013).

171. Song, X., Zhou, C., Fu, F., Chen, Z. & Wu, Q. Effect of high-pressure homogenization on particle size and film properties of soy protein isolate. *Ind. Crops Prod.* **43,** 538–544 (2013).

172. Abbas, S. *et al.* Fabrication of polymeric nanocapsules from curcumin-loaded nanoemulsion templates by self-assembly. *Ultrason. Sonochem.* **23,** 81–92 (2015).

173. Prego, C. *et al.* Chitosan-PEG nanocapsules as new carriers for oral peptide delivery. Effect of chitosan pegylation degree. *J. Control. Release* **111,** 299–308 (2006).

174. Abellan-Pose, R. *et al.* Polyaminoacid Nanocapsules for Drug Delivery to the Lymphatic System: Effect of the Particle Size. *Int. J. Pharm.* **509,** 107–117 (2016).

175. Chorny, M., Fishbein, I., Danenberg, H. D. & Golomb, G. Lipophilic drug loaded nanospheres prepared by nanoprecipitation: Effect of formulation variables on size, drug recovery and release kinetics. *J. Control. Release* **83,** 389–400 (2002).

176. Shinoda, K. & Saito, H. The Stability of O/W type emulsions as functions of temperature and the HLB of emulsifiers: The emulsification by PIT-method. *J. Colloid Interface Sci.* **30,** 258–263 (1969).

177. Ševčíková, P., Kašpárková, V., Vltavská, P. & Krejčí, J. On the preparation and characterization of nanoemulsions produced by phase inversion emulsification. *Colloids Surfaces A Physicochem. Eng. Asp.* **410,** 130–135 (2012).

178. Anton, N., Gayet, P., Benoit, J.-P. & Saulnier, P. Nano-emulsions and nanocapsules by the PIT method: an investigation on the role of the temperature cycling on the emulsion phase inversion. *Int. J. Pharm.* **344,** 44–52 (2007).

179. Keohane, K., Rosa, M., Coulter, I. S. & Griffin, B. T. Enhanced colonic delivery of ciclosporin A self-emulsifying drug delivery system encapsulated in coated minispheres. *Drug Dev. Ind. Pharm.* **42,** 245–253 (2015).

180. Van Speybroeck, M. *et al.* Incomplete desorption of liquid excipients reduces the in vitro and in vivo performance of self-emulsifying drug delivery systems solidified by adsorption onto an inorganic mesoporous carrier. *Mol. Pharm.* **9,** 2750–2760 (2012).

181. Abdalla, A. & Mäder, K. Preparation and characterization of a self-emulsifying pellet formulation. *Eur. J. Pharm. Biopharm.* **66,** 220–226 (2007).

182. Wu, L. *et al.* A Self-microemulsifying Drug Delivery System (SMEDDS) for a Novel Medicative Compound Against Depression: a Preparation and Bioavailability Study in Rats. *AAPS PharmSciTech* **16,** 1051–1058 (2015).

183. Julianto, T., Yuen, K. H. & Noor, A. M. Improved bioavailability of vitamin E with a self emulsifying formulation. *Int. J. Pharm.* **200,** 53–57 (2000).

184. Nazzal, S., Smalyukh, I. I., Lavrentovich, O. D. & Khan, M. A. Preparation and in vitro characterization of a eutectic based semisolid self-nanoemulsified drug delivery system (SNEDDS) of ubiquinone: Mechanism and progress of emulsion formation. *Int. J. Pharm.* **235,** 247–265 (2002).

185. Thakare, P., Mogal, V., Borase, P., Dusane, J. & Kshirsagar, S.

Review Article A review on self-emulsified drug delivery system Self-emulsifying. **3,** 140–153 (2016).

186. Gursoy, R. N. & Benita, S. Self-emulsifying drug delivery systems (SEDDS) for improved oral delivery of lipophilic drugs. *Biomed. Pharmacother.* **58,** 173–182 (2004).

187. Miller, C. A. Spontaneous Emulsification Produced by Diffusion - A Review. *Colloids and Surfaces* **29,** 89–102 (1988).

188. Obitte, N. C., Rohan, L. C., Adeyeye, C. M., Parniak, M. a & Esimone, C. O. The utility of self-emulsifying oil formulation to improve the poor solubility of the anti HIV drug CSIC. *AIDS Res. Ther.* **10,** 14 (2013).

189. Reiss, H. Entropy-induced dispersion of bulk liquids. *J. Colloid Interface Sci.* **53,** 61–70 (1975).

190. Komaiko, J., Sastrosubroto, A. & McClements, D. J. Formation of Oil-in-Water Emulsions from Natural Emulsifiers Using Spontaneous Emulsification: Sunflower Phospholipids. *J. Agric. Food Chem.* **63,** 10078–10088 (2015).

191. Sugumar, S., Mukherjee, A. & Chandrasekaran, N. Nanoemulsion formation and characterization by spontaneous emulsification: investigation of its antibacterial effects on Listeria monocytogenes. *Asian J. Pharm.* **9,** 23–28 (2015).

192. Saberi, A. H., Fang, Y. & McClements, D. J. Fabrication of vitamin E-enriched nanoemulsions: Factors affecting particle size using spontaneous emulsification. *J. Colloid Interface Sci.* **391,** 95–102 (2013).

193. Andey, T. *et al.* Formulation, pharmacokinetic, and efficacy studies of mannosylated self-emulsifying solid dispersions of

noscapine. *PLoS One* **11,** 7–9 (2016).

194. Yang, S., Gursoy, R. N., Lambert, G. & Benita, S. Enhanced Oral Absorption of Paclitaxel in a Novel Self-Microemulsifying Drug Delivery System with or without Concomitant Use of P-Glycoprotein Inhibitors. *Pharm. Res.* **21,** 261–270 (2004).

195. Seo, Y. G. *et al.* Development of docetaxel-loaded solid self-nanoemulsifying drug delivery system (SNEDDS) for enhanced chemotherapeutic effect. *Int. J. Pharm.* **452,** 412–420 (2013).

196. Benival, D. M. & Devarajan, P. V. In situ lipidization as a new approach for the design of a self microemulsifying drug delivery system (SMEDDS) of doxorubicin hydrochloride for oral administration. *J. Biomed. Nanotechnol.* **11,** 913–922 (2015).

197. Soliman, K. A., Ibrahim, H. K. & Ghorab, M. M. Formulation of avanafil in a solid self-nanoemulsifying drug delivery system for enhanced oral delivery. *Eur. J. Pharm. Sci.* **93,** 447–455 (2016).

198. Dash, R. N., Mohammed, H., Humaira, T. & Ramesh, D. Design, optimization and evaluation of glipizide solid self-nanoemulsifying drug delivery for enhanced solubility and dissolution. *Saudi Pharm. J.* **23,** 528–540 (2015).

199. Rege, B. D., Kao, J. P. Y. & Polli, J. E. E ffects of nonionic surfactants on membrane transporters in Caco-2 cell monolayers. *Eur. J. Pharm. Sci.* **16,** 237–246 (2002).

200. Bradshaw-Pierce, E. L. *et al.* Tumor P-glycoprotein correlates with efficacy of PF-3758309 in in vitro and in vivo models of colorectal cancer. *Front. Pharmacol.* **4,** 1–11 (2013).

201. Ramge, P. *et al.* Polysorbate-80 coating enhances uptake of polybutylcyanoacrylate (PBCA)-nanoparticles by human and

bovine primary brain capillary endothelial cells. *Eur. J. Neurosci.* **12,** 1931–1940 (2000).

202. Knudson, W., Knudson, W., Clodfelter, K., Lu, B. & Weinstein, R. S. Solutol HS 15, Nontoxic Polyoxyethylene Esters of 12-Hydroxystearic Acid, Reverses Multidrug Resistance. *Cancer Res.* **51,** 897–902 (1991).

203. Cornaire, G. *et al.* Impact of excipients on the absorption of P-glycoprotein substrates in vitro and in vivo. *Int. J. Pharm.* **278,** 119–131 (2004).

204. Gullapalli, R. P. & Sheth, B. B. Influence of an optimized non-ionic emulsifier blend on properties of oil-in-water emulsions. *Eur. J. Pharm. Biopharm.* **48,** 233–238 (1999).

205. Wang, L., Dong, J., Chen, J., Eastoe, J. & Li, X. Design and optimization of a new self-nanoemulsifying drug delivery system. *J. Colloid Interface Sci.* **330,** 443–448 (2009).

206. Ali, M. H., Moghaddam, B., Kirby, D. J., Mohammed, A. R. & Perrie, Y. The role of lipid geometry in designing liposomes for the solubilisation of poorly water soluble drugs. *Int. J. Pharm.* **453,** 225–232 (2013).

207. Oyarzun-Ampuero, F. a, Rivera-Rodríguez, G. R., Alonso, M. J. & Torres, D. Hyaluronan nanocapsules as a new vehicle for intracellular drug delivery. *Eur. J. Pharm. Sci.* **49,** 483–90 (2013).

208. Qiu, Y. *et al.* Surface chemistry and aspect ratio mediated cellular uptake of Au nanorods. *Biomaterials* **31,** 7606–7619 (2010).

209. Chen, H., He, J., Tang, H. & Yan, C. Porous silica nanocapsules and nanospheres: Dynamic self-assembly synthesis and application in controlled release. *Chem. Mater.* **20,** 5894–5900

(2008).

210. Ramadan, A. *et al.* Oral fondaparinux: use of lipid nanocapsules as nanocarriers and in vivo pharmacokinetic study. *Int. J. Nanomedicine* **6,** 2941–2951 (2011).

211. Elbaz, N. M., Ziko, L., Siam, R. & Mamdouh, W. Core-Shell Silver/Polymeric Nanoparticles-Based Combinatorial Therapy against Breast Cancer In-vitro. *Nat. Publ. Gr.* **6,** 30729 (2016).

212. Peer, D. & Margalit, R. Loading mitomycin C inside long circulating hyaluronan targeted nano-liposomes increases its antitumor activity in three mice tumor models. *Int. J. Cancer* **108,** 780–9 (2004).

213. Hamelers, I. H. L., van Loenen, E., Staffhorst, R. W. H. M., de Kruijff, B. & de Kroon, A. I. P. M. Carboplatin nanocapsules: a highly cytotoxic, phospholipid-based formulation of carboplatin. *Mol. Cancer Ther.* **5,** 2007–12 (2006).

214. Domingos, R. F. *et al.* Characterizing manufactured nanoparticles in the environment: Multimethod determination of particle sizes. *Environ. Sci. Technol.* **43,** 7277–7284 (2009).

215. Shang-Hsiu Hu, San-Yuan Chen, X. G. Multifunctional Nanocapsules for Simultaneous Encapsulation of Hydrophilic and Hydrophobic Compounds and On-Demand Release. *ACS Nano* **6,** 2558–2565 (2013).

216. Kowalczyk, B., Lagzi, I. & Grzybowski, B. A. Nanoseparations: Strategies for size and/or shape-selective purification of nanoparticles. *Curr. Opin. Colloid Interface Sci.* **16,** 135–148 (2011).

217. Won, J., Yang, S. & Na, K. Gemcitabine-releasing polymeric films

for covered self-expandable metallic stent in treatment of gastrointestinal cancer. *Int. J. Pharm.* **427,** 276–283 (2012).

218. Lozano, M. V. *et al.* Polyarginine nanocapsules: A new platform for intracellular drug delivery. *J. Nanoparticle Res.* **15,** 1–15 (2013).

219. González-Aramundiz, J. V., Olmedo, M. P., González-Fernández, Á., Fernández, M. J. A. & Csaba, N. S. Protamine-based nanoparticles as new antigen delivery systems. *Eur. J. Pharm. Biopharm.* **97,** 51–59 (2015).

220. Zanotto-Filho, A. *et al.* Curcumin-loaded lipid-core nanocapsules as a strategy to improve pharmacological efficacy of curcumin in glioma treatment. *Eur. J. Pharm. Biopharm.* **83,** 156–167 (2013).

221. Mcclements, D. J. Critical Review of Techniques and Methodologies for Characterization of Emulsion Stability Critical Review of Techniques and Methodologies for Characterization of Emulsion Stability. *Crit. Rev. Food Sci. Nutr.* **47,** 611–649 (2015).

222. Moore, T. L. *et al.* Chem Soc Rev media and impact on cellular interactions †. *Chem. Soc. Rev.* **44,** 6287–6305 (2015).

223. Tan, S. W., Billa, N., Roberts, C. R. & Burley, J. C. Surfactant effects on the physical characteristics of Amphotericin B-containing nanostructured lipid carriers. *Colloids Surfaces A Physicochem. Eng. Asp.* **372,** 73–79 (2010).

224. Storm, G., Belliot, S., Daemenb, T. & Lasic, D. D. Surface modification of nanoparticles to oppose uptake by the mononuclear phagocyte system. *Adv. Drug Deliv. Rev.* **17,** 31–48 (1995).

225. Souza, S. D. A Review of In Vitro Drug Release Test Methods for

Nano-Sized Dosage Forms. *Adv. Pharm.* **2014,** 1–12 (2014).

226. Souza, S. S. D. & Deluca, P. P. Expert Review. **23,** 460–474 (2006).

227. He, H. *et al.* An in vitro and in vivo study of gemcitabine-loaded albumin nanoparticles in a pancreatic cancer cell line. *Int. J. Nanomedicine* **10,** 6825–6834 (2015).

228. Liu, Y. *et al.* Dual targeting folate-conjugated hyaluronic acid polymeric micelles for paclitaxel delivery. *Int. J. Pharm.* **421,** 160–9 (2011).

229. Xu, H. *et al.* Development of High-Content Gemcitabine PEGylated Liposomes and Their Cytotoxicity on Drug-Resistant Pancreatic Tumour Cells. *Pharm. Res.* **31,** 2583–2592 (2014).

230. Lozano, M. V. *et al.* Highly efficient system to deliver taxanes into tumor cells: Docetaxel-loaded chitosan oligomer colloidal carriers. *Biomacromolecules* **9,** 2186–2193 (2008).

231. Jaidev, L. R., Krishnan, U. M. & Sethuraman, S. Gemcitabine loaded biodegradable PLGA nanospheres for in vitro pancreatic cancer therapy. *Mater. Sci. Eng. C* **47,** 40–47 (2015).

232. Bunzen, H. & Kolehmainen, E. In Situ Formation of Steroidal Supramolecular Gels Designed for Drug Release. *Molecules* **18,** 3745–3759 (2013).

233. Li, Y. *et al.* Formation and Controlled Drug Release Using a Three-Component Supramolecular Hydrogel for Anti- Schistosoma Japonicum Cercariae. *Nanomaterials* **6,** 1–9 (2016).

234. Limón, D. *et al.* Novel nanostructured supramolecular hydrogels for the topical delivery of anionic drugs. *Eur. J. Pharm. Biopharm.* **96,** 421–436 (2015).

235. Bastiancich, C. *et al.* Lauroyl-gemcitabine-loaded lipid nanocapsule hydrogel for the treatment of glioblastoma. *J. Control. Release* **225,** 283–293 (2016).

236. Sharma, N., Madan, P. & Lin, S. Effect of process and formulation variables on the preparation of parenteral paclitaxel-loaded biodegradable polymeric nanoparticles : A co-surfactant study. *Asian J. Pharm. Sci.* **11,** 404–416 (2016).

237. Takeuchi, H., Lehr, C. & Maincent, P. Design of rolipram-loaded nanoparticles : comparison of two preparation methods. *J. Control. Release* **71,** 297–306 (2001).

238. Lamprecht, A., Bouligand, Y. & Benoit, J. New lipid nanocapsules exhibit sustained release properties for amiodarone. *J. Control. Release* **84,** 59–68 (2002).

239. Ritger, P. L. & Peppas, N. A. A simple equation for description of solute release. *J. Control. Release* **5,** 23–36 (1987).

240. Sciences, H., Dash, S., Murthy, P. N., Nath, L. & Chowdhury, P. Kinetic modeling on drug release from controlled drug delivery systems. *Acta Pol. Pharm.* **67,** 217–23 (2010).

241. Antonow, M. B. *et al.* Development and Physicochemical Characterization of Desonide-Loaded Nanocapsule Suspensions. *Adv. Mater. Sci. Eng.* **2016,** 1–12 (2016).

242. Jäger, E. *et al.* Sustained Release from Lipid-Core Nanocapsules by Varying the Core Viscosity and the Particle Surface Area. *J. Biomed. Nanotechnol.* **5,** 130–140 (2009).

243. Hong, S. P., Wen, J., Bang, S., Park, S. & Song, S. Y. CD44-positive cells are responsible for gemcitabine resistance in pancreatic cancer cells. *Int. J. Cancer* **125,** 2323–31 (2009).

244. Li, X. P., Zhang, X. W., Zheng, L. Z. & Guo, W. J. Expression of CD44 in pancreatic cancer and its significance. *Int. J. Clin. Exp. Pathol.* **8,** 6724–6731 (2015).

245. Rall, C. J. N. & Rustgi, A. K. CD44 isoform expression in primary and metastatic pancreatic adenocarcinoma. *Cancer Res.* **55,** 1831–1835 (1995).

246. Dalla, E. *et al.* Biochimica et Biophysica Acta Targeting gemcitabine containing liposomes to CD44 expressing pancreatic adenocarcinoma cells causes an increase in the antitumoral activity. *BBA - Biomembr.* **1828,** 1396–1404 (2013).

247. Lesley, J., Hascall, V. C., Tammi, M. & Hyman, R. Hyaluronan binding by cell surface CD44. *J. Biol. Chem.* **275,** 26967–75 (2000).

248. Arpicco, S. *et al.* Hyaluronic acid-coated liposomes for active targeting of gemcitabine. *Eur. J. Pharm. Biopharm.* **85,** 373–80 (2013).

249. Li, C. *et al.* Complete Regression of Well-established Tumors Using a Novel Water-soluble Poly (l-Glutamic Acid) -Paclitaxel Conjugate Complete Regression of Well-established Tumors Using a Novel Water-soluble. *Cancer Res.* **58,** 2404–2409 (1998).

250. Li, C. *et al.* Tumor Irradiation Enhances the Tumor-specific Distribution of Poly (l-glutamic acid) -conjugated Paclitaxel and Its Antitumor Efficacy Tumor Irradiation Enhances the Tumor-specific Distribution of Poly (L -glutamic acid) -conjugated Paclitaxel and Its. *Clin. Cancer Res.* **6,** 2829–2834 (2000).

251. Liu, T. *et al.* A poly (L -glutamic acid) -combretastatin A4 conjugate for solid tumor therapy : Markedly improved therapeutic efficiency through its low tissue penetration in solid tumor. *Acta*

Biomater. **53,** 179–189 (2017).

252. Cabral, H. *et al.* Targeted therapy of spontaneous murine pancreatic tumors by polymeric micelles prolongs survival and prevents peritoneal metastasis. *Proc. Natl. Acad. Sci.* **110,** 11397–11402 (2013).

253. Maya, S., Sarmento, B., Lakshmanan, V. K., Menon, D. & Jayakumar, R. Actively targeted cetuximab conjugated ??-poly(glutamic acid)-docetaxel nanomedicines for epidermal growth factor receptor over expressing colon cancer cells. *J. Biomed. Nanotechnol.* **10,** 1416–1428 (2014).

254. Xu, R. *et al.* An injectable nanoparticle generator enhances delivery of cancer therapeutics. *Nat. Biotechnol.* **34,** 1–7 (2016).

255. Mori-Iwamoto, S. *et al.* A proteomic profiling of gemcitabine resistance in pancreatic cancer cell lines. *Mol. Med. Rep.* **1,** 429–434 (2008).

256. Kapse-Mistry, S., Govender, T., Srivastava, R. & Yergeri, M. Nanodrug delivery in reversing multidrug resistance in cancer cells. *Front. Pharmacol.* **5,** 1–22 (2014).

257. Garcion, E. *et al.* A new generation of anticancer, drug-loaded, colloidal vectors reverses multidrug resistance in glioma and reduces tumor progression in rats. *Mol. Cancer Ther.* **5,** 1710–22 (2006).

258. Amaral, L., Engi, H., Viveiros, M. & Molnar, J. Comparison of Multidrug Resistant Efflux Pumps of Cancer and Bacterial Cells with Respect to the Same Inhibitory Agents. *In Vivo (Brooklyn).* **21,** 237–244 (2007).

259. Velingkar, V. S. & Dandekar, V. D. Modulation of P- Glycoprotein

mediated multidrug resistance (MDR) in cancer using chemosensitizers. *Internatioinal J. Pharma Sci. Res.* **1,** 104–111 (2010).

260. Gottesman, M. M., Fojo, T. & Bates, S. E. Multidrug Resistance in Cancer: Role of Atp-Dependent Transporters. *Nat. Rev. Cancer* **2,** 48–58 (2002).

261. Scheffer, G. L. *et al.* The drug resistance-related protein LRP is the human major vault protein. *Nat. Med.* **1,** 578–582 (1995).

262. Hoffmann, K., Bekeredjian, R., Schmidt, J., Büchler, M. W. & Märten, A. Effects of the high-affinity peptide reversin 121 on multidrug resistance proteins in experimental pancreatic cancer. *Tumor Biol.* **29,** 351–358 (2009).

263. Scott, A. M., Wolchok, J. D. & Old, L. J. Antibody therapy of cancer. *Nat. Rev.* **12,** 278–287 (2012).

264. Jones, S. K. & Merkel, O. M. Tackling breast cancer chemoresistance with nano-formulated siRNA. *Gene Ther.* **23,** 821–828 (2016).

265. Abdallah, H. M., Al-Abd, A. M., El-Dine, R. S. & El-Halawany, A. M. P-glycoprotein inhibitors of natural origin as potential tumor chemo-sensitizers: A review. *J. Adv. Res.* **6,** 45–62 (2015).

266. Long, J. *et al.* Overcoming Drug Resistance i. *Expert Opin Ther Targets* **15,** 817–828 (2012).

267. Landesman-Milo, D. *et al.* Hyaluronan grafted lipid-based nanoparticles as RNAi carriers for cancer cells. *Cancer Lett.* **334,** 221–7 (2013).

268. Singh, M. S. & Lamprecht, A. P-glycoprotein inhibition of drug resistant cell lines by nanoparticles. *Drug Dev. Ind. Pharm.* **42,**

325–331 (2016).

269. Lamprecht, A. & Benoit, J.-P. Etoposide nanocarriers suppress glioma cell growth by intracellular drug delivery and simultaneous P-glycoprotein inhibition. *J. Control. Release* **112,** 208–13 (2006).

270. Qazzaz, M. E. *et al.* In vitro anticancer properties and biological evaluation of novel natural alkaloid jerantinine B. *Cancer Lett.* **370,** 185–197 (2016).

271. He, Q. *et al.* A pH-responsive mesoporous silica nanoparticles-based multi-drug delivery system for overcoming multi-drug resistance. *Biomaterials* **32,** 7711–7720 (2011).

272. Kievit, F. M. *et al.* Doxorubicin loaded iron oxide nanoparticles overcome multidrug resistance in cancer in vitro. *J. Control. Release* **152,** 76–83 (2011).

273. Krieger, M. L. *et al.* Overcoming cisplatin resistance of ovarian cancer cells by targeted liposomes in vitro. *Int. J. Pharm.* **389,** 10–17 (2010).

274. Jia, Y., Peng, J., Chen, J. & Lu, S. Co-encapsulation of magnetic Fe 3 O 4 nanoparticles and doxorubicin into biodegradable PLGA nanocarriers for intratumoral drug delivery. *Internatioinal J. Nanomedicine* **7,** 1697–1708 (2012).

275. Nsereko, S. & Amiji, M. Localized delivery of paclitaxel in solid tumors from biodegradable chitin microparticle formulations. *Biomaterials* **23,** 2723–2731 (2002).

276. Xu, X., Chen, X., Wang, Z. & Jing, X. Ultrafine PEG – PLA fibers loaded with both paclitaxel and doxorubicin hydrochloride and their in vitro cytotoxicity. *Eur. J. Pharm. Biopharm.* **72,** 18–25 (2009).

277. Ranganath, S. H. & Wang, C. Biomaterials Biodegradable microfiber implants delivering paclitaxel for post-surgical chemotherapy against malignant glioma. **29,** 2996–3003 (2008).

278. Eckardstein, K. L. Von, Patt, S., Kratzel, C., Kiwit, C. W. & Reszka, R. Local chemotherapy of F98 rat glioblastoma with paclitaxel and carboplatin embedded in liquid crystalline cubic phases. *J. Neurooncol.* **72,** 209–215 (2005).

279. Al-abd, A. M., Hong, K., Song, S. & Kuh, H. Pharmacokinetics of doxorubicin after intratumoral injection using a thermosensitive hydrogel in tumor-bearing mice. *J. Control. Release* **142,** 101–107 (2010).

280. Cristini-robbe, O. *et al.* Local Drug Delivery Strategy for Cancer Treatment: Use of Biocompatible Sol-Gel-Derived Porous Materials. *New J. Glas. Ceram.* **2013,** 74–79 (2013).

281. Xiong, L. *et al.* An injectable drug-loaded hydrogel based on a supramolecular polymeric prodrug. *Chem. Commun.* **51,** 14644–14647 (2015).

282. Kyun, W. *et al.* Biomaterials Docetaxel-loaded thermoresponsive conjugated linoleic acid-incorporated poloxamer hydrogel for the suppression of peritoneal metastasis of gastric cancer. *Biomaterials* **34,** 1433–1441 (2013).

283. Nagahama, K. *et al.* Self-Assembling Polymer Micelle / Clay Nanodisk / Doxorubicin Hybrid Injectable Gels for Safe and E ffi cient Focal Treatment of Cancer. *Biomacromolecules* **16,** 880–889 (2015).

284. Mao, Y., Li, X., Chen, G. & Wang, S. Thermosensitive Hydrogel System With Paclitaxel Liposomes Used in Localized Drug Delivery System for In Situ Treatment of Tumor : Better Antitumor Ef fi

cacy and Lower Toxicity. *J. Pharm. Sci.* **105,** 194–204 (2016).

285. Yeon, D. *et al.* Synergistic anti-tumor activity through combinational intratumoral injection of an in-situ injectable drug depot. *Biomaterials* **85,** 232–245 (2016).

286. Ranganath, S. H., Kee, I. M. E. P.-P. M. : D. D. with N. Z.-O. R. and I. A. for M. B. T. C., Krantz, W. B., Chow, P. K. & Wang, C. Hydrogel Matrix Entrapping PLGA-Paclitaxel Microspheres : Drug Delivery with Near Zero-Order Release and Implantability Advantages for Malignant Brain Tumour Chemotherapy. *Pharm. Res.* **26,** 2101–2114 (2009).

287. Ozeki, T. *et al.* Improvement of survival in C6 rat glioma model by a sustained drug release from localized PLGA microspheres in a thermoreversible hydrogel. *Int. J. Pharm.* **427,** 299–304 (2012).

288. Gao, X. Enhanced antitumor effects by docetaxel / LL37- loaded thermosensitive hydrogel nanoparticles in peritoneal carcinomatosis of colorectal cancer. *Internatioinal J. Nanomedicine* **10,** 7291–7305 (2015).

289. Segovia, N. *et al.* Hydrogel Doped with Nanoparticles for Local Sustained Release of siRNA in Breast Cancer. *Adv. Healthc. Mater.* 1–10 (2014). doi:10.1002/adhm.201400235

290. Thu, H., Dass, C. R. & Dunstan, D. E. Injectable chitosan hydrogels for localised cancer therapy. *J. Control. Release 126* **126,** 205–216 (2008).

291. Bhattarai, N., Gunn, J. & Zhang, M. Chitosan-based hydrogels for controlled, localized drug delivery☆. *Adv. Drug Deliv. Rev.* **62,** 83–99 (2010).

292. Kim, S. *et al.* Biomaterials A chitosan / b -glycerophosphate thermo-sensitive gel for the delivery of ellagic acid for the treatment of brain cancer. *Biomaterials* **31,** 4157–4166 (2010).

293. Dai, M. *et al.* A Novel Composite Drug Delivery System : Honokiol Nanoparticles in Thermosensitive Hydrogel Based on Chitosan A Novel Composite Drug Delivery System : Honokiol Nanoparticles in Thermosensitive Hydrogel Based on Chitosan. *J. Nanosci. Nanotechnol.* **9,** 4587–4592 (2009).

294. Li, X. *et al.* A Novel Composite Hydrogel Based on Chitosan and Inorganic Phosphate for Local Drug Delivery of Camptothecin Nanocolloids. *J. Pharm. Sci.* **100,** 232–241 (2011).

295. Desbrisres, J. & Rinaudo, M. I. Formation of a biocompatible polyelectrolyte complex : chitosan-hyaluronan complex stability. *Polym. Bull.* **50,** 91–98 (2003).

296. Florczyk, S. J. *et al.* Biomaterials Porous chitosan-hyaluronic acid scaffolds as a mimic of glioblastoma microenvironment ECM. *Biomaterials* **34,** 10143–10150 (2013).

297. Tian, R. & Niu, R. The development of low-molecular weight hydrogels for applications in cancer therapy. *Nanoscale* **6,** 3474–3482 (2014).

298. Moysan, E. *et al.* An innovative hydrogel of gemcitabine-loaded lipid nanocapsules: when the drug is a key player of the nanomedicine structure. *Soft Matter* (2014). doi:10.1039/c3sm52781f

299. Skilling, K. J., Kellam, B., Ashford, M., Bradshaw, T. D. & Marlow, M. Soft MatterDeveloping a self-healing supramolecular nucleoside hydrogel. *Soft Matter* **12,** 8950–8957 (2016).

300. Greenspan, P. & Fowler, S. D. Spectrofluorometric studies of the lipid probe, nile red. *J. Lipid Res.* **26,** 781–789 (1985).

301. Yao, K. De, Tu, H., Cheng, F., Zhang, J. W. & Liu, J. pH-Sensitivity of the swelling of a chitosan-pectin polyelectrolyte complex. *Die Angew. Makromol. Chemie* **245,** 63–72 (1997).

302. Berger, J., Reist, M., Mayer, J. M., Felt, O. & Gurny, R. Structure and interactions in chitosan hydrogels formed by complexation or aggregation for biomedical applications. *Eur. J. Pharm. Biopharm.* **57,** 35–52 (2004).

303. Ito, T. *et al.* The prevention of peritoneal adhesions by in situ cross-linking hydrogels of hyaluronic acid and cellulose derivatives. *Biomaterials* **28,** 975–983 (2007).

304. Yeo, Y. *et al.* In situ cross-linkable hyaluronan hydrogels containing polymeric nanoparticles for preventing postsurgical adhesions. *Ann. Surg.* **245,** 819–24 (2007).

305. Li, L. *et al.* Biomaterials Biodegradable and injectable in situ cross-linking chitosan-hyaluronic acid based hydrogels for postoperative adhesion prevention. *Biomaterials* **35,** 3903–3917 (2014).

306. Yamane, S., Iwasaki, N., Majima, T. & Funakoshi, T. Feasibility of chitosan-based hyaluronic acid hybrid biomaterial for a novel scaffold in cartilage tissue engineering. *Biomaterials* **26,** 611–619 (2005).

307. Tan, H., Chu, C. R., Payne, K. a. & Marra, K. G. Injectable in situ forming biodegradable chitosan-hyaluronic acid based hydrogels for cartilage tissue engineering. *Biomaterials* **30,** 2499–2506 (2009).

308. Park, H., Choi, B., Hu, J. & Lee, M. Acta Biomaterialia Injectable

chitosan hyaluronic acid hydrogels for cartilage tissue engineering. **9,** 4779–4786 (2013).

309. Deb, S., Abueva, C., Kim, B. & Taek, B. Chitosan – hyaluronic acid polyelectrolyte complex scaffold crosslinked with genipin for immobilization and controlled release of BMP-2. *Carbohydr. Polym.* **115,** 160–169 (2015).

310. Fang, J. Y., Chen, J. P., Leu, Y. L. & Hu, J. W. Temperature-sensitive hydrogels composed of chitosan and hyaluronic acid as injectable carriers for drug delivery. *Eur. J. Pharm. Biopharm.* **68,** 626–636 (2008).

311. Tao, Y., Ai, L., Bai, H. & Liu, X. Synthesis of pH-Responsive Photocrosslinked Hyaluronic Acid-Based Hydrogels for Drug Delivery. *J. Polym. Sci.* **50,** 3507–3516 (2012).

312. Yang, C., Bian, M. & Yang, Z. A polymer additive boosts the anti-cancer efficacy of supramolecular nanofibers of taxol. *Biomater. Sci.* **2,** 651 (2014).

313. Matter, S., Adhia, Y. J., Schloemer, T. H., Perez, M. T. & Mcneil, A. J. Using polymeric additives to enhance molecular gelation : impact of poly (acrylic acid) on pyridine-based gelators †. *Soft Matter* **8,** 430–434 (2012).

314. Pont, G., Chen, L., Spiller, G. & Adams, D. J. The effect of polymer additives on the rheological properties of dipeptide hydrogelators. *Soft Matter* **8,** 7797–7803 (2012).

315. Basrur, V. R., Guo, J., Wang, C. & Raghavan, S. R. Synergistic Gelation of Silica Nanoparticles and a Sorbitol-Based Molecular Gelator to Yield Highly-Conductive Free-Standing Gel Electrolytes. *Appl. Mater. Interfaces* **5,** 262–267 (2013).

316. Mohmeyer, N. & Schmidt, H. A New Class of Low-Molecular-Weight Amphiphilic Gelators. *Chem. Eur. J.* **11,** 863–872 (2005).

317. Menger, F. M. & Caran, K. L. Anatomy of a Gel. Amino Acid Derivatives That Rigidify Water at Submillimolar Concentrations. *J. Am. Chem. Soc.* **122,** 11679–11691 (2000).

318. Altunbas, A., Lee, S. J., Rajasekaran, S. A., Schneider, J. P. & Pochan, D. J. Biomaterials Encapsulation of curcumin in self-assembling peptide hydrogels as injectable drug delivery vehicles. *Biomaterials* **32,** 5906–5914 (2011).

319. Yan, J. *et al.* Ferrocene-containing Thixotropic Molecular Gels: Creation and A Novel Strategy for Water Purification. *J. Colloid Interface Sci.* 374–379 (2015). doi:10.1016/j.jcis.2015.02.044

320. Sutton, S. *et al.* Controlled Release from Modified Amino Acid Hydrogels Governed by Molecular Size or Network Dynamics. *Langmuir* **25,** 10285–10291 (2009).

321. Li, R. *et al.* Encapsulation of 10-Hydroxy Camptothecin in Supramolecular Hydrogel as an Injectable Drug Delivery System. *J. Pharm. Sci.* **104,** 2266–2275 (2015).

322. Song, F., Zhang, L., Shi, J. & Li, N. Colloids and Surfaces B : Biointerfaces Viscoelastic and fractal characteristics of a supramolecular hydrogel hybridized with clay nanoparticles. *Colloids Surfaces B Biointerfaces* **81,** 486–491 (2010).

323. Cheng, C., Tang, M., Wu, C., Simon, T. & Ko, F. New Synthesis Route of Hydrogel through A Bioinspired Supramolecular Approach: Gelation, Binding Interaction, and in Vitro Dressing. *Appl. Mater. Interfaces* **7,** 19306−19315 (2015).

324. Epstein-barash, H. *et al.* Biomaterials A microcomposite hydrogel

for repeated on-demand ultrasound-triggered drug delivery. *Biomaterials* **31,** 5208–5217 (2010).

325. Xuan Zhang, Sharon Bloch, Walter Akers, and S. A. Near-infrared Molecular Probes for In Vivo Imaging. *Curr Protoc Cytom .* 1–28 (2013).

326. Prasmickaite, L. & Bonsted, A. Porphyrin-related photosensitizers for cancer imaging and. *J. Microsc.* **218,** 133–147 (2005).

327. Evan R. Trivedia, b,†, Zhidong Maa, b, c, d,†, Emily A. Waterse, Keith W. Macrenarise, Rohit Subramaniana, b, c, d, Anthony G. M. Barrettff, Thomas J. Meadea, b, c, d, and B. M. & Hoffmanar. Synthesis and characterization of a porphyrazine–Gd(III) MRI contrast agent and in vivo imaging of a breast cancer xenograft model. *Contrast Media Mol Imaging* **9,** 313–322 (2015).

328. Dong, X. *et al.* Thermosensitive porphyrin-incorporated hydrogel with four-arm PEG-PCL copolymer (II): doxorubicin loaded hydrogel as a dual fluorescent drug delivery system for simultaneous imaging tracking in vivo Thermosensitive porphyrin-incorporated hydrogel with f. *Drug Deliv.* **24,** 641–650 (2017).

329. Huang, H. *et al.* Implantable Tin Porphyrin-PEG Hydrogels with pH-Responsive Fluorescence. *Biomacromolecules* **18,** 562−567 (2017).

330. Auger, A., Samuel, J., Poncelet, O. & Raccurt, O. A comparative study of non-covalent encapsulation methods for organic dyes into silica nanoparticles. *Nanoscale Res. Lett.* **6:328,** 1–12 (2011).

331. He, W. *et al.* Core-shell structured gel-nanocarriers for sustained drug release and enhanced antitumor effect. *Int. J. Pharm.* **484,** 163–71 (2015).

332. Nanda, J., Adhikari, B., Basak, S. & Banerjee, A. Formation of Hybrid Hydrogels Consisting of Tripeptide and Di ff erent Silver Nanoparticle-Capped Ligands: Modulation of the Mechanical Strength of Gel Phase Materials. *J. Phys. Chem.* **116,** 12235–12244 (2012).

333. Peters, G. M. Chem Soc Rev nucleoside and nucleotide analogs position and practical applications. *Chem. Soc. Rev.* **45,** 3188–3206 (2016).

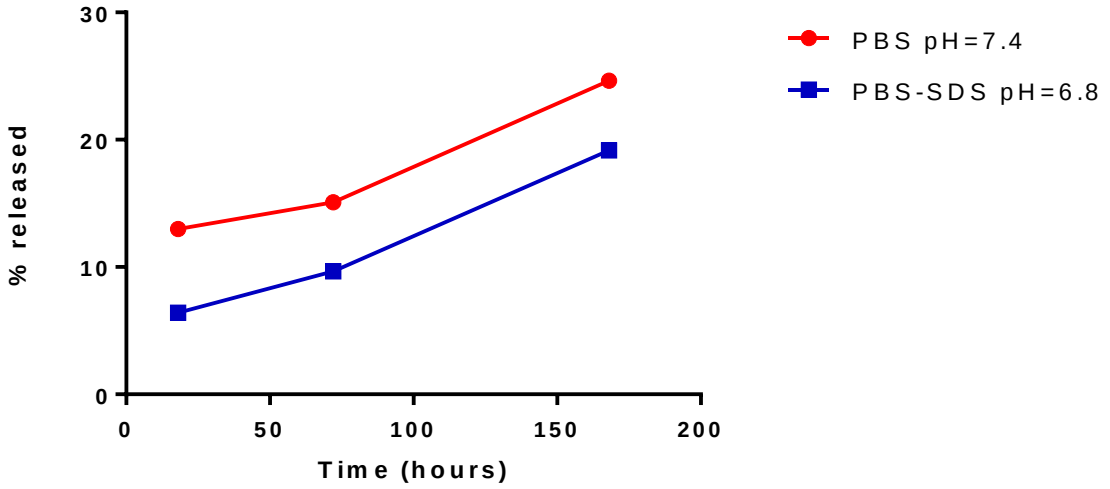
334. Raeburn, J. *et al.* The effect of solvent choice on the gelation and final hydrogel properties of Fmoc–diphenylalanine. *Soft Matter* **11,** 927–935 (2015).

335. Raeburn, J., Zamith Cardoso, A. & Adams, D. J. The importance of the self-assembly process to control mechanical properties of low molecular weight hydrogels. *Chem. Soc. Rev.* **42,** 5143–56 (2013).

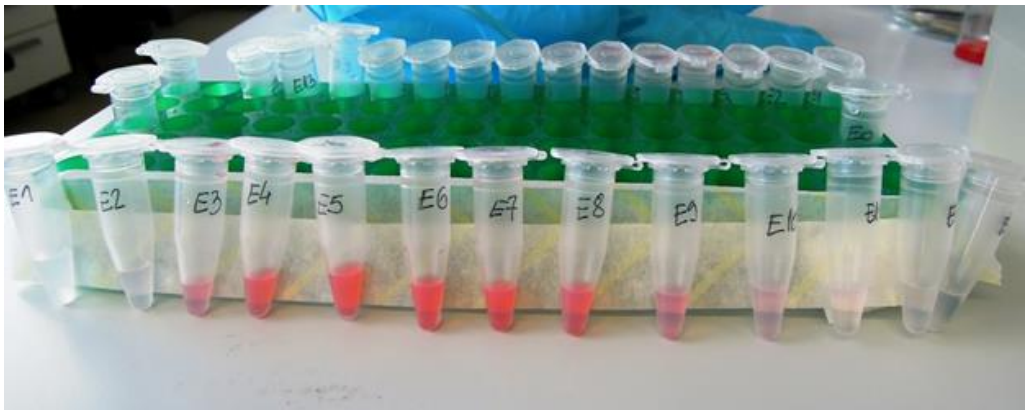
336. Chaudhari, A. K., Han, I. & Tan, J. Multifunctional Supramolecular Hybrid Materials Constructed from Hierarchical Self-Ordering of In Situ Generated Metal-Organic Framework (MOF) Nanoparticles. *Adv. Mater.* **27,** 4438–4446 (2015).

Appendices

Appendix 1. Release of GEM C14 from HA 80 nm NCs in 2 release mediums: PBS (pH=7.4) and PBS+0.1% w/w SDS (pH=6.8). Volume of NCs incubated was 0.5 mL with 12.5 mL of release medium at 37 °C.

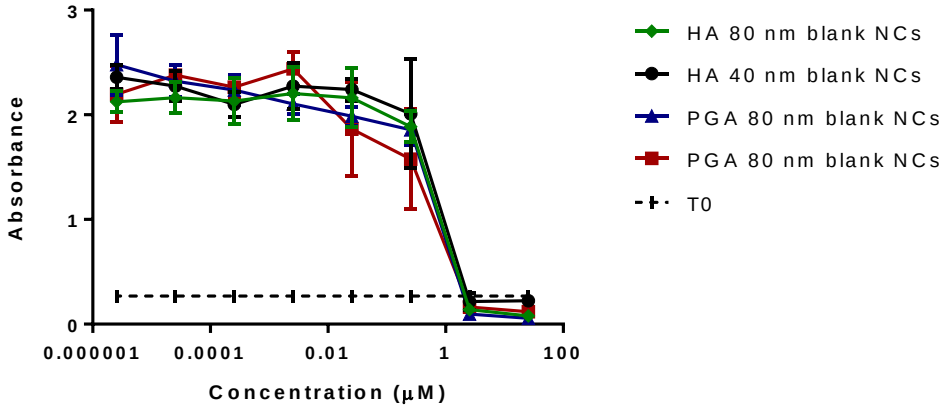


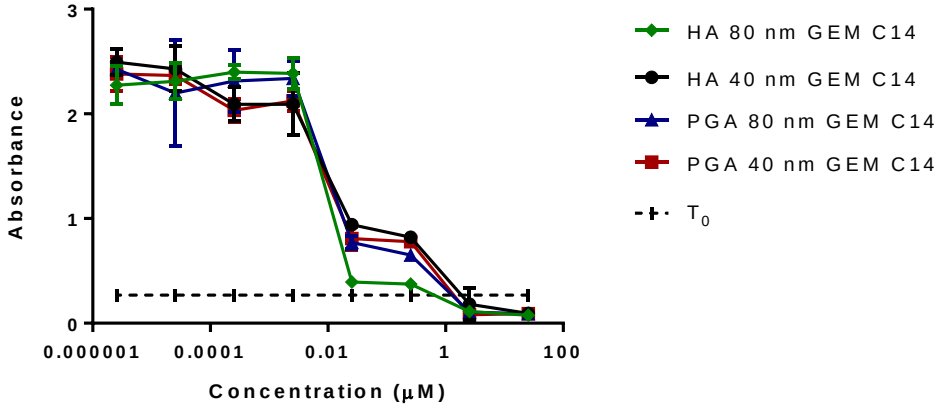
Appendix 2. Image of elutions of HA 80 nm NCs loaded with sudan III dye, collected from SEC column.

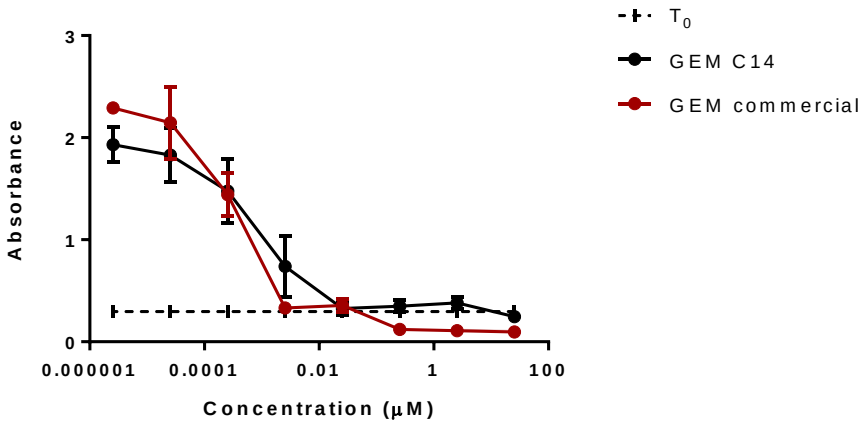


Appendix 3. Growth inhibitory profiles of blank or GEM-C14 loaded NCs and free GEM-HCl or modified GEM on HCT 116 and MIA PaCa-2 cell lines. All 4 types of NCs (HA 80, HA40, PGA 80, PGA 40 nm NCs) were evaluated.

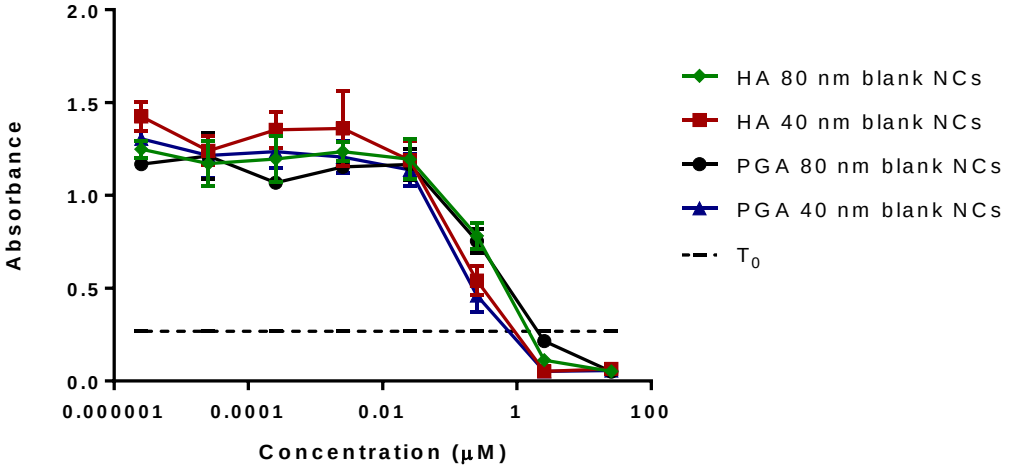
HCT 116

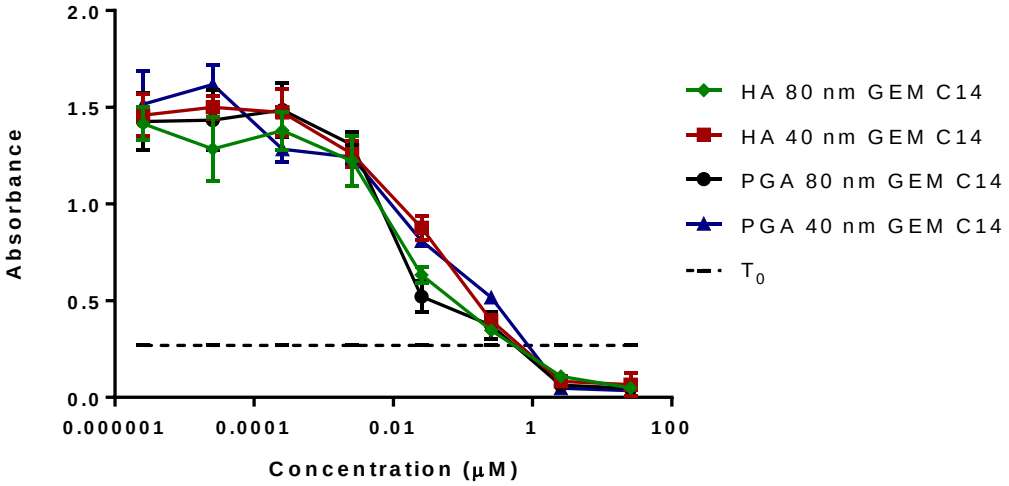

Absorbance
3
2
1
0
0.000001
0.0001
0.01
1
100
Concentration (µM)
HA 80 nm blank NCs
HA 40 nm blank NCs
PGA 80 nm blank NCs
PGA 80 nm blank NCs
T0

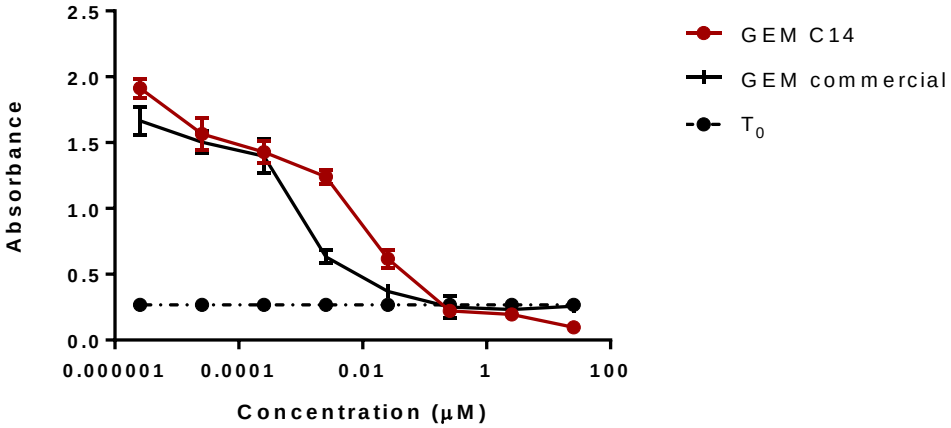

Absorbance
3
2
1
0
0.000001
0.0001
0.01
1
100
Concentration (µM)
HA 80 nm GEM C14
HA 40 nm GEM C14
PGA 80 nm GEM C14
PGA 40 nm GEM C14
T0


Absorbance
3
2
1
0
0.000001
0.0001
0.01
1
100
Concentration (µM)
T0
GEM C14
GEM commercial

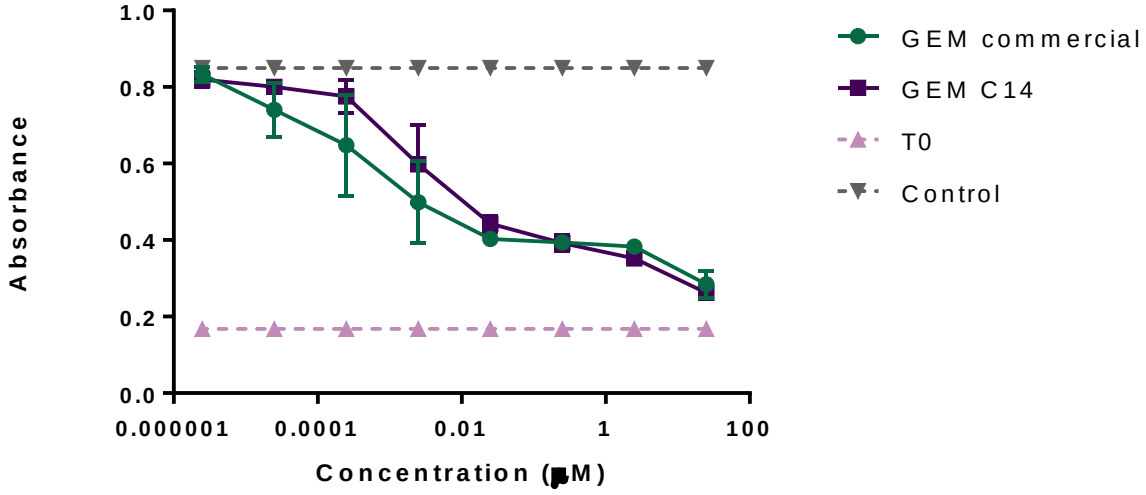
MIA PaCa-2


2.0
1.5
1.0
0.5
0.0
Absorbance
0.000001
0.0001
0.01
1
100
Concentration (µM)
HA 80 nm blank NCs
HA 40 nm blank NCs
PGA 80 nm blank NCs
PGA 40 nm blank NCs
T0

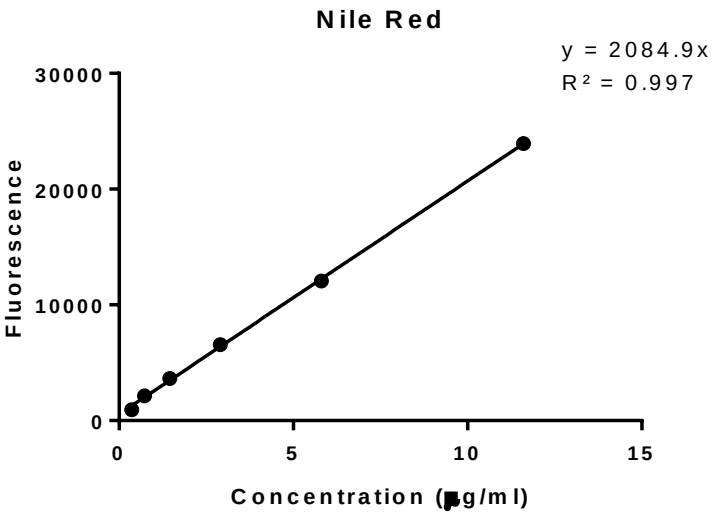

2.0
1.5
1.0
0.5
0.0
Absorbance
0.000001
0.0001
0.01
1
100
Concentration (µM)
HA 80 nm GEM C14
HA 40 nm GEM C14
PGA 80 nm GEM C14
PGA 40 nm GEM C14
T0

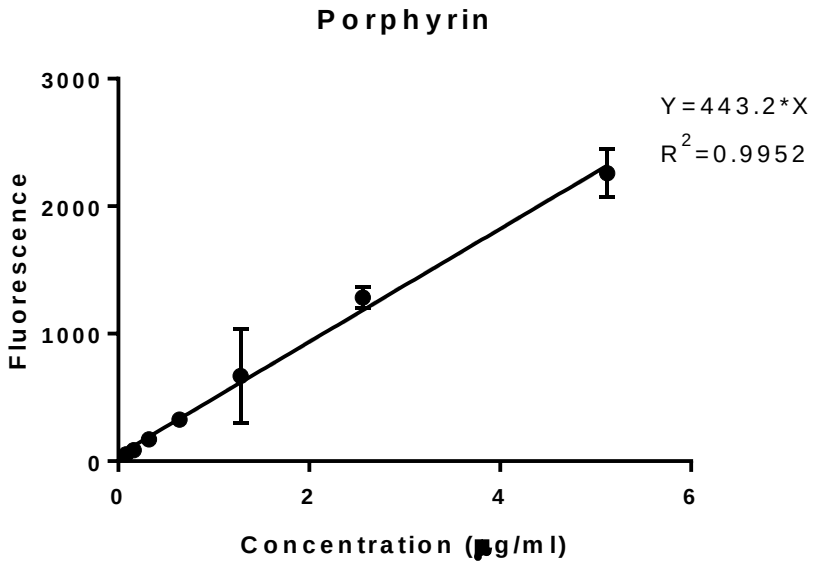

2.5
2.0
1.5
1.0
0.5
0.0
Absorbance
0.000001
0.0001
0.01
1
100
Concentration (µM)
GEM C14
GEM commercial
T0

Appendix 4. Dose response curves illustrating GEM C14 and for GEM-HCl activity on the HCT 116 VR cell line.



Appendix 5. A standard calibration curves of NR and porphyrin





Appendix 6. Image of change in colour upon interaction between DiD and Tween 80

